



TECHNISCHE UNIVERSITÄT MÜNCHEN

Wissenschaftszentrum Weihenstephan für Ernährung, Landnutzung und Umwelt
ZIEL - Institute for Food & Health

**Optimization of liquid chromatography-
mass spectrometry-based methods for the
discovery of microbial and nutritional metabolites**

Nina Sillner

Vollständiger Abdruck der von der Fakultät Wissenschaftszentrum
Weihenstephan für Ernährung, Landnutzung und Umwelt der Technischen
Universität München zur Erlangung des akademischen Grades eines

Doktors der Naturwissenschaften

genehmigten Dissertation.

Vorsitzender: Prof. Dr. Martin Klingenspor

Prüfer der Dissertation:

1. apl. Prof. Dr. Philippe Schmitt-Kopplin
2. Prof. Dr. Dirk Haller

Die Dissertation wurde am 27.06.2019 bei der Technischen Universität
München eingereicht und durch die Fakultät Wissenschaftszentrum
Weihenstephan für Ernährung, Landnutzung und Umwelt am 10.12.2019
angenommen.

Acknowledgments

First of all, I would like to thank my supervisor Prof. Dr. Philippe Schmitt-Kopplin, who gave me the opportunity to do this work in his research group. I also thank you for the freedom you gave me in this research and for your help and support.

I thank Prof. Dr. Dirk Haller, Monika Bazanella and the whole team behind it for the possibility to work on this very interesting project and for the cooperative work and support. Furthermore, I would like to thank Prof. Dr. Michael Rychlik for being part of my thesis committee.

A very special thank you goes to Dr. Alesia Walker for all her support and time throughout the whole thesis. You made it very easy for me to find my way and to familiarize with the topic and the analytical techniques. You always took your time to listen to my problems and helped me out and motivated me.

I thank Dr. Michael Witting for all his help and the many inspiring scientific and non-scientific discussions together with Dr. Alesia Walker. I would also like to thank Dr. Marianna Lucio for helping me in statistical questions and all her support. Many thanks to Jenny Uhl and Astrid Bösl for their support in all administrative matters. Further, I would like to thank Dr. Silke Heinzmann for her help with NMR. I also thank Brigitte Lock for technical assistance in the laboratory and all other colleagues for the discussions, their help and the nice working atmosphere.

Finally, I would like to thank my family who always stood by my side. Your encouragement and endless love have always given me strength to go my way and to write this thesis. My deepest gratitude goes to my parents, my grandparents, my sister Nadine and brother Tobi for their unconditional support and love. Without you I would not be where I am today. Chris, you always stood by my side and gave me your support, love and eventually provided the necessary balance. All of you supported me in all my decisions and always gave me the right advice, even in difficult times.

Abstract

The gastrointestinal tract harbors a complex microbial ecosystem which is strongly influenced by extrinsic factors such as nutrition and drug-intake. Different comprehensive metabolomics tools can be used to better understand the underlying functional processes of host and microbial metabolism.

In the first part of the thesis, an absolute quantification method of bile acids in cecum was setup by using ultra-high pressure liquid chromatography (UHPLC) coupled to ion trap mass spectrometry (MS). Bile acids are key components of co-microbial metabolism and are present in high concentrations in the gastrointestinal tract of mammals. In total, 45 bile acids were profiled and the method was validated including limit of detection and quantification, accuracy, precision, matrix effect and recovery rate. The targeted metabolomics method was applied in order to explore the impact of the anti-diabetic drug metformin on bile acid metabolism in a diabetic mouse model.

In the second part of the thesis, three hydrophilic interaction liquid chromatography (HILIC) stationary phases were studied systematically with varying pH and salt gradients. The goal was to elaborate optimal conditions to perform a non-targeted metabolomics analysis of fecal samples by means of HILIC UHPLC-MS. A set of 150 metabolite standards and a pooled feces sample was analyzed at 18 different conditions and the number of detected features, the ability to separate isomers, precision of the analysis and retention time distribution of metabolite features across all chromatographic runs was evaluated.

Finally, the most appropriate HILIC method was applied for a non-targeted metabolomics approach to screen for differences in the fecal metabolite profiles of formula- and breastfed infants. The subsequent combination of targeted metabolomics including UHPLC, high resolution MS (including QTOF and FT-ICR-MS) and NMR spectroscopy enabled the discovery and identification of novel Amadori products in feces of formula-fed infants. These nutrition markers were directly associated to infant formula milk. Additionally, the fecal excretion of Amadori products was profiled and quantified at several time points over the first 2 years of life.

In this thesis, the necessity of method development and optimization for targeted and non-targeted metabolomics was demonstrated. The application of these

methods emphasized that MS based metabolomics is a powerful tool to discover the impact of exposomal factors like drugs and diet on the metabolome of the gastrointestinal tract.

Zusammenfassung

Der Magen-Darm-Trakt besitzt ein komplexes, mikrobielles Ökosystem, welches stark von extrinsischen Faktoren, wie der Ernährung und Medikamenten, beeinflusst wird. Der Einsatz von verschiedenen Techniken der Metabolomik trägt dazu bei, ein besseres Verständnis von den zugrundeliegenden, funktionellen Prozessen des Wirts- und mikrobiellen Stoffwechsels zu erlangen.

Im ersten Teil der Doktorarbeit wurde eine Methode zur absoluten Quantifizierung von Gallensäuren im Blinddarm mittels UHPLC, gekoppelt an ein Ionenfallen-Massenspektrometer, entwickelt. Gallensäuren sind Schlüsselkomponenten des mikrobiellen Stoffwechsels und kommen in hohen Konzentrationen im Magen-Darm-Trakt von Säugetieren vor. Insgesamt wurden 45 Gallensäuren analysiert und die Methode wurde anhand von Nachweis- und Bestimmungsgrenze, Genauigkeit, Präzision, Matrixeffekt und Wiederfindungsrate validiert. Diese zielgerichtete Metabolomik Methode wurde anschließend angewendet, um die Auswirkungen des Antidiabetikums Metformin auf den Gallensäurestoffwechsel in einem diabetischen Mausmodell zu untersuchen.

Im zweiten Teil der Arbeit wurden drei stationäre Phasen der hydrophilen Interaktions-Flüssigchromatographie (HILIC) systematisch mit unterschiedlichen pH-Werten und Salzgradienten untersucht. Ziel war es, optimale Bedingungen für eine nicht-zielgerichtete Metabolom-Analyse von Stuhlproben mittels HILIC UHPLC-MS zu erarbeiten. Insgesamt wurden 150 verschiedene Metabolite (Standards) und eine gepoolte Stuhlprobe unter 18 verschiedenen chromatographischen Bedingungen analysiert und die Anzahl der detektierten Substanzen, die Fähigkeit zur Trennung von Isomeren, die Präzision der Analyse und die Verteilung der Retentionszeit der Metabolite über alle chromatographischen Läufe bewertet.

Schließlich wurde die am besten geeignete HILIC-Methode für eine nicht-zielgerichtete Metabolom-Analyse angewendet, um nach Unterschieden im Metabolitenprofil im Stuhl von Säuglingsnahrung gefütterten und gestillten Säuglingen zu suchen. Die anschließende Kombination verschiedener analytischer Techniken, einschließlich UHPLC, hochauflösender MS (QTOF und FT-ICR-MS) und NMR Spektroskopie, ermöglichte die Entdeckung und Identifizierung neuer Amadori-Produkte im Stuhl von Säuglingsnahrung gefütterten Kleinkindern. Diese Ernährungsmarker konnten direkt mit den

Proteinen der Säuglingsnahrung assoziiert werden. Darüber hinaus wurde die Ausscheidung von Amadori-Produkten im Stuhl zu mehreren Zeitpunkten in den ersten zwei Lebensjahren analysiert und quantifiziert.

In dieser Arbeit wurde die Notwendigkeit der Methodenentwicklung und -optimierung für die zielgerichtete und nicht-zielgerichtete Metabolomik aufgezeigt. Die Anwendung dieser Methoden hat gezeigt, dass die MS-basierte Metabolomik ein wirksames Instrument ist, um den Einfluss exposomaler Faktoren wie Medikamente und Ernährung auf das Metabolom des Magen-Darm-Trakts zu untersuchen.

Table of Contents

Acknowledgments	III
Abstract	V
Zusammenfassung	VII
Table of Contents	IX
List of Publications	XI
Abbreviations	XIII
1. General Introduction and Methods	1
1.1 Metabolomics.....	1
1.1.1 Metabolomics in gut microbiota research.....	4
1.1.2 Nutritional metabolomics	8
1.1.3 Metabolomics to study the impact of diet on developing infants.....	11
1.1.4 Maillard reaction products in infant formula	13
1.2 Analytical methods in metabolomics	15
1.2.1 Non-targeted vs. targeted metabolomics	16
1.2.2 Liquid chromatography	18
1.2.3 Mass spectrometry	20
2. Metformin impacts cecal bile acid profiles in mice	25
3. Development and Application of a HILIC UHPLC-MS Method for Polar Fecal Metabolome Profiling	27
4. Milk-derived Amadori products in feces of formula-fed infants	29
5. Discussion and Outlook	31

A. Appendix Chapter 2	35
A.1 Original Publication.....	35
A.2 Supplementary Information.....	44
B. Appendix Chapter 3	51
B.1 Original Publication.....	51
B.2 Supplementary Information.....	58
C. Appendix Chapter 4	71
C.1 Original Publication	71
C.2 Supplementary Information	80
Bibliography	93
List of Figures	103
Curriculum Vitae	106
Eidesstattliche Erklärung	108

List of Publications

Publications directly addressed in this thesis:

Sillner, N., Walker, A., Koch, W., Witting, M. & Schmitt-Kopplin, P. Metformin impacts cecal bile acid profiles in mice. *Journal of Chromatography B* 1083, 35-43 (2018).

Sillner, N., Walker, A., Harrieder, E., Schmitt-Kopplin, P. & Witting, M. Development and application of a HILIC UHPLC-MS method for polar fecal metabolome profiling. *Journal of Chromatography B* 1109, 142-148 (2019).

Sillner, N., Walker, A., Hemmler, D., Bazanella, M., Heinzmann, S. S., Haller, D., & Schmitt-Kopplin, P. Milk-derived Amadori products in feces of formula-fed infants. *Journal of Agricultural and Food Chemistry* 67, 28, 8061-8069 (2019).

Further publications within the framework of the doctoral studies:

Kespohl, M., Vachharajani, N., Luu, M., Harb, H., Pautz, S., Wolff, S., Sillner, N., Walker, A., Schmitt-Kopplin, P., Boettger, T., Renz, H., Offermanns, S., Steinhoff, U. & Visekruna, A. The Microbial Metabolite Butyrate Induces Expression of Th1-Associated Factors in CD4+ T Cells. *Frontiers in Immunology* 8, 1036 (2017).

Riba, A., Hassani, K., Walker, A., van Best, N., von Zeschwitz, D., Anslinger, T., Sillner, N., Rosenhain, S., Eibach, D., Maiga-Ascofaré, O., Rolle-Kampczyk, U., Basic, M., Binz, A., Mocek, S., Sodeik, B., Bauerfeind, R., Mohs, A., Trautwein, C., Kießling, F., May, J., Klingenspor, M., Gremse, F., Schmitt-Kopplin, P., Bleich, A., Torow, N., von Bergen & M., Hornef, M. W. Disturbed bile homeostasis and microbiota composition by intestinal protozoan infection causing metabolic dysregulation and growth impairment. *Submitted for publication*.

Abbreviations

ACN	Acetonitrile
B	Breastfed
BA	Bile acids
bar	SI unit for pressure
CA	Cholic acid
CDCA	Chenodeoxycholic acid
CID	Collision-induced dissociation
δ	Chemical shift
Da	Dalton
<i>db/db</i>	BKS.Cg-dock7 ^m +/- Lepr ^{db} /J
DDA	Data dependent acquisition
EIC	Extracted ion chromatogram
ESI	Electrospray ionization
(+) ESI	Positive electrospray ionization
(-) ESI	Negative electrospray ionization
eV	Electron volt
F-	Formula-fed without probiotics
F+	Formula-fed with probiotics
FruAcLys	<i>N</i> -deoxyfructosylacetyllysine
FruLeulle	<i>N</i> -deoxyfructosylleucylisoleucine
FruLys	ϵ - <i>N</i> -deoxyfructosyllysine
FruMetAla	<i>N</i> -deoxyfructosylmethionylalanine
FT-ICR-MS	Fourier Transform Ion Cyclotron Resonance Mass Spectrometry
GC Gas	Chromatography
GCA	Glycocholic acid
GCDCA	Glycochenodeoxycholic acid
GC-MS	Gas chromatography-mass spectrometry
HILIC	Hydrophilic interaction liquid chromatography
HMDB	Human Metabolome Database
HMO	Human milk oligosaccharide
HPLC	High performance liquid chromatography
LacLeulle	<i>N</i> -deoxylactulosylleucylisoleucine

LacLys	ϵ - <i>N</i> -deoxylactulosyllysine
LC	Liquid Chromatography
LC-MS	Liquid chromatography-mass spectrometry
MeOH	Methanol
mL	Milliliter
mL/min	Milliliter/Minute
MS	Mass Spectrometry
MHz	Megahertz
MS/MS	Tandem mass spectrometry
min	Minutes
<i>m/z</i>	Mass-to-charge ratio
NH ₄ Ac	ammonium acetate
(q)NMR	(quantitative) Nuclear magnetic resonance
OTU	Operational taxonomic unit
ppm	Parts per million
Q-MS	Quadrupole-MS
Q-TOF-MS	Quadrupole Time-of-flight-MS
RP	Reversed phase
rRNA	Ribosomal ribonucleic acid
SCFA	Short-chain fatty acid
T	Tesla
TOF	Time-of-flight
TSP	trimethylsilylpropionate
UHPLC	Ultrahigh-performance liquid chromatography
UHT	Ultra-high temperature
wt	Wildtype

1. General Introduction and Methods

1.1 Metabolomics

The scientific discipline “Metabolomics” and “Metabonomics” were defined by Fiehn and Nicholson (1-3). Metabolomics aims the comprehensive identification and quantification of all metabolites in a biological system (3). The term metabonomics, however, is defined as the quantitative measurement of the metabolic responses of multicellular systems to pathophysiological stimuli or genetic modifications (1, 2).

The metabolome is defined as the sum of all metabolites given in a biological system under particular physiological conditions either secreted by cells or tissues (exometabolome) or within (endometabolome) the cells tissue (2).

At the beginning of every metabolic process genes are transcribed into RNA and translated into proteins and enzymes. The end products or intermediates of enzymatic reactions are defined as metabolites. Therefore, metabolites are the end point of the systems biology cascade and metabolomics is closest of all levels to an observed phenotype (3, 4).

The metabolome is the terminal downstream product of the genome and its composition is the result of complex interactions between the genome, transcriptome, proteome and the environment. Therefore it is a key point in the interpretation of a biological system (5).

Furthermore, metabolites represent the most informative snapshot of the biochemical activity of an organism (6). They have a broad range of biological activities responsible for many cellular functions and regulatory processes, e.g. energy production and storage or signal transfer (7). Metabolomics approaches can be used to study the intrinsic functions of metabolites and how they influence particular phenotypes.

The metabolome of an organism not only consists of endogenous compounds determined by the genome. It is a complex mixture of metabolites from commensal microorganisms, diet and other life-style and environmental factors like drug-intake (Figure 1-1) and reflects the functional output of an organism due to these different stimuli (2).

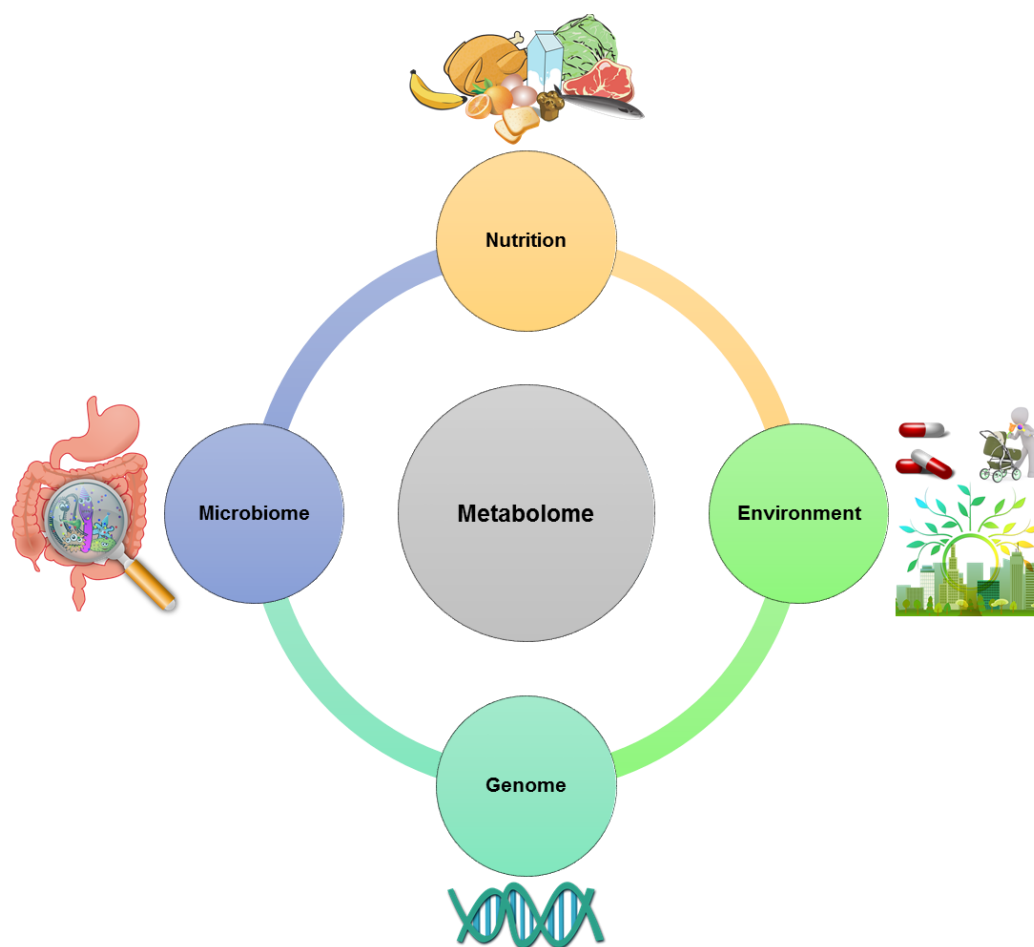


Figure 1-1. Factors shaping the metabolome of an organism or biological sample.

Metabolomics is a fast developing research area in the field of life sciences and complements other -omics techniques such as genomics, transcriptomics and proteomics (8). To date, metabolomics is used to address challenging research objectives including nutrition and food (9-13), microbiome research (14-18), cancer (19) and metabolic diseases (20, 21) and drug discovery (22). Metabolomics is also widely used in plant research (23). In fact, plants have very complex metabolic pathways and produce an enormous number of metabolites. The relative proportions in terms of numbers of publications in the year 2018 including metabolomics and the corresponding research field in the title, keywords, or abstract was determined with the PubMed Central (PMC) database (Figure 1-2).

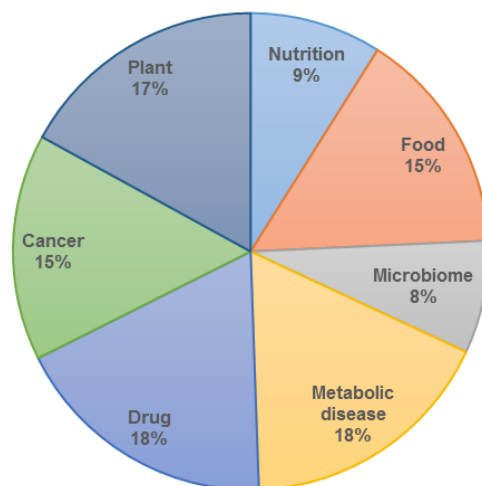


Figure 1-2. Distribution of metabolomics publications in different research areas in 2018. Number of publications were obtained by searching the corresponding keywords (e.g. metabolom* & nutrition) in the PubMed Central (PMC) database for the year 2018. The fractions were calculated by dividing the number obtained from each area by the total number of publications found with the keyword metabolom* (5,430).

The use of metabolomics also has to potential to develop new biomarkers in the medical field (24). For this reason, metabolomics is able to open new research perspectives and will continue to be an evolving discipline in the future.

Metabolomics approaches can be applied to a wide variety of biological samples, e.g. different body fluids (plasma, urine), feces, breath, cells or tissues. The current technologies in metabolomics, especially in the field of high resolution mass spectrometry, are able to detect thousands of metabolites in one sample (25).

However, this aspect gives rise to many challenges in terms of technology, experimental design, data analysis, and data integration (26). By definition, all metabolites in a biological sample are measured within a metabolomics experiment. However, the chemical complexity of metabolites is determined by different polarities and functional groups. For example, sugars are very polar metabolites, whereas fatty acids and lipids are non-polar. Furthermore, the concentration ranges between different metabolite classes or even within specific metabolite classes can be from mg/mL to pg/mL. Therefore, it is almost impossible to study the whole metabolome simultaneously within one experiment (7). In most cases the identity of several metabolites remains unknown. Despite all heterogeneity and diversity in the metabolome, new discoveries can reveal cellular pathways and enhance our understanding of cell metabolism and physiology (6, 27).

1.1.1 Metabolomics in gut microbiota research

The human gastrointestinal tract consists of the oral cavity, esophagus, stomach, small and large intestine (including cecum). These organs are responsible for the digestion of food including carbohydrates, proteins and fats. The colon harbors around 10^{11} bacterial cells/ mL content (28), including around 2,000 different bacterial species (29). The intestinal microbiota is also sometimes described as an additional organ (30). Specific bacteria support our bodies with essential nutrients, such as vitamin B12, through homeostatic symbiosis (31).

The term human microbiome refers to the sum of genomes from living microorganisms in the human being, including bacteria, viruses, archaea and fungi (32, 33). The gut microbiota refers to the microbial community. In mammals, the dominating bacterial phyla in the gut are *Bacteroidetes*, *Firmicutes*, *Actinobacteria* and *Proteobacteria* (34). The intestinal microbiota strongly influences the digestion of food and provides compounds serving as an additional energy source (35). It also plays a role in the development and regulation of the host immune system (36), but it can be also related to specific diseases (37).

Different gastrointestinal disorders, such as inflammatory bowel diseases have been shown to be associated with imbalances in the bacterial communities (38). But also, metabolic disorders like diabetes and obesity, and even neurodegenerative disorders such as Parkinson's disease were found to be influenced by the gut microbiota (39-41). Such imbalances can be influenced by lifestyle factors such as nutrition. For example, the so called Western diet is associated to a less diverse microbiota (39). Conversely, it has been proposed that a healthy condition is associated with a high diversity within the microbial ecosystem. Therefore, the diversity of the microbiota is often in relation with its stability and robustness (42).

Commensals in the gastrointestinal tract produce a variety of different metabolites (43). One of the most investigated compound class are the short chain fatty acids (SCFAs), which are generated by the fermentation of carbohydrates, amino acids and lactic acid in the gut (44). SCFAs have several health-promoting effects. Butyrate is known as major energy source for several colonocytes (45), improves insulin sensitivity (46) and influences the immune system. Physiological intestinal concentrations of SCFAs within the millimolar range are diminishing inflammation-mediated processes. However, depending on its concentration butyrate can also have harmful effects on the mucosal immune system (47). Several studies were

conducted to investigate the impact of different carbohydrates on the SCFA profiles in the gut (48, 49). According to the human fecal metabolome database (HFMDDB) (50), the most abundant small molecules in human feces are the SCFAs acetic acid (36 ± 17 mmol/g wet feces), propionic acid (11 ± 5 mmol/g wet feces), and butyric acid (6 ± 3 mmol/g wet feces) (51). Although SCFAs are highly abundant in feces, they actually represent only approximately 5% of the total SCFAs produced by gut bacteria. The majority of SCFAs are absorbed into the intestinal lumen and utilized for energy production (50).

Another very well-known metabolite class which is influenced by the gut microbiota are bile acids. Bile acids have a steroid structure with several hydroxyl groups and a carboxylic acid side-chain. They can be classified into primary (cholic acid and chenodeoxycholic acid) and secondary bile acids (e.g. deoxycholic acid and lithocholic acid). In the liver, cholesterol is converted by classical, acidic or alternative pathways into the primary bile acids followed by conjugation with taurine or glycine and storage in the gall bladder (52). Fat from diet triggers the release of bile acids from the gall bladder into the small intestine where they promote the absorption of lipophilic dietary (53). Indeed, bile acids play an important role in the modulation of lipid, glucose and energy metabolism and cell signaling (54). Bile acids are reabsorbed by enterohepatic circulation in the small intestine. Only a small percentage of 5% escapes into the colon. Here, bacteria convert primary bile acids into secondary bile acids by deconjugation, dehydroxylation or epimerization enzymatic reactions. Bacteria convert primary bile acids into secondary bile acids. By this, the gut microbiota influences the levels and types of bile acids produced and excreted in feces (55, 56). The daily synthesis of bile acids in the liver is about 200 – 600 mg, of which almost the same amount is excreted in feces, i.e. 5% of the total bile acid pool (~ 3 g) (54).

Species mainly involved in the generation of secondary bile acids are *Bacteroides*, *Eubacterium*, *Clostridium* and *Escherichia coli* (57, 58). Also *Bifidobacterium*, *Ruminococcus* and *Lactobacillus* are known to be involved in the bile acid metabolism (56). Some secondary bile acids are considered toxic and influence the microbial communities (50, 59). The hydrolysis of the C24 N-acyl amide bond of conjugated bile acids is catalyzed by bile salt hydrolases. Bile salt hydrolase genes have been detected for example in *Bacteroides fragilis*, *Bacteroides vulgatus*, *Clostridium perfringens*, *Listeria monocytogenes*, and several species of *Lactobacillus* and *Bifidobacterium*. Deconjugation improves the bacterial

colonization of the gastrointestinal tract. After deconjugation, 7 α -dehydroxylation of the primary bile acids is performed mostly by *Clostridium* and *Eubacterium* species (Firmicutes phylum), resulting in deoxycholic acid and lithocholic acid. Furthermore, oxidation and epimerization reactions of 3-, 7- and 12-hydroxy groups to -oxo groups are catalyzed by bacterial bile acid hydroxysteroid dehydrogenases. Most members of Firmicutes possess 3-, and 12-hydroxysteroid dehydrogenases. Whereas, 7 α -hydroxysteroid dehydrogenases are widespread among members of the genera *Clostridium*, *Eubacterium*, *Bacteroides* and *Escherichia*, and 7 β -HSDHs have been detected only in Firmicutes (60).

Also phenolic compounds like phenylacetic acid, and m- and p-hydroxyphenylpropionic acid are of bacterial origin and are fermentation products of proteins (61, 62). It was reported that, e.g. bifidobacteria, are able to produce phenyllactic, 4-hydroxyphenyllactic (63, 64) and indolelactic acid (65) out of the aromatic amino acids phenylalanine, tyrosine and tryptophan, respectively. The degradation of polyphenols and fiber to benzoic acid can be seen in excretion of hippuric acid in urine. Furthermore, peptidoglycans, lipopolysaccharides and possibly other microbiota-derived metabolites act as signaling molecules and can affect inflammation processes (66).

The gut microbiota also generates specific lipids. Recently, sulfonolipids were identified in murine cecum produced by the bacterial genera *Alistipes* and *Odoribacter*. This unusual class of sphingolipids was significantly increased in mice fed with high-fat diets. However, their biological functions are yet unknown (14).

To what extent microbiota-derived products affect the host are only partly understood. The analysis of the metabolome in a complex host - microbiome system related to health or disease is sometimes called meta-metabolomics (33).

To investigate the metabolome in relation to the gut microbiota different types of samples can be used. Besides plasma, the luminal content of the small intestine, cecum and colon or the organ tissue itself is used for analysis in animal model studies. However, spatial variation of gut luminal metabolites has to be considered. This was shown to be directly linked to microbial breakdown of carbohydrates and proteins in the cecum and reabsorption processes in the colon in mice (67).

Non-invasive specimen which can be collected to investigate the impact of the gut microbiota on the metabolome are feces and urine. Indeed, the number of metabolomics studies using intestinal matrices is smaller compared to urine and plasma studies. Maybe this is the case because plasma and urine are established matrices in clinical practice. Since they are fluids they are also easier to handle,

compared to fecal samples. However, the advantage of using feces for microbiome related studies is that the dry matter consists of 25 – 54% bacterial biomass, therefore the percentage of analyzed metabolites with bacterial origin is relatively high (50). Furthermore, the same fecal sample used for 16S rRNA sequencing, metagenome, metatranscriptome and metaproteome analysis can be used for metabolomics analysis (13, 18, 38, 68). By this, an integrative approach that includes microbiome sequencing and comprehensive fecal metabolite analysis is a method of choice. Besides bacterial biomass, feces consists of exfoliated colonic epithelial cells, undigested food residues, macromolecules (e.g. fiber, protein, DNA, polysaccharides) and thousands of small molecules such as sugars, organic acids, and amino acids. Hence, stool contains a variety of molecules that reflect the result of nutrient digestion and absorption by both gut bacteria and the gastrointestinal tract (50).

In addition, hundreds of bio-transformed metabolites such as glycoside and sulfate conjugates can be found in feces, depending on diet and exposure to xenobiotics. In this field there is still the need for systematic identification of these compounds (50).

For these reasons, there is an increasing interest in analyzing the human fecal metabolome to investigate interactions with resident microbes within the gut (16, 50, 69). Indeed, human stool is one of the most complex sample types analyzed in the field of metabolomics (69). The complexity associated with human fecal samples originates from a variety of fluctuating influences and sources. The molecules in the gut originate from ingested, absorbed or inhaled materials such as food and smoke, personal care and hygiene products or anything that humans are exposed to in their environment and daily life. But also metabolites from the human host itself and especially from its microbiota. In animal models the diet and environment can be controlled and standardized therefore, which makes the diversity of the fecal metabolome less complex and more predictable (69).

Despite the fact that fecal metabolomics studies become more popular, the methods for collecting, extracting and analyzing fecal samples are still far from being standardized (16, 50). One of the first metabolomics studies of human feces used headspace gas chromatography coupled to mass spectrometry (GC-MS) to compare volatile organic compounds in patients with infectious gastroenteritis versus healthy controls (70). However, most of the fecal metabolites are non-volatile (50). In the first fecal metabolomics analysis of non-volatiles metabolic profiles between patients with inflammatory bowel disease (IBD) and healthy

controls were compared using nuclear magnetic resonance (NMR) spectroscopy (71).

The increased interest and understanding of the role of the gut microbiome in health and disease resulted in rising numbers of fecal metabolomics studies using advanced analytical technologies with the goal to understand the chemical environment of the gut microbiome (50).

1.1.2 Nutritional metabolomics

The application of metabolomics in nutrition research has become popular in recent years. Metabolomics is very well suited to study the impact of food on our health due to the close interplay between dietary components and human metabolic pathways. Nutritional metabolomics can be used to 1) identify new dietary biomarkers, 2) understand the role of the diet in intervention studies, 3) study diet-related diseases and 4) precision nutrition. (9)

Assessment of food intake is normally done by the use of questionnaires, diaries, or interviews. However, the problem with this kind of assessments is the high tendency of errors and incompleteness due to their subjective nature. These problems could be significantly improved by the use of qualitative nutrition markers. Thus, one of the goals of nutritional metabolomics is the identification and validation of such markers to improve their use for quantitative assessment of recent or more long-term food intake (72). A number of putative nutrition markers were already successfully identified using metabolomics approaches (11, 12). In the future, metabolomics will continue to play a key role in the validation of such markers (9).

Nutrition markers could be used to characterize individual and population dietary habits in order to draw conclusions on the impact of diet and lifestyle on healthy living and prevention of disease. By defining certain nutrition patterns in specimen from individuals or populations a correlation to metadata of e.g. body mass index or medical information could be performed and a linkage of diet and lifestyle behavior to disease prevention and promotion can be facilitated. Nutrition-derived biomarkers can then to be monitored and related to their expected biological effects (73).

Diet plays a significant role in health and disease (74), and can be considered as part of the so called exposome, the totality of exposure individuals experience

throughout their lives (75). An imbalanced diet is associated with different diseases like obesity, diabetes or inflammatory diseases (76). However, to elucidate the reasons and underlying mechanisms of these associations it is necessary to know the molecular composition of food itself, which includes heterogeneous plant- and animal-based nutrients (74, 77). In line with this, metabolomics approaches are currently widely used to investigate different food metabolomes. By this, associations of food components with physiological responses can be made. Metabolomics allows the detection of thousands of chemical entities present in foods and beverages. By this, much more compounds than the classical nutrients, like carbohydrates, lipids and proteins, can be investigated (77).

Nowadays, the interest of the western society is less focusing on sufficient nutrition to avoid diseases and more focusing towards optimizing overall health by the consumption of healthy and so-called functional food (74, 77). Certain dietary patterns can potentially reduce the risk of various diseases, such as cancer, cardiovascular disease, or Alzheimer's disease. Consumption of high levels of antioxidants, for example by eating fruits and vegetables, reduces the risk of cancer (76). However, it has to be noticed that an exceeding intake of supplementations enriched with natural antioxidants, vitamins and phytochemicals could also have harmful effects This can be true even for essential nutrients (76). The interaction of dietary components with the host metabolism is complex (77). The metabolites deriving from food can interact with genes, proteins, enzymes and microenvironment of an organism. An important function of nutrients is anabolism. They serve as building blocks for macromolecules like DNA, polysaccharides, proteins and cell membranes. For example, the fat composition of the diet influences the physical and chemical properties of lipid membranes in animals. Furthermore, dietary metabolites serve as an energy source, participate in cell signaling mechanisms and modulate enzyme activities (77). Essential nutrients required for homeostasis of an organism can be called core nutritional metabolome (74, 77).

Another part of the plant-based food metabolome consists of phytochemicals. Some of these plant metabolites are bioactive. Several of those bioactive compounds play a beneficial role in the prevention of diseases, for example by having anti-oxidative or detoxifying properties (74, 77, 78). By analyzing the food metabolome, also compounds of non-natural origin can be detected, such as herbicides, insecticides and fungicides. These contaminants enter the human body through diet and by this and become part of the host metabolome.

The individual dietary behavior contributes to an individual metabolome. The knowledge provided from nutritional metabolomics has the potential to develop personalized dietary treatments (78). The individual nutritional phenotype may predict a certain response of a subject to interventions and the extent to which the health status might be affected. The identification of individual variations in response to dietary interventions contributes to the development of personalized nutrition. The aim of personalized nutrition is to meet nutritional needs of individual patients for the purpose of decreasing the risk of a disease and achieving overall wellness (77). Recently, it was demonstrated that personalizing dietary advice improved the dietary habits of individuals compared with receiving general healthy eating guidelines (79). An example of where metabolomics has discovered individual responses to dietary interventions is a three-month vitamin D and calcium intervention study, where individual metabolic profiles could predict the response to the intervention. Response to the intervention was for example defined by changes in the parathyroid hormone (80). The use of such individual profiles to personalize nutritional strategies would enhance success of food recommendations (9).

In nutritional metabolomics, it is also important to evaluate the role of gut bacteria in the processing of nutrition-derived molecules. The role of the gut microbiota is emerging as an important potential player in the onset of diet-related diseases (9). With metabolomics alterations in metabolites that originate from microbial co-metabolism can be identified and associated to alterations in the gut microbial community (16, 43, 81).

However, the differentiation between nutritional, microbial and host-derived metabolites is often not possible and remains to be a challenge in metabolomics studies. Following ingestion, the food components are either metabolized in the gastrointestinal tract by enterocytes and commensal bacteria or excreted in an intact form (77). Indeed, the main modulator of the gut microbiota composition is diet. Specific nutrients promote the growth of certain microorganisms, while others are not able to grow under these conditions. Conversely, the resulting microbial phenotypes influence the composition of the host metabolome. Depending on the type of bacteria the microbial metabolites may exhibit beneficial or harmful properties to the host.

After absorption in the gut, dietary metabolites are transported to the liver followed further metabolized and transported through the blood stream to different tissues of the body. In order to fully understand the effects of diet on the host and its

microbiome a holistic view is required by screening metabolites in various specimens, like feces, plasma, urine or organ tissue. Metabolomics provides snapshots of the nutritional status, which, together with the genotype and microenvironment, define metabolic phenotypes that can remain constant for long periods (76).

Furthermore, nutritional metabolomics generates big datasets which opens the door to a new age of research. The integration of metabolomics with genomics, transcriptomics, and proteomics data and the use of bioinformatics (multiomics approach), for example recently performed to study the impact of dietary resistant starch on the human gut microbiome, metaproteome, and metabolome (68), could enable a precise determination of the nutritional status of individuals and populations or prediction of responses to dietary interventions (78).

1.1.3 Metabolomics to study the impact of diet on developing infants

Environmental exposures in early life, for example nutrition, mode of delivery and the use of antibiotics can impact health in later life. Perturbations during the development phase have been associated, e.g. with an increased possibility of developing allergies, asthma and even metabolic syndrome in later life (82, 83). To understand these effects a variety of pediatric studies were conducted, including also metabolomics approaches. Metabolic profiling can be used to characterize the physiological processes during infant development on a molecular level.

Infant nutrition is closely linked to the gut microbiota which plays a vital role in infant development (13, 84). Abnormal patterns of gut microbiota have been linked to sepsis (85) and necrotizing enterocolitis (86), which are two causes of morbidity and mortality in preterm infants. Furthermore, also the development of colic (87), allergic disease (88), and obesity (89) has been associated with the gut microbiota of infants.

The microbiota from exclusively breast-fed infants is dominated by bifidobacteria, whereas the gut of formula-fed infants also settled by other bacterial species, including *E. coli*, *Clostridia*, *Bacteroides*, and *Lactobacilli* (13, 90, 91). The number of studies regarding the effect of diet on infant fecal microbiota and health is relatively high compared to the number of publications studying the influence of diet on the infant fecal metabolome (84).

However, the intestinal microbiota and thus the metabolite profile of fecal samples of infants fed with breast milk differ significantly from the formula fed ones (84). The human milk oligosaccharides (HMOs) in breast milk enable the settlement and the survival of bifidobacteria species in the gut (92). In turn, bifidobacteria influence the composition of the fecal metabolome. In contrast, the more diverse bacterial species in formula-fed infants contribute to a fecal metabolome, which is different compared to breastfed infants (13, 84).

Breast milk is the gold standard for infant nutrition. It contains the appropriate composition of macro- and micronutrients and bioactive compounds, promoting the development of the immune system (93, 94). Infant formula is an alternative nutrition for infants used as sole food or for supplementation. Most infant formula are cow milk based and are supplemented with various micronutrients, like vitamins and polyunsaturated fatty acids. In recent years, also research in the field of probiotics vastly increased.

Chow *et al.* investigated the fecal metabolite profiles of healthy, breast- and formula-fed infants before and during *in vitro* batch culture fermentation (84). An increase of human milk oligosaccharides (HMOs) and other metabolites (e.g. hydroxyphenyllactate, lactate and taurocholic acid sulfate) was detected in the batch culture of breastfed infants. On the contrary, the metabolite profiles of cultures from formula-fed infants had significantly higher amounts of tocopherols, saturated and unsaturated fatty acids and bile acids (84).

Recently, a trial was conducted to study the impact of early-life intervention with bifidobacteria on the healthy infant fecal microbiota and metabolome (13). Also in this study, significant differences in microbiota and metabolites were detected between breast- and formula-fed infants and between infants birthed vaginally or by cesarean delivery. Targeted measurements of the SCFAs profiles were performed and described higher concentrations of propionate, butyrate, valerate and isovalerate in feces of formula-fed infants. Whereas pyruvic and lactic acid were detected at significantly higher concentrations in breastfed infants. The effect of probiotics on the metabolite composition was negligible (13). Samples from the same study were also used in this thesis with the aim to investigate the differences between the nutrition-related polar metabolomes using a non-targeted HILIC UHPLC-MS approach (Chapter 4).

Furthermore, the introduction of solid food changes the gut microbiota composition towards an adult-like microbiota, and thus plays a significant role in the development of infants. For example, the increasing amount complex

carbohydrates play an important role in the microbial production of SCFAs (92), which was also shown by Bazanella *et al.* with increasing concentrations of propionic, butyric, isovaleric, and valeric acid in feces during the first year of life, independent of breast or formula feeding (13).

1.1.4 Maillard reaction products in infant formula

The Maillard reaction describes a reaction between reducing sugars (or more generally carbonyl compounds) and amino compounds, such as amino acids, peptides or proteins. First, spontaneous condensation between the carbonyl and amino group forms an *N*-glycosylamine, which rearranges into a so called Amadori product (1-amino-1-deoxy-2-ketose structure) via enolization. Amadori products undergo further reactions, especially under heat conditions. Their breakdown initiates a multitude of chemical reactions, which continuously produce new intermediates and reaction products. The sum of these products are called (advanced) Maillard reaction products. (95)

Also in infant formula a variety of Maillard reaction products can be found. To ensure microbiological safety, infant formulas undergo extensive heat treatment, which strongly enhances the Maillard reaction. The high amounts of lactose promote the glycation of milk proteins (lactosylation) yielding the Amadori products. Furthermore, advanced glycation end products (e.g. carboxymethyllysine), sugar degradation products, and protein or lipid oxidation products are formed. In fact, 5 – 20% of the protein-bound lysine in infant formula is lactosylated (96). However, the nutritional consequences for formula-fed infants are not completely understood.

The loss of essential amino acid lysine is generally compensated by high protein concentrations in infant formula (97). However, a high protein concentration in infant formulas has been related to negative health effects such as a risk for obesity, therefore must be handled with care (98).

The metabolism of dietary glycation compounds is little investigated, however, low bioavailability or rapid elimination is suggested (96). Moreover, gut microbial degradation of the Amadori product fructosyllysine by specific bacterial strains is possible (99-101). Whether formula-derived Maillard reaction products influence the composition of the infant's gut microbiota is unknown. Further studies dealing with the nutritional consequences of Maillard reaction products are necessary,

since infant formula represent the sole food intake for many infants during the first months of life (96).

1.2 Analytical methods in metabolomics

Mostly two techniques are used for metabolomics: nuclear magnetic resonance (NMR) spectroscopy and mass spectrometry (MS). However, nowadays MS techniques are dominating (9, 102). Data can be acquired in a non-targeted approach, where as many metabolites as possible are measured, or in a targeted approach, where a list of predefined metabolites are measured (9). Each technology has a number of advantages and disadvantages.

The advantages of NMR-based metabolomics is a robust and reproducible analysis and minimal sample preparation, thus allowing relatively high-throughput analysis [6]. This reproducibility is very beneficial for epidemiology studies with large sample sizes. Furthermore, NMR is a non-destructive technique and thus the sample can be used for further experiments after its measurement. Furthermore, NMR spectroscopy provides structural and quantitative information. Structure elucidation is especially needed for the identification of unknown metabolites, a major bottleneck in metabolomics. The major disadvantage of NMR-based metabolomics is the lack of sensitivity. Therefore, only the most abundant metabolites in a biological sample can be detected and analyzed. (9)

MS-based techniques are very sensitive and enable the detection of a broad spectrum of metabolites (103). It is possible to inject the sample directly into the MS system. This is often done in Fourier transform-ion cyclotron resonance mass spectrometry (FT-ICR-MS) experiments, to achieve ultra-high resolving power up to 1,000,000 and a high mass accuracy (< 0.2 ppm). By this, concrete molecular formulas can be assigned to the detected mass signals, supported by isotopic fine structure elucidation, enabling the investigation of the molecular and elemental composition of a sample (104).

However, commonly MS is coupled to chromatography. Chromatographic separation of analytes prior MS detection has important advantages. Isomeric and isobaric compounds are separated from each other and an additional orthogonal property, i.e. retention time, is gained, which enables identification of metabolites. Furthermore, matrix effects and ionization suppressions are reduced due to prior separation of the complex mixtures of molecules in a biological sample. The most common approaches are gas-chromatography (GC) and liquid chromatography (LC). GC-MS is commonly used for the detection of fatty acids and a range of polar metabolites such as amino acids and glycolysis intermediates (9).

The disadvantage of GC-MS is the elaborating sample preparation (derivatization) to make the metabolites volatile prior analysis. For LC-MS, the sample preparation is less extensive and it enables the analysis of a broad range of metabolites, from high to low polarity, depending on the applied column chemistry. Drawbacks of chromatography coupled MS techniques are, that they usually need longer measurement times and the two-dimensionality makes data analysis more complex.

In general, MS-based approaches are less reproducible compared to NMR-based metabolomics, making the analysis of large sample sets challenging. The chemical diversity and range of metabolites in biological samples makes it impossible to measure the whole metabolome using only one technique. The current trend is to use multiple technology platforms in order to achieve maximum coverage of metabolites. (9)

1.2.1 Non-targeted vs. targeted metabolomics

The variety of chemical and physical properties of metabolites and the dynamic range of concentrations across large orders of magnitude makes it necessary to apply an array of different analytical techniques in metabolomics research (5). MS-based metabolomics can be performed in a profiling mode with no prior selection of metabolites, so called non-targeted metabolomics, or in a targeted mode, where specific metabolites or metabolite classes selected prior measurement (5, 9, 69). A schematic overview of the main characteristics of non-targeted and targeted metabolomics is illustrated in Figure 1-3.

The starting point for many metabolomics studies is the non-targeted approach (9). Non-targeted metabolomics is hypothesis generating and used for investigation of metabolites without prior limitations. This unbiased view on the metabolome enables the discovery of novel molecules and pathways or alterations of metabolites in relation to biological interventions or diseases, which were not expected beforehand (1, 5, 69).

Challenges of this approach are the extensive data processing steps and difficulties in identifying unknown metabolites. Different chemometric approaches, such as feature selection and appropriate multivariate statistics, are needed to handle the large datasets generated to get biological meaningful data. These features then require annotation using chemical or biological databases and further

analytical experiments for subsequent identification (5). In fact, on average only 2% of the features from non-targeted LC-MS experiments have been annotated due to limitations in existing public reference data sets (69).

Targeted metabolomics is hypothesis driven and is usually applied, if particular metabolites are expected to be altered in the context of a specific research question. Targeted metabolomics often includes the accurate quantification of the metabolites of interest. For absolute quantification external and labelled internal reference standards are needed (9). By this, the identity of the metabolites can be ensured and analytical variations are drastically reduced. The sample preparation can be specifically optimized for the metabolites of interest. Compared to full scan MS mode, targeted MS methods tend to be more sensitive, because of the types of mass spectrometers used (e.g. triple quadrupoles and ion traps) (69). Moreover, targeted metabolomics has the advantage of comprehensive understanding of a vast array of metabolic processes, enzyme kinetics and established biochemical pathways. Furthermore, novel associations between metabolites may be illuminated in the context of specific physiological states. (5)

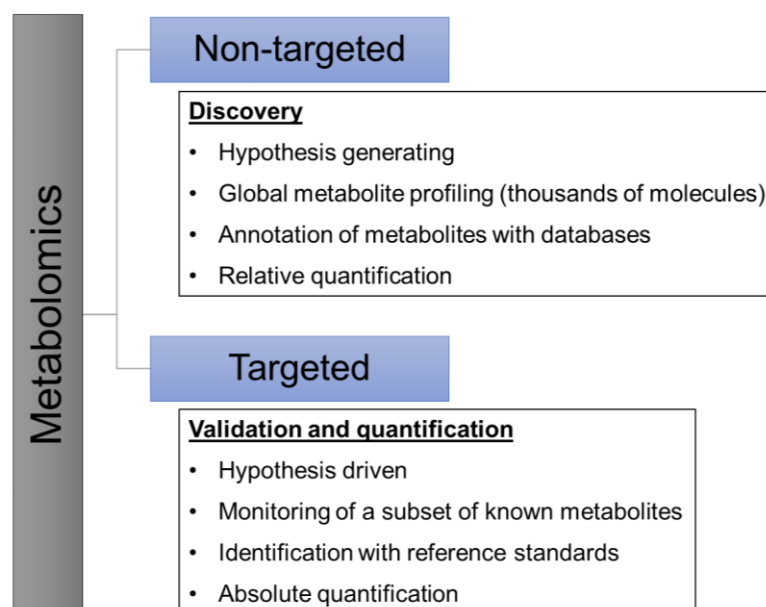


Figure 1-3. Schematic overview and principles of non-targeted and targeted metabolomics.

1.2.2 Liquid chromatography

Nowadays, liquid chromatography coupled to mass spectrometry (LC-MS) is the most frequently used analytical technique in metabolomics. The chromatographic instruments used for this are mostly HPLC or UHPLC ((ultra)high-performance liquid chromatography). Both of them perform well in terms of sensitivity, selectivity and their ability to separate non-volatile and thermal instable compounds. However, UHPLC has the advantage of higher resolution and shorter analysis times ([105](#), [106](#)). LC is a separation method based on the interaction of the analyte with a stationary and a mobile phase. The analytes are carried through the chromatographic column using a liquid mobile phase. During the chromatographic run, many equilibria are generated by the distribution of the analytes between the stationary and the mobile phase. Examples for interactions are hydrogen-bridging, dipole-dipole or ion-dipole interactions, van-der-Waals-forces and hydrophobic interactions ([107](#)). Due to these different interactions, the analytes of the sample elute separated in time.

Most frequently, non-polar stationary phases and polar mobile phases for elution of the analytes are used, which is called reversed-phase (RP) LC. The RP stationary phases are usually based on silica gel and functionalized with unpolar organic residues such as C8 and C18 alkyl chains. The commonly used mobile phases are mixtures of water, methanol or acetonitrile, and additives like formic/ acetic acid and ammonium formate/ acetate. In a RP-LC experiment the polar analytes are not well retained on the column whereas non-polar analytes interact stronger with the stationary phase, resulting in higher retention time values.

However, in the field of metabolomics also the analysis of polar compounds is crucial, since the metabolome consists of many different molecules with a wide range of polarities. In hydrophilic interaction liquid chromatography (HILIC) a combination of hydrophilic stationary phases and organic mobile phases are used ([108](#)). A HILIC gradient mode starts with a high amount of the organic solvent and then increasing the percentage of aqueous solvent over time. HILIC provides a wide range of different retention mechanisms and column selectivities. The stationary phases can be classified in charged (e.g. unbonded silica), neutral (e.g. amide) and zwitterionic phases based on the characteristic of the functional group ([109](#)). In this thesis, candidates from all three types of HILIC columns were used for the comparative analysis of fecal metabolites and a set of 150 metabolites (Chapter 3). The chemical characteristics of the investigated stationary phases are shown in Figure 1-4.

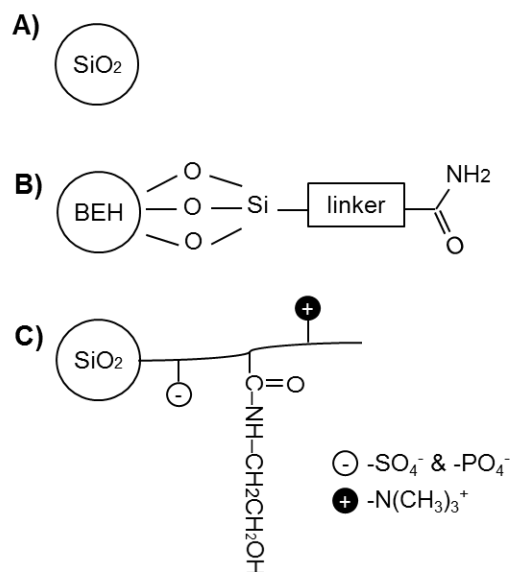


Figure 1-4. Schematic structures of HILIC stationary phases. (A) Unbonded silica, (B) BEH (Ethylene Bridged Hybrid) amide (Waters, ACQUITY UPLC™, Eschborn, Germany), (C) zwitterionic phase (iHILIC®-Fusion, HILICON AB, Umea, Sweden).

Due to the polar stationary phase and a high organic mobile phase, a water-enriched layer is built up on the surface of the stationary phase. The thickness of the water layer depends on the mobile phase composition and the functional groups of the stationary phase. One of the retention mechanisms in HILIC is based on the partitioning of the analytes the mobile phase and the water layer on the surface of the stationary phase. The more hydrophilic an analyte is, the more it is distributed to the water layer, the longer the retention time. Elution of these polar analytes is achieved with an increasing water proportion in the mobile phase (109). Additionally, hydrogen bonding or dipole-dipole interactions can occur. Another retention mechanism in HILIC are electrostatic interactions, especially when charged or zwitterionic stationary phases are used. Depending on the pH value of the mobile phase, the stationary phase and the analytes can be charged. Attraction between of the stationary phase and the analyte occurs if they are contrary charged and repulsion occurs by having the same charge.

Additives are added to control the pH value and the ionic strength of the mobile phase. Buffer salts can decrease or increase electrostatic interactions and therefore influence the retention and peak shapes of the analytes (107, 108, 110).

1.2.3 Mass spectrometry

A mass spectrometer (MS) measures mass-to-charge ratios (m/z) of ions (111). A mass spectrometer consists of three basic components: an ion source, a mass analyzer and a detector for ions. Electrospray ionization (ESI) is the most commonly used ion source, serving as an interface between LC and MS. ESI is a soft ionization technique, as the ionic analytes, dissolved in a solvent, get evaporated at atmospheric pressure. This technique is suitable for molecules with medium to high molecular weights, non-volatile and easily ionizable compounds, including a wide range of polar, unpolar and ionic compounds (112). MS enables sensitive analysis of complex biological samples, and therefore, it is the most common technique in metabolomics. There is a broad spectrum of different mass analyzers ranging from low to high resolution, including ion trap, quadrupole, Time-of-flight (TOF), orbitrap and Fourier transform ion cyclotron resonance (FT-ICR) mass analyzer systems (113). In this thesis, ion trap-, TOF- and FT-ICR-MS systems were used for metabolomics studies.

1.2.3.1 Ion trap mass spectrometry

In an ion trap mass analyzer ions are trapped and stored in an oscillating electric field. The mass spectrum is acquired by ejecting the ions according to their m/z values. Furthermore, stored ions can be selected for fragmentation experiments. The principle of an ion trap is similar to a quadrupole but with different geometry. The ion trap is made up of one ring electrode and two ellipsoid caps at the top and the bottom. Ions generated by an ESI source enter the trap through one of the end-cap electrodes. For trapping the ions in the space between the electrodes, an electric field is generated by applying an oscillating alternating voltage together with a static direct voltage (114, 115). A scheme of an ion trap mass spectrometer, which was used in this thesis (Chapter 2) is shown in Figure 1-5.

The advantage in comparison to a quadrupole is the possibility to store ions of different m/z values inside the trap at the same time. To avoid ion losses by repulsion, because of the same charge of the ions, helium gas is added to remove excess energy from the ions through collisions. Helium gas can also be used for fragmentation experiments. One method for the ejection of ions to acquire the mass spectrum, is the mass selective instability scan. With increasing radio frequency voltage, the trajectory of ions with low m/z values get unstable and are

ejected through the end-cap to reach the detector. With further increase of the radio frequency voltage, the trajectory of ions with higher m/z values get unstable and they are ejected. The maximum number of ions that can be stored in an ion trap is limited due to space-charge effects. Space-charge effects occur due to repulsion of ions with the same charge.

Ion traps have the possibility to perform multistage fragmentation experiments (MS_n). For fragmentation of a certain ion, only the selected m/z ratios are stored inside the trap. After the fragmentation process, MS/MS spectra are detected using an instability scan. To perform further fragmentation experiments (MS₃), a MS/MS-fragment ion is selected, the other ions are ejected and the fragment ion is fragmented again. (114, 115)

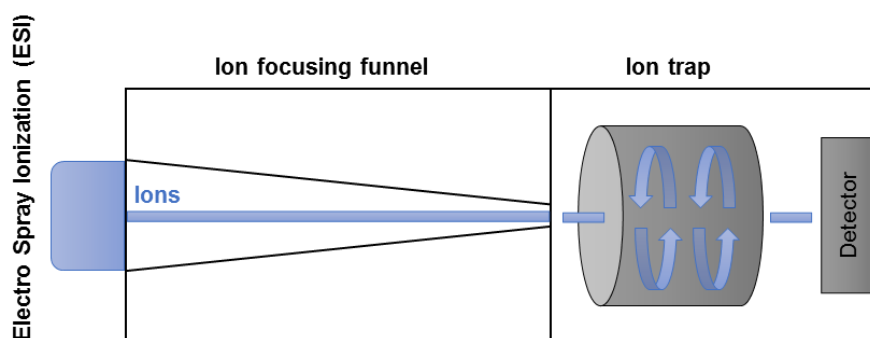


Figure 1-5. Scheme of an iontrap MS (adapted from amaZon ETD user manual, Bruker Daltonics GmbH).

1.2.3.2 Time-of-flight mass spectrometry

Time-of-flight (TOF) mass spectrometers belong to the class of high resolution mass spectrometers. TOF instruments deliver a resolving power of up to 60,000 and a mass accuracy < 5 ppm and are therefore often used in non-targeted metabolomics (25).

A TOF-MS system consists of an ion source (e.g. ESI), ion focusing funnels, a quadrupole as mass filter, followed by a quadrupole as collision cell and the TOF mass analyzer. A scheme of an orthogonal hybrid quadrupole TOF-MS (QTOF-MS), which was used in this thesis, is illustrated in Figure 1-6. The principle of the TOF mass analyzer is the separation of ions with different m/z values due to

different flight times. The smaller the m/z value of an ion, the shorter its flight time through the TOF tube and the earlier its detection. Inside the TOF tube, the accelerator is responsible for pushing the incoming ions orthogonally to the reflector. Here, also the determination of the m/z values takes place by measuring the drift time of the ions after the acceleration until their contact onto the detector unit. The reflector is responsible for compensation of different kinetic energies from ions with the same mass, which leads to a correction of the time of flight and increases the resolving power (115). The detector converts the ion signals into electrical signals, resulting in a mass spectrum.

In a QTOF system, the first quadrupole (Q1) serves as a mass filter and allows the selection of single m/z values or m/z ranges. The second quadrupole is called collision cell (Q2) and can be used in different modes. If a full scan mode MS experiment is performed, the collision cell serves as a further transfer unit, leading the ions into the TOF analyzer. Apart from that, the collision cell can be used for fragmentation (MS/MS) experiments by using collision-induced dissociation (CID) with nitrogen gas.

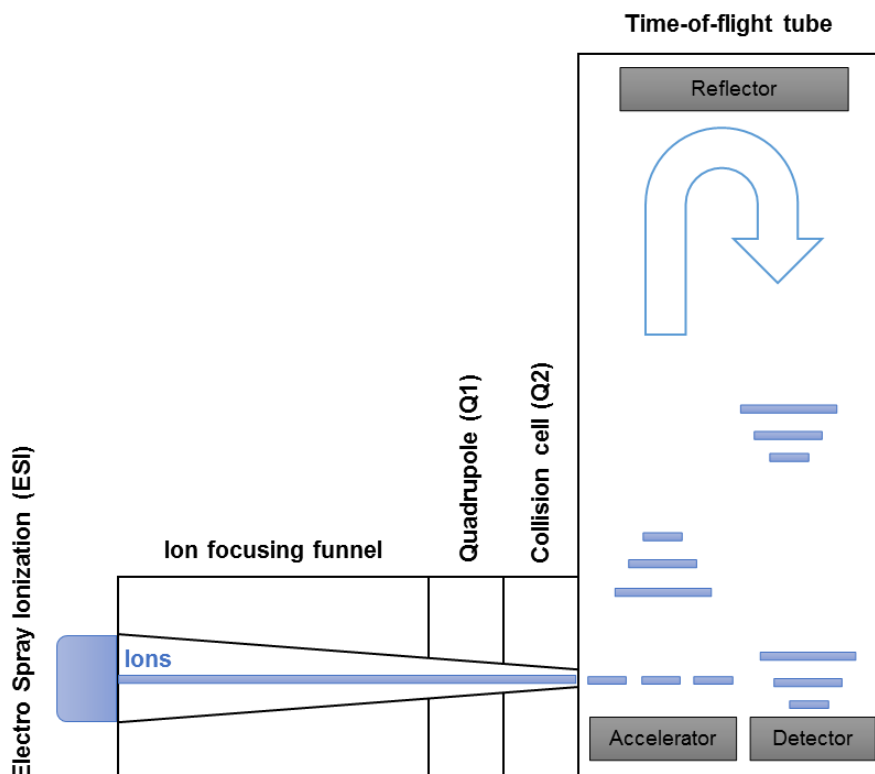


Figure 1-6. Scheme of an orthogonal hybrid QTOF-MS (adapted from maXis™ user manual version 1.1, Bruker Daltonics GmbH).

1.3 Thesis structure and objectives

The aim of this thesis was to develop and optimize analytical methods for metabolomics, using diverse types of liquid chromatographic approaches coupled to different mass spectrometers, to investigate microbial and nutritional metabolites.

The outline of this thesis is summarized in Figure 1-7.

In chapter 2, a targeted metabolomics approach for quantification of 45 bile acids (primary and secondary) in cecum samples is described. UHPLC settings were optimized and the method was validated in terms of accuracy, precision, carry-over and matrix effects. Furthermore, the method was applied to investigate the impact of metformin on the cecal bile acid profiles of wild type and diabetic mice.

Next, a detailed examination of the performance of different types of HILIC columns in dependency of pH values and salt gradient concentrations was performed (Chapter 3). Here, the goal was to develop a convincing method for non-targeted metabolomics of stool samples. To achieve this, a set of 150 metabolite standards and a pooled feces sample was analyzed in terms of detected features, the ability to separate isomers, precision of the analysis, and retention time distribution of metabolites across all chromatographic runs.

Finally, the most suitable non-targeted HILIC method and FT-ICR-MS was applied to screen for differences in the fecal metabolomes of breast- and formula-fed infants (Chapter 4). Four significant markers for the formula-fed fecal metabolome were found and identified as specific Amadori products, originating from infant formula protein glycation by using subsequent targeted metabolomics approaches. The described compounds could serve as nutrition markers for formula feeding in feces of infants.

The appendix contains the original publications of Chapter 2 and 3, and the corresponding supplementary information of Chapter 2 – 4.

Overall, it was demonstrated, that extrinsic factors like drug-intake and diet influence microbial and nutrition-derived metabolite profiles in gut-related samples of mice and humans (cecum and feces). These results were gained by applying different kinds of analytical approaches with main focus on LC-MS techniques.

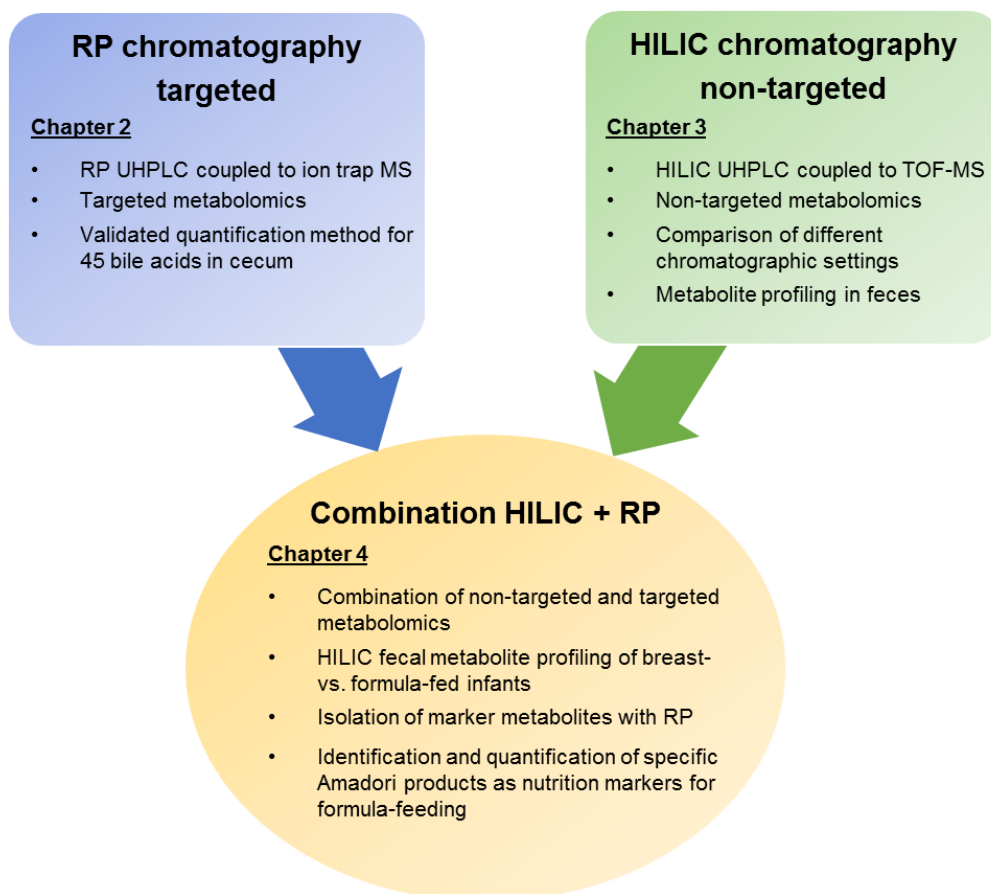


Figure 1-7. Outline of the chapters included in the thesis.

2. Metformin impacts cecal bile acid profiles in mice

Abstract

Bile acids (BAs) are major components of bile synthesized from cholesterol and take part in the digestion of dietary lipids, as well as having signaling functions. They undergo extensive microbial metabolism inside the gastrointestinal tract. Here, we present a method of ultra-high pressure liquid chromatography coupled to ion trap mass spectrometry for quantification of 45 BAs in mouse cecum. The system was validated in regard to sensitivity with limits of detection and quantification (0.6 – 24.9 nM), interday accuracy (102.4%), interday precision (15.2%), recovery rate (74.7%), matrix effect (98.2%) and carry-over effect (< 1.1%). Afterwards, we applied our method to investigate the effect of metformin on BA profiles. Diabetic mice were treated with metformin for 1 day or 14 days. One day of treatment resulted in a significant increase of total BA concentration (2.7-fold increase; *db/db* metformin 5.32 $\mu\text{mol/g}$, *db/db* control mice 1.95 $\mu\text{mol/g}$), most notable in levels of 7-oxodeoxycholic, 3-dehydrocholic and cholic acid. We observed only minor impact on BA metabolism after 14 days of metformin treatment, compared to the single treatment. Furthermore, healthy wild type mice had elevated concentrations of allocholic and ω -muricholic acid compared to diabetic mice. Our method proved the applicability of profiling BAs in cecum to investigate intestinal BA metabolism in diabetes and pharmacological applications.

This chapter was published as Nina Sillner, Alesia Walker, Wendelin Koch, Michael Witting, Philippe Schmitt-Kopplin. Metformin impacts cecal bile acid profiles in mice. *Journal of Chromatography B*, 1083, 35–43, Copyright Elsevier (2018).

Candidate's contributions: Nina Sillner designed the targeted metabolomics research, performed the analytical experiments for optimization and validation of the quantification method, analyzed the data, prepared the figures, wrote and revised the manuscript.

3. Development and Application of a HILIC UHPLC-MS Method for Polar Fecal Metabolome Profiling

Abstract

The fecal metabolome is a complex mixture of endogenous, microbial metabolites, and food derived compounds. Hydrophilic interaction liquid chromatography (HILIC) enables the analysis of polar compounds, which is a valuable alternative to reversed-phase liquid chromatography in the field of metabolomics due to its ability to retain a greater portion of the polar metabolome. The objective of the study was to find the optimal chromatographic solution to perform non-targeted metabolomics of feces by means of HILIC ultra-high-pressure liquid chromatography mass spectrometry (UHPLC-Q-TOF-MS). The performance was systematically investigated analyzing a pooled fecal sample, and mixtures of 150 metabolites from different families, including for example amino acids, amines, indole derivatives, fatty acids and carbohydrates. Three different stationary phases (zwitterionic, amide and unbonded silica) were operated at three pH values (4.6, 6.8 and 9.0), and three salt gradient conditions (5 – 5, 5 – 10 and 5 – 25 mM ammonium acetate). Amide and zwitterionic stationary phases performed similarly at low pH, with highest number of detected standards, which increased by increasing the salt gradient. The amide column showed slightly better performance in terms of separation of isomers and peak widths and remarkably good performance at basic pH, with highest number of metabolite features in the non-targeted analysis. The zwitterionic column operated best in terms of number of detected standards, retention time distribution of standards and metabolite feature across whole chromatographic run. Thus, the zwitterionic column was proven to suit for non-targeted analysis of fecal samples, resulting in good coverage of especially amino acids and carbohydrates.

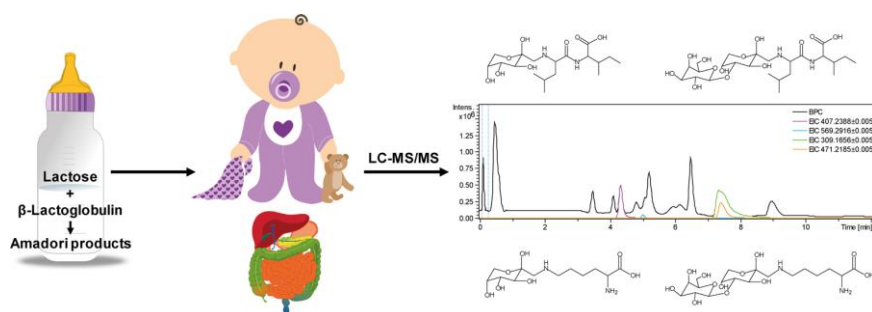
This chapter was published as [Nina Sillner](#), Alesia Walker, Eva-Maria Harrieder, Philippe Schmitt-Kopplin, Michael Witting. Development and Application of a HILIC UHPLC-MS Method for Polar Fecal Metabolome Profiling. *Journal of Chromatography B*, 1109, 142-148, Copyright Elsevier (2019).

Candidate's contributions: Nina Sillner designed the metabolomics research, analyzed the data for the 150 standards and non-targeted fecal metabolomics with 18 chromatographic settings, evaluated the different method suitabilities, prepared the figures, wrote and revised the manuscript.

4. Milk-derived Amadori products in feces of formula-fed infants

Abstract

Food processing of infant formula alters chemical structures, including the formation of Maillard reaction products between proteins and sugars. We detected early Maillard reaction products, so called Amadori products, in stool samples of formula-fed infants. In total, four Amadori products (*N*-deoxylactulosyllysine, *N*-deoxyfructosyllysine, *N*-deoxylactulosylleucylisoleucine, *N*-deoxyfructosylleucylisoleucine) were identified by a combination of complementary non-targeted and targeted metabolomics approaches. Chemical structures were confirmed by preparation and isolation of reference compounds, LC-MS/MS and NMR. The leucylisoleucine Amadori compounds, which most likely originate from β -lactoglobulin, were excreted throughout the first year of life in feces of formula-fed infants, but were absent in feces of breastfed infants. Despite high inter- and intra-individual differences of Amadori products in the infants' stool, solid food introduction resulted in a continuous decrease, proving infant formula as the major source of the excreted Amadori products.



This Chapter was published as [Nina Sillner](#), Alesia Walker, Daniel Hemmler, Monika Bazanella, Silke S. Heinzmann, Dirk Haller, Philippe Schmitt-Kopplin. Milk-derived Amadori products in feces of formula-fed infants. *Journal of Agricultural and Food Chemistry*, 67, 28, 8061-8069, Copyright American Chemical Society (2019).

Candidate's contributions: Nina Sillner designed the metabolomics research, performed all analytical experiments with FT-ICR-MS and UHPLC-MS, prepared and isolated reference compounds for identification, analyzed the data, prepared the figures, wrote and revised the manuscript.

5. Discussion and Outlook

This thesis reports on the targeted and non-targeted mass spectrometry-based profiling of metabolites in cecum and feces samples and the possibilities to cover a broad range of metabolites, from polar to semi-polar molecules by using different chromatographic settings. This enabled a holistic as well as detailed insight into the metabolic composition of samples from the gastrointestinal tract (Chapter 2 and 3).

The quantification method for bile acids enabled a targeted view on this specific metabolite class, allowing to explore the interplay of host, microbes and exogenous factors like drug-intake inside the gut system (Chapter 2).

The developed and optimized HILIC UHPLC-QTOF-MS for non-targeted metabolomics of stool samples (Chapter 3) was successfully applied in a nutrition cohort study, investigating the metabolomes of breast- and formula-fed infants. Non-targeted metabolomics analysis provided an unbiased characterization of metabolic variation introduced by diet to the metabolic phenotype and most significant candidates were selected for an in-depth metabolite identification. Targeted MS/MS experiments, isolation of compounds from feces, preparation of reference compounds, structure elucidation with NMR and quantification of specific Amadori products in feces of formula-fed infants was successfully performed (Chapter 4).

The combination of these different analytical methods enabled the identification of specific Amadori products (*N*-deoxylactulosyl-/ *N*-deoxyfructosyllysine and *N*-deoxylactulosyl-/ *N*-deoxyfructosylleucylisoleucine). Their fecal excretion was quantified at six time points during the first year of life. High concentrations were observed during exclusive formula feeding and decreasing amounts with introduction of solid food were detected. Furthermore, the Amadori products were absent in breastfed infants. Therefore, we think that the described compounds can serve as nutrition markers for formula feeding in infants by analyzing stool samples. This holds especially true for *N*-deoxylactulosyl- and *N*-deoxyfructosylleucylisoleucine, which were directly associated to the whey protein β -lactoglobulin and were not described as metabolites so far. The long-term effects of the consumption of Amadori and, in general, Maillard reaction products in infant food are currently not known (116). Most of the few related studies investigated the consumption of Maillard products in human adults or

animal models (117-120). Our findings demonstrate the necessity for further research dealing for example with absorption and metabolism of Maillard reaction products, including Amadori products.

Most of the nutrition related infant studies focused on the fecal microbiota composition. Only few studies investigated the impact of diet on the infant metabolome. Indeed, both microbiota and metabolites differ significantly between breast- and formula-fed infants (13, 84). Recently, reversed phase UHPLC-QTOF-MS non-targeted profiling described major differences between the metabolite profiles of breast- and formula-fed infants on a global level (13). Based on this study, we were able to identify the previous unknown metabolite *N*-deoxyfructosylleucylisoleucine as the most significant marker for formula-feeding (Chapter 4). Targeted profiling of short chain fatty acids emphasized also the impact of the diet on the gut microbiota and its contribution to the fecal metabolome (13). Besides the described Amadori products in Chapter 4, HILIC UHPLC-QTOF-MS non-targeted profiling revealed that a variety of stool metabolites were altered between breast- and formula-fed infants (Figure 5-1).

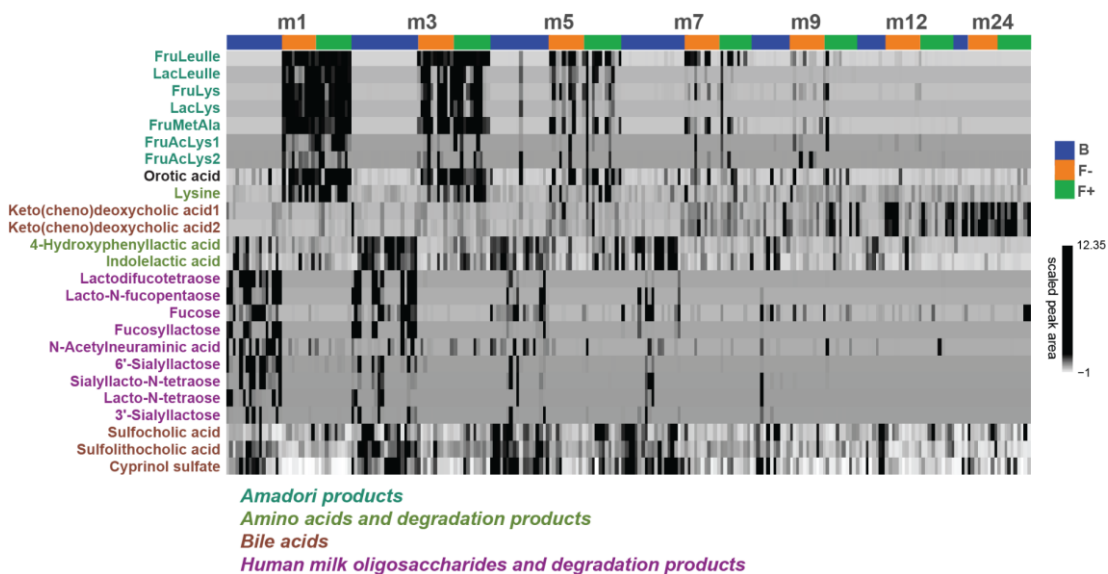


Figure 5-1. Heat map of highly discriminative metabolites mass signals between infants exclusively breastfed (B, blue), exclusively formula-fed without probiotics (F-, orange) and with probiotics (F+, green) over time (month 1 – 24) analyzed by HILIC UHPLC-QTOF-MS (negative ionization mode). Peak areas were unit variance scaled for visualization.

For example in formula-fed infants (F- and F+) the additional putative Amadori products FruMetAla and FruAcLys (*N*-deoxyfructosylmethionylalanine and *N*-deoxyfructosylacetyllysine) can be found during the first months of life. Furthermore, increased levels of lysine and orotic acid were detected. Orotic acid is a known milk marker and was found in infant formula but not in breast milk (121). In the breastfed group two bacterial break-down products from the aromatic amino acids phenylalanine and tryptophan, namely, 4-hydroxyphenyllactic and indolelactic acid were found to be increased from month 1 – 9, demonstrating the impact of altered gut microbiota compositions. Chow et al. (84) recently reported about predominant protein fermentation in fecal samples from formula-fed infants. Furthermore, the chemical composition of stool from breastfed infants was rich in different human milk oligosaccharides (HMOs) and parts of their degradation products fucose and *N*-acetylneuraminic acid, especially in the first 3 months. The presence of HMOs in feces was also described by Chow et al. to be characteristic for breastfed infants (84). Also the bile acid metabolism was different between the feeding groups. The stool of breastfed infants seemed to be dominated by sulfated primary bile acids. However, the formula-fed infants showed higher peak areas for the secondary bile acids ketochenodeoxycholic and ketodeoxycholic acid, indicating distinct microbial activities. A differentiated picture of the whole diet-dependent bile acid composition in infants will be obtained by applying a targeted method as described in Chapter 2 in future research.

In general, the application of metabolomics in nutrition research has become popular because it helps to understand mechanisms underlying dietary interventions. There is a huge potential to find specific dietary biomarkers and to develop long-term disease prevention strategies for example against cardiovascular diseases and obesity. Furthermore, in the future metabolomics will emerge as an promising technology in the field of precision nutrition and medicine (9).

In summary, it was demonstrated that cecal and fecal samples were highly suitable to evaluate the impact of extrinsic factors such as drug intake and diet on the metabolome. High resolution MS methods in combination with liquid chromatography proved to be excellent tools to investigate the metabolite space of feces samples and to discover new nutrition markers.

The identification of unknown metabolites is difficult, repetitive, time consuming and demands several orthogonal analytical methods, including MS/MS, NMR,

fractionation and synthesis. Therefore, unknown identification is still a major bottleneck in metabolomics (122, 123). Precise method development and optimization for targeted as well as non-targeted metabolomics is absolutely necessary to get a deep and valid insight into the chemical composition of biological samples but also to determine the quantity of metabolites for biomarker research. In the future new analytical developments will enable a combined targeted and non-targeted profiling of metabolites, for example in a single measurement (124), by using tandem LC-MS (125) or paired single sample - dual mass spectrometry analyses approach (69), as well as extensive collection of MS/MS spectra for libraries and *in silico* fragmentation tools which will make metabolomics studies more time and cost efficient.

A. Appendix Chapter 2

A.1 Original Publication

Journal of Chromatography B 1083 (2018) 35–43



Contents lists available at ScienceDirect

Journal of Chromatography B

journal homepage: www.elsevier.com/locate/jchromb

Metformin impacts cecal bile acid profiles in mice

Nina Sillner^{a,b}, Alesia Walker^{b,*}, Wendelin Koch^b, Michael Witting^{b,c},
Philippe Schmitt-Kopplin^{a,b,c}

^a ZIEL Institute for Food and Health, Technical University of Munich, Freising, Germany

^b Research Unit Analytical BioGeoChemistry, Helmholtz Zentrum München, Neuherberg, Germany

^c Chair of Analytical Food Chemistry, Technical University of Munich, Freising, Germany



ARTICLE INFO

Keywords:
Bile acids
UHPLC-MS
Quantification
Metformin
db/db mice

ABSTRACT

Bile acids (BAs) are major components of bile synthesized from cholesterol and take part in the digestion of dietary lipids, as well as having signaling functions. They undergo extensive microbial metabolism inside the gastrointestinal tract. Here, we present a method of ultra-high pressure liquid chromatography coupled to ion trap mass spectrometry for quantification of 45 BAs in mouse cecum. The system was validated in regard to sensitivity with limits of detection and quantification (0.6–24.9 nM), interday accuracy (102.4%), interday precision (15.2%), recovery rate (74.7%), matrix effect (98.2%) and carry-over effect (< 1.1%). Afterwards, we applied our method to investigate the effect of metformin on BA profiles. Diabetic mice were treated with metformin for 1 day or 14 days. One day of treatment resulted in a significant increase of total BA concentration (2.7-fold increase; *db/db* metformin 5.32 μmol/g, *db/db* control mice 1.95 μmol/g), most notable in levels of 7-oxodeoxycholic, 3-dehydrocholic and cholic acid. We observed only minor impact on BA metabolism after 14 days of metformin treatment, compared to the single treatment. Furthermore, healthy wild type mice had elevated concentrations of allocholic and ω-muricholic acid compared to diabetic mice. Our method proved the applicability of profiling BAs in cecum to investigate intestinal BA metabolism in diabetes and pharmacological applications.

1. Introduction

Bile acids (BAs) are key compounds in determining co-microbial metabolism in the intestinal tract of mammals. BAs are classified into primary, secondary and tertiary BAs. Cholesterol is converted by classical, acidic or alternative pathways into the primary BAs chenodeoxycholic (CDCA) and cholic acid (CA) [1]. CA and CDCA are common primary BAs detected in human bile, whereas CA and muricholic acid (MCA) are major BAs in mice [2]. In rodents, CDCA is converted into more hydrophilic MCAs, resulting in six unique BAs including alpha (α), beta (β), omega (ω) MCA. Furthermore, BAs undergo taurine (rodents) or glycine (humans) conjugation in hepatocytes before entering the biliary system and excreted into the gut. Here, conjugated BAs are hydrolyzed into their free forms by bile salt hydrolases which are found in several bacteria including Enterococci, Bacteroides, Lactobacillus and Clostridia [3]. Released CA and CDCA are converted by several bacteria (7α-dehydroxylation and 12α-dehydroxylation) into the secondary BAs deoxycholic acid (DCA) and lithocholic acid (LCA), respectively [4]. DCA and LCA can be further

transformed into their isoforms, for example by *Ruminococcus gnavus* [5]. βMCA is converted into the secondary BA ωMCA which is a product of bacterial conversion performed through Clostridium group III or cooperative work of three strains [6].

Recently, BA separation and quantification is preferably performed by liquid chromatography (LC) coupled to mass spectrometry (MS). Here, extensive and tedious preparation steps such as hydrolysis of conjugated BAs and derivatization are not needed compared to gas chromatography (GC) methods [7]. Most of the published methods used octadecyl (C18) reversed-phase (RP) chemistry mainly coupled to triple quadrupole MS. BAs were profiled in humans, mice and rats in many different matrices such as serum, plasma, urine, bile, liver and adipose tissue. There is a large variation in the number of validated and quantified BAs ranging from 9 to 57 BAs with total analysis times between 5 and 32 min. Mouse plasma, urine, bile and liver contain mainly taurine conjugated BAs (TBAs), especially TMCA (α, β and ω) and TCA [8–10]. Reported concentrations vary strongly, for example TCA ranges between 74.1 and 3090 ng/mL in murine serum or plasma samples [8–20].

* Corresponding author at: Helmholtz Zentrum München, Deutsches Forschungszentrum für Gesundheit und Umwelt, Department of Environmental Sciences, Analytical BioGeoChemistry, Ingolstaedter Landstrasse 1, 85764 Neuherberg, Germany.
E-mail address: alesia.walker@helmholtz-muenchen.de (A. Walker).

<https://doi.org/10.1016/j.jchromb.2018.02.029>

Received 11 January 2018; Received in revised form 12 February 2018; Accepted 18 February 2018

Available online 25 February 2018

1570-0232/ © 2018 Elsevier B.V. All rights reserved.

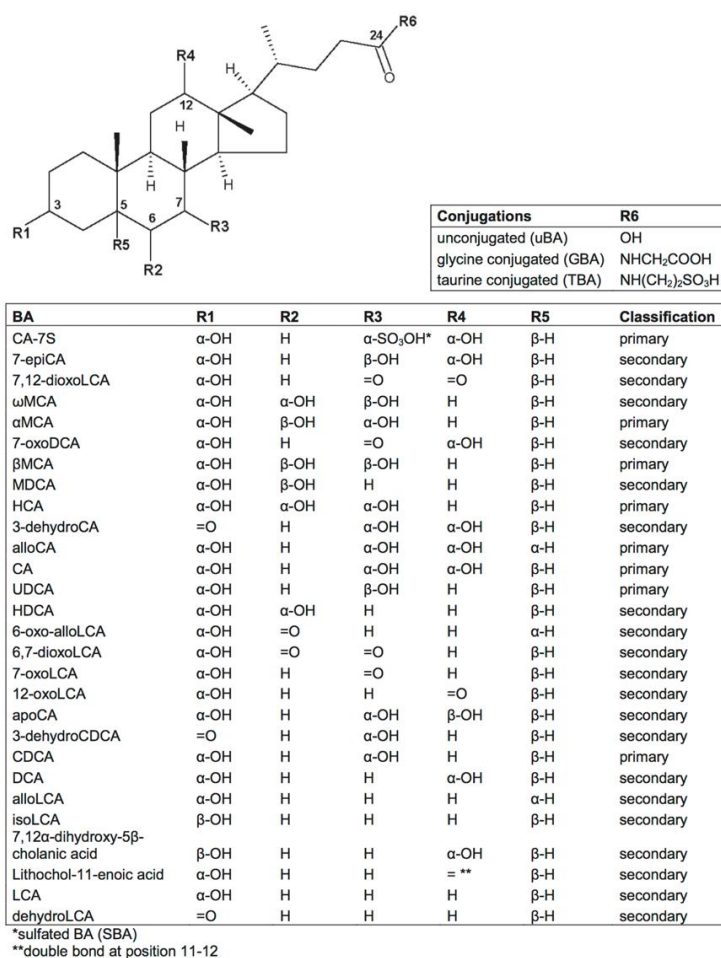


Fig. 1. Chemical structure of bile acids and conjugates.

Few studies quantified BAs in the gastrointestinal tract of mice although BAs are highly abundant and diverse in this organ [13,21]. They are released from the gall bladder into the small intestine, a process triggered by nutrients, promoting absorption of lipophilic dietary compounds [22]. Most BAs are reabsorbed by enterohepatic circulation but a small percentage of 5% escapes into cecum and further into the colon of mice. Here, BAs face extensive bacterial metabolism including deconjugation, dehydroxylation or epimerization. So far, studies analyzing murine cecal content for BA quantities and composition examined their role in the context of germ-free and specific pathogen free mice [23], the impact of diet [24], interplay between FXR receptor and gut microbiota [25], protection from *Clostridium difficile* [26], alcohol consumption [27], and prebiotics [28,29]. Total cecal BA content in mice was reported to range between 0.11 and 20 μmol/g, depending on the number of BAs taken into account [23,24,26–28,30–36].

In this study, a wide range of BAs, 45 in total, were quantified in the luminal content of cecum in mice, performed by UHPLC-MS, with an

octyl reversed-phase chemistry column and an ion trap mass spectrometer. Our method was validated according to intra- and interday accuracy and precision, recovery rate, matrix effect and carry-over. Finally, we applied our method to investigate the effects of metformin on bile acid metabolism in a diabetic mouse model.

2. Material and methods

2.1. Reagents and materials

Forty-five BAs and 4 deuterated BAs were used for validation and quantification purposes. Their specifications are summarized in supplementary information (Table S1). Methanol (MeOH) and acetonitrile were purchased from FLUKA, Sigma-Aldrich (LC-MS grade, CHROMASOLV®, St Louis, MO, USA). Ultrapure water was taken from Milli-Q Integral Water Purification System (Millipore, Billerica, MA, USA), ammonium acetate was purchased from Sigma-Aldrich, and acetic acid

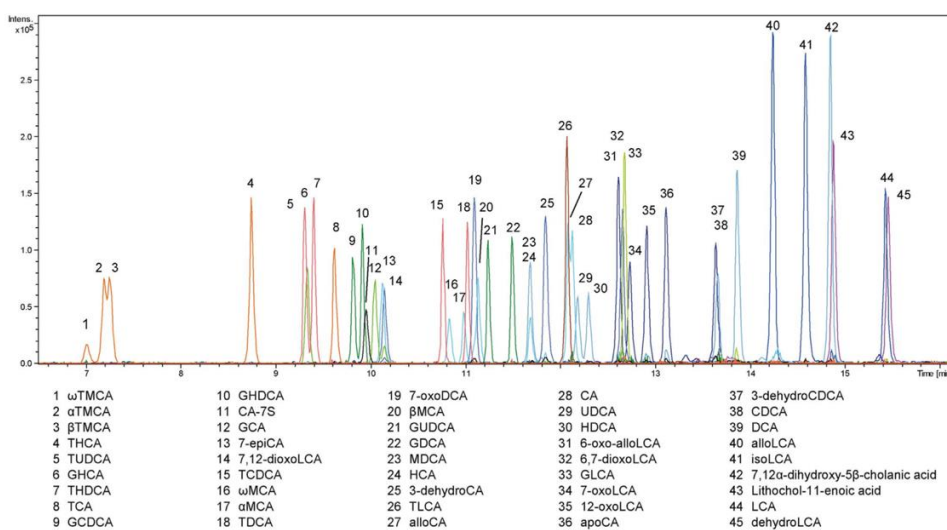


Fig. 2. Extracted ion chromatograms of UHPLC-MS analysis of 45 bile acids, including 10 taurine-conjugated, 7 glycine-conjugated, 1 sulfated and 27 unconjugated BAs.

from Biosolve (Valkenswaard, NL).

2.2. Preparation of stock solutions and calibrations curves

Standard stock solutions of BAs were prepared (1000 mg/L) in MeOH and stored in +4 °C until analysis. As working stock solution, we prepared a mixture of non-deuterated BAs (12.5 mg/L, MeOH). For determination of limit of detection (LOD) and lower limit of quantification (LLOQ), the stock solution was serially half-diluted starting from 5 mg/L to a final concentration of 0.153 μg/L. For quantification of BAs in biological samples, a five-point calibration curve was prepared with a final concentration range between 0.05 mg/L – 0.4 mg/L. The concentration of deuterated BAs (ISs) was kept constant (0.2 mg/L).

2.3. Mouse study

Male homozygous BKS-Cg-*dock7m* +/+ *Leprdb/J* (*db/db*) mice and their nondiabetic controls (*wt*) were used for BA profiling as a complementation of previously published studies [37,38]. Mice were housed in a specific pathogen-free environment. At an age of 3 weeks both *db/db* and *wt* mice were fed a high fat and high carb diet (S0372-E010, Ssniff, Germany). At the beginning of the drug challenge, the mice were fasted for 4 h. Mice (*db/db*) were treated with 300 mg/kg body weight metformin (Sigma Aldrich, St. Louis, MO, USA) by oral gavage. Ten week old *db/db* mice (*n* = 9) had one single treatment with metformin for one day (1D). Eight week old *db/db* mice (*n* = 10) were treated with metformin for 14 days (14D) on a daily basis. Control groups consisting of *wt* and *db/db* mice (*n* = 10 for each group) were treated with a vehicle solution to reproduce the effect of oral gavage [38]. Mice were euthanized by isoflurane (Sigma Aldrich, St. Louis, MO, USA).

2.4. Cecal sample collection and preparation

Luminal content of cecum was taken for BA profiling. The total organ was weighed and the content was carefully squeezed out of the organ, weighed and immediately snap-frozen in liquid nitrogen and

stored at –80 °C. Frozen samples were cut and weighed on dry ice with sterile instruments to prevent bacterial metabolism. About 2 mg of wet cecal content was used for BA extraction. Cold MeOH (1 mL), containing 0.2 mg/L ISs, was added to each sample before extraction. Homogenization and cell disruption was performed with Precellys® Evolution Homogenisator (Bertin Corp., Rockville, Maryland, USA; 4500 rpm, 40 × 3 s, 2 s pause time). Then, samples were centrifuged for 10 min at 21,000g and 4 °C. Supernatants were transferred into sterile Eppendorf tubes and stored at –80 °C before analysis.

2.5. UHPLC-MS analysis

Forty five BAs were separated using an Acquity UHPLC system (Waters, Milford, MA, USA) and a RP column (C8: 1.7 μm, 2.1 × 150 mm, Acquity™ UPLC BEH™) applying a flow rate of 350 μL min⁻¹ with an injection volume of 5 μL (partial loop) and column temperature of 60 °C, respectively. A mixture of isopropanol:acetonitrile:methanol:water (1:1:1:1, v/v) as strong needle wash and an acetonitrile:water (9:1, v/v) mixture as weak needle and seal wash was used. Elution of BAs was performed by following solvent system of 5 mM ammonium acetate and 0.1% acetic acid in water (eluent A) and pure acetonitrile (eluent B). A gradient profile was applied by starting at 10% B for 1 min, increasing to 22% B within 2 min, followed by an increase to 27% B within 4 min, taken over by a linear gradient to 95% B within 13 min. The 95% B was held for 2.5 min, returning to initial 10% B within 2.5 min, resulting in a total run time of 25 min. Prior to next measurement, a pre-run time of 2 min was applied to re-equilibrate the column.

The mass spectrometric analysis was performed on amaZon ETD Ion Trap (Bruker Daltonics GmbH, Bremen, Germany) in full scan mode (50–1000 m/z). BAs and samples were analyzed in negative ionization mode with following settings: dry gas flow rate of 8 L/min, dry gas temperature 250 °C, nebulizer gas pressure 2.0 bar, capillary voltage 4500 V, end plate offset 500 V and acquisition rate of 52 Hz (XtremeScan mode). Maximum accumulation time was set to 200 ms and Ion Charge Control target to 100,000.

Table 1
Limit of detection (LOD), lower limit of quantification (LLOQ) and linearity (R^2).

No.	BA class	BA	LOD [nM]	LLOQ [nM]	R^2
13	uBA	7-epiCA	3.0	6.0	0.9977
14	uBA	7,12-dioxoLCA	3.0	6.0	0.9984
16	uBA	ω MCA	6.0	23.9	0.9941
17	uBA	α MCA	6.0	23.9	0.9967
19	uBA	7-oxoDCA	1.5	6.0	0.9977
20	uBA	β MCA	6.0	23.9	0.9947
23	uBA	MDCa	6.2	12.4	0.9990
24	uBA	HCA	12.0	23.9	0.9983
25	uBA	3-dehydroCA	3.0	6.0	0.9982
27	uBA	alloCA	1.5	3.0	0.9955
28	uBA	CA	6.0	23.9	0.9955
29	uBA	UDCA	3.1	6.2	0.9936
30	uBA	HDCA	3.1	6.2	0.9979
31	uBA	6-oxo-alloLCA	0.8	1.6	0.9963
32	uBA	6,7-dioxoLCA	6.0	12.1	0.9996
34	uBA	7-oxoLCA	1.6	3.1	0.9921
35	uBA	12-oxoLCA	0.8	1.6	0.9960
36	uBA	apoCA	6.3	12.5	0.9974
37	uBA	3-dehydroCDCA	0.8	1.6	0.9963
38	uBA	CDCA	12.4	24.9	0.9966
39	uBA	DCA	3.1	6.2	0.9964
40	uBA	alloLCA	0.8	1.6	0.9977
41	uBA	isoLCA	0.8	1.6	0.9909
42	uBA	7,12 α -dihydroxy-5 β -cholanic acid	0.8	1.6	0.9965
43	uBA	Lithochol-11-enoic acid	0.4	1.6	0.9980
44	uBA	LCA	1.6	6.5	0.9948
45	uBA	dehydroLCA	0.8	1.6	0.9947
1	TBA	ω TMCA	2.3	4.5	0.9947
2	TBA	α TMCA	0.3	0.6	0.9947
3	TBA	β TMCA	0.3	0.6	0.9962
4	TBA	THCA	0.6	1.1	0.9994
5	TBA	TUDCA	0.3	0.6	0.9918
7	TBA	THDCA	0.3	0.6	0.9996
8	TBA	TCA	0.6	2.4	0.9952
15	TBA	TCDCa	0.6	1.2	0.9919
18	TBA	TDCA	0.6	1.2	0.9971
26	TBA	TLCA	0.3	0.6	0.9954
11	SBA	CA-7S	5.0	10.0	0.9996
6	GBA	GHCA	0.6	1.3	0.9971
9	GBA	GCDCa	1.3	2.6	0.9951
10	GBA	GHDCa	0.7	1.4	0.9972
12	GBA	GCA	0.7	2.6	0.9965
21	GBA	GUDCA	0.7	1.4	0.9978
22	GBA	GDCA	0.6	1.3	0.9936
33	GBA	GLCA	1.3	2.7	0.9935

2.6. Method validation

Limit of detection (LOD) and lower limit of quantification (LLOQ) were defined as signal-to-noise ratio > 3 or > 5 , respectively. Accuracy and precision was assessed by standard addition method. A pooled sample of 4–5 mg/mL methanolic cecum extract was used to prepare quality controls (QCs) of three different BA concentrations including low (0.03 mg/L), medium (0.15 mg/L) and high (0.3 mg/L). Six replicates of each QC were analyzed on one day to determine intraday accuracy and precision. This approach was repeated four times to evaluate interday accuracy and precision ($n = 4$).

Recovery rates were determined by comparing peak areas of deuterated BAs inside an unprocessed blank (pure MeOH) containing 0.2 mg/L IS mix against extracted QCs (zero = non-spiked, low, medium and high). BAs were spiked before sample extraction. Matrix effect was assessed by integrating peak areas of deuterated BAs in an unprocessed blank containing 0.2 mg/L IS mix and 4 different QCs (zero, low, medium and high). BAs were spiked after sample extraction. Carry over effects were determined by integration of peak areas of the highest concentration of the calibration curve (0.4 mg/L) and comparing them with peak areas of three subsequent blank injections.

2.7. Data processing and statistical analysis

Targeted peak picking and calibration was performed in QuantAnalysis 2.2 (Bruker Daltonics GmbH, Bremen, Germany) with following settings: retention window 0.05–0.1 min, m/z window 0.3–0.5 Da, Gaussian smoothing window of 0.2 and 3 cycles. Data was exported to comma separated files for further analysis. Boxplots and density plots were illustrated with RStudio (Version 1.0.136) using ggplot2 package [39]. Kruskal-Wallis and post hoc (Dunn) tests were applied for multiple comparison of each BA in the different mouse groups (wt, db/db, db/db metformin; 1D, 14D) using the R package FSA [40]. *p*-Values were adjusted with the Benjamini-Hochberg method. Significance between cecum weights was tested by one-way ANOVA with SigmaPlot 12.0 (Systat Software Inc., San Jose, CA, USA).

3. Results and discussion

3.1. Method validation

Validation was performed for 45 BAs in total, including 1 sulfated (S), 7 glycine (G), 10 taurine (T), 27 unconjugated (u) BAs plus 4 deuterated (d) BAs as internal standards, summarized in Table S1. The common BA steroid structure with varying residues at position 3, 5, 6, 7, 12 and 24 is illustrated in Fig. 1 for all analyzed BAs. The number of BAs used in our method is in the upper range when compared to published studies with 9–57 validated compounds conducted with UHPLC-MS systems [8–20]. Separation was optimized regarding selectivity using a C8 RP column, with ammonium acetate and acetic acid buffer system as mobile phase together with pure acetonitrile for elution. Most other studies used a C18 RP chemistry column for separation [41]. Baseline separation was achieved for almost all BAs (Fig. 2) except for the two epimeric pairs α / β TMCA and alloCA/CA, with a chromatographic peak resolution of 1.27 and 1.00, respectively. However, baseline separation of these BAs was shown in methods with formic acid acidified solvents [9,11,13]. Other critical pairs such as α MCA and β MCA, UDCA and HDCA (including their G- and T-conjugates) were fully resolved.

3.1.1. LOD, LLOQ and linearity

LOD and LLOQ values are as follows, TBAs < GBAs < uBAs, ranging between 0.3 and 12.0 nanomolar (nM) for LOD and between 0.6 and 24.9 nM for LLOQ, shown in Table 1. These values are in line with other methods utilizing triple quadrupole MS instead of ion trap MS [9,19]. The equidistant five-point calibration curve, ranging between 0.05 mg/L and 0.4 mg/L, showed satisfying linear correlation values (R^2), summarized in Table 1.

3.1.2. Accuracy and precision

To overcome the problem with generation of a BA free matrix, we applied standard addition method. For determination of accuracy and precision, QCs were spiked with three concentrations of BAs (low, medium and high) and analyzed six times for intraday and four times for interday experiments. Relative standard deviations (RSDs in %) of precision were calculated as standard deviation divided by mean and multiplied by 100 for intra- and interday measurements for each QC. Accuracy was determined as theoretical concentration divided by measured concentration multiplied by 100. Accuracy values should be within $100 \pm 20\%$ of true values and the RSDs of the determined precision should be $\leq 20\%$, which was achieved for most of the measurements, summarized in Fig. 3A,B and Table S2. Intra- and interday analysis of low spiked QCs showed higher variance, because discrimination of peak areas of endogenous BAs already present in QCs was not always straightforward.

3.1.3. Recovery rate, matrix and carry-over effect

Spike-in experiments of 4 ISs showed a recovery rate between 61

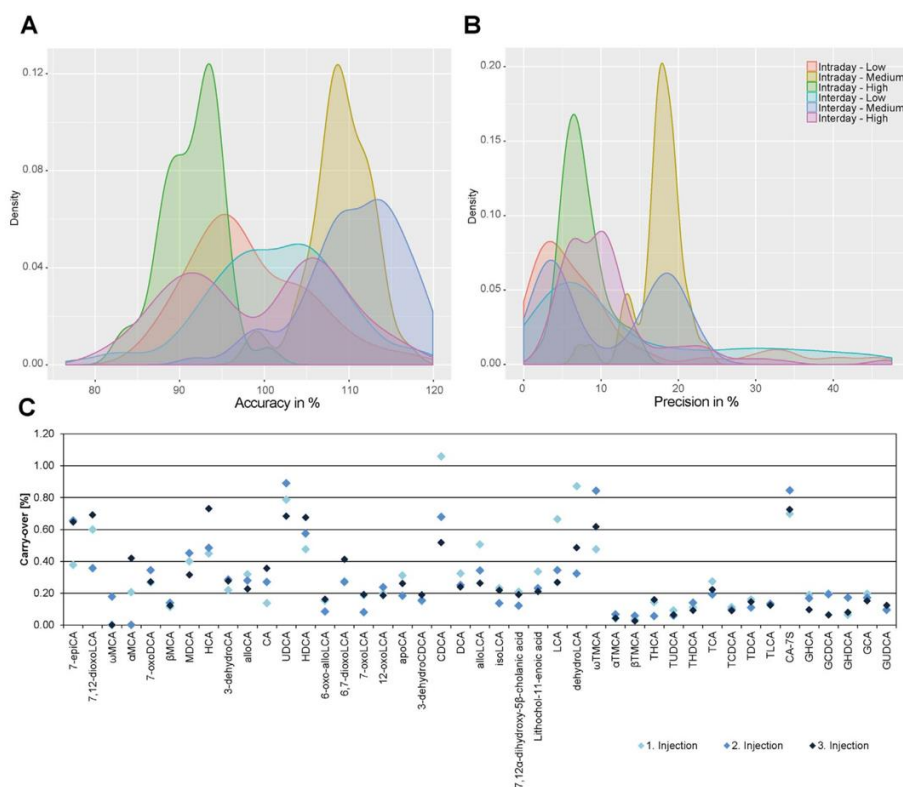


Fig. 3. Accuracy, precision and carry-over validation. (A) Density plot of the distribution of intraday ($n = 6$) and interday ($n = 4$) accuracy and (B) precision for low (0.03 mg/L), medium (0.15 mg/L) and high (0.3 mg/L) BA concentrations in cecum. (C) Carry-over effects of 45 BAs tested for three blank injections after injection of BA mix of 0.4 mg/L.

Table 2

Recovery rate and matrix effect in percentage of internal standards in QC samples with four different concentrations. Data are presented as average of each QC concentration ($n = 3$).

IS	Recovery rate [%]				Matrix effect [%]			
	Zero	Low	Medium	High	Zero	Low	Medium	High
d5-TCA	82.2	69.8	71.1	71.5	63.8	73.8	77.8	69.9
d4-GDCA	82.9	70.6	73.7	72.8	94.9	110.0	116.5	94.5
d4-CA	86.4	71.2	75.7	73.7	98.1	117.7	125.4	101.2
d4-DCA	80.7	68.2	72.5	71.7	98.6	113.8	119.5	95.2

and 106% (Table 2), which is in agreement with other reports [13,14]. Matrix effects were studied by comparing peak areas of ISs in blanks and QCs (zero, low, medium and high). Ionization suppression of ISs ranged between 94.5% and 125.4%, except for d5-TCA, which showed between 69.9% and 77.8% suppression by the matrix depending on spiked BA concentrations (Table 2). Carry-over effect was tested for three blank injections after injection of BA mix of 0.4 mg/L. Here, we calculated a maximum carry-over effect of 1% in the first blank injection, decreasing to 0.89% in the second injection and 0.73% in the third injection. Unconjugated BAs showed a higher carry-over effect compared to TBAs and GBAs (Fig. 3C). Similar effects concerning matrix suppression and carry-over were reported by some groups [17,35],

whereas others didn't observe any significant matrix effects [14,20].

3.2. Determination of BA profiles in diabetic and metformin treated mice

3.2.1. General BA composition in cecum

In order to prove the applicability of our developed method we investigated the BA metabolism inside cecum of a diabetic mouse model treated with metformin. Diabetic (*db/db*) mice were treated with metformin either once (1D) or 14 days (14D). Non-treated *db/db* and wild type littermates (*wt*) served as controls. We observed a significant increase of total cecum weight in *db/db* and metformin mice in both treatments (Fig. 4A). Applying our validated method, we could quantify 20 different BAs in cecal content, including 7 TBAs, 13 uBAs and 1 SBA. This number of quantified BAs in cecum is in the upper range compared to previous studies [26,28,36]. The concentrations of these BAs are summarized in Tables S3 and S4 and a representative chromatogram is shown in Fig. S1. We observed remarkable differences of BA profiles between *wt* and *db/db* mice. Looking at the overall BA composition, *wt* mice were represented by high percentages of ω TMCA and ω MCA (Fig. 4B). Diabetic mice had high proportions of ω TMCA, TCA and DCA, while TCA, ω MCA, 7-oxoDCA and CA were elevated in the metformin treated group (Fig. 4B). Both 14D *db/db* groups had CA-7S and DCA as major BAs. Independent of the treatment duration, the percentage of primary BAs in *wt* mice was approximately 40% of the total BA amount, accordingly secondary BAs accounted for 60% (Tables S3, S4). In

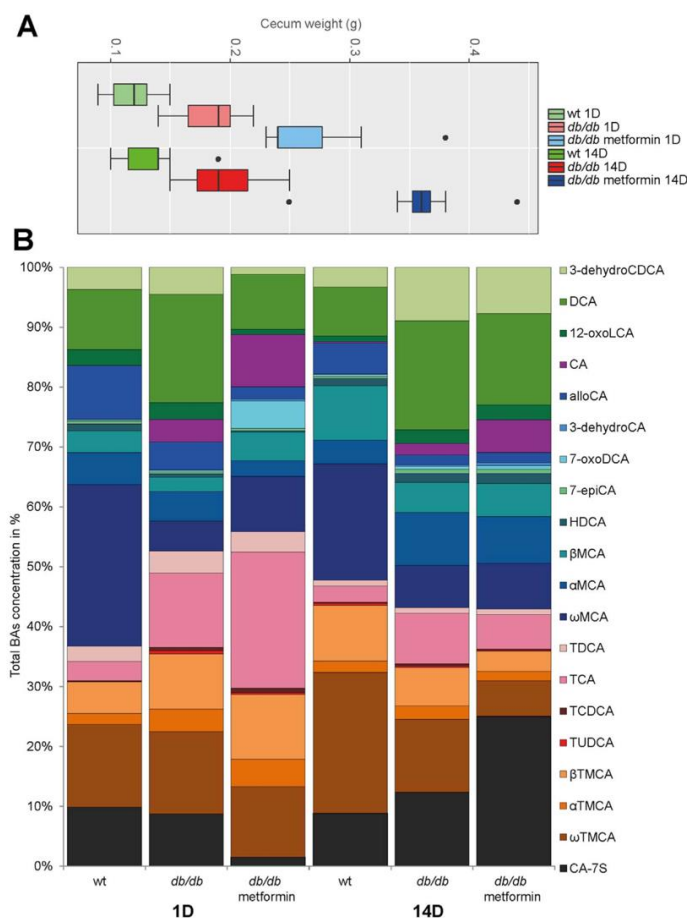


Fig. 4. Cecum weight and total BA profiles of wild type (wt), diabetic (*db/db*) and metformin (*db/db* metformin) treated mice. (A) Total cecum weight after 1D or 14D treatment. (B) Cecal BA composition of wt, *db/db* and *db/db* metformin mice treated for 1D or 14D.

untreated *db/db* mice the relation was 1:1, however, in the *db/db* metformin group primary BAs accounted for roughly 60%. Furthermore, in the 1D groups (Table S3) the proportion of TBAs was lowest in wt (27% of the total concentration) and highest in *db/db* metformin mice (54%). On the other hand, the percentages of uBAs and SBA were highest in wt mice (63% and 10%, respectively) and lowest in the *db/db* metformin group (44% and 1.5%, respectively). The BA ratios in the 14D groups (Table S4) showed opposite behavior, with highest proportion of TBAs in wt (39%) and lowest in *db/db* metformin mice (19%), and lowest ratio of uBAS and SBA in wt (52% and 9%, respectively) and highest in *db/db* metformin mice (58% and 23%, respectively).

3.2.2. Bile acid metabolism in diabetic mice

We observed higher levels of CA and TCDCa and lower levels of ω MCA, alloCA and HDCA in the 1D *db/db* group compared to wt mice (Fig. 5A). Wild type mice of the 14D group had a 4.2-fold higher total BA amount in cecum compared to *db/db* mice (Table S4). Here, β TMCA,

ω MCA, β MCA, alloCA, TUDCA and HDCA were significantly elevated in wt mice and decreased in *db/db* mice (Fig. 5B). Major primary uBAs were β MCA and alloCA in wt mice, whereas CA was very low in concentration or even under the detection limit. AlloCA was highly abundant and seems to be an important primary BA in healthy control mice, whereas in *db/db* mice the ratio of alloCA to CA is similar. Until now, allo BAs were detected in germ-free rabbits, hens and rats and were associated with hepatic cancer [42,43]. Still, we have to point out that alloCA is underrepresented in BA profiling studies probably due to lack of sufficient chromatographic separation from CA. Previous publications consistently reported increased total BA concentrations in diabetic patients or mice, which is contradictory to our results, however, most of them analyzed plasma samples [44–51].

3.2.3. Bile acid metabolism in metformin treated diabetic mice

Single treatment with metformin (1D) resulted in a 2.7-fold increase of total BA concentration in the *db/db* metformin group (5.32 μ mol/g),

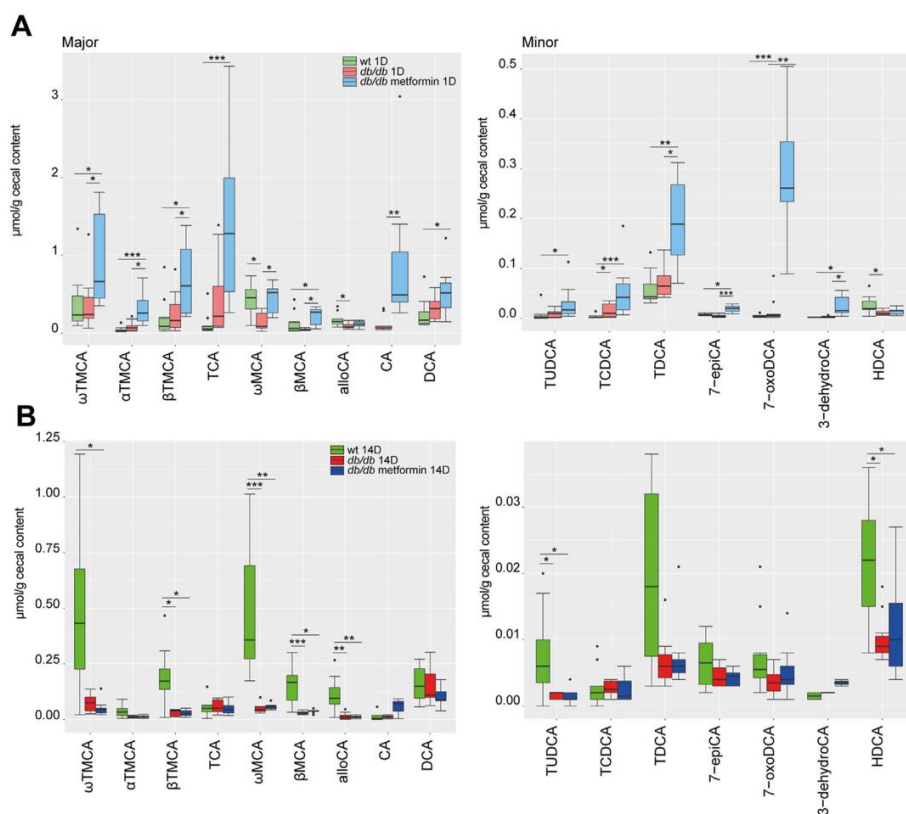


Fig. 5. Boxplots of cecal BA concentrations. (A) Significantly altered BAs in wild type (wt; $n = 10$), diabetic (db/db ; $n = 10$) and metformin treated db/db mice (db/db metformin; $n = 9$) after 1D treatment. (B) Same BAs are displayed for wt ($n = 10$), db/db ($n = 10$) and db/db metformin ($n = 10$) mice after 14D treatment. The BAs are divided into major and minor concentrated ones. *: $p < 0.05$, **: $p < 0.005$, ***: $p < 0.0005$ (Kruskal-Wallis test).

compared to db/db control mice ($1.95 \mu\text{mol/g}$). Similar trends in increased fecal BA excretion after metformin treatment were already reported by Tomkin, Scarpello et al. and Chen et al. [52–54]. Recently, Wu et al. described an increase of total BA concentration in plasma but not in feces [55]. Metformin blocks the reuptake of bile acids in the ileum [56]. Thus, more bile acids could reach distal regions of the intestine, including cecum. In detail, we observed an overall increase of ωTMCA , αTMCA , βTMCA , ωMCA , βMCA , CA, TDCA, 7-epiCA, 7-oxoDCA and 3-dehydroCA, compared to db/db mice (Fig. 5A). A remarkable increase due to metformin was especially shown for 7-oxoDCA, 3-dehydroCA and CA (45.0, 8.1 and 7.5 times, respectively; Table S3). The intermediate BAs 7-oxoDCA, 7-epiCA and 3-dehydroCA are produced from CA by intestinal microbiota by specific hydroxysteroid dehydrogenases [57]. Hence, increased concentrations of these downstream BAs are consistent with the significant increase of CA in metformin treated mice. Only ωMCA and alloCA reached similar concentrations to healthy controls (wt), while all other BAs were significantly lower in wt mice, except for HDCA. On the other hand, oral treatment with metformin for 14D had only slight but not significant effects on BA metabolism in diabetic mice with elevated CA, 3-dehydroCA and CA-7S (Fig. 5B and Table S4). The discrepancy between the 1D and 14D treatment groups in total BA concentrations is likely due to

different sampling times.

4. Conclusion

A quantitative BA profiling method using UHPLC ion trap MS was established and applied to study BA metabolism inside the gastrointestinal tract of mice with focus on cecum. In total, we separated and validated 45 BAs in terms of sensitivity, accuracy, precision, recovery rate, matrix effects and carry-over, reaching overall satisfying results. We implement our method to investigate how metformin is affecting BA profiles inside the mouse cecum. Single treatment with metformin resulted in an increase of total BA concentration. The profiles of 16 out of 20 endogenous BAs were significantly altered including unconjugated, taurine and sulfate conjugated BAs. In particular, remarkable increase was seen for taurine conjugated and oxo-BAs. Healthy control mice were dominated by high abundance of more hydrophilic BAs such as ωTMCA and ωMCA . In summary, this profiling method provided insights into pharmacological impacts of metformin on BA metabolism in the intestine of mice.

Supplementary data to this article can be found online at <https://doi.org/10.1016/j.jchromb.2018.02.029>.

Acknowledgements

The authors thank Deutsche Forschungsgemeinschaft (SPP1656) and ZIEL Institute for Food & Health, Technical University of Munich for the financial support of the work. The project was funded by the German Center for Diabetes Research (DZD) and the Ministry of Education and Research of the Federal Republic of Germany (BMBF) under project no. 0315494A (SysMBo – Systems Biology of Metabotypes).

References

- W.M. Pandak, P. Bohdan, C. Franklund, D.H. Mallonee, G. Eggertsen, I. Björkhem, G. Gil, Z.R. Vlahcevic, P.B. Hylemon, Expression of sterol 12 α -hydroxylase alters bile acid pool composition in primary rat hepatocytes and in vivo, *Gastroenterology* 120 (2001) 1801–1809.
- Thomas Q. de Aguiar Vallim, Elizabeth J. Tarling, Peter A. Edwards, Pleiotropic roles of bile acids in metabolism, *Cell Metab.* 17 (2013) 657–669.
- R.S. Kumar, J.A. Brannigan, A.A. Prabhune, A.V. Pundle, G.G. Dodson, E.J. Dodson, C.G. Suresh, Structural and functional analysis of a conjugated bile salt hydrolase from *Bifidobacterium longum* reveals an evolutionary relationship with penicillin V acylase, *J. Biol. Chem.* 281 (2006) 32516–32525.
- J.M. Ridlon, D.-J. Kang, P.B. Hylemon, Bile salt biotransformations by human intestinal bacteria, *J. Lipid Res.* 47 (2006) 241–259.
- A.S. Devlin, M.A. Fischbach, A biosynthetic pathway for a prominent class of microbiota-derived bile acids, *Nat. Chem. Biol.* 11 (2015) 685–690.
- E.C. Saquet, P.M. Raibaud, C. Mejean, M.J. Riottot, C. Lepreire, P.C. Leglise, Bacterial formation of omega-muricholic acid in rats, *Appl. Environ. Microbiol.* 37 (1979) 1127–1131.
- W.J. Griffiths, J. Sjöwall, Bile acids: analysis in biological fluids and tissues, *J. Lipid Res.* 51 (2010) 23–41.
- Y. Alnouti, L.L. Csanaky, C.D. Klaassen, Quantitative-profiling of bile acids and their conjugates in mouse liver, bile, plasma, and urine using LC-MS/MS, *J. Chromatogr. B Anal. Technol. Biomed. Life Sci.* 873 (2008) 209–217.
- J.C. Garcia-Cañaveras, M.T. Donato, J.V. Castell, A. Lahoz, Targeted profiling of circulating and hepatic bile acids in human, mouse, and rat using a UPLC-MRM-MS-validated method, *J. Lipid Res.* 53 (2012) 2231–2241.
- J. Huang, S.P.R. Bathena, L.L. Csanaky, Y. Alnouti, Simultaneous characterization of bile acids and their sulfate metabolites in mouse liver, plasma, bile, and urine using LC-MS/MS, *J. Pharm. Biomed. Anal.* 55 (2011) 1111–1119.
- J. Han, Y. Liu, R. Wang, J. Yang, V. Ling, C.H. Borchers, Metabolic profiling of bile acids in human and mouse blood by LC-MS/MS in combination with phospholipid-depletion solid-phase extraction, *Anal. Chem.* 87 (2015) 1127–1136.
- S.P. Bathena, S. Mukherjee, M. Olivera, Y. Alnouti, The profile of bile acids and their sulfate metabolites in human urine and serum, *J. Chromatogr. B Anal. Technol. Biomed. Life Sci.* 942–943 (2013) 53–62.
- S.E. Jantti, M. Kivilompolo, L. Ohrnberg, K.H. Pietiläinen, H. Nygren, M. Oresic, T. Hyötyläinen, Quantitative profiling of bile acids in blood, adipose tissue, intestine, and gall bladder samples using ultra high performance liquid chromatography-tandem mass spectrometry, *Anal. Bioanal. Chem.* 406 (2014) 7799–7815.
- G. Lee, H. Lee, J. Hong, S.H. Lee, B.H. Jung, Quantitative profiling of bile acids in rat bile using ultrahigh-performance liquid chromatography-orbitrap mass spectrometry: alteration of the bile acid composition with aging, *J. Chromatogr. B Anal. Technol. Biomed. Life Sci.* 1031 (2016) 37–49.
- Y. Suzuki, R. Kaneko, M. Nomura, H. Naito, K. Kitamori, T. Nakajima, T. Ogawa, H. Hattori, H. Seno, A. Ishii, Simple and rapid quantitation of 21 bile acids in rat serum and liver by UPLC-MS-MS: effect of high fat diet on glycine conjugates of rat bile acids, *Nagoya J. Med. Sci.* 75 (2013) 57–71.
- Y. Liu, Q. Song, J. Zheng, J. Li, Y. Zhao, C. Li, Y. Song, P. Tu, Sensitive profiling of phenols, bile acids, sterols, and eicosanoids in mammalian urine by large volume direct injection-online solid phase extraction-ultra high performance liquid chromatography-polarity switching tandem mass spectrometry, *RSC Adv.* 6 (2016) 81826–81837.
- M.H. Sarafian, M.R. Lewis, A. Pechlivanis, S. Ralphs, M.J. McPhail, V.C. Patel, M.E. Dumas, E. Holmes, J.K. Nicholson, Bile acid profiling and quantification in biofluids using ultra-performance liquid chromatography tandem mass spectrometry, *Anal. Chem.* 87 (2015) 9662–9670.
- E.J. Want, M. Coen, P. Masson, H.C. Keun, J.T.M. Pearce, M.D. Reilly, D.G. Robertson, C.M. Rohde, E. Holmes, J.C. Lindon, R.S. Plumb, J.K. Nicholson, Ultra performance liquid chromatography-mass spectrometry profiling of bile acid metabolites in biofluids: application to experimental toxicology studies, *Anal. Chem.* 82 (2010) 5282–5289.
- H.T. Pham, K. Arnhard, Y.J. Asad, L. Deng, T.K. Felder, L. St. John-Williams, V. Kaever, M. Leadley, N. Mitro, S. Muccio, C. Prehn, M. Rauh, U. Rolle-Kampczyk, J.W. Thompson, O. Uhl, M. Ulaszewska, M. Vogeser, D.S. Wishart, T. Koal, Inter-laboratory robustness of next-generation bile acid study in mice and humans: international ring trial involving 12 laboratories, *J. Appl. Lab. Med.* 1 (2) (2016) 129–142 (An AACCC Publication, DOI).
- K. Minato, M. Suzuki, H. Nagao, R. Suzuki, H. Ochiai, Development of analytical method for simultaneous determination of five rodent unique bile acids in rat plasma using ultra-performance liquid chromatography coupled with time-of-flight mass spectrometry, *J. Chromatogr. B Anal. Technol. Biomed. Life Sci.* 1002 (2015) 399–410.
- C. Parolini, S. Caligari, D. Gilio, S. Manzini, M. Busnelli, M. Montagnani, M. Locatelli, E. Diani, F. Giavarini, D. Caruso, E. Roda, A. Roda, C.R. Sirtori, G. Chiesa, Reduced biliary sterol output with no change in total fecal excretion in mice expressing a human apolipoprotein A-I variant, *Liver Int.* 32 (2012) 1363–1371.
- R.S.P. Benson, S.S. Sidhu, M.N. Jones, R.M. Case, D.G. Thompson, Fatty acid signalling in a mouse enteroendocrine cell line involves fatty acid aggregates rather than free fatty acids, *J. Physiol.* 538 (2002) 121–131.
- Sama I. Sayin, A. Wahlström, J. Felin, S. Jäntti, H.-U. Marschall, K. Bamberg, B. Angelin, T. Hyötyläinen, M. Orešič, F. Bäckhed, Gut microbiota regulates bile acid metabolism by reducing the levels of tauro-beta-muricholic acid, a naturally occurring FXR antagonist, *Cell Metab.* 17 (2013) 225–235.
- R. Kübeck, C. Bonet-Ripoll, C. Hoffmann, A. Walker, V.M. Müller, V.L. Schüppel, I. Lagkouvardos, B. Scholz, K.-H. Engel, H. Daniel, P. Schmitt-Kopplin, D. Haller, T. Clavel, M. Klingspor, Dietary fat and gut microbiota interactions determine diet-induced obesity in mice, *Mol. Metab.* 5 (2016) 1162–1174.
- A. Parsés, N. Sommer, F. Sommer, R. Caesar, A. Molinaro, M. Ståhlman, T.U. Greiner, R. Perkins, F. Bäckhed, Microbiota-induced obesity requires farnesoid X receptor, *Gut* 66 (2017) 429–437.
- N. Studer, L. Desharnais, M. Beutler, S. Brugiroux, M.A. Terrazos, L. Menin, C.M. Schürch, K.D. McCoy, S.A. Kuehne, N.P. Minton, B. Stecher, R. Bernier-Latmani, S. Hapfelmeier, Functional intestinal bile acid 7 α -dehydroxylation by *Clostridium scindens* associated with protection from *Clostridium difficile* infection in a gnotobiotic mouse model, *Front. Cell. Infect. Microbiol.* 6 (2016) 191.
- G. Xie, W. Zhong, H. Li, Q. Li, Y. Qiu, X. Zheng, H. Chen, X. Zhao, S. Zhang, Z. Zhou, S.H. Zeisel, W. Jia, Alteration of bile acid metabolism in the rat induced by chronic ethanol consumption, *FASEB J.* 27 (2013) 3583–3593.
- N. Takemura, M. Hagio, S. Ishizuka, H. Ito, T. Morita, K. Sonoyama, Inulin prolongs survival of intragastrically administered *Lactobacillus plantarum* no. 14 in the gut of mice fed a high-fat diet, *J. Nutr.* 140 (2010) 1963–1969.
- S.-M. Kuo, P.M. Merhige, L.R. Hagey, The effect of dietary prebiotics and probiotics on body weight, large intestine indices, and fecal bile acid profile in wild type and IL10 $^{-/-}$ mice, *PLoS One* 8 (2013) e60270.
- Y. Murakami, S. Tanabe, T. Suzuki, High-fat diet-induced intestinal hyperpermeability is associated with increased bile acids in the large intestine of mice, *J. Food Sci.* 81 (2016) H216–222.
- L. Zhang, R.G. Nichols, J. Correll, I.A. Murray, N. Tanaka, P.B. Smith, T.D. Hubbard, A. Sebastian, I. Albert, E. Hatzakis, F.J. Gonzalez, G.H. Perdew, A.D. Patterson, Persistent organic pollutants modify gut microbiota-host metabolic homeostasis in mice through aryl hydrocarbon receptor activation, *Environ. Health Perspect.* 123 (2015) 679–688.
- O. Kanauchi, I. Serizawa, Y. Araki, A. Suzuki, A. Andoh, Y. Fujiyama, K. Mitsuyama, K. Takaki, A. Toyonaga, M. Sata, T. Bamba, Germinated barley foodstuff, a prebiotic product, ameliorates inflammation of colitis through modulation of the enteric environment, *J. Gastroenterol.* 38 (2003) 134–141.
- S. Narushima, K. Iton, K. Kuruma, K. Uchida, Composition of cecal bile acids in germ-free mice inoculated with human intestinal bacteria, *Lipids* 35 (2000) 639–644.
- S. Narushima, K. Itoh, F. Takamine, K. Uchida, Absence of cecal secondary bile acids in gnotobiotic mice associated with two human intestinal bacteria with the ability to dehydroxylate bile acids in vitro, *Microbiol. Immunol.* 43 (1999) 893–897.
- K.H. Han, H. Tsuchihira, Y. Nakamura, K. Shimada, K. Ohba, T. Aritsuka, H. Uchino, H. Kikuchi, M. Fukushima, Inulin-type fructans with different degrees of polymerization improve lipid metabolism but not glucose metabolism in rats fed a high-fat diet under energy restriction, *Dig. Dis. Sci.* 58 (2013) 2177–2186.
- S. Takahashi, T. Fukami, Y. Masuo, C.N. Brocker, C. Xie, K.W. Krausz, C.R. Wolf, C.J. Henderson, F.J. Gonzalez, Cyp2c7 is responsible for the species difference in bile acid metabolism between mice and humans, *J. Lipid Res.* 57 (2016) 2130–2137.
- A. Walker, M. Lucio, B. Pfützner, M.F. Scheerer, S. Neschen, M.H. de Angelis, A. Hartmann, P. Schmitt-Kopplin, Importance of sulfur-containing metabolites in discriminating fecal extracts between normal and type-2 diabetic mice, *J. Proteome Res.* 13 (2014) 4220–4231.
- S. Neschen, M. Scheerer, A. Seelig, P. Huypens, J. Schultheiss, M. Wu, W. Wurst, B. Rathkolb, K. Suhre, E. Wolf, J. Beckers, M. Hrabec de Angelis, Metformin supports the antidiabetic effect of a sodium glucose cotransporter 2 inhibitor by suppressing endogenous glucose production in diabetic mice, *Diabetes* 64 (2015) 284–290.
- H. Wickham, *ggplot2: Elegant Graphics for Data Analysis*, Springer-Verlag, New York, 2009.
- D.H. Ogle, FSA: Fisheries Stock Analysis (R package version 0.8.17), (2017).
- S. Yin, M. Su, G. Xie, X. Li, R. Wei, C. Liu, K. Lan, W. Jia, Factors affecting separation and detection of bile acids by liquid chromatography coupled with mass spectrometry in negative mode, *Anal. Bioanal. Chem.* (2017), <http://dx.doi.org/10.1007/s00216-017-0489-1>.
- K. Yamasaki, Y. Ayaki, G. Yamasaki, Allocholic acid, a metabolite of 7 α -hydroxycholesterol in the rat and rabbit, *J. Biochem.* 71 (1972) 927–929.
- S.J. Shiffka, M.A. Kane, P.W. Swaan, Planar bile acids in health and disease, *Biochim. Biophys. Acta* 1859 (2017) 2269–2276.
- R.A. Haeusler, B. Astiarraga, S. Camastra, D. Accili, E. Ferrannini, Human insulin resistance is associated with increased plasma levels of 12 α -hydroxylated bile acids, *Diabetes* 62 (2013) 4184–4191.
- K. Uchida, S. Makino, T. Akiyoshi, Altered bile acid metabolism in nonobese, spontaneously diabetic (NOD) mice, *Diabetes* 34 (1985) 79–83.
- B. Cariou, M. Chetiveaux, Y. Zair, E. Pouteau, E. Disse, B. Guyomarc'h-Delassalle,

- M. Laville, M. Krempf, Fasting plasma chenodeoxycholic acid and cholic acid concentrations are inversely correlated with insulin sensitivity in adults, *Nutr. Metab. (Lond.)* 8 (2011) 48.
- [47] M. Wewalka, M.E. Patti, C. Barbato, S.M. Houten, A.B. Goldfine, Fasting serum taurine-conjugated bile acids are elevated in type 2 diabetes and do not change with intensification of insulin, *J. Clin. Endocrinol. Metab.* 99 (2014) 1442–1451.
- [48] D.R. Taylor, J. Alagband-Zadeh, G.F. Cross, S. Omar, C.W. le Roux, R.P. Vincent, Urine bile acids relate to glucose control in patients with type 2 diabetes mellitus and a body mass index below 30 kg/m², *PLoS One* 9 (2014) e93540.
- [49] R.P. Vincent, S. Omar, S. Ghazlan, D.R. Taylor, G. Cross, R.A. Sherwood, L. Fandriks, T. Olbers, M. Werling, J. Alagband-Zadeh, C.W. le Roux, Higher circulating bile acid concentrations in obese patients with type 2 diabetes, *Ann. Clin. Biochem.* 50 (2013) 360–364.
- [50] C. Chen, B. Hu, T. Wu, Y. Zhang, Y. Xu, Y. Feng, H. Jiang, Bile acid profiles in diabetic (db/db) mice and their wild type littermates, *J. Pharm. Biomed. Anal.* 131 (2016) 473–481.
- [51] D.P. Sonne, F.S. van Nierop, W. Kulik, M.R. Soeters, T. Vilsboll, F.K. Knop, Postprandial plasma concentrations of individual bile acids and FGF-19 in patients with type 2 diabetes, *J. Clin. Endocrinol. Metab.* 101 (2016) 3002–3009.
- [52] G.H. Tomkin, Comparison of the effect of parenteral with oral biguanide therapy on vitamin B12 and bile acid absorption, *Ir. J. Med. Sci.* 145 (1976) 340.
- [53] J.H. Scarpello, E. Hodgson, H.C. Howlett, Effect of metformin on bile salt circulation and intestinal motility in type 2 diabetes mellitus, *Diabet. Med.* 15 (1998) 651–656.
- [54] Q. Chen, X. Yang, H. Zhang, X. Kong, L. Yao, X. Cui, Y. Zou, F. Fang, J. Yang, Y. Chang, Metformin impairs systemic bile acid homeostasis through regulating SIRT1 protein levels, *Biochim. Biophys. Acta* 1864 (2017) 101–112.
- [55] H. Wu, E. Esteve, V. Tremaroli, M.T. Khan, R. Caesar, L. Manneras-Holm, M. Stahlman, L.M. Olsson, M. Serino, M. Planas-Felix, G. Xifra, J.M. Mercader, D. Torrents, R. Burcelin, W. Ricart, R. Perkins, J.M. Fernandez-Real, F. Backhed, Metformin alters the gut microbiome of individuals with treatment-naive type 2 diabetes, contributing to the therapeutic effects of the drug, *Nat. Med.* 23 (2017) 850–858.
- [56] D. Carter, H.C. Howlett, N.F. Wiernsperger, C.J. Bailey, Differential effects of metformin on bile salt absorption from the jejunum and ileum, *Diabetes Obes. Metab.* 5 (2003) 120–125.
- [57] S. Fiorucci, E. Distrutti, Bile acid-activated receptors, intestinal microbiota, and the treatment of metabolic disorders, *Trends Mol. Med.* 21 (2015) 702–714.

A.2 Supplementary Information *

Table A.S1 Information on BA standards used for validation and quantification.

No.	Name	Abbreviation	[M - H] ⁻	RT	Salt	Molecular formula	Molecular weight	Internal standard	Supplier	Product number	CAS Number	HMDB ID
1	α -Taurouricolic acid	α TMCA	514.2844	7	Sodium	C ₂₆ H ₄₄ N ₂ O ₇ Na	537.69	d5-TCA	Steraloids	C1889-000		
2	α -Taurouricolic acid	α TMCA	514.2844	7.2	Sodium	C ₂₆ H ₄₄ N ₂ O ₇ Na	537.69	d5-TCA	Steraloids	C1893-000		
3	β -Taurouricolic acid	β TMCA	514.2844	7.3	Sodium	C ₂₆ H ₄₄ N ₂ O ₇ Na	537.69	d5-TCA	Steraloids	C1899-000		HMDB00009832
4	Taurouricolic acid	THCA	514.2844	8.8	Sodium	C ₂₆ H ₄₄ N ₂ O ₇ Na	537.69	d5-TCA	Steraloids	C1887-000		HMDB00011637
5	Tauroursodeoxycholic acid	TUDCA	498.28948	9.3	Sodium	C ₂₆ H ₄₄ N ₂ O ₆ Na	521.69	d4-GDCA	Calbiochem	590549-1GM	14605-22-2	HMDB00008874
6	Glycocholic acid	GHCA	464.30176	9.35	Sodium	C ₂₆ H ₄₂ N ₂ O ₆ Na	487.60	d4-GDCA	Steraloids	C1860-000		HMDB0062157
7	Tauroursodeoxycholic acid	THDCA	498.28948	9.4	Sodium	C ₂₄ H ₄₄ N ₂ O ₆ Na	521.69	d5-TCA	Steraloids	C0892-000	110026-03-4	HMDB000036
8	Taurocholic acid	TCA	514.2844	9.6	Sodium	C ₂₆ H ₄₄ N ₂ O ₇ Na	515.71	d5-TCA	Steraloids	C1965-000	81-24-3	HMDB0000136
9	Glycochenodeoxycholic acid	GDCCA	448.30688	9.8	Sodium	C ₂₆ H ₄₂ N ₂ O ₆ Na	471.61	d4-GDCA	Sigma	G0759-100MG	16564-43-5	HMDB0000898
10	Glycochenodeoxycholic acid	GHCCA	448.30688	9.9	Sodium	C ₂₆ H ₄₂ N ₂ O ₆ Na	471.61	d4-GDCA	Sigma	sc-396740	13042-33-6	HMDB0000138
11	Cholic acid 7-sulfate	CA-7S	487.23711	10	Sodium	C ₂₄ H ₄₀ O ₆ S	488.60	d5-TCA	Santa Cruz	Cay9002532-1	60320-05-0	HMDB0002421
12	Glycocholic acid	GCA	464.30176	10.05	Sodium	C ₂₆ H ₄₃ N ₂ O ₆	465.62	d4-GDCA	Steraloids	C1925-000	475-31-0	HMDB0000138
13	7-epicholic acid	7-epICA	407.2803	10.15	Sodium	C ₂₄ H ₄₀ O ₅	408.57	d4-CA	Santa Cruz	sc-473896	2955-27-3	HMDB0000917
14	7,12-dioxallothricolic acid	7,12-dioxLCA	403.249	10.2	Sodium	C ₂₄ H ₃₆ O ₅	404.54	d4-GDCA	Steraloids	C1500-000	517-33-9	HMDB0000951
15	Tauroursodeoxycholic acid	TUDCA	498.28948	10.8	Sodium	C ₂₆ H ₄₄ N ₂ O ₆ Na	521.69	d4-GDCA	Sigma	T6260-100MG	6009-98-9	HMDB0000951
16	ω -Muricholic acid	ω MCA	407.2803	10.85	Sodium	C ₂₄ H ₄₀ O ₅	408.57	d4-CA	Steraloids	C1888-000	2393-58-0	HMDB0000364
17	α -Muricholic acid	α MCA	407.2803	11	Sodium	C ₂₄ H ₄₀ O ₅	408.57	d4-CA	Steraloids	C1890-000		HMDB0000366
18	Tauroursodeoxycholic acid	TUDCA	498.28948	11.05	Sodium	C ₂₆ H ₄₄ N ₂ O ₆ Na	499.70	d5-TCA	Steraloids	C1160-000		HMDB0000896
19	7-oxodeoxycholic acid	7-oxDCA	405.26465	11.1	Sodium	C ₂₄ H ₃₈ O ₅	406.56	d4-CA	Steraloids	C1250-000	911-40-0	HMDB0000391
20	β -Muricholic acid	β MCA	407.2803	11.15	Sodium	C ₂₄ H ₄₀ O ₅	408.57	d4-CA	Steraloids	C1895-000	2393-59-1	HMDB0000415
21	Glycochenodeoxycholic acid	GHCCA	448.30688	11.25	Sodium	C ₂₆ H ₄₃ N ₂ O ₆	449.62	d4-GDCA	Steraloids	08863-1G	64480-66-6	HMDB0000708
22	Glycochenodeoxycholic acid	GDCCA	448.30688	11.5	Sodium	C ₂₆ H ₄₂ N ₂ O ₆ Na	471.61	d4-GDCA	Calbiochem	361311-5GM	16564-43-5	HMDB0000631
23	Murideoxycholic acid	MDCA	391.28538	11.7	Sodium	C ₂₄ H ₄₀ O ₄	392.57	d4-CA	Steraloids	C0910-000	658-49-5	HMDB0000911
24	Hyocholic acid	HCA	407.2803	11.7	Sodium	C ₂₄ H ₄₀ O ₅	408.57	d4-CA	Steraloids	C1850-000	547-75-1	HMDB0000760
25	3-Dehydrocholic acid	3-dehydroCA	405.26465	11.85	Sodium	C ₂₄ H ₃₈ O ₅	406.56	d4-CA	Steraloids	C1272-000	2304-89-4	HMDB0000592
26	Taurithocholic acid	TLCA	482.29457	12.1	Sodium	C ₂₆ H ₄₄ N ₂ O ₆ Na	505.69	d5-TCA	Sigma	T7515-1G	6042-32-6	HMDB0000722
27	Allocholic acid	alloCA	407.2803	12.1	Sodium	C ₂₄ H ₄₀ O ₅	408.57	d4-CA	Santa Cruz	sc-210779	2464-18-8	HMDB0000605
28	Cholic acid	CA	407.2803	12.15	Sodium	C ₂₄ H ₄₀ O ₅	408.57	d4-CA	Sigma	C1129-25G	81-25-4	HMDB0000619
29	Ursodeoxycholic acid	UDCA	391.28538	12.2	Sodium	C ₂₄ H ₄₀ O ₄	392.57	d4-DCA	Sigma	U6127-1G	128-13-2	HMDB0000946
30	Hyodeoxycholic acid	HDCA	391.28538	12.3	Sodium	C ₂₄ H ₄₀ O ₄	392.57	d4-DCA	Sigma	H8378-5G	83-49-8	HMDB0000733
31	6-oxoallothricolic acid	6-oxo-alloLCA	389.26973	12.6	Sodium	C ₂₄ H ₃₈ O ₄	390.56	d4-DCA	Steraloids	C0720-000	10573-17-8	
32	6,7-dioxallothricolic acid	6,7-dioxLCA	403.249	12.65	Sodium	C ₂₄ H ₃₆ O ₅	404.54	d4-GDCA	Steraloids	C1485-000		
33	Glycolithocholic acid	GLCA	432.31193	12.7	Sodium	C ₂₆ H ₄₂ N ₂ O ₆ Na	455.61	d4-GDCA	Santa Cruz	sc-396741	24404-83-9	HMDB0000698
34	7-oxolithocholic acid	7-oxoLCA	389.26973	12.75	Sodium	C ₂₄ H ₃₆ O ₄	390.56	d4-DCA	Steraloids	C1600-000	4651-67-6	HMDB0000467
35	12-oxolithocholic acid	12-oxoLCA	389.26973	12.9	Sodium	C ₂₄ H ₃₆ O ₄	390.56	d4-DCA	Steraloids	C1650-000	5130-29-0	HMDB0000328
36	Apocholic acid	apoCA	389.26973	13.1	Sodium	C ₂₄ H ₃₈ O ₄	390.56	d4-DCA	Steraloids	C2500-000	641-81-6	
37	3-dehydrochenodeoxycholic acid	3-dehydroCDCA	389.26973	13.6	Sodium	C ₂₄ H ₃₈ O ₄	390.56	d4-DCA	Steraloids	C1706-000		HMDB0000503
38	Chenodeoxycholic acid	CDCA	391.28538	13.65	Sodium	C ₂₄ H ₄₀ O ₄	392.57	d4-DCA	Sigma	C9377-100MG	474-25-9	HMDB0000518
39	Deoxycholic acid	DCA	391.28538	13.9	Sodium	C ₂₄ H ₄₀ O ₄	392.57	d4-DCA	Sigma	D2510-10G	83-44-3	HMDB0000626
40	Allothricolic acid	alloLCA	375.29047	14.2	Sodium	C ₂₄ H ₄₀ O ₃	376.57	d4-DCA	Steraloids	C0700-000	2276-93-9	HMDB0000381
41	lithocholic acid	lithLCA	375.29047	14.6	Sodium	C ₂₄ H ₄₀ O ₃	376.57	d4-DCA	Steraloids	C1475-000	1534-35-6	HMDB0000717
42	7,12-dihydroxy-5 β -cholanic acid	7,12-dihydroxy-5 β -cholanic acid	391.28538	14.85	Sodium	C ₂₄ H ₄₀ O ₄	392.57	d4-DCA	Steraloids	C1170-000	5661-17-6	HMDB00002536
43	3 α -hydroxy-11 β (9 β)-cholanic acid	3 α -hydroxy-11 β (9 β)-cholanic acid	373.27482	14.9	Sodium	C ₂₄ H ₃₈ O ₃	374.56	d4-DCA	Steraloids	C2700-000	1055-37-8	
44	Lithocholic acid	LCA	375.29047	15.4	Sodium	C ₂₄ H ₄₀ O ₃	376.57	d4-DCA	Sigma	L6250-10G	434-13-9	HMDB0000761
45	Dehydrothocholic acid	dehydroLCA	373.27482	15.45	Sodium	C ₂₄ H ₃₈ O ₃	374.56	d4-DCA	Steraloids	C1750-000	1553-56-6	
46	d5-Taurocholic acid	d5-TCA	519.31468	9.6	Sodium	C ₂₆ H ₄₅ H ₉ N ₂ O ₇ Na	542.72		Toronto research chemicals	NC0341860		
47	d4-Glycochenodeoxycholic acid	d4-GDCA	452.33195	11.5	Sodium	C ₂₆ H ₄₃ H ₉ N ₂ O ₆ Na	453.65		Sigma	D-2452		
48	d4-Cholic acid	d4-CA	411.30431	12.15	Sodium	C ₂₄ D ₄ H ₆ O ₅	412.80		Sigma	D-2452		
49	d4-Deoxycholic acid	d4-DCA	395.30939	13.9	Sodium	C ₂₄ D ₄ H ₆ O ₄	396.80		CDN isotopes	D-2941	112076-61-6	

* This chapter was published as [Nina Sillner, Alesia Walker, Wendelin Koch, Michael Witting, Philippe Schmitt-Kopplin. Metformin impacts cecal bile acid profiles in mice. Journal of Chromatography B, 1083, 35–43, Supporting Information. Copyright Elsevier \(2018\).](#)

Table A.S2 Intraday (n = 6) and interday (n = 4) accuracy in RSD% for 45 BAs elaborated by standard addition method with low (0.03 mg/L), medium (0.15 mg/L) and high (0.3 mg/L) spiked quality controls.

No.	BA	Intraday Accuracy %												Interday Accuracy %		
		B0			B1			B2			B3			B0-B3		
		low	medium	high	low	medium	high	low	medium	high	low	medium	high	low	medium	high
1	ωTMCA	96	99	93	27	92	64	80	120	118	133	111	109	84	105	96
2	αTMCA	117	108	90	70	109	74	111	105	106	114	101	108	103	106	95
3	βTMCA	89	104	93	105	97	74	104	108	101	111	110	109	102	105	94
4	THCA	98	109	93	99	99	79	106	116	106	111	110	108	103	109	97
5	TUDCA	96	111	93	77	99	82	106	117	103	101	114	107	95	110	96
6	GHCA	99	104	86	105	115	91	103	112	106	103	114	110	102	111	98
7	THDCA	95	109	93	82	100	81	106	118	105	106	115	105	97	111	96
8	TCA	62	96	90	10	92	76	84	113	105	99	111	115	64	103	96
9	GCDCA	96	108	88	111	105	85	97	115	107	100	111	101	101	110	95
10	GHDCA	97	107	90	117	113	89	99	113	105	107	113	106	105	111	97
11	CA-7S	95	113	87	65	145	86	<LOD	122	104	41	115	113	67	124	98
12	GCA	105	106	89	117	109	87	99	108	105	111	111	110	108	109	98
13	7-epiCA	109	109	90	106	110	89	102	114	103	103	112	116	105	111	99
14	7,12-dioxoLCA	94	109	88	100	119	92	93	114	104	97	113	105	96	114	97
15	TCDCa	75	103	90	105	96	77	104	113	108	103	105	106	97	104	95
16	ωMCA	90	107	88	56	116	87	75	120	105	97	124	117	79	117	99
17	αMCA	77	106	89	80	106	86	103	115	104	118	117	117	94	111	99
18	TDCA	101	108	91	97	100	79	108	109	98	108	110	115	103	107	96
19	7-oxoDCA	96	107	91	98	113	89	106	114	103	104	116	110	101	113	98
20	βMCA	98	111	92	83	110	87	103	119	102	108	118	109	98	114	97
21	GDUDCA	104	108	88	125	112	91	100	107	104	112	111	112	110	110	99
22	GDCA	93	110	83	120	107	81	103	112	105	104	115	113	105	111	95
23	MDCA	103	112	93	104	111	98	111	119	103	108	119	114	107	115	102
24	HCA	113	108	91	93	109	90	109	115	106	118	114	117	108	112	101
25	3-dehydroCA	109	105	89	111	105	84	108	114	106	107	113	113	109	109	98
26	TLCA	95	105	91	107	105	82	109	109	104	108	106	108	105	106	96
27	alloCA	103	117	100	83	101	79	106	109	104	103	104	102	99	108	96
28	CA	89	99	84	104	108	85	98	100	98	97	108	110	97	104	94
29	UDCA	107	110	94	100	103	88	107	121	108	107	122	111	105	114	100
30	HDCA	92	113	96	93	106	92	101	122	106	101	119	107	97	115	100
31	6-oxo-alloLCA	96	113	94	103	113	93	104	119	104	100	118	105	101	116	99
32	6,7-dioxoLCA	94	109	89	112	112	88	94	113	103	93	110	103	98	111	96
33	GLCA	95	109	89	108	102	78	98	116	107	96	115	103	99	111	94
34	7-oxoLCA	91	112	93	100	109	93	103	117	103	101	116	106	99	113	99
35	12-oxoLCA	102	109	95	91	108	94	96	119	106	104	117	106	98	113	100
36	apoCA	106	107	92	108	106	89	106	115	107	108	114	108	107	110	99
37	3-dehydroCDCA	104	114	96	98	110	94	99	120	108	112	119	111	103	116	102
38	CDCA	92	109	94	99	107	93	91	117	108	111	120	113	98	113	102
39	DCA	66	98	90	49	98	78	59	122	113	52	121	121	57	110	100
40	alloLCA	86	114	94	93	116	95	99	118	102	104	116	105	96	116	99
41	isoLCA	91	112	94	94	114	97	100	117	103	105	116	106	98	115	100
42	7,12α-dihydroxy-5β-cholanic acid	104	108	93	98	109	92	102	116	107	109	116	108	103	112	100
43	Lithochol-11-enoic acid	92	112	94	97	113	95	99	117	105	100	116	107	97	115	100
44	LCA	96	112	95	96	114	96	94	115	104	105	122	112	98	116	102
45	dehydroLCA	98	112	94	99	114	97	94	116	105	101	118	108	98	115	101

Table A.S2 (continued) Intraday (n = 6) and interday (n = 4) precision in RSD% for 45 BAs elaborated by standard addition method with low (0.03 mg/L), medium (0.15 mg/L) and high (0.3 mg/L) spiked quality controls.

No.	BA	Intraday Precision %												Interday Precision %		
		B0			B1			B2			B3			B0-B3		
		low	medium	high	low	medium	high	low	medium	high	low	medium	high	low	medium	high
1	ωTMCA	40.4	19.0	13.2	97.6	20.4	62.0	22.1	7.0	13.9	16.2	6.4	6.6	44.1	13.2	24.0
2	αTMCA	7.5	12.9	6.8	60.4	18.4	24.1	8.9	2.6	12.7	9.7	4.7	3.1	21.6	4.7	11.7
3	βTMCA	33.5	23.6	12.4	31.4	20.9	9.3	9.6	1.4	12.2	14.5	4.5	2.2	22.2	12.6	9.0
4	THCA	5.0	21.2	7.3	30.0	19.6	12.3	5.4	3.2	10.4	5.9	3.9	6.5	11.6	12.0	9.1
5	TUDCA	3.2	18.7	9.3	39.4	14.7	21.2	6.8	3.3	9.8	4.6	5.4	8.1	13.5	10.5	12.1
6	GHCA	4.3	17.7	7.1	22.2	18.9	7.6	3.7	3.2	12.3	6.1	2.4	7.7	9.1	10.5	8.7
7	THDCA	2.0	20.1	9.4	45.5	16.0	17.4	4.3	2.5	9.6	10.0	2.4	6.3	15.5	10.3	10.7
8	TCA	155.8	17.2	10.9	<LOD	16.0	17.7	20.2	5.6	12.3	30.1	6.5	7.7	68.7	11.3	12.2
9	GCDCA	9.2	18.1	8.6	19.7	17.1	3.4	3.7	3.8	11.9	5.6	3.7	7.0	9.5	10.7	7.7
10	GHDCA	4.4	17.0	7.0	20.2	16.8	19.3	4.0	4.2	12.0	4.7	3.0	6.6	8.3	10.3	11.2
11	CA-7S	97.3	7.1	14.9	138.0	3.2	54.6	<LOD	9.2	13.0	115.6	16.0	14.2	117.0	8.9	24.2
12	GCA	3.2	18.1	8.3	19.3	18.9	7.1	5.0	3.4	12.5	7.4	4.4	5.2	8.7	11.2	8.3
13	7-epiCA	8.9	15.8	4.6	26.1	19.7	24.6	5.1	2.3	11.6	9.9	4.5	9.3	12.5	10.5	12.5
14	7,12-dioxoLCA	15.1	17.4	7.3	44.4	16.8	19.4	9.5	4.4	11.8	6.4	2.7	6.5	18.8	10.3	11.2
15	TCDCa	45.9	22.1	8.1	25.0	18.6	8.4	3.5	5.3	12.1	7.8	5.4	10.2	20.6	12.8	9.7
16	ωMCA	52.8	8.7	7.0	122.8	17.0	51.6	36.1	9.8	11.6	28.8	10.6	10.3	60.1	11.6	20.1
17	αMCA	33.3	14.0	6.9	64.3	20.0	32.0	14.3	3.9	10.6	9.1	5.8	11.7	30.2	10.9	15.3
18	TDCA	8.8	19.8	9.6	29.3	16.4	16.5	3.9	2.5	10.9	10.2	4.1	10.6	13.1	10.7	11.9
19	7-oxoDCA	3.2	17.0	5.1	29.7	21.3	6.9	6.0	1.3	9.8	8.7	6.0	11.2	11.9	11.4	8.2
20	βMCA	3.0	13.3	3.9	62.8	17.2	45.7	8.0	4.9	9.8	7.8	2.7	12.9	20.4	9.5	18.0
21	GDUDCA	6.4	19.2	7.8	17.3	19.0	22.8	3.0	2.6	13.2	3.9	3.5	9.0	7.6	11.1	13.2
22	GDCA	10.0	18.5	4.2	19.5	18.0	15.0	7.1	2.3	12.4	4.6	5.5	7.3	10.3	11.1	9.7
23	MDCA	7.3	15.9	2.0	44.0	22.1	18.5	6.6	3.2	11.1	14.9	3.1	6.2	18.2	11.1	9.4
24	HCA	14.7	16.8	5.3	33.3	19.1	25.9	11.2	3.9	11.1	6.0	2.9	8.8	16.3	10.7	12.8
25	3-dehydroCA	0.8	17.9	7.1	27.4	21.1	47.6	6.0	1.9	10.2	9.8	5.0	9.8	11.0	11.5	18.7
26	TLCA	29.7	21.3	10.6	27.2	18.2	9.4	2.2	4.0	10.8	3.0	3.3	6.2	15.6	11.7	9.3
27	alloCA	23.5	14.1	9.2	76.1	18.0	122.5	14.5	6.0	9.7	15.2	4.1	3.8	32.3	10.5	36.3
28	CA	2.8	19.5	7.1	28.1	23.6	24.6	9.2	1.6	10.9	6.1	3.4	3.4	11.5	12.0	11.5
29	UDCA	1.2	17.7	6.7	37.3	22.6	13.3	5.2	4.0	10.0	9.2	2.2	4.0	13.2	11.6	8.5
30	HDCA	9.3	18.2	5.2	45.0	20.8	27.7	6.5	4.9	10.4	17.7	4.2	5.2	19.6	12.0	12.1
31	6-oxo-alloLCA	2.3	17.7	5.3	37.4	19.0	29.2	4.9	2.8	10.1	6.9	1.2	6.2	12.9	10.1	12.7
32	6,7-dioxoLCA	7.0	19.0	9.2	24.8	16.6	21.6	4.3	3.7	12.6	5.0	3.7	3.9	10.3	10.8	11.8
33	GLCA	1.9	18.1	11.7	21.3	16.2	2.7	3.4	4.8	11.3	4.0	2.7	4.0	7.6	10.4	7.4
34	7-oxoLCA	7.1	19.1	5.0	34.5	21.3	15.9	5.3	2.6	10.0	10.1	2.2	6.5	14.3	11.3	9.3
35	12-oxoLCA	2.4	17.4	5.8	42.9	19.9	30.6	8.2	3.7	11.1	10.7	3.7	5.5	16.0	11.2	13.2
36	apoCA	2.6	18.9	8.4	28.1	20.5	9.2	2.9	1.8	10.2	8.2	2.2	5.0	10.5	10.8	8.2
37	3-dehydroCDCA	10.0	19.9	5.9	37.2	19.9	15.9	10.0	1.8	10.3	16.5	3.6	4.2	18.4	11	

Table A.S3 Endogenous concentrations ($\mu\text{mol/g}$) of BAs in cecum of wild type mice (wt; n = 10) after 1D treatment (vehicle).

No.	BA	wt										Median	25% quantile	75% quantile
		1	2	3	4	5	6	7	8	9	10			
1	ω TMCA	1.34	0.50	0.28	0.62	0.10	0.17	0.18	0.10	0.41	0.15	0.23	0.15	0.48
2	α TMCA	0.13	0.07	0.04	0.04	0.02	0.03	0.03	0.02	0.03	0.02	0.03	0.02	0.04
3	β TMCA	0.85	0.43	0.10	0.20	0.03	0.05	0.05	0.03	0.14	0.08	0.09	0.05	0.19
5	TUDCA	0.05	0.01	0.00	0.00	< LOD	0.00	0.00	< LOD	0.00	0.00	0.00	0.00	0.00
8	TCA	0.51	0.19	0.06	0.09	0.04	0.05	0.05	0.03	0.07	0.04	0.05	0.04	0.08
11	CA-7S	0.06	0.06	0.12	0.44	0.17	0.48	0.57	0.14	0.17	0.31	0.17	0.13	0.41
13	7-epiCA	0.01	0.01	0.01	0.01	0.01	0.01	0.01	0.01	0.01	0.01	0.01	0.01	0.01
15	TCDCa	0.01	0.00	0.00	0.00	0.00	0.00	0.00	0.00	0.00	0.00	0.00	0.00	0.00
16	ω MCA	0.54	0.10	0.57	0.74	0.17	0.55	0.37	0.29	0.57	0.38	0.46	0.31	0.56
17	α MCA	0.18	0.07	0.07	0.28	0.08	0.10	0.10	< LOD	0.05	< LOD	0.09	0.07	0.12
18	TDCA	0.13	0.07	0.06	0.10	0.04	0.04	0.04	0.03	0.05	0.04	0.04	0.04	0.07
19	7-oxoDCA	0.01	0.01	0.01	0.00	0.00	0.00	0.00	0.01	0.00	0.00	0.00	0.00	0.01
20	β MCA	0.32	0.15	0.08	0.43	0.04	0.03	0.03	0.03	0.10	0.03	0.06	0.03	0.14
25	3-dehydroCA	0.00	< LOD	0.00	< LOD	< LOD	< LOD	< LOD	< LOD	< LOD	< LOD	0.00	0.00	0.00
27	alloCA	0.30	0.18	0.18	0.34	0.08	0.13	0.12	0.11	0.17	0.10	0.15	0.11	0.18
28	CA	< LOD	< LOD	< LOD	< LOD	< LOD	< LOD	< LOD	< LOD	< LOD	< LOD	-	-	-
30	HDCA	0.04	0.00	0.03	0.07	0.01	0.04	0.02	0.02	0.02	0.02	0.02	0.02	0.03
35	12-oxoLCA	0.05	0.05	0.06	0.04	0.04	0.04	0.04	0.04	0.04	0.05	0.04	0.04	0.05
37	3-dehydroCDCA	0.08	0.07	0.10	0.07	0.06	0.05	0.06	0.05	0.06	0.06	0.06	0.06	0.07
39	DCA	0.41	0.18	0.29	0.73	0.21	0.13	0.12	0.11	0.16	0.12	0.17	0.12	0.27
Total concentration ($\mu\text{mol/g}$)		5.01	2.17	2.07	4.21	1.11	1.89	1.78	1.02	2.05	1.42	1.97	1.51	2.15
% uBAs		38.42	38.05	68.11	64.34	63.70	56.78	48.86	65.58	57.25	54.69	63.27		
% TBAs		60.46	59.01	26.01	25.23	21.07	17.64	19.41	21.08	34.69	23.49	26.83		
% SBAs		1.12	2.94	5.88	10.43	15.23	25.58	31.72	13.34	8.06	21.82	9.91		
% primary BAs		47.91	54.03	31.43	43.61	41.76	45.91	52.68	35.44	36.16	41.57	38.30		
% secondary BAs		52.09	45.97	68.57	56.39	58.24	54.09	47.32	64.56	63.84	58.43	61.70		

Table A.S3 (continued) Endogenous concentrations ($\mu\text{mol/g}$) of BAs in cecum of diabetic mice (*db/db*, n = 10) after 1D treatment (vehicle).

No.	BA	<i>db/db</i>										Median	25% quantile	75% quantile
		1	2	3	4	5	6	7	8	9	10			
1	ω TMCA	0.27	0.12	0.50	0.19	0.20	1.27	0.58	0.21	0.06	0.33	0.24	0.19	0.46
2	α TMCA	0.03	0.04	0.22	0.07	0.03	0.18	0.10	0.07	0.03	0.07	0.07	0.03	0.10
3	β TMCA	0.08	0.04	0.53	0.13	0.07	0.82	0.37	0.19	0.03	0.36	0.16	0.07	0.37
5	TUDCA	0.00	< LOD	0.01	0.00	0.00	0.02	0.01	0.01	< LOD	0.01	0.01	0.00	0.01
8	TCA	0.08	0.12	1.27	0.19	0.08	1.39	0.55	0.25	0.07	0.62	0.22	0.09	0.60
11	CA-7S	0.06	0.48	0.17	0.29	0.29	0.14	0.09	0.04	0.23	0.07	0.15	0.07	0.27
13	7-epiCA	0.00	0.01	0.01	0.01	0.01	0.01	0.00	0.00	0.00	0.00	0.00	0.00	0.01
15	TCDCa	0.00	0.00	0.03	0.01	0.00	0.03	0.02	0.01	0.00	0.03	0.01	0.00	0.03
16	ω MCA	0.26	0.07	0.09	0.11	0.32	0.29	0.07	0.02	0.06	< LOD	0.09	0.07	0.26
17	α MCA	0.02	0.09	0.03	0.10	0.09	< LOD	0.09	0.09	0.09	0.06	0.09	0.06	0.09
18	TDCA	0.07	0.05	0.09	0.10	0.05	0.14	0.08	0.05	0.04	0.06	0.06	0.05	0.09
19	7-oxoDCA	0.00	0.01	0.03	0.01	0.00	0.09	0.01	0.00	0.00	0.00	0.01	0.00	0.01
20	β MCA	0.04	0.04	0.05	0.07	0.03	0.07	0.05	0.03	0.03	0.04	0.04	0.04	0.05
25	3-dehydroCA	< LOD	0.00	0.01	< LOD	0.00	0.00	0.00	< LOD	0.00	< LOD	0.00	0.00	0.00
27	alloCA	0.15	0.08	0.05	0.08	0.09	0.16	0.12	0.07	0.06	0.07	0.08	0.07	0.11
28	CA	< LOD	0.06	0.29	0.07	0.04	0.32	0.09	0.06	0.06	0.07	0.07	0.06	0.09
30	HDCA	0.01	0.01	0.01	0.02	0.02	0.01	0.01	0.01	0.01	0.01	0.01	0.01	0.01
35	12-oxoLCA	0.06	0.05	0.05	0.08	0.06	0.05	0.05	0.05	0.05	0.05	0.05	0.05	0.06
37	3-dehydroCDCA	0.08	0.09	0.09	0.13	0.11	0.06	0.07	0.07	0.07	0.07	0.08	0.07	0.09
39	DCA	0.59	0.26	0.38	0.47	0.33	0.42	0.30	0.15	0.16	0.15	0.32	0.19	0.41
Total concentration ($\mu\text{mol/g}$)		1.81	1.61	3.92	2.09	1.83	5.47	2.68	1.38	1.07	2.07	1.95	1.66	2.53
% uBAs		67.13	47.11	27.96	53.87	60.20	26.95	32.29	40.33	56.43	25.32	47.34		
% TBAs		29.51	22.88	67.77	32.48	23.85	70.52	64.22	56.83	22.37	71.47	43.94		
% SBAs		3.36	30.01	4.27	13.65	15.95	2.53	3.49	2.85	21.19	3.21	8.71		
% primary BAs		25.88	59.45	67.60	47.36	39.91	57.41	56.15	59.34	55.93	67.56	50.86		
% secondary BAs		74.12	40.55	32.40	52.64	60.09	42.59	43.85	40.66	44.07	32.44	49.14		

Table A.S3 (continued) Endogenous concentrations ($\mu\text{mol/g}$) of BAs in cecum of metformin treated *db/db* mice (*db/db* metformin, $n = 9$) after 1D treatment.

No.	BA	<i>db/db</i> metformin									Median	25% quantile	75% quantile
		1	2	3	4	5	6	7	8	9			
1	ω TMCA	1.65	0.93	0.45	0.36	1.81	0.35	1.53	0.66	0.54	0.66	0.45	1.53
2	α TMCA	0.35	0.26	0.10	0.16	0.71	0.17	0.48	0.42	0.14	0.26	0.16	0.42
3	β TMCA	1.08	0.79	0.26	0.21	1.12	0.24	1.38	0.61	0.44	0.61	0.26	1.08
5	TUDCA	0.03	0.03	0.01	0.00	0.11	0.01	0.06	0.02	0.02	0.02	0.01	0.03
8	TCA	2.00	1.28	0.33	0.26	3.43	0.53	2.23	1.39	0.66	1.28	0.53	2.00
11	CA-7S	0.08	0.04	0.28	0.17	0.07	0.49	0.08	0.15	0.07	0.08	0.07	0.17
13	7-epiCA	0.01	0.01	0.02	0.03	0.02	0.02	0.02	0.02	0.01	0.02	0.01	0.02
15	TCDCa	0.07	0.04	0.01	0.01	0.18	0.02	0.08	0.04	0.02	0.04	0.02	0.07
16	ω MCA	0.57	0.20	0.40	0.57	0.69	0.52	0.26	0.64	0.26	0.52	0.26	0.57
17	α MCA	0.14	0.02	0.12	0.33	0.23	0.25	0.03	0.23	0.09	0.14	0.09	0.23
18	TDCa	0.31	0.13	0.12	0.13	0.28	0.26	0.27	0.19	0.07	0.19	0.13	0.27
19	7-oxoDCA	0.26	0.09	0.11	0.35	0.29	0.23	0.24	0.51	0.47	0.26	0.23	0.35
20	β MCA	0.29	0.06	0.06	0.31	0.27	0.11	0.31	0.34	0.25	0.27	0.11	0.31
25	3-dehydroCA	0.01	0.01	0.00	0.02	0.06	0.01	0.01	0.04	0.04	0.01	0.01	0.04
27	alloCA	0.16	0.12	0.15	0.12	0.05	0.07	0.12	0.15	0.09	0.12	0.09	0.15
28	CA	1.04	0.40	0.26	0.60	3.04	0.32	0.43	1.40	0.49	0.49	0.40	1.04
30	HDCA	0.02	0.01	0.02	0.01	0.02	0.02	0.01	0.00	0.01	0.01	0.01	0.02
35	12-oxoLCA	0.05	0.05	0.04	0.07	0.05	0.17	0.06	0.04	0.04	0.05	0.04	0.06
37	3-dehydroCDCA	0.07	0.08	0.07	0.05	0.06	0.29	0.08	0.05	0.05	0.07	0.05	0.08
39	DCA	0.72	0.31	0.52	0.61	0.39	1.22	0.64	0.33	0.15	0.52	0.33	0.64
Total concentration ($\mu\text{mol/g}$)		8.92	4.84	3.31	4.36	12.89	5.32	8.33	7.23	3.91	5.32	4.36	8.33
% uBAs		37.54	27.72	53.12	70.14	40.14	60.98	26.71	51.76	49.90	44.17		
% TBAs		61.53	71.54	38.35	26.03	59.32	29.81	72.37	46.11	48.23	54.36		
% SBA		0.93	0.73	8.53	3.83	0.55	9.22	0.92	2.13	1.88	1.47		
% primary BAs		58.90	62.69	47.52	49.76	71.52	41.60	62.42	65.75	58.21	58.81		
% secondary BAs		41.10	37.31	52.48	50.24	28.48	58.40	37.58	34.25	41.79	41.19		

Table A.S3 (continued) Ratios of bile acid (BA) concentrations ($\mu\text{mol/g}$) in wild type (*wt*; $n = 10$), diabetic (*db/db*, $n = 10$) and metformin treated *db/db* mice (*db/db* metformin; $n = 9$) after 1D treatment.

No.	BA	$\mu\text{mol/g}$ ratio		
		<i>db/db</i> /wt	<i>db/db</i> metformin/wt	<i>db/db</i> metformin/ <i>db/db</i>
1	ω TMCA	1.041	2.864	2.752
2	α TMCA	2.158	8.406	3.896
3	β TMCA	1.832	6.925	3.780
5	TUDCA	4.165	8.129	1.952
8	TCA	4.006	23.501	5.867
11	CA-7S	0.915	0.497	0.543
13	7-epiCA	0.689	2.835	4.115
15	TCDCa	5.772	23.517	4.075
16	ω MCA	0.192	1.148	5.977
17	α MCA	0.957	1.600	1.672
18	TDCa	1.498	4.386	2.929
19	7-oxoDCA	1.313	59.094	45.018
20	β MCA	0.685	4.429	6.469
25	3-dehydroCA	0.780	6.353	8.142
27	alloCA	0.537	0.776	1.444
28	CA	-	-	7.469
30	HDCA	0.510	0.744	1.460
35	12-oxoLCA	1.130	1.077	0.953
37	3-dehydroCDCA	1.254	1.060	0.845
39	DCA	1.876	3.063	1.633
Total concentration ($\mu\text{mol/g}$)		0.991	2.702	2.727
% uBAs		0.748	0.698	0.933
% TBAs		1.638	2.026	1.237
% SBA		0.880	0.149	0.169
% primary BAs		1.328	1.535	1.156
% secondary BAs		0.796	0.668	0.838

Table A.S4 Endogenous concentrations ($\mu\text{mol/g}$) of BAs in cecum of wild type mice (wt; n = 10) after 14D treatment (vehicle).

No.	BA	wt										Median	25% quantile	75% quantile
		1	2	3	4	5	6	7	8	9	10			
1	ω TMCA	0.29	0.02	0.02	0.60	0.27	0.58	0.70	0.71	1.19	0.21	0.43	0.23	0.68
2	α TMCA	0.02	0.01	0.00	0.04	0.03	0.05	0.06	0.05	0.09	0.02	0.03	0.02	0.05
3	β TMCA	0.15	0.01	0.02	0.16	0.19	0.20	0.24	0.31	0.47	0.13	0.17	0.14	0.23
5	TUDCA	0.01	0.00	0.00	0.01	0.02	0.00	0.00	0.01	0.02	0.01	0.01	0.00	0.01
8	TCA	0.06	0.01	0.01	0.06	0.15	0.05	0.04	0.05	0.15	0.03	0.05	0.03	0.06
11	CA-7S	0.13	2.59	3.17	0.20	0.13	0.35	0.80	0.05	0.06	0.02	0.16	0.07	0.69
13	7-epiCA	0.01	0.00	0.00	0.01	0.00	0.01	0.01	0.01	0.01	0.00	0.01	0.00	0.01
15	TCDCa	0.00	0.00	0.00	0.00	0.01	0.00	0.00	0.00	0.01	0.00	0.00	0.00	0.00
16	ω MCA	0.27	0.35	0.36	0.86	0.28	0.78	1.01	0.44	0.24	0.17	0.36	0.27	0.69
17	α MCA	0.06	0.05	0.14	0.14	0.04	0.27	0.27	0.07	0.08	0.06	0.07	0.06	0.14
18	TDCA	0.01	0.00	0.00	0.02	0.01	0.03	0.03	0.03	0.04	0.01	0.02	0.01	0.03
19	7-oxoDCA	0.00	0.01	0.00	0.02	0.00	0.01	0.00	0.01	0.02	0.01	0.01	0.00	0.01
20	β MCA	0.08	0.03	0.20	0.16	0.09	0.30	0.18	0.18	0.29	0.08	0.17	0.09	0.20
25	3-dehydroCA	0.00	0.00	0.00	< LOD	0.00	< LOD	0.00	< LOD	0.00	< LOD	0.00	0.00	0.00
27	alloCA	0.07	0.01	0.07	0.27	0.07	0.13	0.15	0.12	0.19	0.04	0.10	0.07	0.14
28	CA	0.00	< LOD	0.00	< LOD	0.00	< LOD	< LOD	< LOD	0.06	< LOD	0.00	0.00	0.02
30	HDCA	0.02	0.02	0.01	0.04	0.01	0.03	0.08	0.02	0.03	0.02	0.02	0.02	0.03
35	12-oxoLCA	0.01	0.02	0.01	0.07	< LOD	< LOD	< LOD	0.02	< LOD	0.02	0.02	0.01	0.02
37	3-dehydroCDCA	0.05	0.06	0.05	0.11	0.03	0.09	< LOD	0.06	0.06	0.07	0.06	0.05	0.07
39	DCA	0.06	0.08	0.10	0.23	0.14	0.27	0.25	0.16	0.22	0.09	0.15	0.10	0.23
Total concentration ($\mu\text{mol/g}$)		1.28	3.28	4.19	2.97	1.48	3.15	3.83	2.29	3.21	1.00	3.06	1.68	3.26
% uBAs		48.50	19.63	22.98	63.51	45.88	59.93	51.05	47.20	37.15	56.09	52.27		
% TBAs		41.35	1.49	1.28	29.91	45.50	29.09	28.07	50.51	61.07	41.57	38.88		
% SBA		10.15	78.88	75.74	6.58	8.63	10.98	20.88	2.29	1.78	2.34	8.84		
% primary BAs		44.05	82.40	86.36	34.32	47.78	42.81	45.09	36.50	43.21	38.84	41.70		
% secondary BAs		55.41	17.58	13.62	65.47	51.05	57.04	54.83	63.03	56.18	60.54	58.30		

Table A.S4 (continued) Endogenous concentrations ($\mu\text{mol/g}$) of BAs in cecum of diabetic mice (*db/db*, n = 10) after 14D treatment (vehicle).

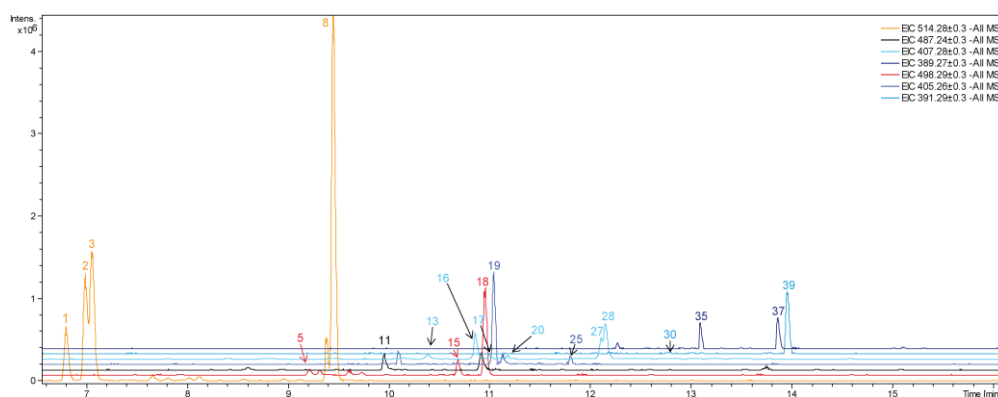
No.	BA	<i>db/db</i>										Median	25% quantile	75% quantile
		1	2	3	4	5	6	7	8	9	10			
1	ω TMCA	0.14	0.10	0.09	0.05	0.03	0.03	0.08	0.04	0.07	0.13	0.07	0.04	0.10
2	α TMCA	0.02	0.01	0.01	0.01	0.01	0.01	0.02	0.01	0.01	0.02	0.01	0.01	0.02
3	β TMCA	0.04	0.04	0.04	0.03	0.01	0.01	0.04	0.01	0.04	0.04	0.04	0.02	0.04
5	TUDCA	0.00	0.00	0.00	0.00	0.00	0.00	0.00	0.00	0.00	0.00	0.00	0.00	0.00
8	TCA	0.04	0.06	0.05	0.09	0.02	0.03	0.10	0.02	0.09	0.09	0.05	0.04	0.09
11	CA-7S	0.09	0.05	0.14	0.05	2.09	0.05	0.06	0.44	0.15	0.05	0.07	0.05	0.15
13	7-epiCA	0.01	0.00	0.00	0.00	0.00	0.00	0.00	0.01	0.01	0.01	0.00	0.00	0.01
15	TCDCa	0.00	0.00	0.00	0.00	0.00	0.00	0.00	0.00	0.00	0.00	0.00	0.00	0.00
16	ω MCA	0.10	0.03	0.10	0.04	0.04	0.03	0.06	0.04	< LOD	0.04	0.04	0.04	0.06
17	α MCA	0.04	0.04	0.07	0.05	0.06	0.04	0.06	0.05	0.05	0.07	0.05	0.04	0.06
18	TDCA	0.02	0.00	0.01	0.00	0.00	0.00	0.01	0.01	0.01	0.01	0.01	0.00	0.01
19	7-oxoDCA	0.01	0.00	0.01	0.00	0.00	0.00	0.00	0.00	0.00	0.00	0.00	0.00	0.00
20	β MCA	0.02	0.03	0.04	0.03	0.04	0.02	0.04	0.03	0.02	0.03	0.03	0.02	0.03
25	3-dehydroCA	< LOD	< LOD	< LOD	< LOD	0.00	< LOD	< LOD	< LOD	< LOD	< LOD	0.00	0.00	0.00
27	alloCA	0.05	0.01	0.00	0.00	< LOD	0.00	0.01	0.01	0.02	0.03	0.01	0.00	0.02
28	CA	< LOD	< LOD	< LOD	< LOD	0.02	< LOD	< LOD	< LOD	< LOD	0.00	0.01	0.01	0.02
30	HDCA	0.01	0.01	0.01	0.01	0.01	0.01	0.01	0.02	0.01	0.02	0.01	0.01	0.01
35	12-oxoLCA	< LOD	0.01	< LOD	0.01	0.02	0.01	0.02	0.01	< LOD	< LOD	0.01	0.01	0.02
37	3-dehydroCDCA	0.05	0.04	0.07	0.05	0.06	0.04	0.06	0.05	< LOD	< LOD	0.05	0.05	0.06
39	DCA	0.30	0.07	0.10	0.10	0.14	0.06	0.11	0.11	0.24	0.23	0.11	0.10	0.20
Total concentration ($\mu\text{mol/g}$)		0.94	0.52	0.74	0.53	2.54	0.36	0.67	0.87	0.73	0.79	0.73	0.56	0.85
% uBAs		62.44	46.98	53.83	55.61	15.18	61.11	55.61	39.95	47.89	54.65	56.83		
% TBAs		27.56	43.20	27.64	35.84	2.67	24.18	36.01	10.05	30.98	38.61	30.83		
% SBA		10.00	9.82	18.53	8.55	82.15	14.70	8.37	50.00	21.13	6.74	12.34		
% primary BAs		32.75	46.97	46.42	48.85	88.23	47.32	49.16	66.47	53.51	43.99	47.37		
% secondary BAs		67.03	52.75	53.38	50.80	11.75	52.52	50.60	33.47	46.21	55.73	52.63		

Table A.S4 (continued) Endogenous concentrations ($\mu\text{mol/g}$) of BAs in cecum of metformin treated *db/db* mice (*db/db* metformin, $n = 9$) after 14D treatment.

No.	BA	<i>db/db</i> metformin										Median	25% quantile	75% quantile
		1	2	3	4	5	6	7	8	9	10			
1	ω TMCA	0.02	0.04	0.05	0.02	0.04	0.07	0.03	0.05	0.14	0.04	0.04	0.03	0.05
2	α TMCA	0.01	0.01	0.02	0.01	0.01	0.02	0.01	0.01	0.02	0.02	0.01	0.01	0.02
3	β TMCA	0.01	0.02	0.03	0.03	0.01	0.05	0.04	0.02	0.02	0.04	0.03	0.02	0.04
5	TUDCA	0.00	0.00	0.00	0.00	0.00	0.00	0.00	0.00	0.00	0.00	0.00	0.00	0.00
8	TCA	0.02	0.05	0.07	0.04	0.03	0.07	0.06	0.03	0.03	0.10	0.04	0.03	0.06
11	CA-7S	0.39	0.17	0.24	0.11	0.52	0.09	0.17	0.12	0.27	0.04	0.17	0.11	0.26
13	7-epiCA	0.00	0.01	0.00	0.00	0.01	0.00	0.00	0.01	0.01	0.00	0.00	0.00	0.01
15	TCDCa	0.00	0.00	0.00	0.00	0.00	0.00	0.00	0.00	0.00	0.01	0.00	0.00	0.00
16	ω MCA	< LOD	< LOD	< LOD	0.04	0.05	0.06	0.05	0.06	0.08	0.06	0.06	0.05	0.06
17	α MCA	0.05	0.06	0.04	0.05	0.06	0.05	0.05	0.06	0.06	0.07	0.05	0.05	0.06
18	TDCA	0.00	0.01	0.01	0.01	0.01	< LOD	0.01	0.01	0.02	0.00	0.01	0.01	0.01
19	7-oxoDCA	0.00	0.00	0.00	0.00	0.01	0.01	0.00	0.00	0.01	0.01	0.00	0.00	0.01
20	β MCA	0.02	0.04	0.03	0.04	0.04	0.04	0.04	0.04	0.04	0.05	0.04	0.04	0.04
25	3-dehydroCA	< LOD	< LOD	< LOD	< LOD	< LOD	0.00	< LOD	< LOD	< LOD	0.00	0.00	0.00	0.00
27	alloCA	0.02	0.00	0.01	0.01	0.01	< LOD	0.00	0.02	0.02	< LOD	0.01	0.01	0.02
28	CA	< LOD	< LOD	< LOD	< LOD	0.00	0.07	< LOD	< LOD	< LOD	0.09	0.07	0.04	0.08
30	HDCA	0.01	0.02	0.01	0.01	0.02	0.00	0.01	0.01	0.03	0.01	0.01	0.01	0.02
35	12-oxoLCA	0.01	0.02	0.02	0.01	0.02	< LOD	0.01	0.02	0.02	< LOD	0.02	0.01	0.02
37	3-dehydroCDCA	0.04	0.06	0.05	0.05	0.06	< LOD	0.05	0.05	0.08	< LOD	0.05	0.05	0.06
39	DCA	0.08	0.14	0.12	0.08	0.13	< LOD	0.06	0.09	0.18	0.04	0.09	0.08	0.13
Total concentration ($\mu\text{mol/g}$)		0.70	0.64	0.70	0.53	1.02	0.54	0.59	0.58	1.03	0.59	0.61	0.59	0.70
% uBAs		35.44	53.32	41.18	57.57	39.58	45.21	47.20	59.91	51.05	55.98	57.79		
% TBAs		8.85	19.72	25.09	21.38	9.16	38.16	24.60	19.05	23.05	37.98	18.52		
% SBA		55.70	26.96	33.73	21.05	51.26	16.63	28.20	21.04	25.89	6.03	23.70		
% primary BAs		74.39	54.71	61.71	55.91	67.62	72.31	63.41	49.11	44.47	70.68	60.03		
% secondary BAs		25.56	45.18	37.97	43.82	32.33	27.00	36.23	50.68	55.44	28.90	39.97		

Table A.S4 (continued) Ratios of bile acid (BA) concentrations ($\mu\text{mol/g}$) in wild type (*wt*; $n = 10$), diabetic (*db/db*, $n = 10$) and metformin treated *db/db* mice (*db/db* metformin; $n = 9$) after 14D treatment.

No.	BA	$\mu\text{mol/g}$ ratio		
		<i>db/db</i> /wt	<i>db/db</i> metformin/wt	<i>db/db</i> metformin/ <i>db/db</i>
1	ω TMCA	0.171	0.098	0.572
2	α TMCA	0.393	0.330	0.839
3	β TMCA	0.226	0.148	0.655
5	TUDCA	0.248	0.206	0.831
8	TCA	1.022	0.884	0.865
11	CA-7S	0.461	1.040	2.256
13	7-epiCA	0.620	0.644	1.037
15	TCDCa	1.020	0.798	0.782
16	ω MCA	0.120	0.161	1.339
17	α MCA	0.732	0.746	1.019
18	TDCA	0.330	0.328	0.994
19	7-oxoDCA	0.610	0.756	1.238
20	β MCA	0.182	0.230	1.267
25	3-dehydroCA	1.064	2.240	2.106
27	alloCA	0.102	0.118	1.151
28	CA	2.822	16.948	6.006
30	HDCA	0.403	0.440	1.093
35	12-oxoLCA	0.760	0.946	1.245
37	3-dehydroCDCA	0.895	0.871	0.973
39	DCA	0.738	0.588	0.797
Total concentration ($\mu\text{mol/g}$)		0.240	0.201	0.837
% uBAs		1.087	1.105	1.017
% TBAs		0.793	0.476	0.601
% SBA		1.396	2.679	1.920
% primary BAs		1.136	1.440	1.267
% secondary BAs		0.903	0.686	0.759

**Figure A.S1** Extracted ion chromatograms of 20 quantified endogenous BAs in mouse cecum. Numbers refer to Table A.S1.

B. Appendix Chapter 3

B.1 Original Publication

Journal of Chromatography B 1109 (2019) 142–148



Contents lists available at ScienceDirect

Journal of Chromatography B

journal homepage: www.elsevier.com/locate/jchromb



Development and application of a HILIC UHPLC-MS method for polar fecal metabolome profiling



Nina Sillner^{a,b}, Alesia Walker^a, Eva-Maria Harrieder^a, Philippe Schmitt-Kopplin^{a,b,c}, Michael Witting^{a,c,*}

^a Research Unit Analytical BioGeoChemistry, Helmholtz Zentrum München, Neuherberg, Germany

^b ZIEL Institute for Food and Health, Technical University of Munich, Freising, Germany

^c Chair of Analytical Food Chemistry, Technical University of Munich, Freising, Germany

ARTICLE INFO

Keywords:
Hydrophilic interaction liquid chromatography
HILIC
UHPLC-MS
Metabolomics
Non-targeted
Feces

ABSTRACT

The fecal metabolome is a complex mixture of endogenous, microbial metabolites, and food derived compounds. Hydrophilic interaction liquid chromatography (HILIC) enables the analysis of polar compounds, which is a valuable alternative to reversed-phase liquid chromatography in the field of metabolomics due to its ability to retain a greater portion of the polar metabolome. The objective of the study was to find the optimal chromatographic solution to perform non-targeted metabolomics of feces by means of HILIC ultra-high-pressure liquid chromatography mass spectrometry (UHPLC-Q-TOF-MS). The performance was systematically investigated analyzing a pooled fecal sample, and mixtures of 150 metabolites from different families, including for example amino acids, amines, indole derivatives, fatty acids and carbohydrates. Three different stationary phases (zwitterionic, amide and unbonded silica) were operated at three pH values (4.6, 6.8 and 9.0), and three salt gradient conditions (5–5, 5–10 and 5–25 mM ammonium acetate). Amide and zwitterionic stationary phases performed similarly at low pH, with highest number of detected standards, which increased by increasing the salt gradient. The amide column showed slightly better performance in terms of separation of isomers and peak widths and remarkably good performance at basic pH, with highest number of metabolite features in the non-targeted analysis. The zwitterionic column operated best in terms of number of detected standards, retention time distribution of standards and metabolite feature across whole chromatographic run. Thus, the zwitterionic column was proven to suit for non-targeted analysis of fecal samples, resulting in good coverage of especially amino acids and carbohydrates.

1. Introduction

Metabolome profiling studies are often performed using reversed-phase (RP) chromatography because of its robust and reproducible separation characteristics and the coverage of a wide range of metabolites. However, most biological matrices contain plenty polar metabolites, which cannot be retained on RP stationary phases. Thus, hydrophilic interaction liquid chromatography (HILIC) became more and more popular in the field of metabolomics for separation of polar compounds. The term HILIC was first introduced by Andrew J. Alpert to describe the combination of hydrophilic stationary phases and organic mobile phases [1]. HILIC offers a wide variety of different retention mechanisms and column selectivities. Stationary phases can be classified in neutral ligand (e.g. amide), charged (e.g. unbonded silica) and

zwitterionic phases (e.g. sulfobetaine) based on the characteristics of the functional group. Besides the different column chemistries, the separation properties in HILIC are also dependent on the pH value and buffer salt concentration [2]. The most commonly used buffers are ammonium formate or acetate. HILIC has often been used for analyzing hydrophilic compounds in urine and plasma to increase the coverage of the metabolome [3–6]. Yet, HILIC represents a challenge in metabolomics because it is less reproducible and requires longer equilibration time than RP chromatography [7,8]. Only a few studies used HILIC for the analysis of fecal samples so far [9–14], and mostly in combination with RP measurements. Feces represents a challenging matrix influenced by many factors such as diet, gut microbiota, and the host metabolism. The optimal fecal sample preparation for a targeted HILIC-MS/MS method was already investigated [10]. However, there is

* Corresponding author at: Helmholtz Zentrum München, Deutsches Forschungszentrum für Gesundheit und Umwelt, Department of Environmental Sciences, Analytical BioGeoChemistry, Ingolstaedter Landstrasse 1, 85764 Neuherberg, Germany.
E-mail address: michael.witting@helmholtz-muenchen.de (M. Witting).

<https://doi.org/10.1016/j.jchromb.2019.01.016>

Received 19 October 2018; Received in revised form 14 December 2018; Accepted 23 January 2019

Available online 04 February 2019

1570-0232/ © 2019 Elsevier B.V. All rights reserved.

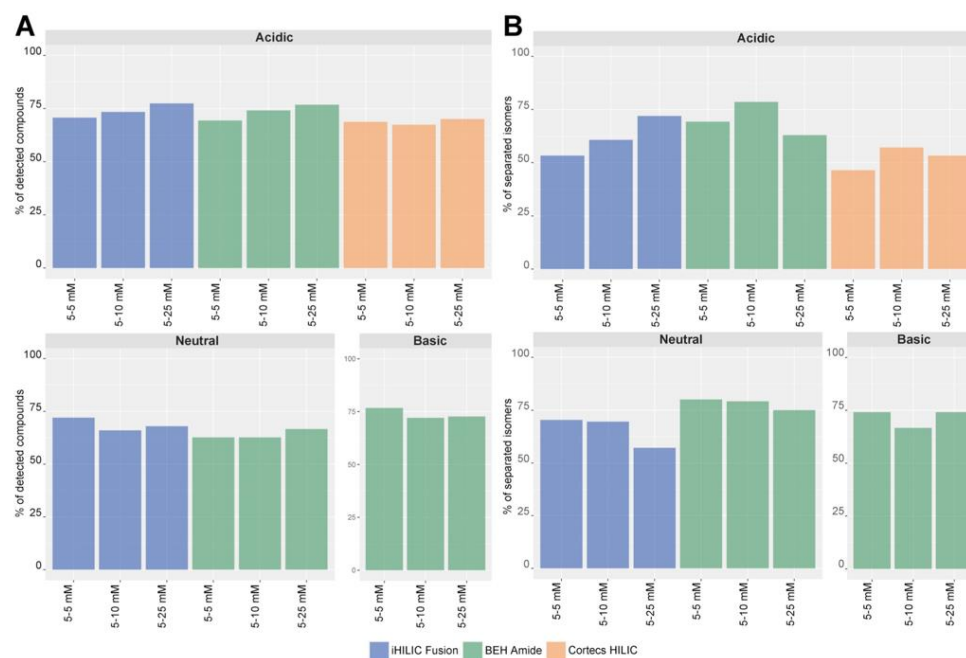


Fig. 1. Detection of analyzed standards and separation of isomeric substances under different HILIC conditions. Comparison of analyzed standards under acidic, neutral and basic pHs for iHILIC Fusion, BEH Amide and Cortecs HILIC at 5–5 mM, 5–10 mM and 5–25 mM NH_4Ac . (A) Percentage of detected metabolites in each condition, taken into account number of detected against injected metabolites ($n = 150$). (B) Percentage of separated isomeric pairs for each condition, taking into account number of detected isomeric metabolites and number of separated isomers.

currently no study comparing different HILIC columns and conditions for non-targeted metabolome profiling in feces.

In the present work we aimed to find the optimal chromatographic settings for non-targeted metabolomics of fecal samples using HILIC-MS. Therefore, three different HILIC columns (zwitterionic, amide and unbonded silica) were compared at different pH values (depending on the column specifications) and three salt gradient conditions. Parameters were evaluated in terms of number of detected features, separation of isomers, precision and repartition of the metabolic features along the chromatographic runs using standard mixtures and fecal samples.

2. Materials and methods

2.1. Reagents and materials

A set of 150 analytical grade standards were purchased from different vendors as summarized in Table S1. Four/nine standard mixtures were prepared to a final concentration of 0.0122/0.0139 mg/mL in 75% acetonitrile (LiChrosolv®, hypergrade for LC-MS, Merck KGaA, Darmstadt, Germany). MilliQ H_2O was derived from Milli-Q Integral Water Purification System (Billerica, MA, United States of America). Methanol (LiChrosolv®, hypergrade for LC-MS), ammonium acetate (NH_4Ac) and ammonium hydroxide ($\geq 25\%$ in water) were obtained from Merck KGaA, Darmstadt, Germany. Glacial acetic acid was purchased from Biosolve, Valkenswaard, Netherlands.

2.2. Fecal sample preparation

Metabolite extraction from infant stool samples was prepared as described in Bazanella et al. [15]. A pooled methanol stool extract ($n = 468$) was evaporated at 40 °C (Savant, SPD121P, SpeedVac Concentrator, ThermoFisher Scientific, Waltham, Massachusetts, United States of America) and reconstituted with 75% acetonitrile to perform HILIC coupled to mass spectrometry (MS) analysis.

2.3. LC-MS conditions

The pooled fecal sample and a set of 150 metabolites (Table S1) were analyzed on a time of flight mass spectrometer (maXis, Bruker Daltonics, Bremen, Germany), coupled to an UHPLC system (Acquity, Waters, Eschborn, Germany). Internal calibration of the mass spectrometer (MS) was done by injecting ESI-L Low Concentration Tuning Mix (Agilent, Santa Clara, CA, United States of America). External Calibration of the MS was ensured by injecting ESI-L Low Concentration Tuning Mix (1:4 diluted in 75% acetonitrile) in the first 0.3 min of each LC-MS run, introduced by a switching valve. Mass spectra were acquired in positive and negative ionization mode (\pm ESI). ESI parameters were as follows: nitrogen flow rate of 10 L/min, dry heater of 200 °C, nebulizer pressure of 2.0 bar and capillary voltage of 4500 V. Data was acquired in line and profile mode with an acquisition rate of 5 Hz, within a mass range of 50–1500 Da.

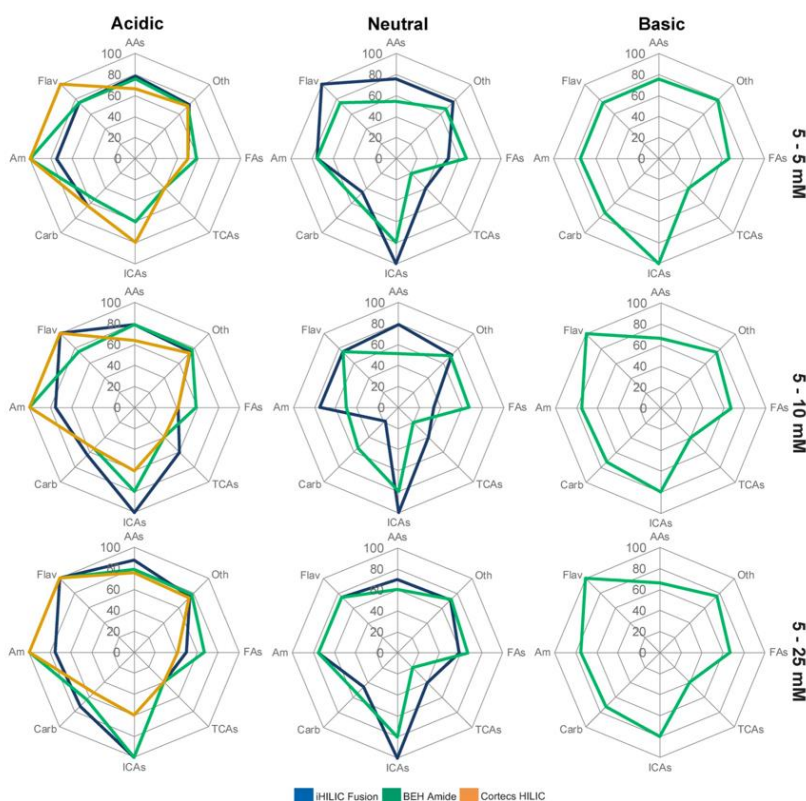


Fig. 2. Selectivity of metabolite subclasses for the different HILIC conditions. Standards were translated by the Chemical Translation Service and classified by ClassyFire using compound name and InChIKey information; compounds were classified into eight different categories, including amino acids, peptides and analogues (AAs), Flavones (Flav), Amines (Am), Carbohydrates and carbohydrate conjugates (Carb), Indolyl carboxylic acids and derivatives (ICAs), Tricarboxylic acids and derivatives (TCAs), Fatty acids and conjugates (FAs) and Others (Oth; with < 4 compounds per subclass).

2.4. Chromatographic conditions

Three different HILIC columns were compared: a charge modulated hydroxyethyl amide (zwitterionic) HILIC column (iHILIC®-Fusion UHPLC column, SS, 100 × 2.1 mm, 1.8 μm, 100 Å, (HILICON AB, Umea, Sweden)), an ethylene Bridged Hybrid (BEH) amide (ACQUITY UPLC BEH Amide column, 100 × 2.1 mm, 1.7 μm, 130 Å, (Waters, Eschborn, Germany)) and a solid-core particle (unbonded silica) CORTECS HILIC column (CORTECS UPLC HILIC column, 100 × 2.1 mm, 1.6 μm, 90 Å (Waters, Eschborn, Germany)).

A stock solution of 0.5 M NH₄Ac was either adjusted to pH 4.6 (acidic), 6.8 (neutral) or 9.0 (basic) with glacial acetic acid or 25% ammonium hydroxide, respectively.

Mobile phases for HILIC separation consisted of 5 mM NH₄Ac in 95% acetonitrile (A) (A; acidic, neutral or basic) and 5, 10 or 25 mM NH₄Ac in 5% acetonitrile (B; acidic, neutral or basic). Elution of metabolites was performed with a flow rate of 0.5 mL/min, using a 0.1–99.9% phase B gradient over 7.5 min. After a pre-run time of 5 min at 0.1% B, 0.1% B was kept for 2 min with increasing to 99.9% B within 7.5 min. 99.9% B was kept constant for 2.5 min with fast decrease to 0.1% B within 0.1 min. The column oven temperature was set to 40 °C and 1 μL sample was injected by partial loop (10 μL). Weak and strong

wash consisted of 95% acetonitrile and 10% acetonitrile, respectively.

2.5. Data processing and analysis

Raw LC-MS data were processed with Genedata Refiner MS software (Genedata GmbH, Munich, Germany), including chemical noise subtraction, intensity cutoff filter, calibration, chromatographic peak picking, deisotoping, blank subtraction and metabolite library search with The Human Metabolome Database (HMDB) for MS1 level (± 0.005 Da) for targeted and non-targeted analysis of standards and stool samples [16]. Metabolite subclass classification was done with ClassyFire Batch [17] by the Fiehn Lab (<http://cfb.fiehnlab.ucdavis.edu/>) and the subclass name was taken for metabolite classification for standards and annotated metabolites. Standard classification was done by translating compound name into InChIKeys with the chemical translation service (<http://cts.fiehnlab.ucdavis.edu/>) [18].

3. Results and discussion

We evaluated the behavior of three HILIC columns under three different pHs (acidic, neutral or basic) and salt gradient conditions (5–5, 5–10 or 5–25 mM NH₄Ac) in acetic acid/ammonium hydroxide

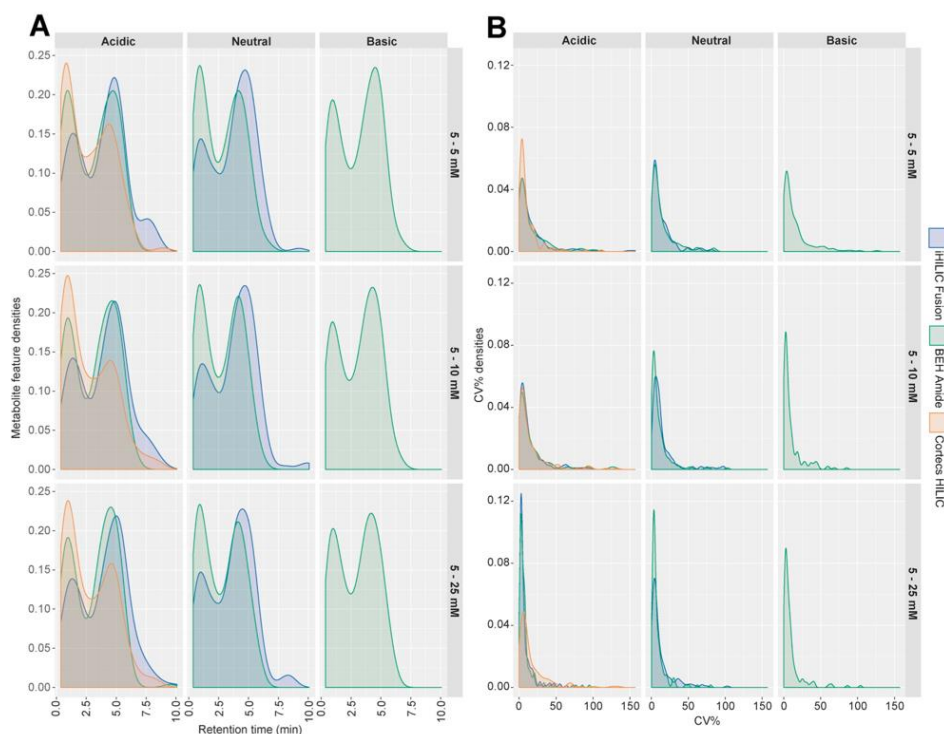


Fig. 3. Retention time and precision distribution of detected standards. (A) Density distribution of retention times across the chromatographic run for each HILIC condition and (B) Precision of triplicate injections of analyzed standards, expressed in percentage of coefficient of variation (CV%).

buffered conditions. All UHPLC columns (iHILIC Fusion, BEH Amide and Cortecs HILIC) were assessed under acidic conditions, two (iHILIC Fusion, BEH Amide) were performed under neutral and one (BEH Amide) under basic conditions, depending on the vendor specifications for each column (pH range iHILIC Fusion: 2–8, BEH Amide: 2–12, Cortecs HILIC: 1–5). In total, we analyzed 150 different metabolite standards, classified into amino acids, fatty acids, tricarboxylic acids, indole derivatives, carbohydrates, amines, flavones and others and a pooled fecal sample with in total 18 different chromatographic settings in positive and negative electrospray ionization mode. The majority of HILIC application based studies in targeted and non-targeted metabolomics are performed with particle sizes above 2 μm [8]. Few studies performed analyses using sub-2 μm HILIC columns with different numbers of tested compounds [3,4,6,19,20].

3.1. Evaluation of the HILIC conditions using standards

The number of detected metabolites ranged between 62.7% and 77.3%, with highest percentages given under acidic (average: 71.9%) or basic (average: 73.8%) pH, but having limited column chemistry (BEH Amide) for comparison at pH 9 (Fig. 1A). Under neutral pH, only 66.3% of all measured standards were detected. Under acidic conditions, the increase of NH_4Ac salt resulted in a higher percentage of detected compounds for all column chemistries with the highest values for iHILIC Fusion (77.3%) and BEH Amide (76.7%) under 5–25 mM NH_4Ac conditions (Fig. 1A). We could also observe that iHILIC Fusion and BEH Amide had higher signal to noise ratios compared to Cortecs HILIC,

despite same injected concentrations on all columns (exemplarily shown for indole-3-lactic acid in Fig. S1). However, iHILIC Fusion showed broader peak widths. Twenty metabolites couldn't be detected in all 18 conditions, possibly being under limit of detection for the used concentration (~ 13 ppm).

3.2. Analysis of resolution of isomers and selectivity of metabolite classes

In our set, we had 15 isomeric pairs (36 substances with 2, 3 or 4 isomers within the pairs) for which we analyzed chromatographic separation. Here, we considered the following, 2 pairs (both detected and separated or no separation), 3 pairs (3 or 2 detected, 3, 2 or 1 resolved or no separation), 4 pairs (4, 3 or 2 detected with 1, 2, 3 or 4 resolved or no separation), summarized in Table S2. Almost all settings reached over 50% of separated isomers, except for Cortecs HILIC pH 4.6, 5–5 mM NH_4Ac (Fig. 1B). Highest percentage of isomer separation ($\geq 75\%$) was reached for BEH Amide (acidic, 5–10 mM, and neutral, 5–5/10/25 mM). Under acidic conditions the increase of the salt gradient led to an increase of separation of isomers for iHILIC Fusion, whereas BEH Amide and Cortecs HILIC didn't show such a behavior (Fig. 1B). At pH 6.8, less isomers were separated with iHILIC Fusion and BEH Amide. BEH Amide performed well at basic pH, reaching $\sim 74\%$ for 5–5 and 5–25 mM and a small decrease at 5–10 mM condition. For example, for iHILIC Fusion (acidic, 5–25 mM), we could detect 32 substances and resolve 8 pairs (Table S2), whereas for BEH Amide with highest % of separated isomers (neutral at all gradients), we could only detect 20 (5–5 mM) or 24 (5–10 mM and 5–25 mM) substances and

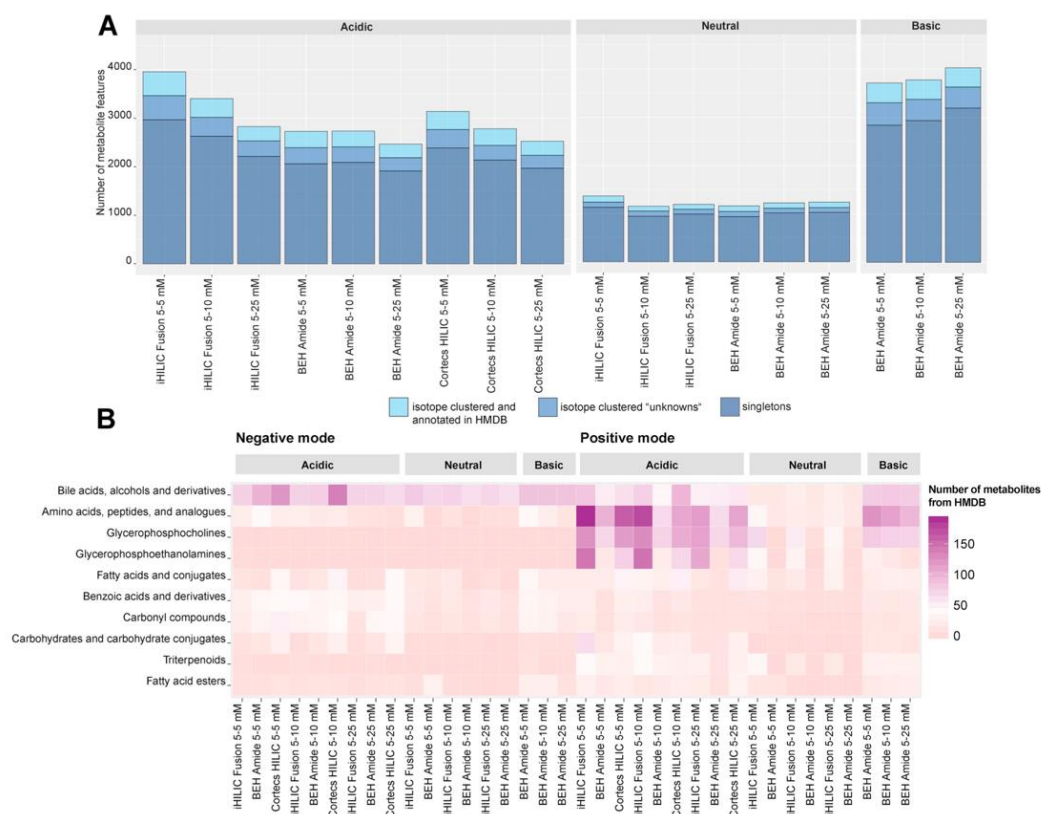


Fig. 4. Non-targeted analysis of stool sample performed at 18 different HILIC conditions. (A) Number of detected metabolite features, categorized into singletons (mass and retention time), isotope clustered features (compounds with recognized isotope pattern and retention time) with or without ("unknowns") HMDB annotation (± 0.005 Da, MS1), analyzed in positive ESI mode. (B) Metabolite features were annotated with HMDB and categorized by ClassyFire into different subclasses using InChIKey information. Top ten subclasses are illustrated for negative or positive ESI mode across all eighteen different HILIC runs.

resolve 4 or 5 pairs, respectively. Some representative examples, analyzed at acidic, 5–25 mM NH_4Ac condition for each column, are shown in Fig. S2. For example, under acidic conditions, BEH Amide was able to resolve the 4 L-leucine isomers (L-isoleucine:L-leucine:L-norleucine:L-tert-leucine) into two peaks consisting of (L-leucine + L-norleucine and L-isoleucine + L-tert-leucine, Fig. S2) at 5–25 mM NH_4Ac .

Overall, under basic and acidic pH, we observed higher coverage, regarding the subclass comparison (Fig. 2). Amino acids, peptides and analogues (AAs) were mostly preferred under acidic conditions using iHILIC Fusion and BEH Amide with an 87.9% coverage for iHILIC Fusion at 5–25 mM condition, which is similar to Sampsonidis et al. [19]. They showed high coverage of amines and amino acids for amide and zwitterionic columns at pH 4. Flavones and amines are 100% covered by Cortecs HILIC using any salt gradient, whereas a full coverage of amines is also shown for BEH Amide (acidic; Fig. 2). The class of flavones was also fully detected by the BEH Amide and iHILIC Fusion at 5–25 mM NH_4Ac concentration. We observed higher counts of the carbohydrates and carbohydrate conjugates (Carb) class for iHILIC Fusion, with 72.3% under 5–25 mM condition and BEH Amide (basic; all salt gradients). Indolyl carboxylic acids and derivatives (ICAs) were preferred under acidic conditions with 100% for iHILIC Fusion for 5–10 mM and 5–25 mM NH_4Ac . Moreover, neutral pH resulted in full

coverage of ICAs, using iHILIC Fusion at all salt gradients (Fig. 2). Tricarboxylic acids and derivatives (TCAs) and fatty acids and conjugates (FAs) were poorly recovered at each pH, but FAs had higher counts (8/12, 66.7%) for BEH Amide at neutral and basic pH for all salt gradients. Altogether, iHILIC Fusion at acidic pH or BEH Amide at basic pH had the best abilities to cover high percentage of metabolite classes.

3.3. Retention time distribution and precision of analyzed standards

Preferably, retention time distribution should be uniformly given across the whole retention time axis with as few as possible compounds detected in the void volume. For example, Cortecs HILIC showed poor retention for the tested compounds, resulting in a high density between 0.0 and 2.5 min under acidic conditions for all salt gradients (Fig. 3A). BEH Amide and iHILIC Fusion had higher densities between 2.5 and 10 min at low pH throughout all salt gradients. The small peak density at ~8 min at 5–5 mM NH_4Ac , for iHILIC Fusion moved to earlier retention times by increasing the salt gradient. Neutral pH resulted in lower retention times for BEH Amide for all salt gradients whereas no big differences were observed for this column at basic pH (Fig. 3A). Precision was assessed by calculating the coefficient of variation (CV) in % of the peak areas of triplicate injections for all detected metabolites.

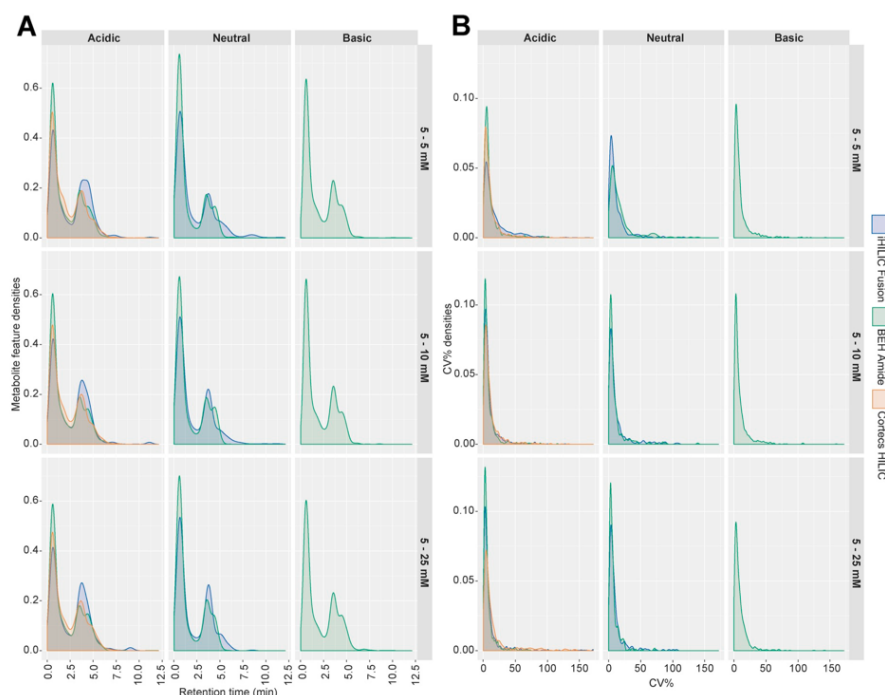


Fig. 5. Retention time repartition and precision of metabolite features detected in stool sample. (A) Retention time distribution in min of metabolite features across the 18 HILIC chromatographic runs. (B) Precision of metabolite features from triplicate injections, expressed in CV%.

Most of the detected peaks showed CVs below 20% (Fig. 3B). Highest density of CV% \leq 20% was observed for acidic conditions at highest concentration of NH_4Ac for iHILIC Fusion, followed by BEH Amide.

3.4. Non-targeted evaluation of the HILIC conditions using fecal sample

We compared the same chromatographic conditions for a pooled feces sample. The objective was to maximize the number of detected metabolite features with good reproducibility and repartition of these features along the chromatographic run. We calculated the total number of metabolite features as a sum of isotope clustered features and singletons, for which no matching isotopes were found by the used software. Among all tested conditions, BEH Amide operated at basic pH provided the highest number of metabolite features (pos: 4026 at 5–25 mM NH_4Ac , neg: 1045 at 5–10 mM NH_4Ac) (Fig. 4A, S3). At low pH, most features were detected with iHILIC Fusion in positive mode (3958, 3402 and 2827 for 5–5, 5–10 and 5–25 mM NH_4Ac , respectively) and with Cortecs HILIC in negative mode (949, 867 and 634 for 5–5, 5–10 and 5–25 mM NH_4Ac , respectively). Interestingly, the number of detected metabolite features decreased by increasing the NH_4Ac concentration at pH 4.8, whereas the opposite was true for pH 9 (pos mode). Overall, the number of detected metabolite features in feces was much higher in positive mode, compared to negative mode, independently of the chromatographic settings. The opposite was reported by Marcobal et al., however, they analyzed mouse feces and used a column which is strictly speaking classified as aqueous normal-phased, thus, no adequate comparison is possible [12]. For annotation with HMDB only isotope clustered features were used. Here, the maximal number of HMDB annotated features was reached with iHILIC

Fusion at acidic pH and 5–5 mM NH_4Ac in positive mode with 493 annotations (Cortecs HILIC acidic pH and 5–5 mM NH_4Ac with 150 annotations in negative mode, Fig. S3) and the least annotations with iHILIC Fusion 5–25 mM NH_4Ac at neutral pH in positive and negative mode.

In order to gain an overview of the metabolite classes detected in feces under the 18 different conditions, the HMDB annotated features (RT > 0.8 min) were classified with ClassyFire Batch and the ten most abundant subclasses were selected for representation (Fig. 4B). Overall, the highest number of metabolites were classified under acidic, the fewest under neutral conditions. The most abundant metabolite class in negative mode was “bile acids, alcohols and derivatives”. Here, the Cortecs HILIC was the most prominent one (5–10 and 5–25 mM NH_4Ac). Also the compound classes fatty acids, benzoic acids, carbonyl compounds and carbohydrates and conjugates/derivatives reached the highest numbers with Cortecs HILIC for all salt gradients at acidic pH. In positive mode, the most abundant metabolite class was “amino acids, peptides and analogues”, followed by glycerophosphocholines and glycerophosphoethanolamines. Especially the iHILIC Fusion column detected the highest numbers in those compound classes, followed by Cortecs HILIC, while numbers were slightly decreasing with increasing NH_4Ac concentrations. In contrast, BEH Amide detected more of the mentioned classes under basic conditions. Moreover, with iHILIC Fusion more carbohydrates and carbohydrate conjugates, as well as triterpenoids were found compared to the other columns.

From the 150 evaluated standards approximately 50 were identified in feces under acidic and basic pH. At neutral pH < 30 were found with BEH Amide and roughly 40 with iHILIC Fusion. A detailed list of detected standards in feces in consideration of possible isomer separation

can be found in Table S3. Virgiliou et al. detected more metabolites under neutral conditions using BEH Amide compared to acidic pH, however, their findings aren't referred to fecal samples [6].

3.5. Retention time repartition and precision of metabolite features of fecal sample

The best repartition along the chromatographic run was observed for iHILIC Fusion under acidic conditions with lowest density between 0 and 2.5 min and highest density between 2.5 and 7 min (Fig. 5A). Additionally, only with iHILIC Fusion features with retention times above 8 min were detected. At neutral pH, both, iHILIC Fusion and BEH Amide, showed worse repartition with higher densities for early retaining metabolites (0–2.5 min). The precision of the triplicates gave overall good results for all tested conditions (Fig. 5B). Under acidic and neutral pH the CV% values improved with increasing salt gradient. The best results with the highest density under 20% were achieved for BEH Amide 5–25 mM NH₄Ac at pH 4.6. Also iHILIC Fusion reached good CV% values, especially at acidic pH and 5–25 mM NH₄Ac. In comparison, Cortecs HILIC showed the worst density distribution.

4. Conclusion

In the present study we compared three different HILIC chemistries operated under acidic, neutral and basic pH and increasing salt gradients. The performance was evaluated for a set of 150 endogenous compounds and infant stool samples, in terms of number of detected features or metabolite classes, separation of isomeric pairs, distribution along the chromatographic run and precision. The major goal was to find a HILIC method which covers the broadest space of polar metabolites in feces. The unbonded silica Cortecs HILIC column was not convincing in regards of retention time distribution, precision and number of recovered standards. Overall, BEH Amide and the zwitterionic iHILIC Fusion performed similarly satisfying under the studied acidic conditions, whereas neutral pH achieved the worst results. For basic pH no comparison between columns was possible, due to limitations in pH tolerances, though the results of the non-targeted analysis were very promising and would require more detailed examination. The increase of salt gradient concentration improved the number of detected standards. The opposite behavior was observed in terms of number of metabolite features in the non-targeted analysis of feces. However, high salt gradients reduce the risk of carry-over for late eluting compounds, especially for zwitterionic columns. BEH Amide showed sharp peaks, slightly better separation of some isomers and increased coverage of amines and fatty acids. The iHILIC Fusion column demonstrated throughout the highest number of detected standards and metabolite features in the non-targeted analysis at acidic pH. Furthermore, it showed the best repartition of the metabolic features along the chromatographic run and a good coverage of metabolite classes like amino acids and carbohydrates in standards and non-targeted analysis of feces. In summary, we think that using the zwitterionic iHILIC Fusion column under acidic conditions offers the best prerequisites to study the polar fecal metabolome in our future non-targeted metabolomics studies.

Supplementary data to this article can be found online at <https://doi.org/10.1016/j.jchromb.2019.01.016>.

Acknowledgements

The authors thank Dirk Haller and Monika Bazanella from the Chair of Nutrition and Immunology and ZIEL Institute of Food & Health at the Technical University of Munich for providing the fecal samples. Furthermore, we thank Brigitte Look from the Research Unit Analytical BioGeoChemistry at the Helmholtz Zentrum München for sample

extraction.

This research did not receive any specific grant from funding agencies in the public, commercial, or not-for-profit sectors.

References

- [1] A.J. Alpert, Hydrophilic-interaction chromatography for the separation of peptides, nucleic acids and other polar compounds, *J. Chromatogr.* 499 (1990) 177–196.
- [2] Y. Guo, S. Gaiki, Retention behavior of small polar compounds on polar stationary phases in hydrophilic interaction chromatography, *J. Chromatogr. A* 1074 (2005) 71–80.
- [3] K. Contrepolis, L. Jiang, M. Snyder, Optimized analytical procedures for the untargeted metabolomic profiling of human urine and plasma by combining hydrophilic interaction (HILIC) and Reverse-Phase Liquid Chromatography (RPLC)-mass spectrometry, *Mol. Cell. Proteomics* 14 (2015) 1684–1695.
- [4] H.G. Gika, G.A. Theodoridis, I.D. Wilson, Hydrophilic interaction and reversed-phase ultra-performance liquid chromatography TOF-MS for metabolomic analysis of Zucker rat urine, *J. Sep. Sci.* 31 (2008) 1598–1608.
- [5] W. Koch, S. Forcisi, R. Lehmann, P. Schmitt-Kopplin, Sensitivity improvement in hydrophilic interaction chromatography negative mode electrospray ionization mass spectrometry using 2-(2-methoxyethoxy)ethanol as a post-column modifier for non-targeted metabolomics, *J. Chromatogr. A* 1361 (2014) 209–216.
- [6] C. Virgiliou, I. Sampsonidis, H.G. Gika, N. Raikos, G.A. Theodoridis, Development and validation of a HILIC-MS/MS multitargeted method for metabolomics applications, *Electrophoresis* 36 (2015) 2215–2225.
- [7] K. Spagou, H. Tsoukali, N. Raikos, H. Gika, I.D. Wilson, G. Theodoridis, Hydrophilic interaction chromatography coupled to MS for metabolomic/metabolomic studies, *J. Sep. Sci.* 33 (2010) 716–727.
- [8] D.Q. Tang, L. Zou, X.X. Yin, C.N. Ong, HILIC-MS for metabolomics: an attractive and complementary approach to RPLC-MS, *Mass Spectrom. Rev.* 35 (2016) 574–600.
- [9] W. Barton, N.C. Penney, O. Cronin, I. Garcia-Perez, M.G. Molloy, E. Holmes, F. Shanahan, P.D. Cotter, O. O'Sullivan, The microbiome of professional athletes differs from that of more sedentary subjects in composition and particularly at the functional metabolic level, *Gut* 67 (2018) 625–633.
- [10] O. Deda, A.C. Chatziioannou, S. Fasoula, D. Palachanis, N. Raikos, G.A. Theodoridis, H.G. Gika, Sample preparation optimization in fecal metabolic profiling, *J. Chromatogr. B Anal. Technol. Biomed. Life Sci.* 1047 (2017) 115–123.
- [11] E. Lofffield, E. Vogtmann, J.N. Sampson, S.C. Moore, H. Nelson, R. Knight, N. Chia, R. Sinha, Comparison of collection methods for fecal samples for discovery metabolomics in epidemiologic studies, *Cancer Epidemiol. Biomark. Prev.* 25 (2016) 1483–1490.
- [12] A. Marcobal, P.C. Kashyap, T.A. Nelson, P.A. Aronov, M.S. Donia, A. Spormann, M.A. Fischbach, J.L. Sonnenburg, A metabolomic view of how the human gut microbiota impacts the host metabolome using humanized and gnotobiotic mice, *ISME J.* 7 (2013) 1933.
- [13] A. McMillan, J.B. Renaud, G.B. Gloor, G. Reid, M.W. Sumarah, Post-acquisition filtering of salt cluster artefacts for LC-MS based human metabolomic studies, *J. Cheminf.* 8 (2016) 44.
- [14] J.J.J. van der Hoof, J. Wandy, F. Young, S. Padmanabhan, K. Gerasimidis, K.E.V. Burgess, M.P. Barrett, S. Rogers, Unsupervised discovery and comparison of structural families across multiple samples in untargeted metabolomics, *Anal. Chem.* 89 (2017) 7569–7577.
- [15] M. Bazanella, T.V. Maier, T. Clavel, I. Lagkouvardos, M. Lucio, M.X. Maldonado-Gomez, C. Autran, J. Walter, L. Bode, P. Schmitt-Kopplin, D. Haller, Randomized controlled trial on the impact of early-life intervention with bifidobacteria on the healthy infant fecal microbiota and metabolome, *Am. J. Clin. Nutr.* 106 (2017) 1274–1286.
- [16] D.S. Wishart, Y.D. Feunang, A. Marcu, A.C. Guo, K. Liang, R. Vazquez-Fresno, T. Sajed, D. Johnson, C. Li, N. Karu, Z. Sayeeda, E. Lo, N. Assempour, M. Berjanskii, S. Singhal, D. Arndt, Y. Liang, H. Badran, J. Grant, A. Serra-Cayuela, Y. Liu, R. Mandal, V. Neveu, A. Pon, C. Knox, M. Wilson, C. Manach, A. Scalbert, HMDB 4.0: the human metabolome database for 2018, *Nucleic Acids Res.* 46 (2018) D608–d617.
- [17] Y. Djoumbou Feunang, R. Eisner, C. Knox, L. Chepelev, J. Hastings, G. Owen, E. Fahy, C. Steinbeck, S. Subramanian, E. Bolton, R. Greiner, D.S. Wishart, ClassyFire: automated chemical classification with a comprehensive, computable taxonomy, *J. Cheminf.* 8 (2016) 61.
- [18] G. Wohlgenuth, P.K. Haldiya, E. Willighagen, T. Kind, O. Fiehn, The chemical translation service—a web-based tool to improve standardization of metabolomic reports, *Bioinformatics* 26 (2010) 2647–2648.
- [19] I. Sampsonidis, M. Witting, W. Koch, C. Virgiliou, H.G. Gika, P. Schmitt-Kopplin, G.A. Theodoridis, Computational analysis and ratiometric comparison approaches aimed to assist column selection in hydrophilic interaction liquid chromatography-tandem mass spectrometry targeted metabolomics, *J. Chromatogr. A* 1406 (2015) 145–155.
- [20] H.G. Gika, G.A. Theodoridis, U. Vrhovsek, F. Mattivi, Quantitative profiling of polar primary metabolites using hydrophilic interaction ultrahigh performance liquid chromatography-tandem mass spectrometry, *J. Chromatogr. A* 1259 (2012) 121–127.

B.2 Supplementary Information *

Table B.S1 Detailed information on analyzed standards.

Name	Classification	Mix I [acidic]	Mix II [neutral and basic]	Producer	HMDB ID
N,N-Dimethylglycine	Amino acids, peptides, and analogues	A	D	Sigma	HMDB00092
Fumaric acid	Others	A	A	Sigma	HMDB00134
Benzoic acid	Others	A	A	Sigma-Aldrich	HMDB01870
L-Leucine	Amino acids, peptides, and analogues	A	A	Sigma	HMDB00687
Phenylacetic acid	Others	A	D	Aldrich	HMDB00209
L-Methionine	Amino acids, peptides, and analogues	A	A	Sigma-Aldrich	HMDB00696
Pimelic acid	Fatty acids and conjugates	A	B	Aldrich	HMDB00857
3-Methyl-Histidine	Amino acids, peptides, and analogues	A	B	Sigma	HMDB00479
2-Keto-3-deoxy-D-gluconate	Others	A	D	Sigma	HMDB01353
Citric acid	Tricarboxylic acids and derivatives	A	B	Sigma	HMDB00094
L-Tryptophan	Indolyl carboxylic acids and derivatives	A	A	Sigma-Aldrich	HMDB00929
Uridine	Others	A	B	Sigma	HMDB00296
3-Methylcytidine	Others	A	A	/	No result
1-Methyladenosine	Others	A	B	Sigma	HMDB03331
N ² -Methylguanosine	Others	A	C	Sigma	HMDB05862
Fructose-1,6-bisphosphate	Carbohydrates and carbohydrate conjugates	A	A	Sigma	HMDB0001058
Glutathione, ox.	Amino acids, peptides, and analogues	A	A	Sigma	HMDB03337
Choline	Others	B	A	Sigma	HMDB00097
L-Proline	Amino acids, peptides, and analogues	B	D	Sigma-Aldrich	HMDB00162
Nicotinamide	Others	B	B	Sigma	HMDB01406
L-Norleucine	Amino acids, peptides, and analogues	B	B	Sigma	HMDB01645
N-Methylnicotinamide	Others	B	A	Aldrich	HMDB03152
L-Glutamine	Amino acids, peptides, and analogues	B	B	Sigma	HMDB00641
D-Arabinose	Carbohydrates and carbohydrate conjugates	B	B	Sigma	HMDB0029942
Tryptamine	Others	B	C	Aldrich	HMDB00303
Cis-Aconitic acid	Tricarboxylic acids and derivatives	B	D	Aldrich	HMDB00072
Hippuric acid	Others	B	A	Sigma	HMDB00714
DI-Isocitric acid	Tricarboxylic acids and derivatives	B	C	Sigma	HMDB00193
Indole-3-lactic acid	Indolyl carboxylic acids and derivatives	B	B	Aldrich	HMDB00671
Pseudouridine	Others	B	C	/	HMDB00767
Glucose-1-phosphate	Carbohydrates and carbohydrate conjugates	B	D	Sigma	HMDB0001586
N ⁶ -Methyladenosine	Others	B	D	/	HMDB04044
7-Methylguanosine	Others	B	A	Sigma	HMDB01107
Arachidonoyl Ethanolamide	Amines	B	B	Biomol	HMDB04080
Glyceric acid	Carbohydrates and carbohydrate conjugates	C	C	Sigma	HMDB00139
Succinic acid	Others	C	A	Sigma	HMDB00254
Taurine	Others	C	C	Sigma	HMDB00251
L-tert-Leucine	Amino acids, peptides, and analogues	C	C	Aldrich	No result
Anthranilic acid	Others	C	B	Sigma-Aldrich	HMDB01123
D-Ribose	Carbohydrates and carbohydrate conjugates	C	C	Sigma	HMDB0000283
Carnitine	Others	C	D	Sigma	HMDB0000062
Suberic acid	Fatty acids and conjugates	C	A	Aldrich	HMDB00893
D-Galactose	Carbohydrates and carbohydrate conjugates	C	A	Sigma-Aldrich	HMDB0000143
N-Acetylglutamic acid	Amino acids, peptides, and analogues	C	D	Sigma	HMDB0001138
3-Indoxylsulfate	Others	C	C	Aldrich	HMDB00682
Biotin	Others	C	D	Sigma-Aldrich	HMDB00030
Adenosine	Others	C	B	Sigma	HMDB00050
Guanosine	Others	C	A	Sigma	HMDB00133
Palmitoyl Ethanolamide	Others	C	B	Biomol	HMDB02100
Riboflavin	Others	C	C	Sigma	HMDB00244
NADH	Others	C	C	Sigma	HMDB0001487

* This chapter was published as [Nina Sillner](#), Alesia Walker, Eva-Maria Harrieder, Philippe Schmitt-Kopplin, Michael Witting. Development and Application of a HILIC UHPLC-MS Method for Polar Fecal Metabolome Profiling. Journal of Chromatography B, 1109, 142-148, *Supporting Information*. Copyright Elsevier (2019).

Table B.S1 (continued) Detailed information on analyzed standards.

Name	Classification	Mix I [acidic]	Mix II [neutral and basic]	Producer	HMDB ID
L-Serine	Amino acids, peptides, and analogues	D	B	Sigma	HMDB00187
Levulinic acid	Tricarboxylic acids and derivatives	D	B	Aldrich	HMDB00958
Isethionic acid	Others	D	D	Aldrich	HMDB03903
S-Malic acid	Others	D	B	Aldrich	HMDB00744
2-Oxoglutaric acid	Others	D	A	Sigma-Aldrich	HMDB00208
3-Phenylpropionic acid	Others	D	D	Aldrich	HMDB00764
L-Fucose	Carbohydrates and carbohydrate conjugates	D	A	Sigma-Aldrich	HMDB00174
D-Glucose	Carbohydrates and carbohydrate conjugates	D	B	Aldrich	HMDB00122
3-Indolepropionic acid	Indolyl carboxylic acids and derivatives	D	A	Aldrich	HMDB02302
L-Hydroxytryptophan	Others	D	D	Aldrich	HMDB000472
Palmitic acid	Fatty acids and conjugates	D	A	Sigma	HMDB00220
5-Ethyluridine	Others	D	C	/	No result
N ⁴ -Acetylcytidine	Others	D	B	Sigma	HMDB05923
Quercetin	Flavones	D	C	Sigma	HMDB05794
S-Adenosyl-L-homocysteine	Others	D	D	Sigma	HMDB00939
FAD	Others	D	D	Sigma	HMDB01248
p-Cresol	Others	E	D	Sigma	HMDB01858
Betain	Others	E	C	Sigma	HMDB00875
1,2,3-Trihydroxybenzene	Others	E	A	Sigma	HMDB0013674
Methylsuccinic acid	Fatty acids and conjugates	E	B	Aldrich	HMDB01844
Caprylic acid	Fatty acids and conjugates	E	C	Aldrich	HMDB00482
2-Hydroxyphenylacetic acid	Others	E	A	Sigma	HMDB00669
L-Phenylalanine	Amino acids, peptides, and analogues	E	B	Sigma-Aldrich	HMDB00159
L-Arginine	Amino acids, peptides, and analogues	E	C	Sigma-Aldrich	HMDB00517
D-Mannose	Carbohydrates and carbohydrate conjugates	E	C	Sigma	HMDB00169
Ferulic acid	Others	E	D	Aldrich	HMDB00954
Chorismic acid	Tricarboxylic acids and derivatives	E	A	Sigma	HMDB00958
2'-O-Methylcytidine	Others	E	B	Sigma	No result
Inosine	Others	E	D	Sigma	HMDB00195
Kaempferol	Flavones	E	C	Sigma	HMDB05801
Arachidonic acid	Fatty acids and conjugates	E	D	Sigma	HMDB01043
S-Adenosyl-L-methionine	Others	E	A	Sigma	HMDB0001185
Hypotaurine	Others	F	A	Aldrich	HMDB00965
L-Valine	Amino acids, peptides, and analogues	F	D	Sigma-Aldrich	HMDB00883
1,3,5-Trihydroxybenzene	Others	F	B	Aldrich	HMDB0013675
L-Asparagine	Amino acids, peptides, and analogues	F	C	Sigma	HMDB00168
Spermidine	Amines	F	D	Sigma	HMDB01257
3-Hydroxyphenylacetic acid	Others	F	B	Aldrich	HMDB00440
3-(4-Hydroxyphenyl)-propionic acid	Others	F	C	Aldrich	HMDB02199
Indole-3-acetic acid	Indolyl carboxylic acids and derivatives	F	D	Sigma	HMDB00197
Theobromine	Others	F	D	Sigma	HMDB02825
Gluconic acid	Carbohydrates and carbohydrate conjugates	F	A	Sigma-Aldrich	HMDB00625
Carnosine	Others	F	B	Sigma	HMDB00033
5-Methylcytidine	Others	F	C	/	HMDB00982
Glucose-6-phosphate	Carbohydrates and carbohydrate conjugates	F	A	Sigma	HMDB01401
Apigenin	Flavones	F	A	Sigma	HMDB02124
Retinol	Others	F	A	Sigma	HMDB00305
Glutathione, red	Others	F	A	Sigma-Aldrich	HMDB00125
2-Methylbutyric acid	Fatty acids and conjugates	G	A	Aldrich	HMDB02176
L-Homoserine	Amino acids, peptides, and analogues	G	B	Sigma	HMDB00719

Table B.S1 (continued) Detailed information on analyzed standards.

Name	Classification	Mix I [acidic]	Mix II [neutral and basic]	Producer	HMDB ID
Oxaloacetic acid	Others	G	A	Sigma	HMDB00223
L-Omithine	Amino acids, peptides, and analogues	G	D	Aldrich	HMDB00214
4-Hydroxyphenylacetic acid	Others	G	C	Santa Cruz	HMDB00020
Uric acid	Others	G	D	Sigma	HMDB00289
N-Acetyl-L-omithine	Amino acids, peptides, and analogues	G	B	Sigma	HMDB03357
L-Citrulline	Amino acids, peptides, and analogues	G	A	Sigma	HMDB00904
L-Tyrosine	Amino acids, peptides, and analogues	G	A	Sigma-Aldrich	HMDB00158
Indole pyruvic acid	Indolyl carboxylic acids and derivatives	G	C	Aldrich	HMDB0060484
Myristic acid	Fatty acids and conjugates	G	C	Sigma	HMDB00806
2'-C-Methylcytidine	Others	G	D	Sigma	No result
Myristoyl Ethanolamide	Amines	G	B	Biomol	No result
Luteolin	Flavones	G	D	Sigma	HMDB05800
N ² -N ² -Dimethylguanosine	Others	G	B	Sigma	HMDB04824
N ⁶ -Threonylcarbamoyladenine	Others	G	B	/	No result
ATP	Others	G	C	Aldrich	HMDB00538
Isovaleric acid	Fatty acids and conjugates	H	B	Aldrich	HMDB00718
Uracile	Others	H	B	Sigma	HMDB00300
L-Threonine	Amino acids, peptides, and analogues	H	C	Sigma-Aldrich	HMDB00167
Creatine	Amino acids, peptides, and analogues	H	C	Sigma	HMDB00064
L-Aspartic acid	Amino acids, peptides, and analogues	H	A	Sigma	HMDB00191
L-Lysine	Amino acids, peptides, and analogues	H	C	Sigma	HMDB00182
L-Histidine	Amino acids, peptides, and analogues	H	D	Sigma	HMDB00177
Cysteic acid	Amino acids, peptides, and analogues	H	A	Sigma	HMDB02757
2-Isopropylmalic acid	Fatty acids and conjugates	H	B	Aldrich	HMDB00402
4-Pyridoxic acid	Others	H	B	Sigma-Aldrich	HMDB00017
Sebacic acid	Fatty acids and conjugates	H	B	Aldrich	HMDB00792
Thymidine	Others	H	D	Sigma	HMDB00273
2'-O-Methyluridine	Others	H	B	AldrichCPR	No result
γ-Linolenic acid	Others	H	C	Sigma	HMDB03073
Catechin	Others	H	B	Sigma	HMDB02780
γ-Linolenoyl Ethanolamide	Amines	H	C	Biomol	HMDB13625
NAD+	Others	H	B	Sigma-Aldrich	HMDB0000902
Valeric acid	Fatty acids and conjugates	I	C	Aldrich	HMDB00892
Creatinine	Amino acids, peptides, and analogues	I	C	Sigma	HMDB00562
L-Cysteine	Amino acids, peptides, and analogues	I	D	Aldrich	HMDB00574
L-Isoleucine	Amino acids, peptides, and analogues	I	D	Sigma-Aldrich	HMDB00172
L-Homocysteine	Amino acids, peptides, and analogues	I	C	Santa Cruz	HMDB0000742
L-Glutamic acid	Amino acids, peptides, and analogues	I	D	Sigma	HMDB00148
Allantoin	Others	I	A	Sigma-Aldrich	HMDB00462
1-Methyl-Histidine	Amino acids, peptides, and analogues	I	C	Aldrich	HMDB00001
Serotonine	Others	I	C	Sigma-Aldrich	HMDB00259
N-α-Acetyllysine	Amino acids, peptides, and analogues	I	C	Sigma	HMDB00446
O-Acetyl-L-carnitine	Others	I	D	Sigma	HMDB0000201
Cytidine	Others	I	A	Sigma	HMDB00089
5-Methyluridine	Others	I	C	Aldrich	HMDB00884
2'-O-Methyladenosine	Others	I	A	Sigma	HMDB0004326
2'-O-Methylguanosine	Others	I	D	/	No result
N ⁶ -Isopentenyladenosine	Others	I	D	/	No result
Reserpine	Others	I	D	Sigma	HMDB0014351

Table B.S1 (continued) Retention times (min) measured in negative ionization mode.

Name	[M-H] ⁻	Retention time [min]																		
		NEGATIVE																		
		Acidic					Neutral					Basic								
		iHILIC Fusion 5-5 mM	BEH Amide 5-5 mM	Cortex HILIC 5-5 mM	HILIC Fusion 5-10 mM	BEH Amide 5-10 mM	Cortex HILIC 5-10 mM	HILIC Fusion 5-25 mM	BEH Amide 5-25 mM	Cortex HILIC 5-25 mM	iHILIC Fusion 5-5 mM	BEH Amide 5-5 mM	HILIC Fusion 5-10 mM	BEH Amide 5-10 mM	HILIC Fusion 5-25 mM	BEH Amide 5-25 mM	BEH Amide 5-5 mM	BEH Amide 5-10 mM	BEH Amide 5-25 mM	
N,N-Dimethylglycine	102.0561	x	x	x	x	x	x	x	x	x	x	x	x	x	x	x	x	x	x	x
Fumaric acid	115.0037	x	5.1	x	x	5.1	x	x	x	x	x	x	x	x	x	x	x	x	x	x
Benzoic acid	121.0295	1.6	1.6	x	1.6	1.6	1.5	1.7	1.6	1.5	1.7	1.7	2.7	1.7	2.9	1.7	1.8	1.8	1.8	
L-Leucine	130.0874	4.8	4.3	4.2	4.9	4.3	4.4	4.8	4.3	4.4	4.3	4.3	4.9	4.3	4.8	4.3	4.3	4.3	4.3	
Phenylacetic acid	135.0452	1.5	1.4	1.6	1.5	1.4	1.7	1.6	1.4	1.8	1.6	1.6	2.7	1.6	2.9	1.7	1.7	1.7	1.7	
L-Methionine	148.0438	5.2	x	x	5.2	4.5	x	5.1	4.5	x	x	x	5.2	x	5	4.5	4.5	4.5	4.4	
Pimelic acid	159.0663	5	4.7	4.6	5.1	4.6	4.6	5.1	4.6	4.6	4.8	4.8	4.9	4.8	5	4.9	4.8	4.8	4.9	
3-Methyl-Histidine	168.0779	7.9	5.4	x	7.8	5.5	x	7.5	x	x	x	x	x	x	x	x	x	x	x	
2-Keto-3-deoxy-D-gluconate	177.0405	5.1	x	x	5.2	4.7	x	5.2	4.7	x	x	x	x	x	5	x	4.5	4.5	x	
Citric acid	191.0197	x	x	x	x	x	x	x	x	x	x	x	x	x	x	x	x	x	x	
L-Tryptophan	203.0826	x	x	x	x	x	x	4.8	4.3	x	x	x	x	x	x	x	4.2	4.2	4.2	
Uridine	243.0623	2.8	2.7	0.8	2.8	2.7	0.9	2.8	2.7	0.9	2.6	2.6	x	2.6	2.8	2.6	2.6	2.6	2.6	
3-Methylcytidine	257.0779	1.3	0.8	0.8	1.3	1.2	0.8	1.3	1.2	0.8	1.2	1.2	1.3	1.2	1.3	1.2	1.2	1.2	1.2	
1-Methyladenosine	280.1051	2.2	1.8	1.1	2.2	1.8	1.2	2.2	1.8	1.2	x	x	x	x	x	x	1.8	1.8	1.8	
N ² -Methylguanosine	296.1000	4.2	x	2.7	4.2	x	2.9	4.2	x	3	x	x	x	x	x	x	x	x	x	
Fructose-1,6-bisphosphate	338.9888	x	x	x	x	x	x	x	x	x	x	x	x	x	x	x	5.3	5.4	x	
Glutathione, ox.	611.1447	x	x	x	x	x	x	x	x	x	x	x	x	x	x	x	x	x	x	
Choline	103.0997	x	x	x	x	x	x	x	x	x	x	x	x	x	x	x	x	x	x	
L-Proline	114.0561	x	x	x	x	x	x	x	x	x	x	x	x	x	x	x	x	x	x	
Nicotinamide	121.0407	x	x	x	x	x	x	x	x	x	x	x	x	x	x	x	x	x	x	
L-Norleucine	130.0874	4.8	4.3	4.2	4.9	4.3	4.4	4.8	4.3	4.4	4.3	4.3	4.9	4.3	4.8	4.3	4.3	4.3	4.3	
N-Methylnicotinamide	135.0564	x	0.7	x	x	0.7	x	0.8	0.7	x	0.7	0.7	0.8	0.7	0.8	0.7	0.7	0.7	0.7	
L-Glutamine	145.0619	5.6	5	x	5.6	5.1	x	5.5	5.1	x	x	x	5.7	x	5.6	x	5	5	x	
D-Arabinose	149.0456	3.6	x	1.2	3.5	x	1.3	3.6	x	1.3	x	x	x	x	x	x	x	x	x	
Tryptamine	159.0928	x	x	x	x	x	x	4.6	3.6	x	3.6	3.6	x	x	x	x	x	x	x	
Cis-Aconitic acid	173.0092	5.1	4.9	4.5	5.2	4.8	4.6	5.2	4.9	4.6	x	x	5	x	5.2	x	5	5.1	5.2	
Hippuric acid	178.0510	3.7	3.7	3.5	3.7	3.7	3.6	3.7	3.7	3.6	3.7	3.7	4	3.7	4	3.7	3.7	3.7	3.7	
DH-socitric acid	191.0197	x	x	x	x	x	x	x	x	x	x	x	x	x	x	x	x	x	x	
Indole-3-lactic acid	204.0666	3.8	x	x	3.9	3.4	x	3.9	3.4	x	3.3	3.3	4	3.3	4	3.3	3.3	3.3	3.3	
Pseudouridine	243.0623	4.1	4	1.2	4	4	1.3	4	4	1.4	4	4	4.1	4	4.1	4	4	4	4	
Glucose-1-phosphate	259.0224	x	x	x	x	x	x	5.7	x	x	x	x	x	x	x	x	x	x	x	
N ⁶ -Methyladenosine	280.1051	2.2	1.8	1.1	2.2	1.8	1.2	2.2	1.8	1.2	1.8	1.8	2	1.8	2.1	1.8	1.8	1.8	1.8	
7-Methylguanosine	297.1073	x	x	x	x	x	x	x	x	x	x	x	x	x	x	x	x	x	x	
Arachidonoyl Ethanolamide	346.2752	0.6	0.5	x	0.6	0.5	x	0.5	0.5	x	0.5	0.5	0.6	0.5	0.6	0.5	0.5	0.5	0.5	
Glyceric acid	105.0193	x	x	x	x	x	x	x	x	x	x	x	x	x	x	x	x	x	x	
Succinic acid	117.0193	x	x	x	x	4.7	x	5.2	4.7	4.6	x	x	4.9	x	x	x	4.8	4.9	5	
Taurine	124.0074	4.9	4.5	4	4.8	4.5	4	4.8	4.5	4	4.5	4.5	4.9	4.5	4.9	4.5	4.4	4.5	4.5	
L-tert-Leucine	130.0874	4.8	4.3	4.2	4.9	4.3	4.4	4.8	4.4	4.4	x	4.3	4.9	4.4	4.8	4.4	4.3	4.3	4.3	
Anthranilic acid	136.0404	1.3	1.1	1	1.3	1.2	1	1.4	1.2	1.1	1.2	1.2	2.1	1.2	2.2	1.2	1.3	1.3	1.4	
D-Ribose	149.0456	2.5	2.2	0.9	2.5	2.2	1	2.5	2.2	1	2.1	2.1	x	2.1	2.6	2.1	2.1	2.1	2.1	
Carnitine	160.0979	x	x	x	x	x	x	x	x	x	x	x	x	x	x	x	x	x	x	
Suberic acid	173.0819	5	4.5	4.5	5	4.5	4.5	5	4.5	4.6	4.7	4.7	4.8	4.7	5	4.7	4.7	4.7	4.8	
D-Galactose	179.0561	4.5	4.5	2	4.5	4.5	2.3	4.5	4.3	2.4	3.7	3.7	x	3.7	4	3.7	3.7	3.7	3.7	
N-Acetylglutamic acid	188.0564	5.1	5	4.6	5.1	5.1	4.6	5.2	5.1	4.7	4.9	4.9	4.9	5	5.1	5.1	5	5	5.1	
3-Indoxylsulfate	212.0023	0.6	0.6	0.4	0.6	0.6	0.4	0.6	0.6	0.4	0.5	0.5	0.7	0.5	0.7	0.5	0.5	0.5	0.5	
Biotin	243.0809	4.1	4	4	4.1	4	4	4.1	x	4	x	x	x	x	x	x	4.2	4.2	4.2	
Adenosine	266.0891	x	x	x	x	x	x	x	x	x	x	x	x	x	x	x	x	x	x	
Guanosine	282.0844	4.5	4.2	3	4.4	4.2	3.1	4.5	4.2	3.2	4.2	4.2	4.5	4.2	4.5	4.2	4.2	4.2	4.2	
Palmitoyl Ethanolamide	298.2752	x	x	x	x	x	x	x	x	x	x	x	x	x	x	x	x	x	x	
Riboflavin	375.1296	x	x	1.7	x	x	1.8	x	x	1.8	3.8	3.8	3.8	3.8	3.8	3.8	3.8	3.8	3.8	
NADH	664.1175	x	x	x	x	x	x	x	x	x	x	x	x	x	x	x	x	x	x	

Table B.S1 (continued) Retention times (min) measured in negative ionization mode.

Name	[M-H] ⁻	Retention time [min]																		
		NEGATIVE																		
		Acidic				Neutral				Basic										
		!HILIC Fusion 5-5 mM	BEH Amide 5-5 mM	Cortecs HILIC 5-5 mM	HILIC Fusion 5-10 mM	BEH Amide 5-10 mM	Cortecs HILIC 5-10 mM	!HILIC Fusion 5-25 mM	BEH Amide 5-25 mM	Cortecs HILIC 5-25 mM	!HILIC Fusion 5-5 mM	BEH Amide 5-5 mM	HILIC Fusion 5-10 mM	BEH Amide 5-10 mM	!HILIC Fusion 5-25 mM	BEH Amide 5-25 mM	BEH Amide 5-5 mM	BEH Amide 5-10 mM	BEH Amide 5-25 mM	
L-Serine	104.0353	x	x	x	x	x	x	x	x	x	x	x	x	x	x	x	x	x	x	x
Levulinic acid	115.0401	2	2.1	2.7	2	2.1	2.9	2.2	2.1	3	2.6	2.6	3.7	2.6	3.8	2.6	2.7	2.7	2.8	2.8
Isethionic acid	124.9914	2.1	3.3	0.7	2	3.3	0.7	2.1	3.3	0.7	2.7	2.7	2.1	2.7	2.2	2.8	2.7	2.7	2.8	2.8
S-Malic acid	133.0143	x	x	x	x	x	x	x	x	x	x	x	x	x	x	x	x	x	x	x
2-Oxoglutaric acid	145.0143	5	x	x	5.1	x	x	x	x	5	x	x	x	4.9	x	5	x	x	4.9	x
3-Phenylpropionic acid	149.0608	1	0.7	0.5	1	0.7	1.1	1.1	0.7	1.2	1.1	1.1	1.4	1.1	1.5	1.1	1.1	1.1	1.1	1.1
L-Fucose	163.0612	2.7	2.6	1.1	2.7	2.6	1.2	2.7	2.6	1.2	2.5	2.5	3.2	2.5	3.3	2.4	3.1	2.8	3.2	3.2
D-Glucose	179.0561	x	x	x	x	x	x	x	x	x	4.4	4.4	x	4.4	x	4.4	4.4	4.4	4.4	4.4
3-Indolepropionic acid	188.0717	1.3	1	1	1.3	1	1.1	1.4	1	1.1	1.2	1.2	2.2	1.2	2.3	1.2	1.2	1.2	1.2	1.2
L-Hydroxytryptophan	219.0775	x	x	x	x	x	x	x	x	x	x	x	x	x	x	x	x	x	x	x
Palmitic acid	255.2330	x	1.2	x	x	1.2	x	x	1.2	x	0.6	0.6	x	0.6	x	0.6	0.6	0.6	0.6	0.6
5-Ethyluridine	267.0623	2.1	1.7	x	2	1.7	1.2	2.1	1.7	1.2	1.7	1.7	2.1	1.7	2.1	1.7	1.7	1.7	1.7	1.7
N ⁶ -Acetylcytidine	284.0888	3.1	2.9	x	3	2.9	1.3	3.1	2.9	1.4	2.8	2.8	3.2	2.8	3.2	2.8	2.8	2.8	2.8	2.8
Quercetin	301.0354	x	x	0.6	6.4	x	0.9	5.6	x	1	0.7	0.7	4	0.7	4	1.8	x	x	x	x
S-Adenosyl-L-homocysteine	383.1143	5.5	x	x	5.5	5.1	x	5.5	5.1	x	x	x	x	x	x	x	x	x	x	x
FAD	784.1498	x	x	x	x	x	x	x	x	x	x	x	x	x	x	x	x	x	x	x
p-Cresol	107.0502	x	x	0.7	x	0.7	x	0.8	x	x	x	x	x	x	x	x	x	x	x	x
Betain	116.0717	x	x	x	x	x	x	x	x	x	x	x	x	x	x	x	x	x	x	x
1,2,3-Trihydroxybenzene	125.0244	x	x	x	x	x	x	x	x	x	x	x	x	x	x	x	1.1	0.9	1.1	1.1
Methylsuccinic acid	131.0350	4.9	4.1	4	5	4.1	4.1	5	4	4.2	4.4	4.4	x	4.4	x	4	4.4	4	4.2	4.2
Caprylic acid	143.1078	0.7	0.7	0.7	x	0.7	x	0.7	0.7	x	0.8	0.8	x	0.8	0.8	0.8	0.7	0.8	0.8	0.8
2-Hydroxyphenylacetic acid	151.0401	1.4	1	0.7	1.4	1	0.7	1.4	1	0.7	1.4	1	0.7	0.8	0.8	1.5	0.7	1.5	0.7	1
L-Phenylalanine	164.0717	4.9	4.2	4.1	4.9	4.3	4.5	4.9	4.3	4.5	4.3	4.3	4.8	4.3	4.7	4.3	4.2	4.2	4.2	4.2
L-Arginine	173.1044	7.6	5.6	x	7.3	5.6	x	6.9	x	x	x	x	x	x	x	x	x	x	x	x
D-Mannose	179.0561	4.5	4.3	2	4.5	4.3	2.3	4.5	4.3	2.4	4.3	4.3	x	4.3	4.5	4.3	4.4	4.4	4.4	4.4
Ferulic acid	193.0506	2.2	1.6	1.3	2.2	1.7	1.5	2.4	1.7	1.5	x	x	x	x	3.7	2	2.1	2.1	2.1	2.1
Chorismic acid	225.0405	x	x	x	5	x	x	x	x	x	x	x	x	x	x	x	x	x	x	x
2'-O-Methylcytidine	256.0939	4	3	2.5	3.9	3	2.4	3.8	x	2.4	3	3	3.7	3	3.7	3	3	3	3	3
Inosine	267.0735	4	3.8	1.9	4	3.8	2.7	4	3.7	2.6	3.7	3.7	4.1	3.8	4.1	3.8	3.7	3.7	3.8	3.8
Kaempferol	285.0405	3.5	0.7	0.6	3.5	0.8	1.1	3.5	0.7	1.3	0.7	0.7	3.9	0.7	3.9	0.7	0.7	0.7	0.7	0.7
Arachidonic acid	303.2330	0.6	0.6	0.5	0.6	0.6	0.5	0.6	0.6	0.5	0.6	0.6	0.7	0.6	0.7	0.6	0.6	0.6	0.6	0.6
S-Adenosyl-L-methionine	397.1300	x	x	x	x	x	x	x	x	x	x	x	x	x	x	x	x	x	x	x
Hypotaurine	108.0125	x	x	x	x	x	x	x	x	x	x	x	x	x	x	x	x	x	x	x
L-Valine	116.0717	x	x	x	x	x	x	x	x	x	x	x	x	x	x	x	x	x	x	x
1,3,5-Trihydroxybenzene	125.0244	2	3.3	0.7	2	3.3	0.7	2	3.3	0.7	0.7	0.7	x	0.7	2.4	0.7	0.7	0.7	0.7	0.7
L-Asparagine	131.0462	x	5.2	x	6.1	5.2	x	x	5.2	x	x	x	x	x	x	x	x	x	x	x
Spermidine	144.1506	x	x	x	x	x	x	x	x	x	x	x	x	x	x	x	x	x	x	x
3-Hydroxyphenylacetic acid	151.0401	3.7	3	2.3	3.6	3.1	2.5	3.7	3	2.6	3.3	3.3	4.1	3.3	4.2	3.4	3.4	3.4	3.4	3.4
3-(4-Hydroxyphenyl)-propionic acid	165.0557	2.2	1.5	3.1	2.1	1.6	1.3	2.3	1.5	1.3	1.8	1.8	3.5	1.8	3.6	1.8	2	2	2	2
Indole-3-acetic acid	174.0560	1.9	1.4	1.3	1.9	1.4	1.4	2	1.4	1.4	1.6	1.6	3.4	1.6	3.5	1.6	1.7	1.7	1.7	1.7
Theobromine	179.0575	x	0.8	0.7	x	0.8	0.7	x	x	0.7	0.8	0.8	0.8	0.8	0.8	0.8	0.8	0.8	0.8	0.8
Gluconic acid	195.0510	6.7	6.1	4.8	6.7	6.1	x	6.8	5.9	x	x	x	x	x	x	x	4.9	x	5.1	5.1
Carnosine	225.0993	6.5	5.4	6	6.5	5.4	6	6.3	5.4	5.9	5.5	5.5	6.4	5.4	6.3	5.3	5.3	5.3	5.3	5.3
5-Methylcytidine	256.0939	4.4	3.9	x	4.3	3.9	3.4	4.2	3.9	x	3.9	3.9	4.2	3.9	4.2	3.9	3.9	3.8	3.9	3.9
Glucose-6-phosphate	259.0224	5.5	5.6	4.9	6	5.4	5	6.1	5.7	5	5.5	5.5	5.5	5.6	5.7	5.7	5.5	5.5	5.7	5.7
Apigenin	269.0456	1.5	0.7	0.5	1.5	0.7	0.6	1.5	0.7	0.5	0.7	0.7	0.9	0.7	0.9	0.7	0.7	0.7	0.7	0.7
Retinol	285.2224	x	x	x	x	x	x	x	x	x	x	x	x	x	x	x	x	x	x	x
Glutathione, red	306.0765	x	x	x	x	x	x	x	x	x	x	x	x	x	x	x	x	x	x	x
2-Methylbutyric acid	101.0608	x	x	x	x	x	x	x	x	x	x	x	x	x	x	x	x	x	x	x
L-Homoserine	118.0510	x	x	x	x	x	x	5.5	5	x	x	x	5.7	x	x	x	x	x	x	x

Table B.S1 (continued) Retention times (min) measured in negative ionization mode.

Name	[M-H] ⁻	Retention time [min]																		
		NEGATIVE																		
		Acidic						Neutral						Basic						
		HILIC Fusion 5-5 mM	BEH Amide 5-5 mM	Cortex HILIC 5-5 mM	HILIC Fusion 5-10 mM	BEH Amide 5-10 mM	Cortex HILIC 5-10 mM	HILIC Fusion 5-25 mM	BEH Amide 5-25 mM	Cortex HILIC 5-25 mM	HILIC Fusion 5-5 mM	BEH Amide 5-5 mM	HILIC Fusion 5-10 mM	BEH Amide 5-10 mM	HILIC Fusion 5-25 mM	BEH Amide 5-25 mM	BEH Amide 5-5 mM	BEH Amide 5-10 mM	BEH Amide 5-25 mM	
Oxaloacetic acid	130.999	x	x	x	x	x	x	x	x	x	x	x	x	x	x	x	x	x	x	x
L-Ornithine	131.083	x	x	x	x	x	x	x	x	x	x	x	x	x	x	x	x	x	x	x
4-Hydroxyphenylacetic acid	151.040	3.6	2.6	1.9	3.6	2.6	2.1	3.6	x	2.1	x	x	x	x	x	x	3.2	3.2	3.3	
Uric acid	167.021	x	x	x	x	x	x	x	x	x	x	x	x	x	x	x	x	x	x	x
N-Acetyl-L-ornithine	173.093	x	x	x	x	x	x	x	x	x	5	5	5.5	5	5.5	5	5	x		5
L-Citrulline	174.088	5.7	5.1	x	5.6	5.1	x	5.6	5.1	x	x	x	x	x	x	x	5.2	5.1	5.1	
L-Tyrosine	180.067	x	x	x	x	x	x	4.6	x	x	x	x	x	x	x	x	x	x	x	x
Indole pyruvic acid	202.051	0.6	0.5	0.5	0.6	0.5	0.5	0.6	0.5	0.5	0.5	0.5	0.6	0.5	0.6	0.5	0.6	0.5	x	x
Myristic acid	227.202	x	x	x	x	x	x	x	x	x	0.6	0.6	x	0.6	0.7	0.6	0.6	0.6	0.6	0.6
2'-C-Methylcytidine	256.094	4.3	3.8	x	4.2	3.7	2.7	4.2	3.7	2.7	3.7	3.7	4.2	3.7	4.2	3.8	3.7	3.7	3.7	3.7
Myristoyl Ethanolamide	270.244	0.6	0.6	0.6	0.6	0.5	0.6	0.6	0.6	0.6	0.6	0.6	0.6	0.6	0.6	0.6	x	x	x	x
Luteolin	285.040	0.8	0.7	0.6	3.5	3.4	0.6	x	3.7	0.5	x	x	x	x	x	x	x	x	x	x
N ⁶ -N ² -Dimethylguanosine	310.116	3.8	3.5	2.4	3.7	3.5	2.5	3.7	3.5	2.6	3.5	3.5	3.8	3.5	3.8	3.5	3.5	3.5	3.5	3.5
N ⁶ -Threonylcarbamoyladenose	411.127	x	x	x	x	x	x	x	x	x	x	4.8	x	4.8	x	4.6	4.7	4.7		
ATP	505.988	x	x	x	x	x	x	x	x	x	x	x	x	x	x	x	x	x	x	x
Isovaleric acid	101.061	x	x	x	x	x	x	x	x	x	x	x	x	x	x	x	x	x	x	x
Uracile	111.020	1.3	1.2	0.7	1.3	1.2	0.7	1.3	1.2	0.7	1.2	1.2	1.3	x	1.2	x	1.2	x	1.2	
L-Threonine	118.051	x	x	x	x	x	x	5.7	5	x	x	x	6	x	x	x	x	x	x	x
Creatine	130.062	5.2	4.8	4.7	5.2	4.8	4.7	x	x	4.7	x	x	x	x	x	x	x	x	x	x
L-Aspartic acid	132.030	x	x	x	6.1	x	x	x	x	x	x	x	x	x	x	x	x	x	x	x
L-Lysine	145.098	7.5	5.7	x	7.2	5.7	x	6.8	5.6	x	5	5	5.5	5	x	x	x	x	x	x
L-Histidine	154.062	8.4	x	x	8.3	x	x	8.1	x	x	x	x	x	x	x	x	x	x	x	x
Cysteic acid	167.997	5.2	5.1	4.3	5.2	5.1	x	5.3	5.1	x	x	x	5	x	5.1	x	4.9	4.9	5	
2-Isopropylmalic acid	175.062	x	x	x	x	x	x	4.8	x	x	x	x	x	5.7	x	x	x	x	x	x
4-Pyridoxic acid	182.046	1.8	0.8	0.5	1.6	0.8	0.6	1.4	0.8	0.5	0.7	0.7	0.8	0.7	0.9	0.7	0.7	0.7	0.7	0.7
Sebacic acid	201.113	4.6	3.9	4.1	4.6	3.9	4.3	4.6	3.8	4.3	4.4	4.4	4.8	4.4	4.8	4.3	4.4	4.4	4.4	4.4
Thymidine	241.083	1.5	1.4	0.7	1.5	1.4	0.7	1.5	1.4	0.8	1.3	1.3	1.5	1.3	1.5	1.3	1.3	1.3	1.3	1.3
2'-O-Methyluridine	257.078	1.3	x	0.8	1.3	1.2	0.8	1.3	1.2	0.8	1.2	1.2	1.3	1.2	1.3	1.2	1.2	1.2	1.2	1.2
γ-Linolenic acid	277.217	0.6	0.6	0.6	0.6	0.6	0.6	0.6	0.6	0.6	0.6	0.6	0.7	0.6	0.7	0.6	0.6	0.6	0.6	0.6
Catechin	289.072	x	0.7	0.5	5.9	0.7	0.5	5.6	2.3	0.5	0.7	0.7	x	0.7	x	0.7	2.1	x	1.8	
γ-Linolenoyl Ethanolamide	322.275	0.6	0.5	x	0.6	0.5	x	0.6	0.5	x	x	x	x	x	x	x	x	x	x	x
NAD ⁺	663.109	x	x	x	x	x	x	x	x	x	x	x	x	x	x	x	x	x	x	x
Valeric acid	101.061	x	x	x	x	x	x	x	x	x	x	x	x	x	x	x	x	x	x	x
Creatinine	112.052	x	x	x	x	x	x	x	x	x	3	3	x	x	x	x	2.9	2.9	3	
L-Cysteine	120.012	x	x	x	x	x	x	x	x	x	x	x	x	x	x	x	x	x	x	x
L-Isoleucine	130.087	4.8	4.3	4.2	4.9	4.3	x	4.8	4.4	4.4	4.3	4.3	4.9	4.4	4.8	4.4	4.3	4.3	4.3	4.3
L-Homocysteine	134.028	x	x	x	x	x	x	x	x	x	1.6	1.6	2.1	1.6	2.1	1.6	x	x	x	
L-Glutamic acid	146.046	5.4	5.3	x	x	5.3	x	5.5	5.3	x	x	x	5.2	x	5.4	x	5.1	x	x	
Allantoin	157.037	3.8	3.5	0.9	3.8	3.5	0.9	3.8	3.4	1	3.4	3.4	3.8	3.4	3.8	3.4	3.4	3.4	3.4	3.4
1-Methyl-Histidine	168.078	x	x	x	x	x	x	x	x	x	x	x	x	x	x	x	x	x	x	x
Serotonine	175.088	x	x	x	x	x	x	x	x	x	x	x	x	x	x	x	x	x	x	x
N-α-Acetyllysine	187.109	5.4	5	5.1	5.4	4.9	5.1	5.4	5	5.1	5	5	5.5	5	5.5	5	5	x		5
O-Acetyl-L-carnitine	202.108	x	x	x	x	x	x	x	x	x	x	x	x	x	x	x	x	x	x	x
Cytidine	242.078	4.5	4	3.2	4.4	4	3.3	4.3	4	3.3	x	x	4.3	4	4.3	4	4	4	4	4
5-Methyluridine	257.078	2.3	2.2	0.8	2.3	2.2	0.8	2.3	2.2	0.8	2.1	2.1	2.4	2.1	2.3	2.1	2.1	2.1	2.1	2.1
2'-O-Methyladenosine	280.105	1.7	1.3	1.1	1.6	1.3	1.2	1.6	1.3	x	1.4	1.4	1.6	1.4	1.6	1.4	1.4	1.4	1.4	1.4
2'-O-Methylguanosine	296.100	4	3.7	2	4	3.6	2.1	4	3.6	2.1	3.6	3.6	4	3.6	4	3.6	3.6	3.6	3.6	3.6
N ⁶ -Isopentenyladenosine	334.152	1.1	0.8	0.7	1.1	0.8	0.7	1	0.8	0.7	1	1	1	1	0.9	1	0.8	0.8	0.8	
Reserpine	607.266	4.1	0.5	2.8	4	0.5	2.6	3.9	0.5	x	x	x	x	x	x	0.5	x	x		

Table B.S1 (continued) Retention times (min) measured in positive ionization mode.

Name	[M+H] ⁺	Retention time [min]																	
		POSITIVE																	
		Acidic						Neutral						Basic					
		IHLIC Fusion 5-5 mM	BEH Amide 5-5 mM	Cortecs HILIC 5-5 mM	IHLIC Fusion 5-10 mM	BEH Amide 5-10 mM	Cortecs HILIC 5-10 mM	IHLIC Fusion 5-25 mM	BEH Amide 5-25 mM	Cortecs HILIC 5-25 mM	IHLIC Fusion 5-5 mM	BEH Amide 5-5 mM	IHLIC Fusion 5-10 mM	BEH Amide 5-10 mM	IHLIC Fusion 5-25 mM	BEH Amide 5-25 mM	BEH Amide 5-10 mM	BEH Amide 5-25 mM	
N,N-Dimethylglycine	104.0706	x	x	x	x	x	x	x	x	x	x	x	x	x	x	x	x	x	x
Fumaric acid	117.0182	x	x	x	x	x	x	x	x	x	x	x	x	x	x	x	x	x	x
Benzoic acid	123.0441	x	x	x	x	x	x	x	x	x	x	x	x	x	x	x	x	x	x
L-Leucine	132.1019	4.9	4.3	4.2	4.9	4.3	4.4	4.8	4.3	4.4	5.1	4.3	4.9	4.3	4.9	4.3	4.3	4.3	4.3
Phenylacetic acid	137.0597	x	x	x	x	x	x	x	x	x	x	x	x	x	x	x	x	x	x
L-Methionine	150.0583	5.1	x	x	5.2	x	x	5.1	x	4.6	5.6	4.5	x	4.5	x	4.5	4.5	4.4	4.4
Pimelic acid	161.0808	5	4.7	x	5.1	4.6	x	5.1	4.6	x	4.9	x	4.9	x	x	x	4.8	x	x
3-Methyl-Histidine	170.0924	8	5.3	6.1	7.9	5.5	7	7.6	5.4	6.9	9.2	5.6	8.1	5.5	7.8	5.4	5.7	5.5	5.4
2-Keto-3-deoxy-D-gluconate	179.0550	x	x	x	x	x	x	x	x	x	4.5	x	x	4.4	x	4.4	x	x	4.4
Citric acid	193.0343	x	x	x	x	x	x	x	x	x	x	x	x	x	x	x	x	x	x
L-Tryptophan	205.0972	x	x	x	4.8	x	4.8	4.3	x	5.2	x	4.8	x	4.7	x	4.3	4.2	4.2	4.2
Uridine	245.0768	2.8	2.7	0.8	2.8	2.6	0.9	2.8	2.7	0.9	2.9	2.6	2.9	2.6	2.9	2.6	2.5	2.5	2.6
3-Methylcytidine	259.0925	x	1.2	0.7	1.3	1.2	0.7	1.3	1.2	0.8	1.3	1.2	1.3	1.2	1.3	1.2	1.2	1.2	1.2
1-Methyladenosine	282.1197	2.2	1.7	1.1	2.2	1.8	1.2	2.2	1.8	1.2	2.3	1.8	2.2	1.8	2.2	1.8	1.8	1.8	1.8
N ² -Methylguanosine	298.1146	x	x	2.7	4.2	3.9	2.8	x	3.9	3	4.3	x	4	3.9	x	3.9	3.6	3.6	3.6
Fructose-1,6-bisphosphate	341.0033	x	x	x	x	x	x	x	1.2	x	x	x	x	x	x	x	x	x	x
Glutathione, ox.	613.1592	x	x	x	x	x	x	x	x	x	x	x	x	x	x	x	x	x	x
Choline	105.1143	x	x	x	x	x	x	x	x	x	x	x	x	x	x	x	x	x	x
L-Proline	116.0706	5.1	4.5	4.6	5.1	4.5	4.7	5.1	4.5	4.7	5.3	4.5	5.2	x	5.1	0.7	4.5	4.5	4.5
Nicotinamide	123.0553	1	0.8	0.8	1	0.8	0.8	1	0.8	0.8	1	0.9	0.9	0.9	1	0.8	0.9	0.9	0.9
L-Norleucine	132.1019	x	4.3	4.2	4.9	4.3	4.4	4.8	4.3	4.4	5.1	4.3	4.9	4.3	4.9	4.3	4.3	4.3	4.3
N-Methylnicotinamide	137.0709	0.9	0.7	0.8	0.9	0.7	0.8	0.8	0.7	0.8	0.8	0.7	0.8	0.7	0.8	0.7	0.7	0.7	0.7
L-Glutamine	147.0764	5.6	5	4.6	5.5	5	5	5.5	5	5	6	x	5.7	x	5.6	x	5	5	1.1
D-Arabinose	151.0601	x	x	x	x	x	x	x	x	x	x	x	x	x	x	x	2.2	2.2	2.2
Tryptamine	161.1073	x	3.5	3.8	4.6	3.5	3.7	4.6	3.5	3.7	4.2	3.6	4.2	3.6	4.1	3.6	3.5	3.6	3.5
Cis-Aconitic acid	175.0237	5.1	x	x	5.2	x	x	5.2	4.9	x	x	x	x	x	x	x	x	x	x
Hippuric acid	180.0655	x	3.7	3.5	x	3.7	3.5	x	3.7	3.6	4	3.7	4	3.7	4	3.7	3.7	3.7	3.7
Di-Isocitric acid	193.0343	x	x	x	x	x	x	x	x	x	x	x	x	x	x	x	x	x	x
Indole-3-lactic acid	206.0812	3.8	x	3.3	3.9	3.4	x	3.9	3.4	x	3.3	4	3.3	4	3.3	3.4	3.3	3.3	3.3
Pseudouridine	245.0768	x	x	1.3	x	x	1.3	x	x	x	4.1	4	4.1	4	4.1	4	4	4	4
Glucose-1-phosphate	261.0370	x	x	x	x	x	x	x	x	x	x	x	x	x	x	x	x	x	x
N ⁶ -Methyladenosine	282.1197	2.2	1.7	1.1	2.2	1.8	1.2	2.2	1.8	1.2	2.3	1.8	2.2	1.8	2.2	1.8	1.8	1.8	1.8
7-Methylguanosine	299.1219	4.9	4.6	4.5	4.9	x	4.5	4.8	4.6	4.5	5	x	5	x	4.9	x	4.6	x	x
Arachidonoyl Ethanolamide	348.2897	0.6	0.5	0.5	0.6	0.5	0.5	0.6	0.5	0.5	0.6	0.6	0.6	0.6	0.6	0.5	0.5	0.6	0.6
Glyceric acid	107.0339	x	x	x	x	x	x	x	x	x	x	x	x	x	x	x	x	x	x
Succinic acid	119.0339	x	x	x	x	x	x	x	x	x	x	x	x	x	x	1.3	x	x	x
Taurine	126.0219	4.9	4.5	4	4.9	4.5	4	4.9	4.5	4	4.8	4.5	4.9	4.5	4.9	4.5	4.4	4.5	4.5
L-tert-Leucine	132.1019	4.9	4.3	4.2	4.9	4.3	4.4	4.8	4.3	4.4	5.1	4.3	4.9	4.3	4.9	4.3	4.3	4.3	4.3
Anthranilic acid	138.0550	1.3	1.1	x	1.4	1.1	1.1	1.4	1.2	1.1	2.2	1.3	2.2	1.2	2.2	1.3	1.2	1.2	1.3
D-Ribose	151.0601	x	2.2	x	x	x	x	x	x	x	x	x	x	x	x	x	x	x	x
Carnitine	162.1125	5.4	4.8	5.4	5.5	4.8	5.5	5.5	4.8	5.5	5.5	4.8	5.5	4.8	5.5	4.8	4.8	4.8	4.8
Suberic acid	175.0965	5	x	x	5	4.5	x	x	4.5	4.6	4.8	4.7	4.9	4.7	5	4.8	4.7	4.7	x
D-Galactose	181.0707	x	x	x	x	x	x	x	x	x	x	x	x	x	x	3.7	3.7	3.7	3.7
N-Acetylglutamic acid	190.0710	5.1	5.1	4.6	5.1	5.1	4.6	5.2	5.1	4.7	x	4.9	4.9	5	5.1	x	5	5	x
3-Indoxylsulfate	214.0169	x	x	x	x	x	x	x	x	x	x	x	x	x	x	x	x	x	x
Biotin	245.0954	4.1	4	4	4.1	4	4	4.1	4	4	4.5	x	4.5	4.2	4.5	4.2	4.2	4.2	4.2
Adenosine	268.1037	4.3	x	2.8	4.2	x	2.8	4.2	x	x	3.4	2.8	3.4	2.8	3.4	2.8	x	x	x
Guanosine	284.0990	4.5	4.2	3	4.5	4.2	3.1	4.5	4.2	3.2	4.5	4.2	4.5	4.2	4.5	4.2	4.2	4.2	4.2
Palmitoyl Ethanolamide	300.2897	x	x	x	x	x	x	x	x	x	x	x	x	x	x	x	x	x	x
Riboflavine	377.1441	3.8	3.8	1.7	3.8	3.8	1.8	3.8	3.8	1.9	3.8	3.8	3.8	3.8	3.8	3.8	3.8	3.8	3.8
NADH	666.1320	x	x	x	x	x	x	x	x	x	x	x	x	x	x	x	x	x	x

Table B.S1 (continued) Retention times (min) measured in positive ionization mode.

Name	[M+H] ⁺	Retention time [min]																	
		POSITIVE																	
		Acidic						Neutral						Basic					
		IHLIC Fusion 5-5 mM	BEH Amide 5-5 mM	Cortecs HILIC 5-5 mM	IHLIC Fusion 5-10 mM	BEH Amide 5-10 mM	Cortecs HILIC 5-10 mM	IHLIC Fusion 5-25 mM	BEH Amide 5-25 mM	Cortecs HILIC 5-25 mM	IHLIC Fusion 5-5 mM	BEH Amide 5-5 mM	IHLIC Fusion 5-10 mM	BEH Amide 5-10 mM	IHLIC Fusion 5-25 mM	BEH Amide 5-25 mM	BEH Amide 5-10 mM	BEH Amide 5-25 mM	
L-Serine	106.0499	x	x	x	x	x	x	x	x	x	x	x	x	x	x	x	x	x	
Levulinic acid	117.0546	2	2.1	2.7	x	2	2.7	2.2	2.1	3	3.7	2.6	3.7	2.5	3.8	2.6	2.7	2.7	2.8
Isethionic acid	127.0060	x	x	x	x	x	x	x	x	x	x	x	x	x	x	x	x	x	x
S-Malic acid	135.0288	x	x	x	x	x	x	x	x	x	x	x	x	x	x	x	x	x	x
2-Oxoglutaric acid	147.0288	x	x	x	x	x	x	x	x	x	x	x	x	x	x	x	x	x	x
3-Phenylpropionic acid	151.0754	x	x	x	x	x	x	x	x	x	x	x	x	x	x	x	x	x	x
L-Fucose	165.0757	x	x	x	x	x	x	x	x	x	x	x	x	x	x	x	x	x	x
D-Glucose	181.0707	x	x	x	x	x	x	x	x	x	x	x	x	x	x	x	x	x	x
3-Indolepropionic acid	190.0863	1.3	1	1	1.4	1	x	1.4	1	1.1	2.2	1.2	2.2	1.2	2.3	1.2	1.2	1.2	1.2
L-Hydroxytryptophan	221.0921	x	x	x	x	x	x	x	x	3.2	x	x	x	0.7	x	0.7	x	x	x
Palmitic acid	257.2475	x	x	x	x	x	x	x	x	x	x	x	x	x	x	x	x	x	x
5-Ethyluridine	269.0768	2.1	1.7	0.6	2.1	1.7	0.7	2.1	1.7	0.6	2.1	1.7	2.1	1.6	2.1	1.6	1.6	1.7	1.7
N ⁴ -Acetylcytidine	286.1034	3.1	2.9	1.2	3.1	2.9	1.3	3.1	2.9	1.4	3.2	2.8	3.2	2.8	3.2	2.8	2.8	2.8	2.8
Quercetin	303.0499	x	x	x	x	x	x	5.6	3.2	x	0.7	x	0.7	x	x	0.7	0.7	0.7	0.7
S-Adenosyl-L-homocysteine	385.1289	5.5	5.1	5.1	5.5	5.1	5.1	5.5	5.1	5.1	5.9	x	5.6	x	5.6	x	5.3	x	5.1
FAD	786.1644	5	x	x	5	5.2	x	5.1	5.3	x	4.8	x	x	x	x	x	5.1	x	x
p-Cresol	109.0648	x	x	x	x	x	x	x	x	x	x	x	x	x	x	x	x	x	x
Betain	118.0863	x	x	x	x	4.3	x	x	4.3	x	4.8	4.3	4.8	4.3	4.8	4.3	4.3	4.3	4.3
1,2,3-Trihydroxybenzene	127.0390	x	x	x	x	x	x	x	x	x	x	x	x	x	x	x	x	x	x
Methylsuccinic acid	133.0495	x	x	x	x	x	4.1	x	x	4.1	x	x	x	x	x	x	x	x	x
Caprylic acid	145.1223	x	x	x	x	x	x	x	x	x	x	x	x	x	x	x	x	x	x
2-Hydroxyphenylacetic acid	153.0546	x	x	x	x	x	x	x	x	x	x	x	x	x	x	x	x	x	x
L-Phenylalanine	166.0863	x	4.2	4.1	4.9	4.3	x	4.8	4.3	x	5.1	4.3	4.9	4.3	4.8	4.3	4.3	4.3	4.3
L-Arginine	175.1190	7.4	5.6	5.9	7.2	5.6	6.2	6.9	5.6	6.1	x	6.4	10	6.2	8.5	5.9	6.2	6.1	5.8
D-Mannose	181.0707	x	x	x	x	x	x	x	x	x	x	x	x	x	x	x	x	x	x
Ferulic acid	195.0652	x	1.6	x	2.3	1.6	1.4	2.4	1.7	1.5	x	0.5	x	x	x	x	x	x	x
Chorismic acid	227.0550	x	x	x	x	x	x	x	x	x	x	x	x	x	x	x	x	x	x
2'-O-Methylcytidine	258.1084	4	x	x	x	x	x	4.2	3	x	3.7	3	3.6	3	3.7	3	2.9	3	3
Inosine	269.0881	4.5	3.8	1.9	4.1	3.8	2	4.1	3.7	2.1	4.1	3.8	4.1	3.8	4.1	3.8	3.7	3.7	3.7
Kaempferol	287.0550	3.5	0.7	x	3.5	0.8	1.1	3.6	0.8	1.3	x	0.7	3.5	0.7	3.5	0.7	0.8	0.7	0.7
Arachidonic acid	305.2475	x	x	x	x	x	x	x	x	x	x	x	x	x	x	x	x	x	x
S-Adenosyl-L-methionine	399.1445	7.9	5.8	x	7.9	6	7.5	7.5	5.9	x	x	6.6	x	x	x	x	6.8	6.3	6
Hypotaurine	110.0270	x	x	x	x	x	x	x	x	x	x	x	x	x	x	x	x	x	x
L-Valine	118.0863	x	x	4.3	x	x	x	5.5	x	6.4	4.8	x	5.2	4.3	4.8	4.3	4.6	x	x
1,3,5-Trihydroxybenzene	127.0390	x	x	x	x	x	x	x	x	x	x	x	x	x	x	x	x	x	x
L-Asparagine	133.0608	x	5.1	5.3	6	5.1	5.2	5.9	5.2	5.3	6.8	x	6.3	x	x	x	5.4	x	x
Spermidine	146.1652	x	6.4	8.9	x	6.5	8.5	9.9	9.5	8	x	x	x	x	x	x	x	x	x
3-Hydroxyphenylacetic acid	153.0546	x	x	x	x	x	x	x	x	x	x	x	x	x	x	x	x	x	x
3-(4-Hydroxyphenyl)-propionic acid	167.0703	x	x	x	x	x	x	x	x	x	x	x	x	x	x	x	x	x	x
Indole-3-acetic acid	176.0706	1.9	1.4	1.3	2	1.3	1.3	2	1.4	1.4	x	1.6	3.4	1.6	3.5	1.6	1.6	1.7	1.7
Theobromine	181.0720	0.9	0.8	0.7	0.9	0.8	0.7	0.9	0.8	0.7	0.9	0.8	0.9	0.8	0.9	0.8	0.8	0.8	0.8
Gluconic acid	197.0656	x	x	x	x	x	x	x	x	x	x	x	x	x	x	x	x	x	x
Carnosine	227.1139	6.5	5.4	5.9	6.5	5.4	6	6.3	5.4	5.9	6.2	5.4	6.4	5.4	6.3	5.3	5.3	5.3	5.3
5-Methylcytidine	258.1084	4.4	3.9	3.3	4.3	3.9	3.4	4.2	3.9	3.5	x	x	4.1	x	x	x	x	x	x
Glucose-6-phosphate	261.0370	5.6	x	4.9	5.7	5.6	5.1	5.8	5.7	5.1	5.4	5.5	5.4	5.5	5.7	5.7	5.5	5.5	5.7
Apigenin	271.0601	1.4	0.7	0.5	1.4	0.7	0.6	0.9	0.7	0.6	0.9	0.7	0.9	0.7	0.9	0.7	0.7	0.7	0.7
Retinol	287.2370	x	0.5	x	x	0.5	x	x	0.5	x	x	x	x	x	x	x	x	x	x
Glutathione, red	308.0911	x	x	x	x	x	x	x	x	x	x	x	x	x	x	x	x	x	x
2-Methylbutyric acid	103.0754	x	x	x	x	x	x	x	x	x	x	x	x	x	x	x	x	x	x
L-Homoserine	120.066	5.6	4.9	x	x	5	x	5.7	5	5	6.1	x	5.7	x	x	x	5.1	x	4.9

Table B.S1 (continued) Retention times (min) measured in positive ionization mode.

Name	[M+H] ⁺	Retention time [min]																		
		POSITIVE																		
		Acidic						Neutral						Basic						
		IHLIC Fusion 5-5 mM	BEH Amide 5-5 mM	Corcos HILIC 5-5 mM	IHLIC Fusion 5-10 mM	BEH Amide 5-10 mM	Corcos HILIC 5-10 mM	IHLIC Fusion 5-25 mM	BEH Amide 5-25 mM	Corcos HILIC 5-25 mM	IHLIC Fusion 5-5 mM	BEH Amide 5-5 mM	IHLIC Fusion 5-10 mM	BEH Amide 5-10 mM	IHLIC Fusion 5-25 mM	BEH Amide 5-25 mM	BEH Amide 5-5 mM	BEH Amide 5-10 mM	BEH Amide 5-25 mM	
Oxaloacetic acid	133.013	x	x	x	x	x	x	x	x	x	x	x	x	x	x	x	x	x	x	x
L-Ornithine	133.097	7.5	5.7	6.1	7.3	5.7	6.4	6.9	5.6	6.2	5.5	x	9.8	x	8.5	x	6.5	6.1	5.9	
4-Hydroxyphenylacetic acid	153.055	x	x	x	x	x	x	x	x	x	x	x	x	x	x	x	x	x	x	x
Uric acid	169.036	x	x	x	x	x	x	x	x	x	x	x	x	x	x	x	x	x	x	x
N-Acetyl-L-ornithine	175.108	5.4	5	5	5.4	4.9	5	5.4	5	5	5.5	5	5.5	5	5.5	5	4.9	5	5	
L-Citrulline	176.103	5.6	5.1	4.8	5.7	5.1	5.1	5.6	5.1	5.1	6	5.2	5.7	x	5.7	5.2	5.2	5.2	5.2	
L-Tyrosine	182.081	5.1	x	x	5.1	x	x	5.1	4.6	x	x	x	x	x	5.1	x	4.6	4.5	4.5	
Indole pyruvic acid	204.066	0.7	0.6	0.5	0.7	x	0.5	0.7	0.6	0.6	0.7	0.6	0.6	0.6	0.6	0.6	0.6	x	x	
Myristic acid	229.216	x	x	x	x	x	x	x	x	x	x	x	x	x	x	x	x	x	x	x
2'-C-Methylcytidine	258.108	4.4	3.8	2.5	4.3	3.8	2.5	4.2	3.8	2.8	4.2	3.7	4.1	3.7	4.1	3.7	3.7	3.7	3.7	
Myristoyl Ethanolamide	272.258	0.6	0.6	0.6	0.6	0.6	0.6	0.6	0.6	0.6	0.6	0.6	0.6	0.6	0.6	0.6	0.6	0.6	0.6	
Luteolin	287.055	x	0.7	x	x	x	1.1	5.7	3.7	0.5	2.1	x	x	x	x	x	x	2.7	0.7	
N ² -N ² -Dimethylguanosine	312.130	x	x	2.4	3.8	3.5	2.4	3.7	3.5	2.6	3.8	3.5	3.8	3.5	3.8	3.5	3.5	3.5	3.5	
N ⁶ -Threonylcarbamoyladenosine	413.142	x	x	x	x	x	x	x	x	x	4.8	4.6	4.8	4.7	4.8	4.7	4.7	4.7	4.7	
ATP	508.003	x	x	x	x	x	x	x	x	x	x	x	x	x	x	x	x	x	x	
Isovaleric acid	103.075	x	x	x	x	x	x	x	x	x	x	x	x	x	x	x	x	x	x	
Uracile	113.035	1.3	1.2	0.6	1.3	1.2	0.7	1.3	1.2	0.7	1.3	1.2	1.3	1.2	1.3	1.2	1.2	1.2	1.2	
L-Threonine	120.066	5.6	4.9	x	5.8	5	4.2	5.7	5	4.2	6.5	x	5.9	x	x	x	x	x	x	
Creatine	132.077	5.2	4.8	4.7	5.2	4.8	4.7	5.1	4.8	x	5.2	4.8	5.2	4.8	5.2	4.8	4.8	4.8	4.8	
L-Aspartic acid	134.045	x	5.3	x	x	5.4	x	6.2	x	x	6.4	x	6.1	x	x	x	5.4	5.2	x	
L-Lysine	147.113	7.4	5.6	6.1	7.1	5.6	6.3	6.8	5.6	6.2	5.5	x	5.5	x	8.4	5.9	6.2	x	5.9	
L-Histidine	156.077	8.2	5.8	6.3	8.2	6	7.4	8.2	5.3	7.6	x	x	x	x	x	x	6.6	x		
Cysteic acid	170.012	5.1	5.1	x	x	5.1	x	5.3	5.1	x	5.1	x	5	x	5.1	5	5	4.9	x	
2-Isopropylmalic acid	177.077	x	x	x	x	x	x	x	x	x	x	x	x	x	x	x	x	x	x	
4-Pyridoxic acid	184.060	1.7	x	0.9	1.3	1.5	0.5	1.4	0.8	0.5	0.9	0.7	0.8	0.7	0.9	0.7	0.7	0.7	0.7	
Sebacic acid	203.128	4.7	3.9	4.1	x	3.8	4.1	4.6	3.8	4.2	4.8	4.4	4.8	4.4	4.8	4.4	4.4	4.4	4.4	
Thymidine	243.098	1.5	1.3	0.7	1.5	1.3	0.7	1.5	1.3	0.7	1.5	1.3	1.5	1.3	1.5	1.3	1.3	1.3	1.3	
2'-O-Methyluridine	259.092	x	1.2	0.7	1.3	1.2	0.7	1.3	1.2	0.8	1.3	1.2	x	1.2	x	1.2	1.2	1.2	1.2	
γ-Linolenic acid	279.232	0.6	0.6	x	0.6	0.6	x	0.6	0.6	x	x	x	x	x	x	x	x	x	x	
Catechin	291.086	x	x	x	x	x	x	x	2	x	x	x	6	0.7	x	0.7	x	x	1.9	
γ-Linolenoyl Ethanolamide	324.290	0.6	0.5	0.5	0.6	0.5	0.5	0.6	0.5	0.5	0.6	0.6	0.6	x	0.6	0.6	0.5	0.6	0.6	
NAD ⁺	665.124	x	x	x	x	x	x	x	x	x	x	x	x	x	x	x	x	x	x	
Valeric acid	103.075	x	x	x	x	x	x	x	x	x	x	x	x	x	x	x	x	x	x	
Creatinine	114.066	4.6	2.8	3.3	4.6	2.8	3.3	4.4	2.8	3.3	3.8	3.1	3.8	3	3.8	2.9	2.9	3	3	
L-Cysteine	122.027	x	x	x	x	x	x	x	x	x	x	x	x	x	x	x	x	x	x	
L-Isoleucine	132.102	4.9	4.3	4.2	4.9	4.3	4.4	4.8	4.3	4.4	5.1	4.3	4.9	4.3	4.9	4.3	4.3	4.3	4.3	
L-Homocysteine	136.043	4.7	x	x	x	x	x	6.3	x	x	x	x	x	x	x	x	x	x	x	
L-Glutamic acid	148.060	5.3	5.2	x	5.4	5.2	x	5.5	5.3	5	5.3	5.1	5.2	5	5.4	5.2	5	5.1	5.2	
Allantoin	159.051	3.8	3.5	0.9	x	3.4	0.9	3.8	3.5	1	3.8	3.4	3.8	3.4	3.8	3.4	3.4	3.4	3.4	
1-Methyl-Histidine	170.092	8	5.7	6.1	8.8	5.5	8.4	8.8	5.4	8.5	x	x	x	x	x	x	x	x	x	
Serotonine	177.102	x	x	3.8	x	3.9	3.8	4.6	3.9	3.8	4.5	2	4.2	2	4.1	2	1.9	1.9	3.9	
N-α-Acetyllysine	189.123	5.4	5	5.1	5.4	4.9	5.1	5.4	5	5.1	5.5	5	5.5	5	5.5	5	5	5	5	
O-Acetyl-L-carnitine	204.123	5	4.5	5.3	5	4.5	5.4	5	4.5	5.3	1	0.8	1.3	0.8	0.9	0.7	0.8	0.8	0.8	
Cytidine	244.093	4.5	4	3.2	4.4	4	3.2	4.4	4	3.4	4.3	x	4.3	4	4.3	4	4	4	4	
5-Methyluridine	259.092	2.3	2.2	0.7	2.3	2.2	0.7	2.3	2.2	0.8	2.4	2.1	2.3	2.1	2.3	2.1	2.1	2.1	2.1	
2'-O-Methyladenosine	282.120	1.6	1.3	1.1	1.6	1.3	1.2	1.6	1.4	1.2	1.6	1.4	1.6	1.4	1.6	1.4	1.4	1.4	1.4	
2'-O-Methylguanosine	298.115	x	3.7	2	4	3.6	2	4	3.6	2.1	4	3.6	4.2	3.6	4	3.6	3.9	3.9	3.9	
N ⁶ -Isopentenyladenosine	336.167	1.3	0.8	0.7	1	0.8	0.7	1	0.8	0.7	1	1	1	0.8	0.9	0.8	0.8	0.8	0.8	
Reserpine	609.2807	4.1	0.5	2.8	4	0.5	2.6	3.9	0.5	1.5	0.8	0.5	x	x	x	x	0.5	0.5	0.5	

Table B.S2 Number of detected isomeric pairs (x = not detected).

Isomeric pairs - Number of detected compounds	Acidic									Neutral					Basic			
	iHILIC Fusion 5-5 mM	iHILIC Fusion 5-10 mM	iHILIC Fusion 5-25 mM	BEH Amide 5-5 mM	BEH Amide 5-10 mM	BEH Amide 5-25 mM	Correxs HILIC 5-5 mM	Correxs HILIC 5-10 mM	Correxs HILIC 5-25 mM	iHILIC Fusion 5-5 mM	iHILIC Fusion 5-10 mM	iHILIC Fusion 5-25 mM	BEH Amide 5-5 mM	BEH Amide 5-10 mM	BEH Amide 5-25 mM	BEH Amide 5-5 mM	BEH Amide 5-10 mM	BEH Amide 5-25 mM
Betain; L-Valine	x	x	x	x	x	x	x	x	x	2	2	2	x	2	2	2	x	x
1,2,3-Trihydroxybenzene; 1,3,5-Trihydroxybenzene	x	x	x	x	x	x	x	x	x	x	x	x	x	x	x	2	2	2
L-Isoleucine; L-Leucine; L-Norleucine; L-tert-Leucine	4	4	4	4	4	4	4	4	4	4	4	4	4	4	4	4	4	4
Pseudouridine; Uridine	2	2	2	2	2	2	2	2	2	2	2	2	2	2	2	2	2	2
2'-C-Methylcytidine; 2'-O-Methylcytidine; 5-Methylcytidine	3	3	3	3	3	3	3	3	3	3	3	3	3	3	3	3	3	3
2'-O-Methyluridine; 3-Methylcytidine; 5-Methyluridine	3	3	3	3	3	3	3	3	3	3	3	3	3	3	3	3	3	3
1-Methyladenosine; 2'-O-Methyladenosine; N ⁶ -Methyladenosine	3	3	3	3	3	3	3	3	3	3	3	3	3	3	3	3	3	3
2'-O-Methylguanosine; N ² -Methylguanosine	2	2	2	x	2	2	2	2	2	2	2	x	x	2	2	2	2	2
D-Galactose; D-Glucose; D-Mannose	2	2	2	2	2	2	2	2	2	2	x	x	2	3	3	3	3	3
2-Hydroxyphenylacetic acid; 3-Hydroxyphenylacetic acid; 4-Hydroxyphenylacetic acid	3	3	3	3	3	2	3	3	3	2	2	2	2	2	2	3	3	3
Kaempferol; Luteolin	2	2	2	2	2	2	2	2	2	2	x	x	x	x	x	x	2	2
L-Homoserine; L-Threonine	2	x	2	2	2	2	x	x	2	2	2	x	x	x	x	x	x	x
Glucose-1-phosphate; Glucose-6-phosphate	x	x	2	x	x	x	x	x	2	x	x	x	x	x	x	x	x	x
D-Arabinose; D-Ribose	2	2	2	x	x	x	2	2	2	x	x	x	x	x	x	x	x	x
1-Methyl-Histidine; 3-Methyl-Histidine	2	2	2	2	2	2	2	2	2	x	x	x	x	x	x	x	x	x

Table B.S2 (continued) Number of separated isomeric pairs (ns = not separated).

Isomeric pairs - Separated compounds	Acidic									Neutral					Basic			
	iHILIC Fusion 5-5 mM	iHILIC Fusion 5-10 mM	iHILIC Fusion 5-25 mM	BEH Amide 5-5 mM	BEH Amide 5-10 mM	BEH Amide 5-25 mM	Correxs HILIC 5-5 mM	Correxs HILIC 5-10 mM	Correxs HILIC 5-25 mM	iHILIC Fusion 5-5 mM	iHILIC Fusion 5-10 mM	iHILIC Fusion 5-25 mM	BEH Amide 5-5 mM	BEH Amide 5-10 mM	BEH Amide 5-25 mM	BEH Amide 5-5 mM	BEH Amide 5-10 mM	BEH Amide 5-25 mM
Betain; L-Valine	ns	ns	ns	ns	ns	ns	ns	ns	ns	ns	2	ns	ns	ns	ns	2	ns	ns
1,2,3-Trihydroxybenzene; 1,3,5-Trihydroxybenzene	ns	ns	ns	ns	ns	ns	ns	ns	ns	ns	ns	ns	ns	ns	ns	2	ns	2
L-Isoleucine; L-Leucine; L-Norleucine; L-tert-Leucine	ns	ns	ns	2	2	2	2	ns	ns	1	ns	ns	2	3	2	ns	ns	ns
Pseudouridine; Uridine	2	2	2	2	2	2	2	2	2	2	2	2	2	2	2	2	2	2
2'-C-Methylcytidine; 2'-O-Methylcytidine; 5-Methylcytidine	3	3	2	3	3	3	2	3	3	2	2	2	3	3	3	3	3	3
2'-O-Methyluridine; 3-Methylcytidine; 5-Methyluridine	2	2	2	2	2	2	ns	ns	2	2	2	2	2	2	2	2	2	2
1-Methyladenosine; 2'-O-Methyladenosine; N ⁶ -Methyladenosine	2	2	2	2	2	2	ns	ns	ns	2	2	2	2	2	2	2	2	2
2'-O-Methylguanosine; N ² -Methylguanosine	2	2	2	ns	2	2	2	2	2	2	2	ns	ns	2	2	2	2	2
D-Galactose; D-Glucose; D-Mannose	ns	ns	ns	2	2	ns	ns	ns	ns	ns	2	3	3	3	2	2	2	2
2-Hydroxyphenylacetic acid; 3-Hydroxyphenylacetic acid; 4-Hydroxyphenylacetic acid	3	2	3	3	3	2	3	3	3	2	2	2	2	2	2	3	3	3
Kaempferol; Luteolin	ns	ns	2	ns	2	2	ns	2	2	2	ns	ns	ns	ns	ns	2	2	2
L-Homoserine; L-Threonine	ns	ns	2	ns	ns	ns	ns	ns	ns	2	2	ns	ns	ns	ns	ns	ns	ns
Glucose-1-phosphate; Glucose-6-phosphate	ns	ns	2	ns	ns	ns	ns	ns	ns	2	ns	ns	ns	ns	ns	ns	ns	ns
D-Arabinose; D-Ribose	2	2	2	ns	ns	ns	2	2	2	ns	ns	ns	ns	ns	ns	ns	ns	ns
1-Methyl-Histidine; 3-Methyl-Histidine	ns	2	2	2	2	ns	ns	2	ns	ns	ns	ns	ns	ns	ns	ns	ns	ns
Detected	30	28	32	26	28	27	28	28	30	27	23	21	20	24	24	27	27	27
Separated	16	17	23	18	22	17	13	16	16	19	16	12	16	19	18	20	18	20
% of separated isomers	53	61	72	69	79	63	46	57	53	70	70	57	80	79	75	74	67	74
Number of fully detected and resolved pairs	5	5	8	5	7	5	4	7	6	6	5	3	4	5	5	6	5	6
% of resolved isomeric pairs	33	33	53	33	47	33	27	47	40	40	33	20	27	33	33	40	33	40

Table B.S3 Fecal metabolites matched with analyzed standards. Possible isomer separation was taken into account; (y = detected in feces, x = not detected in feces).

Detected standards in feces	Acidic						Neutral						Basic					
	iHILIC Fusion 5-5 mM	BEH Amide 5-5 mM	Cortex HILIC 5-5 mM	iHILIC Fusion 5-10 mM	BEH Amide 5-10 mM	Cortex HILIC 5-10 mM	iHILIC Fusion 5-25 mM	BEH Amide 5-25 mM	Cortex HILIC 5-25 mM	iHILIC Fusion 5-5 mM	BEH Amide 5-5 mM	iHILIC Fusion 5-10 mM	BEH Amide 5-10 mM	iHILIC Fusion 5-25 mM	BEH Amide 5-25 mM	BEH Amide 5-5 mM	BEH Amide 5-10 mM	BEH Amide 5-25 mM
Benzoic acid	y	x	x	x	x	y	x	x	y	x	x	x	x	x	x	y	y	y
Isethionic acid	y	y	y	y	y	y	y	y	y	y	y	y	y	y	y	y	y	y
Methylsuccinic acid	y	y	y	y	x	y	y	y	x	x	x	x	x	x	x	x	x	x
Phenylacetic acid	y	y	y	y	y	y	y	y	y	y	y	y	y	y	y	y	y	y
Anthranilic acid	y	x	x	y	x	x	y	x	x	x	x	x	x	x	x	x	x	x
3-Hydroxyphenylacetic acid; 4-Hydroxyphenylacetic acid	y	x	x	y	x	x	y	x	x	x	x	x	x	x	x	y	y	y
4-Hydroxyphenylacetic acid	x	y	y	x	y	y	x	x	y	x	x	x	x	x	x	x	x	x
3-Hydroxyphenylacetic acid	x	y	y	x	y	x	x	y	x	x	x	x	x	x	x	x	x	x
Pimelic acid	y	x	x	y	y	x	x	y	x	y	y	y	x	x	x	x	x	y
3-(4-Hydroxyphenyl)-propionic acid	y	y	x	y	y	y	y	y	y	y	y	y	y	x	y	y	y	y
3-Indolepropionic acid	y	y	y	y	y	y	y	y	y	x	y	x	y	y	y	y	y	y
3-Indoxylsulfate	y	x	y	y	x	y	y	x	x	x	x	x	x	x	x	x	x	x
Inosine	y	y	y	y	y	y	y	y	x	x	x	x	x	x	y	y	y	y
Arachidonic acid	y	y	y	y	y	y	y	y	y	y	y	y	y	y	y	y	y	y
Uracile	y	y	y	y	y	y	y	y	y	x	y	y	y	y	y	y	y	y
Creatinine	y	y	y	y	y	y	y	y	y	y	y	y	y	y	y	y	y	y
L-Proline	y	y	y	y	y	y	y	x	y	x	y	x	y	x	y	y	y	y
Taurine	y	y	y	y	y	y	y	y	y	y	y	y	y	y	y	y	y	y
Creatine	y	y	y	y	y	y	y	x	y	y	y	x	y	x	y	x	y	y
L-Ornithine	y	x	x	y	x	x	y	x	x	x	x	x	x	x	x	x	x	x
N-Methylnicotinamide	y	y	y	y	y	y	x	y	y	y	y	y	y	y	y	y	y	y
L-Glutamine	y	y	x	x	y	y	y	y	y	x	y	x	y	x	y	y	y	y
L-Lysine	y	y	y	y	y	y	y	x	x	x	x	x	y	x	x	y	y	y
L-Glutamic acid	y	y	x	y	x	y	y	y	x	x	x	x	x	x	x	y	y	y
L-Methionine	y	x	x	y	x	x	x	x	y	x	x	x	x	x	x	y	y	y
3-Phenylpropionic acid	y	y	x	y	x	y	y	x	y	y	y	y	y	y	y	y	y	y
L-Histidine	y	x	x	y	x	y	y	x	x	x	x	x	x	x	x	x	x	x
Carnitine	y	y	y	y	y	y	y	y	y	y	y	y	y	y	y	y	y	y
N-Acetyl-L-ornithine	y	y	x	y	y	x	y	y	x	y	x	y	y	x	y	y	y	y
L-Arginine	y	y	y	y	y	y	y	y	x	x	y	x	y	y	y	y	y	y
L-Citrulline	y	y	y	y	y	y	y	y	y	x	y	x	y	x	y	y	y	y
L-Tyrosine	y	x	x	y	x	x	x	y	x	x	x	x	x	x	x	y	y	y
4-Pyridoxic acid	y	y	y	y	y	y	y	y	y	y	y	y	y	y	y	y	y	y
N-Acetylglutamic acid	y	y	x	y	y	x	x	y	x	x	y	x	y	x	y	y	y	y
O-Acetyl-L-carnitine	y	x	x	x	x	x	x	x	y	x	x	x	x	x	x	x	x	x
Thymidine	y	y	y	y	y	y	y	y	y	y	y	y	y	y	y	y	y	y
Cytidine	y	x	y	y	x	y	y	x	y	x	x	x	x	x	x	x	x	x
Uridine	y	y	y	y	y	y	y	y	y	y	x	y	x	y	y	y	y	y
Biotin	y	x	y	y	x	y	y	x	y	x	x	x	x	x	x	x	x	x
Adenosine	y	x	y	y	x	y	y	x	x	y	x	y	x	y	x	x	x	x
Apigenin	y	y	y	y	y	y	x	y	y	x	x	x	x	x	x	y	y	y
Myristoyl Ethanolamide	y	y	y	y	y	y	y	y	y	x	y	y	y	y	y	y	y	y
γ-Linolenic acid	y	y	y	y	y	y	y	y	y	y	y	y	y	y	y	y	y	y
Guanosine	y	x	y	y	x	y	y	x	y	x	x	x	x	x	x	x	x	x
γ-Linolenoyl Ethanolamide	y	y	y	y	y	y	y	y	y	y	y	y	x	y	y	y	y	y
Arachidonoyl Ethanolamide	y	y	y	y	y	y	y	y	y	y	y	y	y	y	y	y	y	y
Riboflavine	y	y	y	y	y	y	y	y	x	x	x	x	x	x	x	y	y	y
Caprylic acid	x	y	x	x	y	x	y	x	x	y	x	x	y	x	y	y	y	y
Palmitic acid	x	y	x	x	y	x	x	y	x	x	y	x	y	x	y	y	y	y
L-Phenylalanine	x	y	y	y	y	x	y	y	x	y	x	y	x	y	x	y	y	y
3-Methyl-Histidine	x	y	x	y	x	x	x	x	x	x	x	x	x	x	x	y	x	x
Indole-3-acetic acid	x	y	y	x	y	y	y	x	x	x	x	x	x	y	x	y	y	y
Retinol	x	y	x	x	y	x	x	y	x	x	x	x	x	x	x	x	x	x
D-Arabinose; D-Ribose	x	x	y	x	x	x	x	x	x	x	x	x	x	x	x	x	x	x
D-Arabinose	x	x	x	x	x	x	y	x	y	x	x	x	x	x	x	x	x	x
D-Ribose	y	y	y	y	y	y	y	x	y	y	x	y	y	y	y	y	y	y
2-Hydroxyphenylacetic acid	x	x	y	x	x	x	x	x	x	x	x	x	x	x	x	x	x	x

C. Appendix Chapter 4

C.1 Original Publication

Milk-Derived Amadori Products in Feces of Formula-Fed Infants

Nina Sillner,^{†,‡} Alesia Walker,^{*,†,‡} Daniel Hemmler,^{†,§} Monika Bazanella,^{||} Silke S. Heinzmann,[†] Dirk Haller,^{‡,||} and Philippe Schmitt-Kopplin^{†,‡,§}

[†]Research Unit Analytical BioGeoChemistry, Helmholtz Zentrum München, 85764 Neuherberg, Germany

[‡]ZIEL Institute for Food and Health, Technical University of Munich, 85354 Freising, Germany

[§]Chair of Analytical Food Chemistry, Technical University of Munich, 85354 Freising, Germany

^{||}Chair of Nutrition and Immunology, Technical University of Munich, 85354 Freising, Germany

S Supporting Information

ABSTRACT: Food processing of infant formula alters chemical structures, including the formation of Maillard reaction products between proteins and sugars. We detected early Maillard reaction products, so-called Amadori products, in stool samples of formula-fed infants. In total, four Amadori products (*N*-deoxylactulosyllysine, *N*-deoxyfructosyllysine, *N*-deoxylactulosylleucylisoleucine, *N*-deoxyfructosylleucylisoleucine) were identified by a combination of complementary nontargeted and targeted metabolomics approaches. Chemical structures were confirmed by preparation and isolation of reference compounds, LC-MS/MS, and NMR. The leucylisoleucine Amadori compounds, which most likely originate from β -lactoglobulin, were excreted throughout the first year of life in feces of formula-fed infants but were absent in feces of breastfed infants. Despite high inter- and intraindividual differences of Amadori products in the infants' stool, solid food introduction resulted in a continuous decrease, proving infant formula as the major source of the excreted Amadori products.

KEYWORDS: Amadori products, Maillard reaction, metabolomics, infant formula, milk marker, fructosyllysine

■ INTRODUCTION

In the first months of life the only source of food for infants is breast milk or infant formula. During infant formula production and subsequent storage, Maillard reaction products are formed. For example, Amadori products, such as *ε*-*N*-deoxylactulosyllysine (LacLys), originate from lactosylation of 5–20% of the protein-bound lysine in infant formula.¹ In comparison, the glycation of protein-bound lysine in human breast milk is much lower however, depending on maternal nutrition. Under acidic conditions LacLys is partially released from milk proteins in the form of furosine, which is often used as an indicator of the degree of lysine glycosylation.^{2,3} Clawin-Rädecker and Schlimme reported about 20–25 mg furosine/100 g of protein in breast milk from women in Germany.⁴ Very low or nondetectable (below 6 mg furosine/100 g of protein) contents were measured in breast milk from women in Poland. But, in infant formula concentrations from 1320 to 1550 mg furosine/100 g of protein were detected.⁵ However, the nutritional consequences for formula-fed infants are not completely understood. Studies have shown that *ε*-*N*-deoxyfructosyllysine (FruLys) was not available as a lysine source *in vivo*; therefore, a significant loss of nutritional value was suggested.⁶ This loss is normally compensated by an increased protein amount in formula.¹ Also the bioavailability and excretion of milk-derived Amadori products ingested by formula-fed infants are largely unknown. In different intervention studies with adults or rats only 3–10% of peptide-bound Amadori products were absorbed and rapidly excreted via urine, whereas most of the Amadori products were suggested to be fermented by the gut microbiota.^{7–9} In *in vitro* tests, FruLys was not actively transported by intestinal cells but rather absorbed by diffusion.^{10,11} Different glycated dipeptides,

however, might be absorbed and cross the basolateral membrane after amino acid hydrolysis inside colonic cells.¹²

Occasionally, novel food markers can be identified in nutrition studies by nontargeted metabolomics profiling without prior focusing on ingredients or metabolites.^{13–15} In the present work, we conducted a multistep analytical approach to discover and identify milk-derived Amadori products in feces of formula-fed infants. This was achieved by comparing fecal samples from formula-fed and breastfed infants at several time points during their first year of life using a combination of liquid chromatography, mass spectrometry, and nuclear magnetic resonance spectroscopy.

■ MATERIALS AND METHODS

Study Design. Stool samples ($n = 244$, Table S1) from healthy infants, who received infant formula with ($n = 11$, F+) or without ($n = 11$, F-) bifidobacteria (*B. bifidum*, *B. breve*, *B. infantis*, *B. longum*) or exclusively breast milk ($n = 20$, B), were collected over a period of two years in a randomized, double-blinded, placebo-controlled intervention trial as described elsewhere.¹⁶ For metabolomics analysis, fecal samples of months 1, 3, 5, 7, 9, 12, and 24 were selected. The trial was registered at the German Clinical Trials Register under number DRKS00003660, and the protocol was approved by the ethics committee of the medical faculty of the Technical University of Munich (approval no. 5324/12).

Chemicals. L-Lysine, D-(+)-glucose, α -lactose monohydrate, and trimethylsilylpropionate (TSP; 98%) were purchased from Sigma-Aldrich (Steinheim, Germany). Leucylisoleucine was purchased from Bachem (Bubendorf, Switzerland), and *ε*-*N*-deoxyfructosyllysine

Received: March 26, 2019

Revised: May 14, 2019

Accepted: June 17, 2019

Published: June 17, 2019

(dihydrochloride) was purchased from Abcam (Cambridge, U.K.). Milli-Q water (18.2 M Ω) was derived from a Milli-Q Integral Water Purification System (Billerica, MA, USA). Acetonitrile (ACN; LiChrosolv, hypergrade for LC-MS), methanol (LiChrosolv, hypergrade for LC-MS), and ammonium acetate (NH₄Ac) were obtained from Merck (Darmstadt, Germany). Glacial acetic acid was purchased from Biosolve (Valkenswaard, Netherlands).

Fecal Sample Preparation. Metabolite extraction from infant stool samples was prepared with methanol as described previously.¹⁶ For direct infusion Fourier transform ion cyclotron resonance mass spectrometry (FT-ICR-MS) analysis, the extracts were diluted 1:1000 (v/v) with methanol. For ultrahigh-performance liquid chromatography-tandem mass spectrometry (UHPLC-MS/MS) measurements, the methanol extracts were evaporated under vacuum at 40 °C (SpeedVac Concentrator, Savant SPD121P, ThermoFisher Scientific, Waltham, MA, USA) and reconstituted with ACN/H₂O 75:25 (v/v). A pooled sample was generated from all fecal extracts for quality control purposes. All samples were stored at -80 °C in tightly closed tubes.

Direct Infusion FT-ICR Mass Spectrometry. Ultrahigh-resolution FT-ICR mass spectra of diluted fecal extracts from 1-month-old infants were acquired with a 12 T Bruker Solarix mass spectrometer (Bruker Daltonics, Bremen, Germany) equipped with an APOLLO II electrospray source in negative ionization mode. The diluted samples were infused into the electrospray ion source with a flow rate of 2 μ L/min. Settings for the ion source were a drying gas temperature of 180 °C, a drying gas flow of 4 L/min, and a capillary voltage of 3600 V. The spectra were acquired with a time-domain of 4 megawords, and 150 scans were accumulated within a mass range of 123–1000 Da. The mass spectrometer was first externally calibrated by ion clusters of arginine (57 nmol/mL in methanol). Internal calibration of each spectrum was conducted with a reference list containing omnipresent fatty acids. Raw spectra were post-processed by Compass DataAnalysis 4.2 (Bruker Daltonics, Bremen, Germany), and mass signals with a signal-to-noise ratio of at least 6 were exported to mass lists. All exported features were aligned into a matrix containing averaged mass signals values (maximum peak alignment window width: \pm 0.5 ppm) and corresponding intensities of all analyzed samples.¹⁷ FT-ICR artifacts (side lobes) were filtered as described elsewhere.¹⁸ Only *m/z* features of monoisotopic candidates were retained in the matrix. Assignment of molecular formulas by mass difference network analysis was performed as recently described.¹⁹

For van Krevelen diagrams, the intensities of the mass signals measured in either formula-fed (*n* = 19) or breastfed (*n* = 16) infants were averaged. Moreover, for better visualization molecular formulas of fatty acids with very high signal intensities were excluded.

UHPLC-MS/MS Analysis. Fecal sample extracts and standard substances (in ACN/H₂O 75:25, v/v) were analyzed by UHPLC (Acquity, Waters, Milford, MA, USA) coupled to a time-of-flight (TOF) mass spectrometer (MS) (maXis, Bruker Daltonics, Bremen, Germany). Hydrophilic interaction liquid chromatography (HILIC) was performed using an iHILIC-Fusion UHPLC column SS (100 \times 2.1 mm, 1.8 μ m, 100 Å, HILICON AB, Umea, Sweden). Chromatographic settings were the same as previously described¹⁰ with some modifications (injection volume of 5 μ L; eluent A consisted of 5 mmol/L NH₄Ac (pH 4.6) in 95% ACN (pH 4.6) and eluent B consisted of 25 mmol/L NH₄Ac (pH 4.6) in 30% ACN with a runtime of 12.1 min, followed by reconditioning for 5 min after each sample, respectively). Every tenth injection a pooled fecal sample was used as a quality control for subsequent batch normalization.

Calibration of the MS was done by injecting ESI-L Low Concentration Tuning Mix (Agilent, Santa Clara, CA, USA) prior to the measurements. Additionally, ESI-L Low Concentration Tuning Mix (diluted 1:4 (v/v) with 75% ACN) was injected in the first 0.3 min of each UHPLC-MS run by a switching valve for internal recalibration. Mass spectra were acquired in positive and negative electrospray ionization mode (\pm ESI). Parameters of the ESI source were a nitrogen flow rate of 10 L/min, a dry heater set at 200 °C, a nebulizer pressure of 2 bar, and a capillary voltage of 4000 V. Data were acquired in line and in profile mode with an acquisition rate of 5 Hz within a mass range of 50–1500 Da. Data-dependent MS/MS experiments were performed in

automated MS/MS mode. After each precursor scan, the five most abundant ions (absolute intensity threshold \geq 2000 au) were subjected to MS/MS. Each fecal sample was measured in duplicates with a collision energy of 10 and 35 eV, respectively.

Raw UHPLC-MS data were processed with Genedata Expressionist Refiner MS 11.0 (Genedata GmbH, Munich, Germany), including chemical noise subtraction, intensity cutoff filter, calibration, chromatographic peak picking, deisotoping, and metabolite library search against the Human Metabolome Database (HMDB)²¹ for MS1 level spectra (\pm 0.005 Da). Peak areas of duplicates were averaged and normalized to fecal weight. Batch normalization based on consecutive quality control measurement samples (pooled sample) was performed after missing value imputation (randomized number between 1.0 and 1.2, based on lowest value of the data matrix).

Targeted MS/MS experiments of different Amadori products were performed in multiple reaction monitoring mode (MRM) at 20 eV in positive ionization mode. The MS/MS fit score between standards and Amadori products in fecal samples were calculated with the Bruker Compass DataAnalysis 4.2 software (Bruker Daltonics, Bremen, Germany). The score indicates how well the masses and intensities of the reference compound spectra agree with those found in the spectrum of a pooled fecal sample.

Preparation of Reference Amadori Products. Glucose was mixed with either leucylisoleucine or lysine, and lactose was mixed with either leucylisoleucine or lysine (1 mL, 0.2 mol/L in Milli-Q purified water, respectively). The four reaction mixtures were heated in closed glass vials for 1 h at 100 °C,²² cooled to room temperature, and stored at -20 °C. For quantitative measurements *N*-deoxyfructosylleucylisoleucine (FruLeulle) was purified by diluting the mixture 1:5 (v/v) with Milli-Q water and subsequent isolation by HPLC-MS. The isolated fractions containing FruLeulle were pooled and dried using a vacuum Schlenk line. The dried product was dissolved in Milli-Q water. Finally, the concentration of the FruLeulle stock solution was determined with NMR (0.73 mmol/L).

Isolation of *N*-Deoxyfructosyl-*N*-Deoxylactulosylleucylisoleucine from Feces. To analyze the structures of *N*-deoxyfructosyl- and *N*-deoxylactulosylleucylisoleucine (FruLeulle and LacLeulle) by NMR spectroscopy, 6 fecal samples (methanol extracts) from formula-fed infants were selected. The Amadori products were isolated from in total 1 mL (50 mg feces/mL methanol) of the fecal extracts by HPLC-MS. Afterward, the fractions containing either FruLeulle or LacLeulle were pooled and evaporated under vacuum at 40 °C (SpeedVac Concentrator, Savant SPD121P, ThermoFischer Scientific, Waltham, MA, USA).

High-Pressure Liquid Chromatography-Based Isolation of Amadori Products. The Amadori products FruLeulle and LacLeulle were semi-preparatively purified by high-pressure liquid chromatography (HPLC) using an Agilent 1290 Infinity LC system (Santa Clara, CA, USA) with an Xbridge Prep C8 column (5 μ m, 10 \times 100 mm, Waters (Milford, MA, USA)). An isocratic method with 93% 5 mmol/L NH₄Ac and 0.1% acetic acid in water and ACN/H₂O 7:93 (v/v) with a runtime of 14 min was used. The flow rate, column temperature, and injection volume was 3 mL/min, 60 °C, and 100 μ L, respectively. The sample manager was cooled to 5 °C. The Amadori products were collected with a Gilson 215 Liquid Handler (Middleton, WI, USA), while the specific collection time windows were monitored with an amaZon ETD ion trap mass spectrometer (Bruker Daltonics GmbH, Bremen, Germany). Therefore, the flow was split 10:1 post-column (QuickSplit, ASI, Richmond, CA, USA).

Amadori Product Quantification. Stock solutions of the reference compounds FruLeulle and FruLys were prepared in Milli-Q water and stored at -20 °C until analysis. The concentration of the stock solution of FruLeulle was determined as 0.73 mmol/L and of FruLys as 12.4 mmol/L using qNMR. For quantification of FruLeulle and FruLys in fecal samples, the stock solutions were diluted with ACN/H₂O 75:25 (v/v), and a six-point calibration curve was prepared with a concentration range of 0.073–17.3 μ mol/L for FruLeulle and of 1.24–124 μ mol/L for FruLys. Six representative formula-fed children (*n* = 3 F- and *n* = 3 F+) were selected randomly, and fecal samples from months 1, 3, 5, 7, 9, and 12 were diluted 1:20 (v/v) with ACN/H₂O

75:25 (v/v) and analyzed with HILIC UHPLC-TOF-MS (positive ionization mode) as described in the main part. The data were processed with QuantAnalysis 2.2 (Bruker Daltonics GmbH, Bremen, Germany) using a quadratic curve fit.

Nuclear Magnetic Resonance Spectroscopy. The chemical standard leucylisoleucine, the prepared and purified FruLeulle, and the isolated Amadori products FruLeulle and LacLeulle from feces were each dissolved in 70 μL of aqueous NMR buffer (15% D_2O containing TSP) and transferred to 2 mm outer diameter NMR vials. NMR experiments were carried out on a Bruker 800 MHz spectrometer (Bruker Biospin, Rheinstetten, Germany) operating at 800.35 MHz and equipped with a quadrupole inverse cryogenic probe. The spectrometer used a standard one-dimensional (1D) pulse-sequence noesygppr1d [recycle delay (RD)-90°-t1-90°-mixing time (tm)-90°-acquire] free-induction decay with water presaturation during a relaxation delay of 2 s, a mixing time (tm) set to 200 ms, and a 90° pulse of 9.6 μs . Spectra were acquired with 1024 scans into 64 K data points with a spectral width of 12 ppm. For 2D NMR spectra, phase-sensitive sensitivity-improved 2D TOCSY data with water suppression by gradient-tailored excitation (Watergate) (3-9-19) and using decoupling in the presence of scalar interactions (DIPSI-2) were acquired. For each spectrum, 19228 \times 1024 data points were collected, with an acquisition time of 1 s, 16 dummy scans, and a mixing time of 20 ms. The number of scans was adjusted according to the concentration of the sample, ranging from 8 to 256 scans. The spectral widths were set to 12 and 12 ppm in the F2 and F1 dimensions, respectively.

Additionally, quantitative NMR (qNMR) measurements were performed to determine the exact concentrations of the FruLeulle and FruLys stock solutions. For this, 50 μL of D_2O solvent containing 1 mg/mL internal standard TSP was mixed with 150 μL of the FruLeulle or FruLys stock solution and transferred to a 3 mm NMR tube. ^1H NMR experiment (noesygppr1d) with 128 scans, 16 dummy scans, and a relaxation delay of 30 s was performed, achieving full relaxation of all protons and therefore was a quantitative experiment. All other parameters were set as described previously. Peaks were integrated with TopSpin, and the integrals were calibrated to TSP peaks (9H) and stoichiometrically corrected.

Other Methods. Details of acid hydrolysis of infant formula are given in the Supporting Information.

RESULTS AND DISCUSSION

Nontargeted Metabolomic Screening of Feces from Formula-Fed and Breastfed Infants using FT-ICR-MS. Stool samples of one-month-old children fed either with breastmilk or infant formula were measured by FT-ICR-MS. Assigned molecular formulas were visualized in van Krevelen diagrams to represent a large amount of compounds in a two-dimensional space using the H/C and O/C ratios of molecular formulas.²³ Unique signatures were found for formula-fed (Figure 1) and breastfed (Figure S1) infants with dominant distinctions in nitrogen containing compounds (CHON; orange). In formula-fed infants the O/C ratios between 0.4 and 0.7 were very prominent. The most intense CHON compounds were assigned to $\text{C}_{18}\text{H}_{34}\text{N}_2\text{O}_8$, $\text{C}_{24}\text{H}_{44}\text{N}_2\text{O}_{13}$, $\text{C}_{12}\text{H}_{24}\text{N}_2\text{O}_7$, and $\text{C}_{18}\text{H}_{34}\text{N}_2\text{O}_{12}$ (Figure 1). Mass-signal-based annotation using the Human Metabolome Database (HMDB) resulted in only one match, namely for fructosyllysine (FruLys, $\text{C}_{12}\text{H}_{24}\text{N}_2\text{O}_7$), which is a well-known Amadori product in human nutrition.²⁴ Therefore, we suggested that the other abundant CHON containing metabolites could also belong to the class of Amadori products. Amadori products are formed during heating or storage processes of food. In the initial stage of the Maillard reaction, the free ϵ -amino group of lysine in food proteins reacts with reducing sugars, such as glucose or lactose, resulting in the formation of, for example, FruLys.²⁴ The exclusively formula-fed infants from this cohort consumed infant formula, which was supplemented with whey powder.

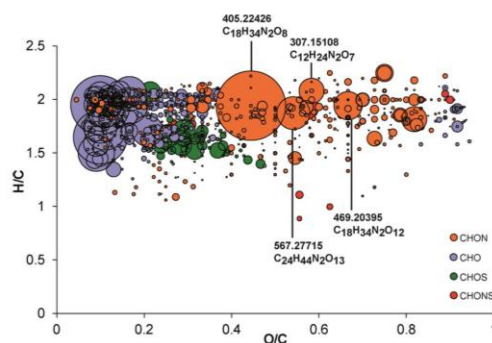


Figure 1. Chemical composition of feces from 1-month-old infants, who were exclusively fed with infant formula (average of signal intensity of $n = 19$ fecal samples), acquired by FT-ICR-MS in negative ionization mode. Calculated molecular formulas were categorized into four compositional groups: CHO (blue), CHON (orange), CHOS (green), and CHONS (red). The van Krevelen diagram plots the H/C vs O/C atomic ratios of the computed molecular formulas. Putative Amadori products are highlighted with measured m/z values and calculated molecular formulas.

Supplementation of whey is frequently used to adapt the cow's milk casein to whey ratio (82:18) to that of human milk (40:60).²⁵ Whey proteins are richer in lysine than casein, and it can be expected that more Amadori products are formed.²⁶ Up to 20% of the lysine residues in cow milk-based formula are blocked by Amadori products.²⁷ The main Amadori product in infant formula is LacLys, which results from the condensation of lactose with lysine residues (lactosylation) of milk proteins, especially with those of the major whey protein β -lactoglobulin. The LacLys content is approximately 3-fold higher in infant formula than in UHT-sterilized liquid cow milk, since infant formulas are more rigorously heat treated for microbiological safety and long shelf life.²⁸ Heat-induced lactosylation of β -lactoglobulin was found at several lysine residues and the N-terminal leucine.^{29–34}

Our assumption of possible Amadori products in stool samples of formula-fed infants was supported by further UHPLC-MS/MS measurements. We analyzed all stool samples and screened them for mass signals, representing the four most intense CHON-containing compounds found by FT-ICR-MS analysis (Figure 1). Due to the polar characteristics of Amadori products, we used a HILIC UHPLC-MS/MS method. An exemplary chromatogram of a fecal sample from one formula-fed infant at the age of one month is shown in Figure 2. All four mass signals were detected within an error of ± 0.005 Da ($\text{C}_{18}\text{H}_{34}\text{N}_2\text{O}_8$, pink; $\text{C}_{24}\text{H}_{44}\text{N}_2\text{O}_{13}$, blue; $\text{C}_{12}\text{H}_{24}\text{N}_2\text{O}_7$, green; $\text{C}_{18}\text{H}_{34}\text{N}_2\text{O}_{12}$, orange). A typical fragment observed for $\text{C}_{18}\text{H}_{34}\text{N}_2\text{O}_8$ and $\text{C}_{24}\text{H}_{44}\text{N}_2\text{O}_{13}$ with m/z 245.1860 in MS/MS experiments (Figure 3C and G) was annotated as leucylisoleucine, which coincides with the N-terminal amino acid sequence of β -lactoglobulin. Also, the calculated molecular formulas from the FT-ICR-MS screening supported the assumption of leucylisoleucine Amadori products with glucose and lactose ($\text{C}_{18}\text{H}_{34}\text{N}_2\text{O}_8$ and $\text{C}_{24}\text{H}_{44}\text{N}_2\text{O}_{13}$). Interestingly, only the dipeptide leucylisoleucine Amadori products and no mass signals for fructosyl-/lactosylleucine were detected in feces. To verify our assumptions reference substances were prepared and isolated.

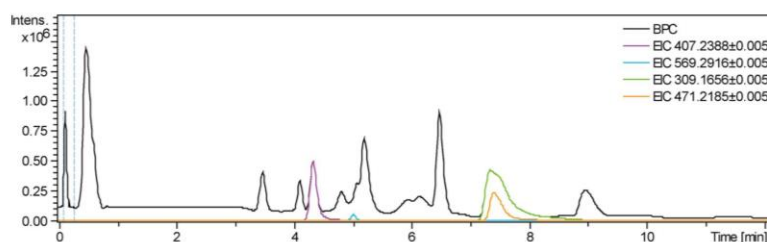


Figure 2. Representative chromatogram of a fecal sample (child ID 25, age 1 month, formula-fed) separated by hydrophilic interaction liquid chromatography (HILIC) and detected in positive ionization mode by TOF-MS. Base peak chromatogram (BPC, black) and extracted ion chromatograms (EICs) of the m/z values referring to the putative Amadori products FruLeulle ($[M + H]^+ = 407.2388$, pink), LacLeulle ($[M + H]^+ = 569.2916$, blue), FruLys ($[M + H]^+ = 309.1656$, green), and LacLys ($[M + H]^+ = 471.2185$, orange); extracted with ± 0.005 Da.

Identification of Fecal Amadori Products using UHPLC-MS/MS and NMR.

Chemical structures were confirmed by comparison of retention time, MS/MS fragmentation patterns, and spiking experiments. The prepared reference compounds FruLeulle and LacLeulle (Figure 3A and E, blue) showed the same retention time as the according peak in the fecal sample (Figure 3A and E, orange), which was further confirmed by spiking of purified reference compounds into fecal samples (Figure 3A and E, green). Additionally, the MS/MS fragmentation patterns were the same (fit score of 99.7% and 99.3%, respectively) (Figure 3B, C and F, G). Chemical structures of FruLeulle and LacLeulle are shown in Figure 3D and H. Matching retention times and MS/MS fragments between the reference substances of FruLys (purchased) and LacLys (prepared reference) and the pooled fecal sample from formula-fed infants are illustrated in Figure S2. All Amadori products showed similar fragmentation patterns (Figure 3B, D and Figure S2B, D). Dominant fragment ions were neutral losses of water [18 Da ($-H_2O$), 36 Da ($-2H_2O$), 54 Da ($-3H_2O$); 84 Da ($-3H_2O-CH_2O$)] and loss of the glucose/lactose moiety (162/324 Da), which are characteristic for this compound class.^{3,35,36}

Furthermore, FruLeulle and LacLeulle were isolated from feces by HPLC, and the structures were verified by NMR spectroscopy (1D 1H Figure 4 and 2D $^1H-^1H$ TOCSY Figures S3–S6). First, NMR spectra of leucylisoleucine were recorded to annotate chemical shifts of each hydrogen atom (Figures 4A and S3). These were 0.893 (3H, t, H-1), 0.925 (3H, d, H-4), 0.967 (6H, dd, H-9, H-10), 1.175 (1H, m, H-2), 1.463 (1H, m, H-2), 1.711 (2H, m, H-7, H-8), 1.788 (1H, m, H-7), 1.832 (1H, m, H-3), 4.069 (1H, t, H-6), and 4.116 (1H, dd, H-5). Second, the prepared product of leucylisoleucine and glucose, i.e., FruLeulle was analyzed and compared to the unconjugated dipeptide (Figures 4B and S4). Slight variations were observed for the chemical shifts, introduced by the conjugation of glucose near H-6 but separated by NH. These were 0.893 (3H, t, H-1), 0.925 (3H, d, H-4), 0.967 (3H, d, H-9 or H-10) and 0.933 (3H, d, H-9 or H-10), 1.19 (1H, m, H-2), 1.463 (1H, m, H-2), 1.665 (1H, m, H-8), 1.688 (1H, m, H-7), 1.833 (1H, m, H-7), 1.85 (1H, m, H-3), 4.012 (1H, t, H-6), and 4.164 (1H, dd, H-5). In addition, a doublet of doublets was observed, arising from the CH_2 connecting the dipeptide and monosaccharide (3.19 (2H, dd, H-11)). Further signals arising from the bound glucose were observed, i.e., 3.70 (1H, m, H-14), 3.73 (1H, dd, H-12), 3.88 (1H, dd, H-13), and 4.01 (2H, m, H-15). Subsequently, these shifts were compared to resonances arising from the proposed FruLeulle in fecal extracts (Figures 4C and S5). Here again

similar resonances were found, confirming the presence of the Amadori product in stool, i.e., 0.893 (3H, t, H-1), 0.925 (3H, d, H-4), 0.967 (3H, d, H-9 or H-10) and 0.933 (3H, d, H-9 or H-10), 1.19 (1H, m, H-2), 1.463 (1H, m, H-2), 1.66 (1H, m, H-8), 1.719 (1H, m, H-7), 1.788 (1H, m, H-7), 1.85 (1H, m, H-3), 4.07 (1H, t, H-6), and 4.164 (1H, dd, H-5). For LacLeulle, similar chemical shifts were found, with an additional resonance at 4.52 ppm (1H, d, H-16) from the galactose moiety (Figure S6).

To verify the presence of Amadori products in the infant formula consumed in this cohort, the formula powder was acid hydrolyzed. Under these conditions Amadori products are released from milk proteins in the form of *N*-(2-furoylmethyl) amino acids.^{2,28,37} Accordingly, mass signals for *N*-(2-furoylmethyl)-lysine (furosine), *N*-(2-furoylmethyl)-leucine, and *N*-(2-furoylmethyl)-leucylisoleucine were detected. Their fragmentation patterns showed typical fragments of lysine (84.082 Da) and leucine/isoleucine (86.097 Da) (Figure S7), which were also present in the Amadori product fragmentation patterns. Penndorf et al.³⁷ identified several *N*-(2-furoylmethyl) amino acids in hypoallergenic but only furosine in conventional (intact protein-containing) infant formulas. However, the detection of *N*-(2-furoylmethyl)-leucine and *N*-(2-furoylmethyl)-leucylisoleucine in our study might be due to different detection methods and general variations between different infant formulas (e.g., differences in whey supplementation).

Fecal Excretion Profiles of the Change of Amadori Products over Time. The fecal excretion of the identified Amadori products in relation to formula consumption was studied in infants within the first year of life (six time points) and at the age of 24 months (no longer formula-fed) by HILIC UHPLC-MS (Figure 5, Table S1). Exclusively breastfed infants served as the control group (B, red). In formula-fed infants (F–, green and F+, blue) the Amadori products were most abundant at the age of 1–3 months. Apart from FruLeulle, we noticed a strong decrease in Amadori profiles after an age of 5 months. By comparison, FruLeulle showed relatively high values up to an age of 9 months (Figure 5A). Most of the formula-fed infants received additionally solid food from month 5 onward (Table S1), which most likely contributed to the reduced excretion of the Amadori products. The lactosylated compounds (Figure 5B and D) declined earlier than the glycosylated ones (Figure 5A and C), which might indicate an enhanced capacity for the digestion of the lactose moiety progressing with time. At the age of 12 months, toddlers receive a much lower amount of formula in relation to their body weight compared to newborns and are fed primarily with solid food. Therefore, most Amadori products

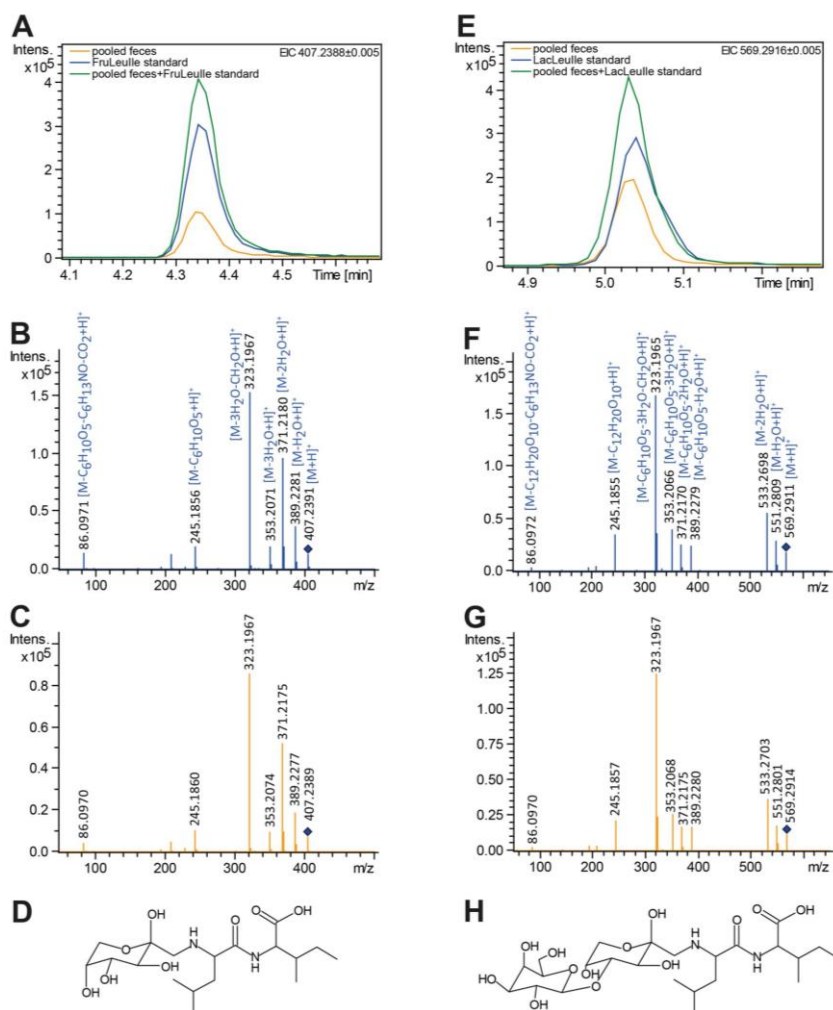


Figure 3. Identification of Leulle Amadori products performed with HILIC LC-MS/MS (positive ionization mode). (A) Extracted ion chromatogram (EIC) of FruLeulle ($[M + H]^+ = 407.2388 \pm 0.005$ Da) in feces (orange), prepared reference compound (blue), and spiking of the purified Amadori product into the pooled fecal extract (green). (B) Collision-induced dissociation MS/MS experiments (20 eV) of the prepared FruLeulle standard and (C) of pooled fecal samples (MS/MS match: fit score of 99.7%). (D) Proposed chemical structure of FruLeulle. (E) EIC of LacLeulle ($[M + H]^+ = 569.2916 \pm 0.005$ Da) in feces (orange), prepared reference compound (blue), and spiking of the purified Amadori product into the pooled fecal extract (green). (F) Collision-induced dissociation MS/MS experiments (20 eV) of the prepared LacLeulle standard and (G) of pooled fecal samples (MS/MS match: fit score of 99.3%). (H) Proposed chemical structure of LacLeulle.

were not detectable any more. Interestingly, FruLeulle was still detectable in low amounts at an age of 12 months (Figure 5A). Besides the displacement of the formula-derived Amadori products by feeding of solid food, the gut microbiota could also play an important role. During the first year of life the gut microbiome significantly changes and becomes more diverse.¹⁶ Many studies have suggested a microbial degradation of FruLys in the intestinal tract^{5–10,38–41} and modulation of the microbiota composition by Maillard reaction products.⁴² This

hypothesis was proven for specific bacterial strains^{43–45} and for fecal suspensions from human adults.⁴⁶ Whether formula-derived Amadori products have an influence on the composition of the infant's gut microbiota or not needs to be investigated. At the age of 24 months Amadori products were no longer detectable. Overall, there were no major differences between the formula-fed group with probiotics (F+, blue, Figure 5) and without probiotics (F–, green; Figure 5). However, the high variation between the different samples of the same month

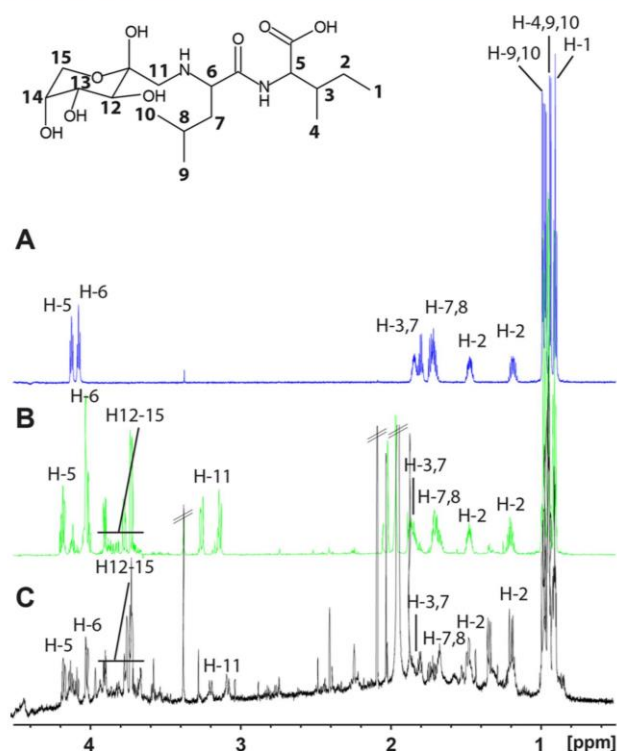


Figure 4. Identification of FruLeulle Amadori products performed with ^1H NMR spectroscopy and structural annotation. (A) Leulle standard, (B) prepared FruLeulle standard, and (C) extracted FruLeulle from fecal samples. Small deviations in the chemical shift for FruLeulle derive from different amounts of NH_4Ac in the two samples.

indicate large interindividual differences. During exclusive breastfeeding no Amadori products were excreted in feces (B, red; Figure 5). However, after the introduction of solid food, we could detect low amounts of Amadori products occasionally, which may originate from other milk sources.

To get a better idea of the quantities of excreted Amadori products in feces, samples from 6 formula-fed individuals were selected and FruLeulle and FruLys were quantified in samples from month 1 to 12 (Figure S8). The concentrations of the stock solutions used for quantification were determined with qNMR (Figure S9). In total, the fecal concentrations of the two Amadori products were high during the first months of life and much lower in months 9 and 12. On average $1.6 \mu\text{mol/g}$ of FruLeulle (Figure S8A) and $15.7 \mu\text{mol/g}$ of FruLys (Figure S8B) were excreted into feces at the age of 3 months. Overall, the concentration of FruLys was much higher than the concentration of FruLeulle. This can be explained due to the fact that the consumed amount of protein-bound FruLys was higher due to multiple lysine residues in whey and casein proteins compared to only one N-terminal glycation site in β -lactoglobulin resulting in FruLeulle. Nevertheless, the excretion of the two Amadori products show interindividual differences; for example, for Child 27 and 75 the FruLys/FruLeulle ratio is lower than for the others. This could be due to individual absorption and excretion kinetics. In rats the fecal excretion of FruLys and LacLys was

reported to be much lower than in urine.^{7,10,47,48} Yet, about 95% of the ingested FruLys was neither found in urine nor in feces and might be metabolized in yet unknown pathways.^{10,49} However, in human infants this ratio seems to be different. Niederweiser et al.⁵⁰ determined a fecal excretion rate of 55% and only 16% in urine for FruLys in infants. Formula-fed preterm infants excreted 1.3–3.9% of the ingested amount of LacLys via urine.⁵¹ The reason for the higher concentrations of FruLys in stool of infants might originate from different microbiota composition compared to adults or rodents. The early life microbiota might not be adapted to the intake of heat-treated proteins, and therefore, degradation is less efficient.⁴⁷ Another reason might be that infants absorb compounds with higher molecular weights more efficiently.¹⁰ However, no data is available for the absorption and distribution rates of FruLeulle. Nevertheless, the metabolic transit of Amadori products depends on their chemical structure.

In summary, we identified milk-derived Amadori products in feces of formula-fed infants by combining nontargeted metabolomics and targeted structure elucidation using MS/MS and NMR in a nutritional intervention study. The most probable dietary source of FruLeulle and LacLeulle is the heat-treated whey protein β -lactoglobulin in infant formula because of its N-terminal sequence. In general, the augmented fecal excretion of FruLys and FruLeulle demonstrates the high load of

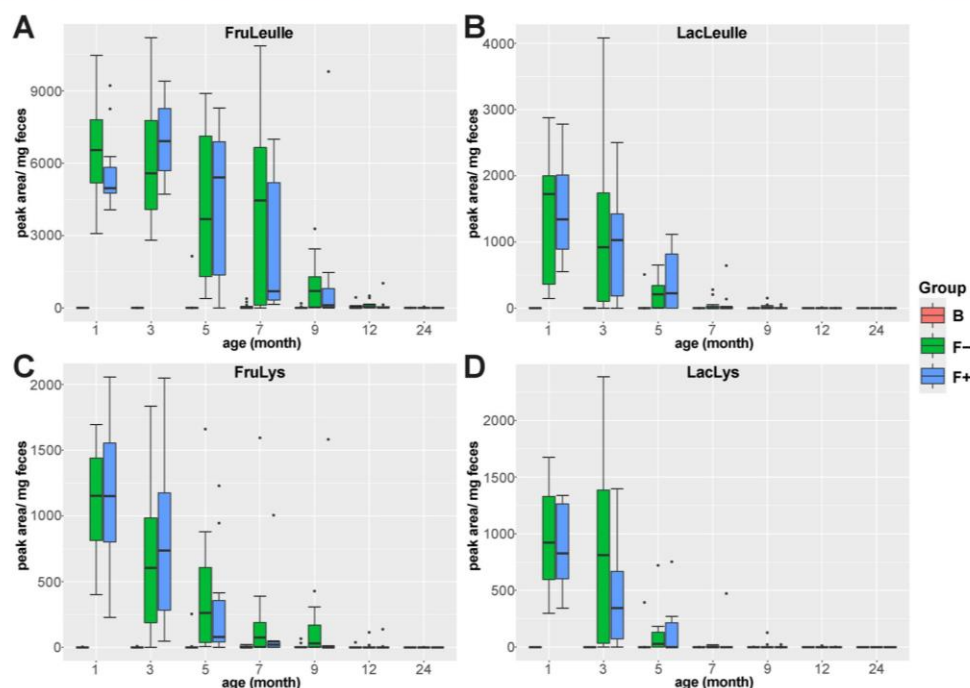


Figure 5. Fecal excretion profiles of the Amadori products (A) FruLeulle, (B) LacLeulle, (C) FruLys, and (D) LacLys during the first 2 years of life. In formula-fed infants (F⁻, without probiotics, green, and F⁺, with probiotics, blue) the amount of excreted Amadori products decreased over time. Breastfed infants (B, red) excreted only very small amounts after introduction of solid food (approximately 5 months).

Maillard reaction products to which formula-fed infants are exposed to during the first months of life. The absorption of the different Amadori products in the gastrointestinal tract and potential modulation of the infants gut microbiota remains to be investigated in future studies.

■ ASSOCIATED CONTENT

Supporting Information

The Supporting Information is available free of charge on the ACS Publications website at DOI: 10.1021/acs.jafc.9b01889.

Methodical details of acid hydrolysis of infant formula; van Krevelen diagram of feces from breastfed infants (Figure S1); LC-MS/MS identification of FruLys and LacLys (Figure S2); 2D-¹H-¹H-TOCSY NMR spectra of leucylisoleucine (Figure S3), prepared reference compound FruLeulle (Figure S4), FruLeulle (Figure S5), and LacLeulle (Figure S6) isolated from feces; fragmentation patterns of *N*-(2-furoylmethyl) amino acids in infant formula after acid hydrolysis (Figure S7); quantitative excretion profiles of FruLeulle and FruLys in selected samples (Figure S8); and qNMR measurements of FruLeulle and FruLys stock solutions (Figure S9) (PDF)

Information on infant cohort and HILIC UHPLC-QTOF-MS analysis of Amadori products in fecal samples (Table S1) (XLSX)

■ AUTHOR INFORMATION

Corresponding Author

*E-mail: alesia.walker@helmholtz-muenchen.de. Tel.: +49 89 3187 4656.

ORCID

Alesia Walker: 0000-0002-1477-2023

Present Address

¹Helmholtz Zentrum München, Deutsches Forschungszentrum für Gesundheit und Umwelt, Department of Environmental Sciences, Research Unit Analytical BioGeoChemistry, Ingolstaedter Landstrasse 1, 85764 Neuherberg, Germany.

Notes

The authors declare no competing financial interest.

■ ABBREVIATIONS USED

ACN, acetonitrile; B, exclusively breastfed; ESI, electrospray ionization; F⁻, formula-fed without probiotics; F⁺, formula-fed with probiotics; FruLeulle, *N*-deoxyfructosylleucylisoleucine; FruLys, *ε*-*N*-deoxyfructosyllysine; FT-ICR-MS, Fourier transform ion cyclotron resonance mass spectrometry; HILIC, hydrophilic interaction liquid chromatography; HPLC, high-performance liquid chromatography; LacLeulle, *N*-deoxylactosylleucylisoleucine; LacLys, *ε*-*N*-deoxylactosyllysine; MS, mass spectrometry/spectrometer; MS/MS, tandem mass spectrometry; *m/z*, mass-to-charge ratio; NH₄Ac, ammonium acetate; (q)NMR, (quantitative) nuclear magnetic resonance spectroscopy; TSP, trimethylsilylpropionate; UHPLC, ultra-

high-performance liquid chromatography; UHT, ultrahigh temperature

REFERENCES

- (1) Pischetsrieder, M.; Henle, T. Glycation products in infant formulas: chemical, analytical and physiological aspects. *Amino Acids* **2012**, *42* (4), 1111–8.
- (2) Erbersdobler, H. F.; Dehn, B.; Nangpal, A.; Reuter, H. Determination of furosine in heated milk as a measure of heat intensity during processing. *J. Dairy Res.* **1987**, *54* (1), 147–151.
- (3) Hegele, J.; Buetler, T.; Delatour, T. Comparative LC–MS/MS profiling of free and protein-bound early and advanced glycation-induced lysine modifications in dairy products. *Anal. Chim. Acta* **2008**, *617* (1), 85–96.
- (4) Clawin-Rädecker, I.; Schlimme, E. Nachweis nichtenzymatisch glycosylierter Proteine in boviner Kolostralmilch und reifer Frauenmilch durch die Bestimmung des Furosingehaltes. *Kieler Milchwirtschaftliche Forschungsberichte* **1998**, *50* (2), 133–145.
- (5) Martysiak-Zurowska, D.; Stolyhwo, A. Content of furosine in infant formulae and follow-on formulae. *Polish Journal of Food and Nutrition Sciences* **2007**, *57* (2), 185–190.
- (6) Finot, P.-A.; Bujard, E.; Mottu, F.; Mauron, J. Availability of the True Schiff's Bases of Lysine. Chemical Evaluation of the Schiff's Base between Lysine and Lactose in Milk. *Protein Crosslinking: Nutritional and Medical Consequences* **1977**, 343–365.
- (7) Finot, P. A.; Magnenat, E. Metabolic Transit of Early and Advanced Maillard Products. *Prog Food Nutr Sci.* **1981**, *5* (1-6), 193–207.
- (8) Erbersdobler, H. F.; Lohmann, M.; Buhl, K. Utilization of Early Maillard Reaction Products by Humans. *Nutritional and Toxicological Consequences of Food Processing* **1991**, 363–370.
- (9) Henle, T.; Schwenger, V.; Ritz, E. Preliminary studies on the renal handling of lactuloselysine from milk products. *Czech Journal of Food Sciences* **2000**, *18*, 101–102.
- (10) Erbersdobler, H. F.; Faist, V. Metabolic transit of Amadori products. *Nahrung* **2001**, *45* (3), 177–81.
- (11) Grunwald, S.; Krause, R.; Bruch, M.; Henle, T.; Brandsch, M. Transepithelial flux of early and advanced glycation compounds across Caco-2 cell monolayers and their interaction with intestinal amino acid and peptide transport systems. *Br. J. Nutr.* **2006**, *95* (6), 1221–8.
- (12) Hellwig, M.; Geissler, S.; Matthes, R.; Peto, A.; Silow, C.; Brandsch, M.; Henle, T. Transport of free and peptide-bound glycated amino acids: synthesis, transepithelial flux at Caco-2 cell monolayers, and interaction with apical membrane transport proteins. *ChemBioChem* **2011**, *12* (8), 1270–9.
- (13) Heinzmann, S. S.; Brown, I. J.; Chan, Q.; Bictash, M.; Dumas, M. E.; Kochhar, S.; Stampler, J.; Holmes, E.; Elliott, P.; Nicholson, J. K. Metabolic profiling strategy for discovery of nutritional biomarkers: proline betaine as a marker of citrus consumption. *Am. J. Clin. Nutr.* **2010**, *92* (2), 436–43.
- (14) O'Sullivan, A.; Gibney, M. J.; Brennan, L. Dietary intake patterns are reflected in metabolomic profiles: potential role in dietary assessment studies. *Am. J. Clin. Nutr.* **2011**, *93* (2), 314–21.
- (15) Heinzmann, S. S.; Holmes, E.; Kochhar, S.; Nicholson, J. K.; Schmitt-Kopplin, P. 2-Furoylglycine as a Candidate Biomarker of Coffee Consumption. *J. Agric. Food Chem.* **2015**, *63* (38), 8615–21.
- (16) Bazanella, M.; Maier, T. V.; Clavel, T.; Lagkouvardos, I.; Lucio, M.; Maldonado-Gomez, M. X.; Autran, C.; Walter, J.; Bode, L.; Schmitt-Kopplin, P.; Haller, D. Randomized controlled trial on the impact of early-life intervention with bifidobacteria on the healthy infant fecal microbiota and metabolome. *Am. J. Clin. Nutr.* **2017**, *106* (5), 1274–1286.
- (17) Lucio, M.; Fekete, A.; Frommberger, M.; Schmitt-Kopplin, P. Metabolomics: High-Resolution Tools Offer to Follow Bacterial Growth on a Molecular Level. *Handbook of Molecular Microbial Ecology* **2011**, 683–695.
- (18) Kanawati, B.; Bader, T. M.; Wanczek, K. P.; Li, Y.; Schmitt-Kopplin, P. Fourier transform (FT)-artifacts and power-function resolution filter in Fourier transform mass spectrometry. *Rapid Commun. Mass Spectrom.* **2017**, *31* (19), 1607–1615.
- (19) Moritz, F.; Kaling, M.; Schnitzler, J. P.; Schmitt-Kopplin, P. Characterization of poplar metabolites via mass difference enrichment analysis. *Plant, Cell Environ.* **2017**, *40* (7), 1057–1073.
- (20) Sillner, N.; Walker, A.; Harrieder, E.-M.; Schmitt-Kopplin, P.; Witting, M. Development and application of a HILIC UHPLC-MS method for polar fecal metabolome profiling. *J. Chromatogr. B: Anal. Technol. Biomed. Life Sci.* **2019**, *1109*, 142–148.
- (21) Wishart, D. S.; Feunang, Y. D.; Marcu, A.; Guo, A. C.; Liang, K.; Vazquez-Fresno, R.; Sajed, T.; Johnson, D.; Li, C.; Karu, N.; Sayeeda, Z.; Lo, E.; Assempour, N.; Berjanskii, M.; Singhal, S.; Arndt, D.; Liang, Y.; Badran, H.; Grant, J.; Serra-Cayuela, A.; Liu, Y.; Mandal, R.; Neveu, V.; Pon, A.; Knox, C.; Wilson, M.; Manach, C.; Scalbert, A. HMDB 4.0: the human metabolome database for 2018. *Nucleic Acids Res.* **2018**, *46* (D1), D608–d617.
- (22) Hemmler, D.; Roullier-Gall, C.; Marshall, J. W.; Rychlik, M.; Taylor, A. J.; Schmitt-Kopplin, P. Evolution of Complex Maillard Chemical Reactions, Resolved in Time. *Sci. Rep.* **2017**, *7* (1), 3227.
- (23) Kim, S.; Kramer, R. W.; Hatcher, P. G. Graphical Method for Analysis of Ultrahigh-Resolution Broadband Mass Spectra of Natural Organic Matter, the Van Krevelen Diagram. *Anal. Chem.* **2003**, *75* (20), 5336–5344.
- (24) Hellwig, M.; Henle, T. Baking, Ageing, Diabetes: A Short History of the Maillard Reaction. *Angew. Chem., Int. Ed.* **2014**, *53* (39), 10316–10329.
- (25) Nasirpour, A.; Scher, J.; Desobry, S. Baby Foods: Formulations and Interactions (A Review). *Crit. Rev. Food Sci. Nutr.* **2006**, *46* (8), 665–681.
- (26) Contreras-Calderón, J.; Guerra-Hernández, E.; García-Villanova, B. Indicators of non-enzymatic browning in the evaluation of heat damage of ingredient proteins used in manufactured infant formulas. *Eur. Food Res. Technol.* **2008**, *227* (1), 117–124.
- (27) Henle, T.; Walter, H.; Klostermeyer, H. Evaluation of the extent of the early Maillard-reaction in milk products by direct measurement of the Amadori-product lactuloselysine. *Z. Lebensm.-Unters. Forsch.* **1991**, *193* (2), 119–22.
- (28) Birlouez-Aragon, I.; Pischetsrieder, M.; Leclère, J.; Morales, F. J.; Hasenkopf, K.; Kientsch-Engel, R.; Ducauze, C. J.; Rutledge, D. Assessment of protein glycation markers in infant formulas. *Food Chem.* **2004**, *87* (2), 253–259.
- (29) Meltretter, J.; Wust, J.; Pischetsrieder, M. Modified peptides as indicators for thermal and nonthermal reactions in processed milk. *J. Agric. Food Chem.* **2014**, *62* (45), 10903–15.
- (30) Meltretter, J.; Wust, J.; Pischetsrieder, M. Comprehensive analysis of nonenzymatic post-translational beta-lactoglobulin modifications in processed milk by ultrahigh-performance liquid chromatography-tandem mass spectrometry. *J. Agric. Food Chem.* **2013**, *61* (28), 6971–81.
- (31) Morgan, F.; Mollé, D.; Henry, G.; Vénien, A.; Léonil, J.; Peltre, G.; Levieux, D.; Maubois, J.-L.; Bouhallab, S. Glycation of bovine β -Lactoglobulin: effect on the protein structure. *Int. J. Food Sci. Technol.* **1999**, *34* (5–6), 429–435.
- (32) Chevalier, F.; Chobert, J.-M.; Mollé, D.; Haertlé, T. Maillard glycation of beta-lactoglobulin with several sugars: comparative study of the properties of the obtained polymers and of the substituted sites. *Lait* **2001**, *81* (5), 651–666.
- (33) Morgan, F.; Bouhallab, S. d.; Mollé, D.; Henry, G.; Maubois, J.-L.; Léonil, J. Lactolation of β -Lactoglobulin Monitored by Electrospray Ionisation Mass Spectrometry. *Int. Dairy J.* **1998**, *8* (2), 95–98.
- (34) Milkovska-Stamenova, S.; Hoffmann, R. Identification and quantification of bovine protein lactosylation sites in different milk products. *J. Proteomics* **2016**, *134*, 112–126.
- (35) Wang, J.; Lu, Y.-M.; Liu, B.-Z.; He, H.-Y. Electrospray positive ionization tandem mass spectrometry of Amadori compounds. *J. Mass Spectrom.* **2008**, *43* (2), 262–264.
- (36) Ruan, D. W.; Wang, H.; Cheng, F. The Maillard Reaction. *The Maillard Reaction in Food Chemistry* **2018**, 1.

- (37) Penndorf, I.; Biedermann, D.; Maurer, S. V.; Henle, T. Studies on N-Terminal Glycation of Peptides in Hypoallergenic Infant Formulas: Quantification of α -N-(2-Furoylmethyl) Amino Acids. *J. Agric. Food Chem.* **2007**, *55* (3), 723–727.
- (38) Sgarbieri, V. C.; Amaya, J.; Tanaka, M.; Chichester, C. O. Nutritional consequences of the Maillard reaction. Amino acid availability from fructose-leucine and fructose-tryptophan in the rat. *J. Nutr.* **1973**, *103* (5), 657–663.
- (39) Mori, B.; Nakatsuji, H. Utilization in Rats of ^{14}C -L-Lysine-labeled Casein Browned by Amino-carbonyl Reaction. *Agric. Biol. Chem.* **1977**, *41* (2), 345–350.
- (40) Erbersdobler, H.; Gunsser, I.; Weber, G. Abbau von Fruktoselysin durch die Darmflora. *Zentralblatt für Veterinärmedizin Reihe A* **1970**, *17* (6), 573–575.
- (41) Lee, K.; Erbersdobler, H.F. Balance Experiments on Human Volunteers with ϵ -Fructoselysine (FL) and Lysinoalanine (LAL). *Maillard Reactions in Chemistry, Food and Health* **2005**, 358–363.
- (42) Seiquer, I.; Rubio, L. A.; Peinado, M. J.; Delgado-Andrade, C.; Navarro, M. P. Maillard reaction products modulate gut microbiota composition in adolescents. *Mol. Nutr. Food Res.* **2014**, *58* (7), 1552–60.
- (43) Wiame, E.; Delpierre, G.; Collard, F.; Van Schaftingen, E. Identification of a pathway for the utilization of the Amadori product fructoselysine in *Escherichia coli*. *J. Biol. Chem.* **2002**, *277* (45), 42523–9.
- (44) Katz, C.; Cohen-Or, I.; Gophna, U.; Ron, E. Z. The Ubiquitous Conserved Glycopeptidase Gcp Prevents Accumulation of Toxic Glycated Proteins. *mBio* **2010**, *1* (3), 1.
- (45) Bui, T. P.; Ritari, J.; Boeren, S.; de Waard, P.; Plugge, C. M.; de Vos, W. M. Production of butyrate from lysine and the Amadori product fructoselysine by a human gut commensal. *Nat. Commun.* **2015**, *6*, 10062.
- (46) Hellwig, M.; Bunzel, D.; Huch, M.; Franz, C. M. A. P.; Kulling, S. E.; Henle, T. Stability of Individual Maillard Reaction Products in the Presence of the Human Colonic Microbiota. *J. Agric. Food Chem.* **2015**, *63* (30), 6723–6730.
- (47) Somoza, V.; Wenzel, E.; Weiß, C.; Clawin-Rädecker, I.; Grübel, N.; Erbersdobler, H. F. Dose-dependent utilisation of casein-linked lysinoalanine, N(epsilon)-fructoselysine and N(epsilon)-carboxymethyllysine in rats. *Mol. Nutr. Food Res.* **2006**, *50* (9), 833–841.
- (48) Rerat, A.; Calmes, R.; Vaissade, P.; Finot, P. A. Nutritional and metabolic consequences of the early Maillard reaction of heat treated milk in the pig. Significance for man. *Eur. J. Nutr.* **2002**, *41* (1), 1–11.
- (49) Förster, A.; Kuhne, Y.; Henle, T. Studies on absorption and elimination of dietary maillard reaction products. *Ann. N. Y. Acad. Sci.* **2005**, *1043* (1043), 474–81.
- (50) Niederwieser, A.; Giliberti, P.; Matasovic, A. N ϵ -1-Deoxyfructosyl-/lysine in urine after ingestion of a lactose free, glucose containing milk formula. *Pediatr. Res.* **1975**, *9*, 867.
- (51) Langhendries, J. P.; Hurrell, R. F.; Furniss, D. E.; Hischenhuber, C.; Finot, P. A.; Bernard, A.; Battisti, O.; Bertrand, J. M.; Senterre, J. Maillard reaction products and lysinoalanine: urinary excretion and the effects on kidney function of preterm infants fed heat-processed milk formula. *J. Pediatr. Gastroenterol. Nutr.* **1992**, *14* (1), 62–70.

C.2 Supplementary Information *

Acid hydrolysis of infant formula and RP UHPLC-MS/MS analysis

Two infant formulas, which were consumed by the infant cohort, were obtained from local retail stores. The powder (20 mg each) was hydrolyzed with 1 mL of 6 N hydrochloric acid in glass vials for 24 h at 110 °C, whereby the vials were flushed with nitrogen gas before closing. After cooling to room temperature, the pH was adjusted to 7 with 12 N sodium hydroxide and the volume was filled up to 2.5 mL with Milli-Q purified water. The hydrolysates were centrifuged (13000 rpm, 10 min) and 500 µL of each supernatant were dried under vacuum and dissolved in 100 methanol.

The remaining salt was removed by centrifugation (14000 rpm, 5 min).

The infant formula hydrolyzates (methanol extracts) were analyzed by UHPLC (Acquity, Waters, Milford, MA, USA) coupled to a time of flight mass spectrometer (maXis, Bruker Daltonics, Bremen, Germany). Reversed-phase chromatography (RP) was performed using a C8 column (1.7 µm, 2.1 × 150 mm, Acquity™ UPLC BEH™, Waters, Milford, MA, USA). The LC settings were the same as previously described.⁽²⁰⁾

Calibration of the MS was done by injecting ESI-L Low Concentration Tuning Mix (Agilent, Santa Clara, CA, USA) prior to the measurements. Additionally, ESI-L Low Concentration Tuning Mix (diluted 1:4 (v/v) with 75% ACN) was injected in the first 0.3 min of each UHPLC-MS run by a switching valve for internal recalibration. Mass spectra were acquired in positive ionization mode. Parameters of the ESI source were: nitrogen flow rate was 10 L/min, dry heater temperature was 200°C, nebulizer pressure was 2 bar and capillary voltage was 4500 V. Data were acquired in line and profile mode with an acquisition rate of 5 Hz within a mass range of 50–1500 Da. MS scan. MS/MS experiments of *N*-(2-furoylmethyl) amino acids were performed in multiple reaction monitoring mode (MRM) at 20 eV.

* This chapter was published as [Nina Sillner](#), Alesia Walker, Daniel Hemmler, Monika Bazanella, Silke S. Heinzmann, Dirk Haller, Philippe Schmitt-Kopplin. Milk-derived Amadori products in feces of formula-fed infants. *Journal of Agricultural and Food Chemistry*, 67, 28, 8061-8069. *Supporting Information*. Copyright American Chemical Society (2019).

Table C.S1 Information on infant cohort and HILIC UHPLC-MS analysis of Amadori products in fecal samples (B = breast milk, F- = infant formula without probiotics, F+ = infant formula with probiotics).

				[M-H]-	405.2252	567.2763	307.1524	469.2048
				RT	4.43	5.05	7.29	7.37
Sample Name	Child ID	Age (month)	Group	Feed	LeulleGlc	LeulleLac	LysGlc	LysLac
11-1	11	1	B	B	0.030399	0.023658	0.025314	0.023865
11-3	11	3	B	B	0.027547	0.022663	0.021095	0.020813
11-5	11	5	B	B	0.028064	0.024441	0.024245	0.023302
11-7	11	7	B	B + solid food	0.020531	0.016528	6.416521	0.015159
12-1	12	1	B	B	0.064042	0.051684	0.051366	0.049659
12-3	12	3	B	B	0.044472	0.050828	0.045559	0.050546
12-7	12	7	B	B + solid food	0.02503	0.025507	0.026053	0.026807
16-3	16	3	B	B	0.033223	0.038077	0.035461	0.035233
16-5	16	5	B	B + solid food	0.01604	0.018533	0.017345	0.018176
16-7	16	7	B	B + solid food	119.6613	0.03059	3.035293	0.027849
23-1	23	1	F-	F-	4880.72	1791.823	835.1149	1383.562
23-3	23	3	F-	F-	5582.87	159.7294	58.58814	0.026749
23-5	23	5	F-	F- + solid food	7672.712	227.3245	63.65294	0.034793
23-7	23	7	F-	F- + solid food	6845.209	53.83839	75.35301	1.086105
23-9	23	9	F-	F- + solid food	1733.502	0.031755	22.3434	0.032376
23-12	23	12	F-	F- + solid food	28.65984	0.031653	2.190044	0.026362
23-24	23	24	F-	solid food	0.051798	0.039772	0.041514	0.043071
24-1	24	1	F-	F-	8037.909	513.2307	806.8194	802.6556
24-3	24	3	F-	F-	2813.364	1959.816	317.0631	1438.198
24-5	24	5	F-	F- + solid food	8888.955	643.4647	1660.426	124.6727
24-7	24	7	F-	F- + solid food	4929.419	10.10962	229.0182	21.44383
24-9	24	9	F-	F- + solid food	2452.665	52.00817	308.4155	22.63938
24-12	24	12	F-	F- + solid food	30.29263	0.022547	0.022807	0.023589
25-1	25	1	F+	F+	4064.999	2029.759	1151.326	1295.769
25-3	25	3	F+	F+	9407.13	1028.3	2048.097	327.8446
25-5	25	5	F+	F+ + solid food	6448.169	1117.198	1229.188	753.2615
25-7	25	7	F+	F+ + solid food	5874.533	643.2717	1005.692	472.6199
25-9	25	9	F+	F+ + solid food	9799.457	56.8465	1582.067	22.8003
25-12	25	12	F+	F+ + solid food	1025.998	0.025689	137.5831	0.023874
25-24	25	24	F+	solid food	0.027504	0.02923	0.02823	0.029744
27-1	27	1	F-	F-	6171.278	2068.291	1463.314	1570.217
27-3	27	3	F-	F-	7814.149	1229.349	603.484	1332.104
27-5	27	5	F-	F- + solid food	1317.219	112.1544	134.7732	27.93683
27-7	27	7	F-	F- + solid food	4457.185	0.03477	16.37367	0.03391
27-9	27	9	F-	F- + solid food	23.23819	0.017976	4.34715	0.018257
27-12	27	12	F-	F- + solid food	41.51971	0.028138	0.026562	0.027235
27-24	27	24	F-	solid food	0.028174	0.030359	0.029739	0.031447
29-1	29	1	F-	F-	3078.987	2874.825	1310.195	1674.523
29-3	29	3	F-	F-	8367.447	2554.074	1643.16	1613.648
29-5	29	5	F-	F- + solid food	970.6401	2.20181	880.4609	11.30277
29-7	29	7	F-	F- + solid food	6457.739	280.4378	1593.962	12.83718
29-9	29	9	F-	F- + solid food	419.3304	0.037518	172.66	0.036474
29-12	29	12	F-	F- + solid food	417.3738	0.044037	17.1465	0.046876
29-24	29	24	F-	solid food	0.024518	0.029352	1.041772	0.028365
30-1	30	1	F-	F-	6923.973	145.3951	549.5674	527.8638
30-3	30	3	F-	F-	4062.362	50.34164	398.8072	68.35814
30-5	30	5	F-	F- + solid food	6055.812	208.2017	261.0104	183.5932

Table C.S1 (continued) Information on infant cohort and HILIC UHPLC-MS analysis of Amadori products in fecal samples (B = breast milk, F- = infant formula without probiotics, F+ = infant formula with probiotics).

30-7	30	7 F-	F- + solid food	3227.72	0.021618	138.5986	4.706154
30-9	30	9 F-	F- + solid food	3283.544	0.020012	104.2772	0.019035
30-12	30	12 F-	F- + solid food	501.8773	8.037319	0.028008	0.031777
31-1	31	1 B	B	0.038985	0.028682	0.030791	0.030038
31-3	31	3 B	B	0.01522	0.018806	0.016635	0.016416
31-5	31	5 B	B	0.018216	0.018375	0.017157	0.016849
31-7	31	7 B	B + solid food	0.023549	0.016822	0.018156	0.018252
31-9	31	9 B	B + solid food	0.035273	0.024436	3.00258	0.026499
31-12	31	12 B	B + solid food	0.042147	0.034308	0.038401	0.0377
31-24	31	24 B	solid food	0.067192	0.048276	0.051344	0.055365
34-1	34	1 B	B	0.018015	0.014142	0.01513	0.014535
34-3	34	3 B	B	0.021368	0.016479	0.019315	0.018911
34-5	34	5 B	B + solid food	0.021025	0.02551	2.048708	0.022361
34-7	34	7 B	B + solid food	0.028394	0.023117	2.02422	0.027832
36-1	36	1 F+	F+	5379.674	1620.142	1429.285	941.4732
36-3	36	3 F+	F+	6918.217	2503.807	1239.686	800.0972
36-5	36	5 F+	F++ solid food	151.9933	9.260036	59.4021	0.016243
36-7	36	7 F+	F++ solid food	383.2124	26.37218	47.93382	0.045944
36-9	36	9 F+	F++ solid food	35.39916	0.024856	0.025968	0.024501
36-12	36	12 F+	F++ solid food	0.025371	0.028151	0.026099	0.027542
36-24	36	24 F+	solid food	0.058457	0.04162	0.042774	0.049007
39-1	39	1 F+	F+	4961.979	553.3896	859.2609	701.9982
39-3	39	3 F+	F+	7993.562	1171.789	730.2295	493.9431
39-5	39	5 F+	F++ solid food	4460.971	971.5635	414.7201	247.1307
39-7	39	7 F+	F++ solid food	6991.32	7.0172	46.86997	0.016466
39-9	39	9 F+	F++ solid food	907.8215	11.95675	11.11352	0.027204
39-12	39	12 F+	F++ solid food	133.5297	0.022227	0.020332	0.021029
43-1	43	1 F+	F+	4847.69	1995.941	227.1225	342.9379
43-3	43	3 F+	F+	5293.913	799.6078	47.40313	102.9375
43-5	43	5 F+	F++ solid food	7510.489	800.4518	61.7856	0.022508
43-7	43	7 F+	F++ solid food	5488.896	137.508	33.92202	0.023231
43-9	43	9 F+	F++ solid food	693.8391	0.013276	5.608192	0.012656
43-12	43	12 F+	F++ solid food	12.05177	0.043896	0.04151	0.04608
43-24	43	24 F+	solid food	0.038076	0.043477	0.039819	0.040377
44-1	44	1 F+	F+	4909.017	955.8195	1407.426	700.0211
44-3	44	3 F+	F+	8893.238	0.02653	450.3308	0.026511
44-5	44	5 F+	F++ solid food	7334.444	0.026977	78.2148	0.023978
44-7	44	7 F+	F++ solid food	697.9181	0.02676	20.68241	0.026514
44-9	44	9 F+	F++ solid food	1475.745	5.526965	9.571373	0.025829
44-12	44	12 F+	F++ solid food	0.01563	0.016141	0.017035	0.016388
44-24	44	24 F+	solid food	0.0457	0.044094	0.04248	0.043983
45-1	45	1 B	B	0.018529	0.01926	0.019362	0.018431
45-3	45	3 B	B	0.024569	0.025162	8.176321	0.020671
45-5	45	5 B	B + solid food	0.021222	0.022232	0.022511	0.022044
45-7	45	7 B	B + solid food	0.043893	0.039683	0.038203	0.039139
46-1	46	1 F+	F+	5291.856	700.014	648.5107	503.471
46-3	46	3 F+	F+	8466.367	302.1923	737.0038	345.2114
46-5	46	5 F+	F++ solid food	0.021304	0.017365	0.018125	0.018979
46-7	46	7 F+	F++ solid food	4903.702	0.032018	2.589137	0.035386
46-9	46	9 F+	F++ solid food	25.22747	0.014523	0.013442	0.012721

Table C.S1 (continued) Information on infant cohort and HILIC UHPLC-MS analysis of Amadori products in fecal samples (B = breast milk, F- = infant formula without probiotics, F+ = infant formula with probiotics).

46-12	46	12 F+	F+ + solid food	54.83285	0.023367	0.022787	0.02281
46-24	46	24 F+	solid food	0.069333	0.049605	0.057121	0.056636
59-3	59	3 B	B	0.04264	0.045787	0.04463	0.045279
59-5	59	5 B	B	0.044708	0.046599	0.046031	0.045686
59-7	59	7 B	B + solid food	0.02704	0.033738	0.028484	0.03177
60-1	60	1 B	B	0.024678	0.028794	0.030908	0.028434
60-3	60	3 B	B	0.036864	0.044388	0.041384	0.038838
60-5	60	5 B	B	2.665363	0.018085	0.015601	0.014989
60-7	60	7 B	B + solid food	26.46408	0.021666	0.021535	0.021377
62-1	62	1 F+	F+	9219.088	2778.548	2056.058	1337.216
62-3	62	3 F+	F+	8067.571	1180.731	976.8632	535.6024
62-5	62	5 F+	F+ + solid food	8287.987	227.1479	298.9886	22.36671
62-7	62	7 F+	F+ + solid food	314.4135	0.038278	0.038936	0.037048
62-9	62	9 F+	F+ + solid food	5.790972	0.027967	0.026351	0.023841
62-12	62	12 F+	F+ + solid food	50.79174	0.038316	0.040774	0.043378
63-1	63	1 B	B	0.04254	0.031122	0.034245	0.035298
63-3	63	3 B	B	0.03731	0.039662	0.034347	0.035557
63-5	63	5 B	B	0.023727	0.020533	0.019003	0.020601
63-7	63	7 B	B + solid food	0.021331	0.022098	0.020648	0.023062
64-1	64	1 F-	F-	10470.32	312.5716	1695.678	483.3049
64-3	64	3 F-	F-	4808.745	0.016577	0.01825	0.018576
64-5	64	5 F-	F- + solid food	2543.32	0.03424	9.896091	0.037412
64-7	64	7 F-	F- + solid food	84.5799	0.025638	0.024155	0.023962
64-9	64	9 F-	F- + solid food	40.11214	0.026856	4.455327	0.024618
64-12	64	12 F-	F- + solid food	23.70247	0.026807	0.024161	0.024984
64-24	64	24 F-	solid food	0.039658	0.045719	0.042782	0.044955
66-1	66	1 B	B	0.042418	0.047013	0.047677	0.048388
66-3	66	3 B	B	0.943099	0.027166	0.026298	0.029238
66-5	66	5 B	B + solid food	0.017082	0.016357	0.016025	0.014871
66-7	66	7 B	B + solid food	0.021345	0.022421	0.022967	0.023101
66-9	66	9 B	B + solid food	16.56801	3.250371	32.73256	0.026534
66-12	66	12 B	B + solid food	97.92702	0.023172	0.022787	0.021315
71-3	71	3 F-	F-	6282.068	4081.131	1834.217	2384.216
71-5	71	5 F-	F- + solid food	6579.307	653.6058	684.033	66.27993
71-7	71	7 F-	F- + solid food	7044.154	205.5159	10.23927	0.015132
71-9	71	9 F-	F- + solid food	825.8429	38.6703	29.93418	0.026235
71-12	71	12 F-	F- + solid food	36.47426	0.035861	0.03418	0.032459
71-24	71	24 F-	solid food	0.052651	0.038375	0.0386	0.041363
75-1	75	1 F-	F-	9259.387	166.1759	400.8095	298.6309
75-3	75	3 F-	F-	11202.94	335.5718	710.7202	757.5983
75-5	75	5 F-	F- + solid food	8643.987	383.0965	532.2005	720.7888
75-7	75	7 F-	F- + solid food	10867.99	0.01773	388.4415	0.021656
75-9	75	9 F-	F- + solid food	844.0064	0.014694	166.1616	0.012186
75-12	75	12 F-	F- + solid food	1.992445	0.017978	0.016053	0.01549
75-24	75	24 F-	solid food	0.024581	0.029074	0.026276	0.02784
76-1	76	1 F-	F-	7110.631	1786.628	1370.078	1165.233
76-3	76	3 F-	F-	4109.133	1519.384	1012.03	937.5258
76-5	76	5 F-	F- + solid food	1284.662	300.4745	6.10344	0.020782
76-7	76	7 F-	F- + solid food	1.17755	0.021207	0.021195	0.021851
76-9	76	9 F-	F- + solid food	5.429427	0.013825	0.011709	0.011783

Table C.S1 (continued) Information on infant cohort and HILIC UHPLC-MS analysis of Amadori products in fecal samples (B = breast milk, F- = infant formula without probiotics, F+ = infant formula with probiotics).

76-24	76	24 F-	solid food	3.248891	0.036986	0.036516	0.034475
80-1	80	1 B	B	0.019398	0.021628	0.020593	0.021539
80-3	80	3 B	B	0.054553	0.040815	4.340475	0.045781
80-5	80	5 B	B + solid food	2146.342	508.8088	253.9288	394.0239
80-7	80	7 B	B + solid food	110.846	0.031166	17.98444	0.029246
80-9	80	9 B	B + solid food	0.030932	0.029682	0.031978	0.030559
80-12	80	12 B	B + solid food	0.022567	0.020887	0.019681	0.022194
80-24	80	24 B	solid food	0.039818	0.045615	0.038868	0.043157
82-1	82	1 B	B	0.026429	0.029543	0.029036	0.028207
82-3	82	3 B	B	0.025006	0.020929	0.023184	0.021887
82-5	82	5 B	B	0.017683	0.020667	2.766804	0.021036
82-7	82	7 B	B + solid food	0.035174	0.031687	0.032056	0.032426
82-9	82	9 B	B + solid food	53.46822	0.016728	5.001914	0.014961
86-1	86	1 F-	F-	4030.443	1660.941	996.8328	826.4652
86-3	86	3 F-	F-	7727.128	0.019392	45.4883	0.018072
86-5	86	5 F-	F+ + solid food	395.2402	0.015461	6.399787	0.015752
86-7	86	7 F-	F+ + solid food	27.45319	0.025326	2.940112	0.02989
86-9	86	9 F-	F+ + solid food	38.86829	0.016155	2.489334	0.013511
86-12	86	12 F-	F+ + solid food	8.479176	0.021749	0.020099	0.020817
86-24	86	24 F-	solid food	0.028072	0.025723	0.024456	0.027522
88-1	88	1 B	B	0.031802	0.036062	0.037012	0.038779
88-3	88	3 B	B	0.020352	0.018267	0.017829	0.017351
88-5	88	5 B	B	0.022317	0.019139	6.834954	0.019396
88-7	88	7 B	B + solid food	0.017383	0.017107	12.29679	0.015961
88-9	88	9 B	B + solid food	4.515869	0.022945	0.022355	1.22994
88-12	88	12 B	B + solid food	3.543567	0.035857	0.030682	0.031225
90-1	90	1 B	B	0.019305	0.021805	0.019632	0.01972
90-3	90	3 B	B	0.021551	0.018904	0.018631	0.017493
90-5	90	5 B	B + solid food	0.037158	0.037681	0.035173	0.035527
90-7	90	7 B	B + solid food	388.2584	0.031361	19.07934	0.031765
92-3	92	3 B	B	0.016381	0.013907	0.0134	0.01415
92-5	92	5 B	B	0.020441	0.019136	0.020407	0.019275
92-7	92	7 B	B + solid food	58.8532	0.02244	15.04533	0.022337
92-12	92	12 B	B + solid food	0.017266	0.017963	0.019346	0.017796
95-1	95	1 B	B	0.048445	0.036712	0.039834	0.037547
95-3	95	3 B	B	0.044303	0.044166	0.0417	0.0432
95-7	95	7 B	B + solid food	252.5689	0.021942	22.22397	0.021349
95-9	95	9 B	B + solid food	189.8155	0.020749	65.87474	0.018427
95-12	95	12 B	B + solid food	434.6342	0.021573	37.32093	0.017059
100-1	100	1 B	B	0.023448	0.018199	3.975629	0.019157
100-3	100	3 B	B	0.01581	0.018422	0.018952	0.017708
100-5	100	5 B	B	0.01695	0.014122	0.014628	0.015142
100-7	100	7 B	B + solid food	0.01974	0.020347	0.018529	0.018977
100-9	100	9 B	B + solid food	6.405732	0.017286	1.362482	0.016572
100-12	100	12 B	B + solid food	12.9028	0.023088	0.553953	0.019006
100-24	100	24 B	solid food	3.381841	0.039471	0.038888	0.041432
102-1	102	1 F+	F+	4645.779	1340.465	994.4343	1257.936
102-3	102	3 F+	F+	4713.134	1668.482	1313.06	1069.385
102-5	102	5 F+	F+ + solid food	5410.648	268.9269	945.306	183.1295
102-7	102	7 F+	F+ + solid food	3173.625	0.022941	4.348681	0.02632

Table C.S1 (continued) Information on infant cohort and HILIC UHPLC-MS analysis of Amadori products in fecal samples (B = breast milk, F- = infant formula without probiotics, F+ = infant formula with probiotics).

102-9	102	9 F+	F++ solid food	109.5796	0.023999	0.024753	0.025727
102-12	102	12 F+	F++ solid food	8.879795	1.386224	1.506048	1.377331
102-24	102	24 F+	solid food	0.029173	0.034888	0.03073	0.031968
105-1	105	1 F+	F+	8252.548	1303.03	1683.87	1268.308
105-3	105	3 F+	F+	5550.674	1842.523	1110.428	1397.211
105-5	105	5 F+	F++ solid food	1997.542	832.1617	288.5633	272.036
105-7	105	7 F+	F++ solid food	195.7658	0.027274	0.029055	0.028685
105-9	105	9 F+	F++ solid food	107.4512	25.61599	0.026726	0.025882
105-12	105	12 F+	F++ solid food	18.04759	0.030021	0.027354	0.02806
105-24	105	24 F+	solid food	0.021742	0.024135	0.021616	0.023202
106-1	106	1 F+	F+	6271.829	2362.048	1678.341	443.8438
106-3	106	3 F+	F+	5826.753	63.52694	115.4738	43.11581
106-5	106	5 F+	F++ solid food	744.356	2.250023	21.36107	0.028328
106-7	106	7 F+	F++ solid food	347.7183	3.475778	19.9162	0.023906
106-9	106	9 F+	F++ solid food	0.023362	0.028175	0.024146	0.025892
106-12	106	12 F+	F++ solid food	48.59373	0.039716	6.484939	0.041032
106-24	106	24 F+	solid food	0.050023	0.058033	0.059674	0.062022
107-1	107	1 B	B	0.030395	0.034933	0.028222	0.03012
107-3	107	3 B	B	0.0423	0.035447	0.038896	0.037396
107-5	107	5 B	B	0.019719	0.021717	0.020286	0.021378
107-9	107	9 B	B + solid food	1.964399	0.028296	0.032728	0.029391
114-1	114	1 F+	F+	4663.503	824.428	744.313	826.4558
114-3	114	3 F+	F+	6090.119	0.027462	59.97435	0.028827
114-5	114	5 F+	F++ solid food	6018.072	0.02211	18.13848	0.021818
114-7	114	7 F+	F++ solid food	150.7144	0.024747	0.023042	0.021151
114-9	114	9 F+	F++ solid food	37.04273	0.022617	0.023788	0.022505
114-12	114	12 F+	F++ solid food	0.035365	0.024842	0.028185	0.029252
114-24	114	24 F+	solid food	0.050425	0.038197	0.045678	0.044608
115-1	115	1 B	B	0.042476	0.04341	0.045546	0.046728
115-3	115	3 B	B	0.053825	0.048243	0.046412	0.053621
115-5	115	5 B	B	0.031935	0.034077	0.033277	0.034983
115-7	115	7 B	B + solid food	13.75874	0.056975	0.058623	0.055045
115-9	115	9 B	B + solid food	0.046962	0.043496	0.044904	0.04352
115-24	115	24 B	solid food	0.048869	0.054127	0.051858	0.056311
126-1	126	1 B	B	0.030898	0.036328	0.036258	0.032545
126-3	126	3 B	B	0.041264	0.046923	0.04305	0.045803
126-5	126	5 B	B + solid food	0.026529	0.027558	0.024562	0.026721
126-7	126	7 B	B + solid food	0.029136	0.021611	4.406153	0.026032
126-9	126	9 B	B + solid food	0.031128	0.037566	0.034971	0.038312
126-24	126	24 B	solid food	0.040648	0.027995	0.031127	0.031922
127-1	127	1 F-	F-	6100.672	2392.39	1506.03	1015.903
127-3	127	3 F-	F-	3462.304	921.3953	958.8837	811.8805
127-5	127	5 F-	F- + solid food	3682.81	8.951646	529.5674	136.9012
127-7	127	7 F-	F- + solid food	137.5753	3.780905	147.5283	19.47951
127-9	127	9 F-	F- + solid food	707.7817	152.4529	428.0896	127.1886
127-12	127	12 F-	F- + solid food	154.0039	3.862017	114.0224	13.03087
127-24	127	24 F-	solid food	48.43847	0.037375	0.037051	0.041144

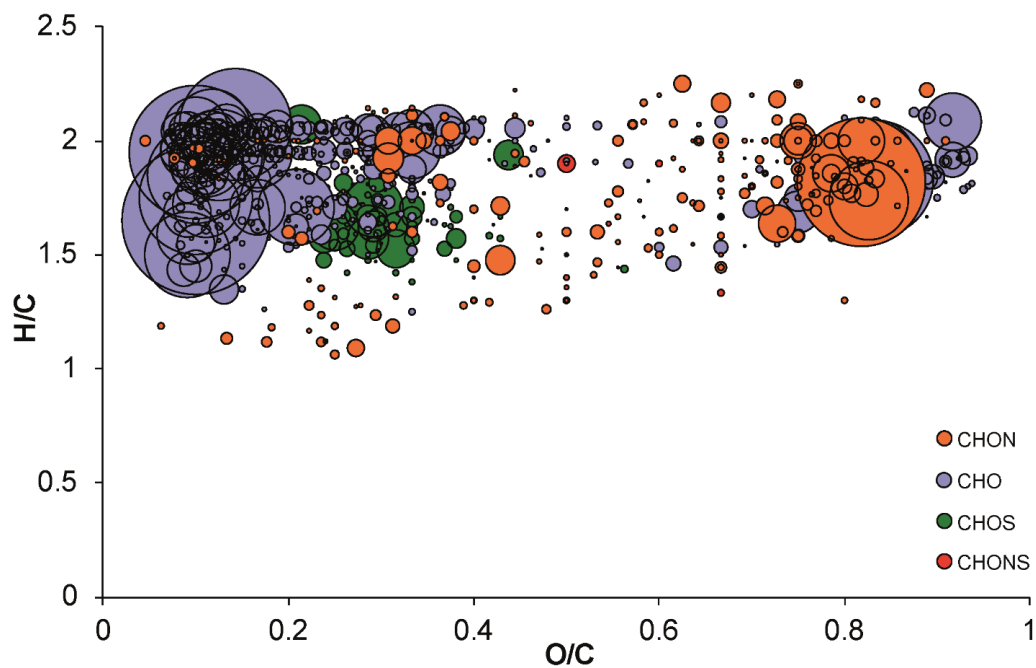


Figure C.S1. Chemical composition of feces from 1-month-old infants, who were exclusively fed with breast milk (average of signal intensity of $n = 16$ fecal samples), acquired by FT-ICR-MS in negative ionization mode. Calculated molecular formulas were categorized into 4 compositional groups: CHO (blue), CHON (orange), CHOS (green) and CHONS (red). The van Krevelen diagram plots the H/C vs. O/C atomic ratios of the computed molecular formulas.

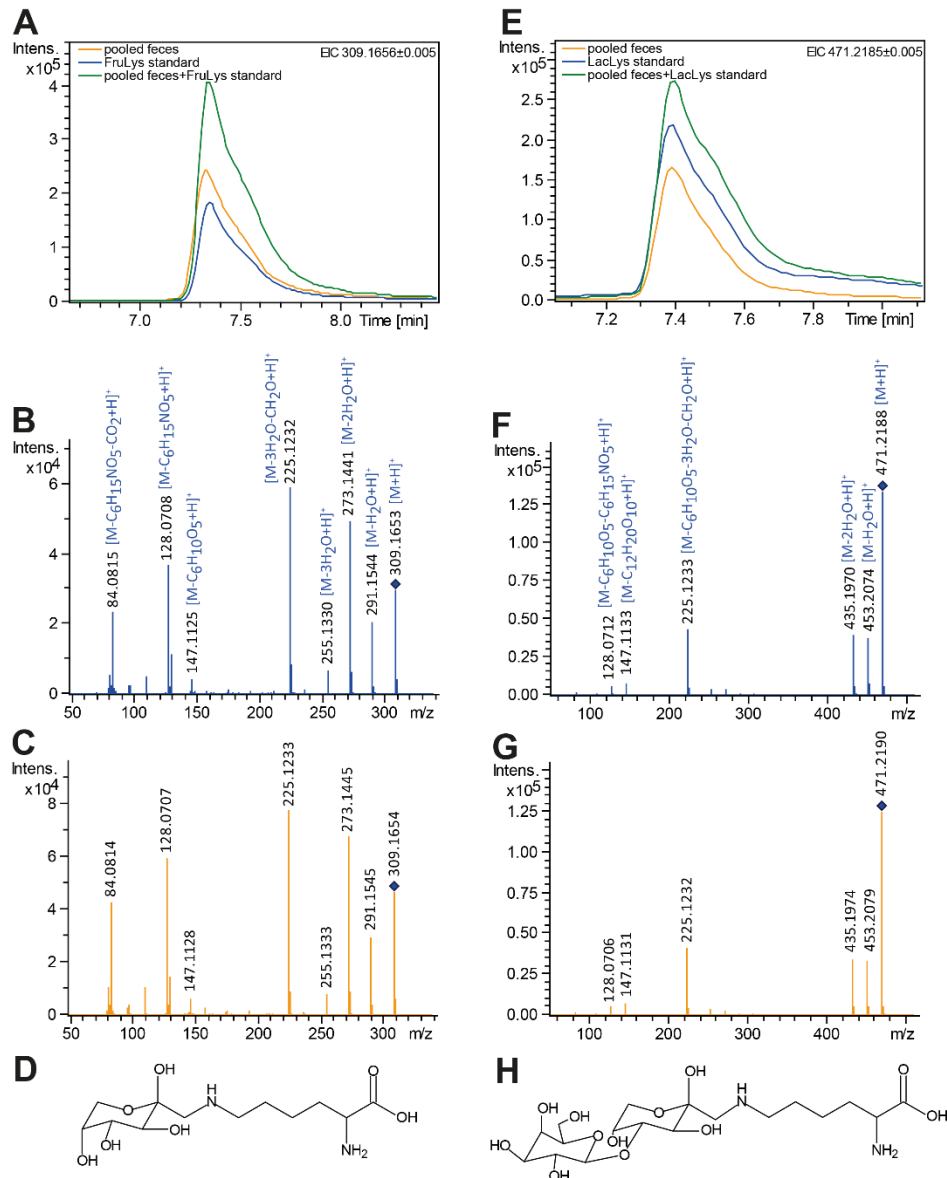


Figure C.S2. Identification of Lys Amadori products performed with HILIC LC-MS/MS (positive ionization mode). (A) Extracted ion chromatogram of FruLys ($[M+H]^+ = 309.1656 \pm 0.005$ Da) in feces (orange), purchased compound (blue) and spiking of the purchased Amadori product into the pooled fecal extract (green). (B) Collision induced dissociation MS/MS experiments (20 eV) of the FruLys standard and (C) of pooled fecal samples (MS/MS match: fit score 99.5%). (D) Chemical structure of FruLys. (E) Extracted ion chromatogram of LacLys ($[M+H]^+ = 471.2185 \pm 0.005$ Da) in feces (orange), prepared reference compound (blue) and spiking of the prepared Amadori product into the pooled fecal extract (green). (F) MS/MS (20 eV) of prepared LacLys standard and (G) of pooled fecal samples (MS/MS match: fit score 99.9%). (H) Chemical structure of LacLys.

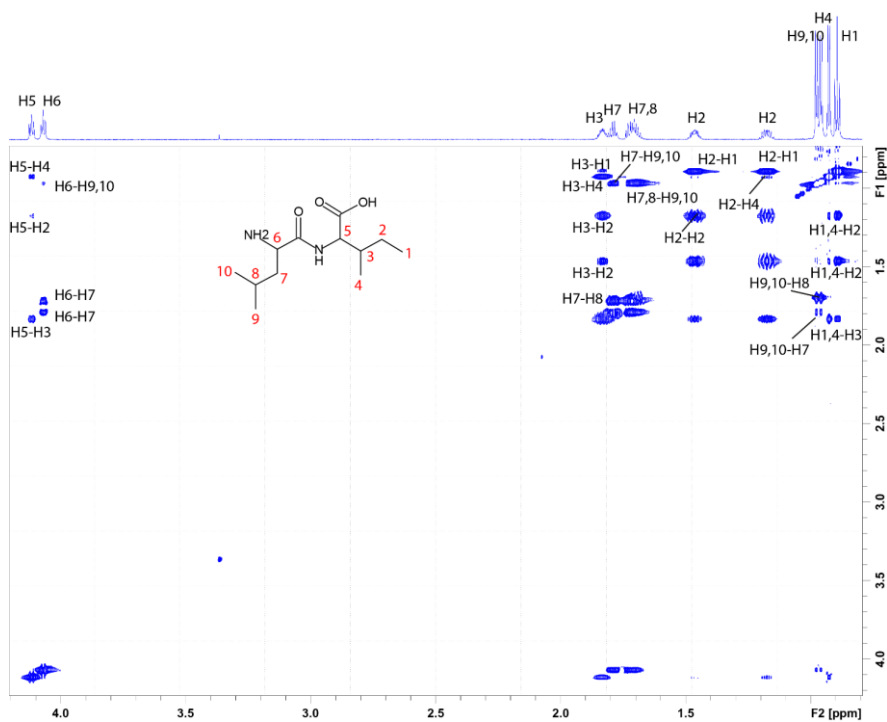


Figure C.S3. 2D ¹H-¹H TOCSY NMR spectrum of the reference standard leucylisoleucine (800 MHz, in 15% D₂O aqueous NMR buffer containing TSP).

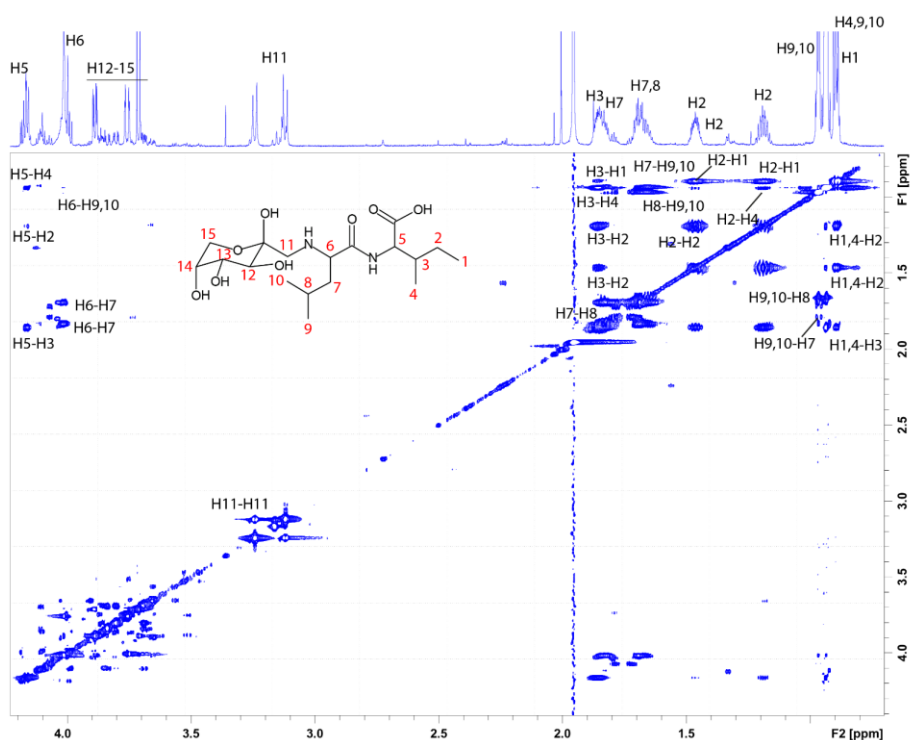


Figure C.S4. 2D ¹H-¹H TOCSY NMR spectrum of the prepared and purified FruLeulle standard (800 MHz, in 15% D₂O aqueous NMR buffer containing TSP).

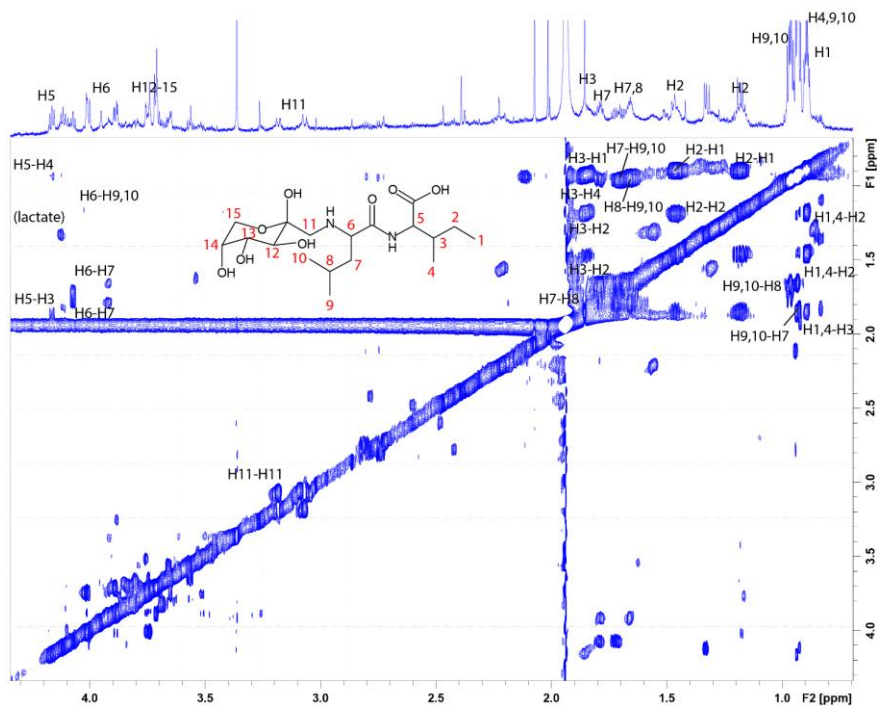


Figure C.S5. 2D ¹H-¹H TOCSY NMR spectrum of extracted FruLeulle from fecal samples (800 MHz, in 15% D₂O aqueous NMR buffer containing TSP).

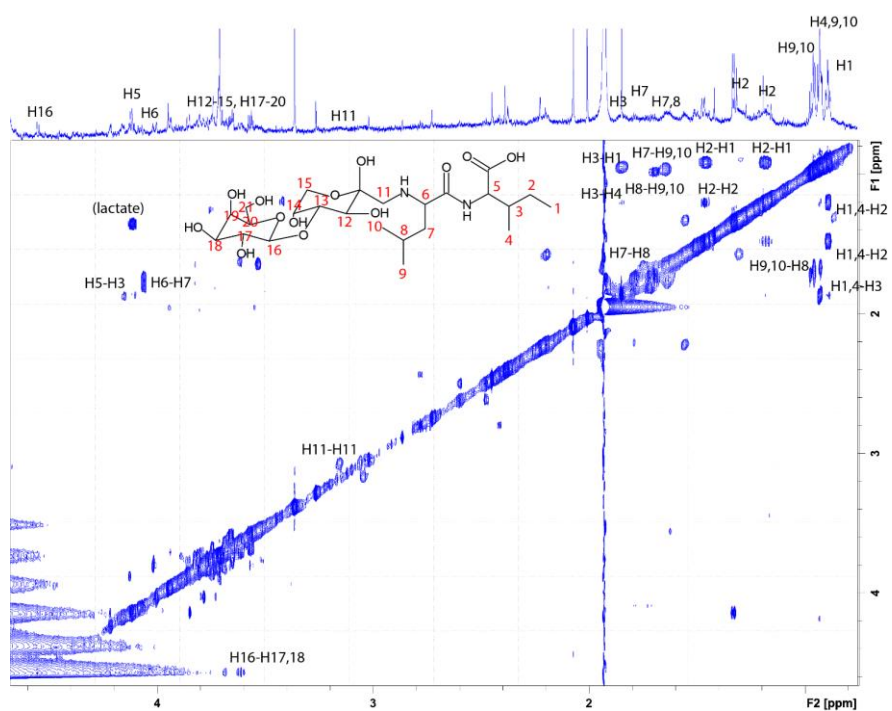


Figure C.S6. 2D ¹H-¹H TOCSY NMR spectrum of extracted LacLeulle from fecal samples (800 MHz, in 15% D₂O aqueous NMR buffer containing TSP).

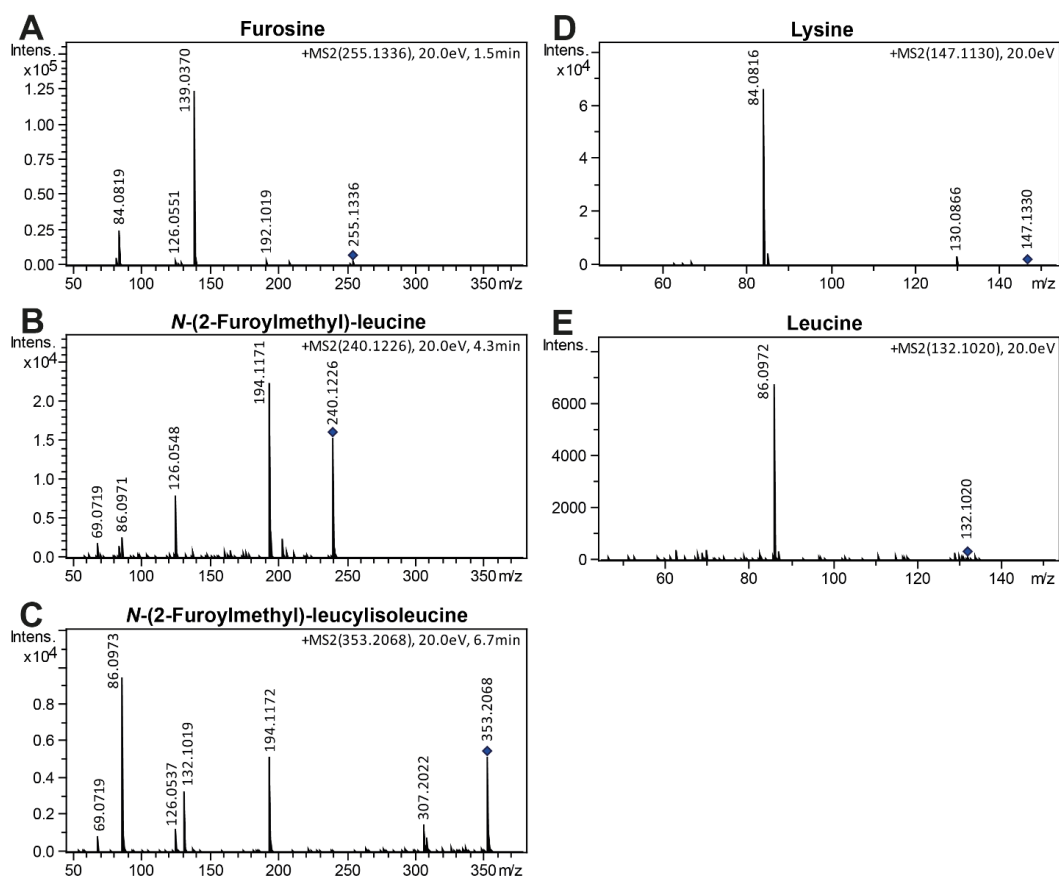


Figure C.S7. Acid hydrolysis of infant formula. Fragmentation patterns of the putative *N*-(2-furoylmethyl) amino acids (A) furosine, (B) *N*-(2-furoylmethyl)-leucine and (C) *N*-(2-furoylmethyl)-leucylisoleucine measured with C8 RP-UHPLC-MS/MS in positive ionization mode with a collision energy of 20 eV. MS/MS of (D) lysine and (E) leucine are shown for comparison.

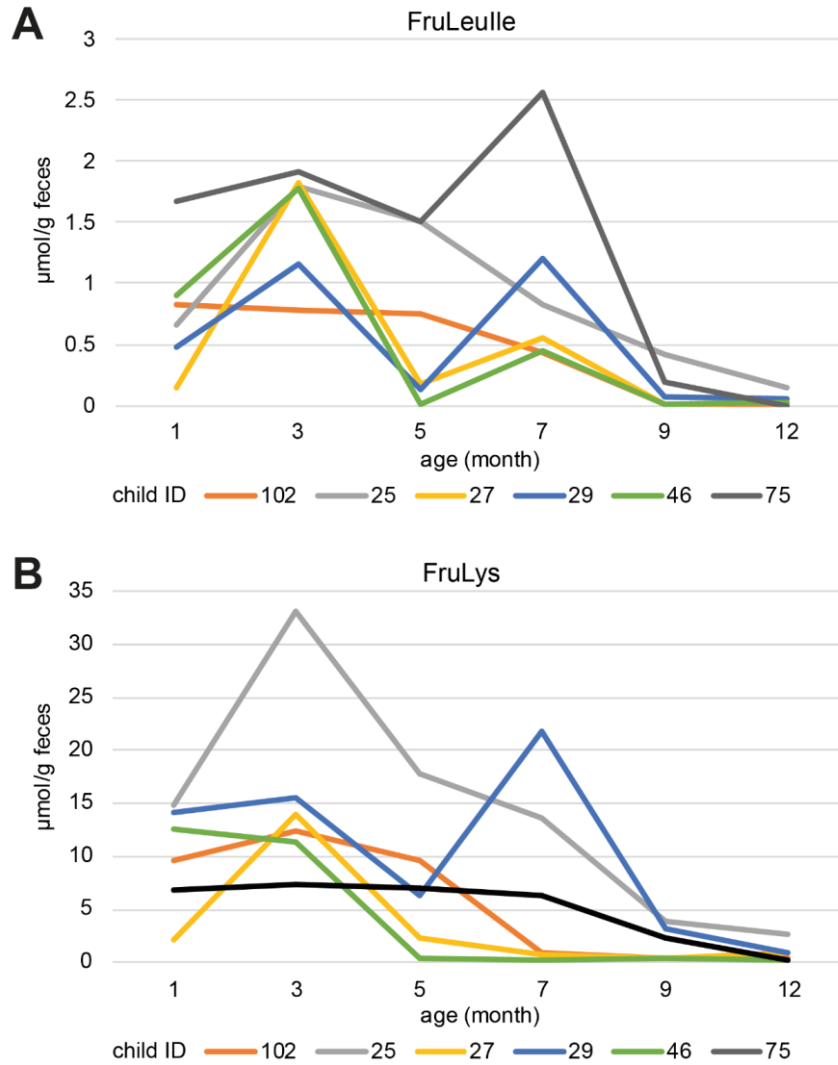


Figure C.S8. Excretion of (A) FruLeulle and (B) FruLys in $\mu\text{mol/g feces}$ during the first year of life. Samples from 6 exemplary formula-fed infants were chosen for quantification.

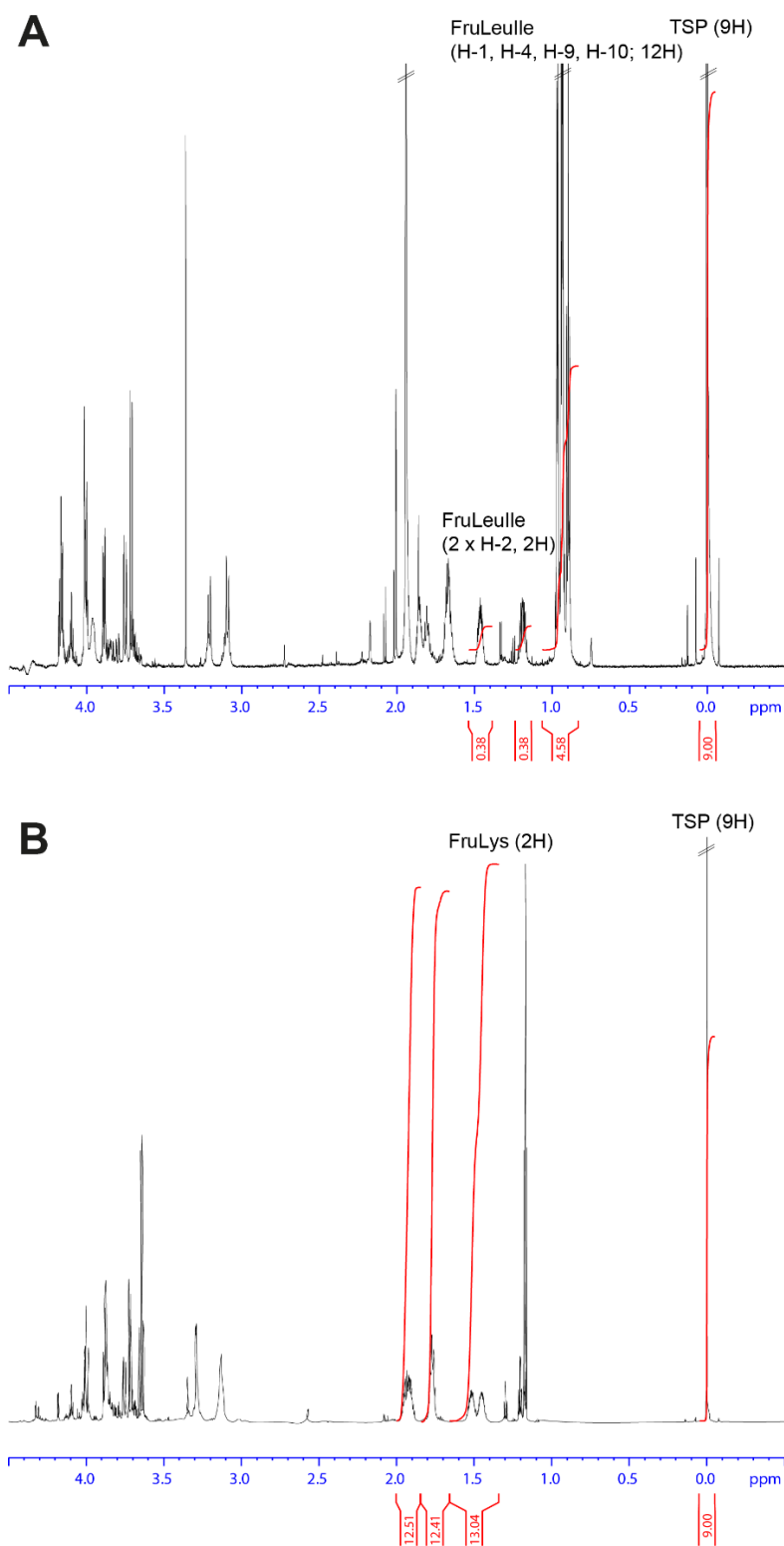


Figure C.S9. ^1H NMR spectra used for quantification of (A) FruLeulle (7.3 mmol/L) and (B) FruLys (12.4 mmol/L) reference stock solutions using 1 mg/mL TSP as internal standard.

Bibliography

1. Nicholson JK, Lindon JC, Holmes E. 'Metabonomics': understanding the metabolic responses of living systems to pathophysiological stimuli via multivariate statistical analysis of biological NMR spectroscopic data. *Xenobiotica*. 1999;29(11):1181-9.
2. Nicholson JK, Wilson ID. Understanding 'Global' Systems Biology: Metabonomics and the Continuum of Metabolism. *Nature Reviews Drug Discovery*. 2003;2(8):668-76.
3. Fiehn O. Metabolomics – the link between genotypes and phenotypes. *Plant Molecular Biology*. 2002;48(1):155-71.
4. Dunn WB, Bailey NJC, Johnson HE. Measuring the metabolome: current analytical technologies. *Analyst*. 2005;130(5):606-25.
5. Roberts LD, Souza AL, Gerszten RE, Clish CB. Targeted Metabolomics. *Current Protocols in Molecular Biology*. 2012;98(1):30.2.1-2.24.
6. Patti GJ, Yanes O, Siuzdak G. Metabolomics: the apogee of the omics trilogy. *Nature Reviews Molecular Cell Biology*. 2012;13:263.
7. Villas-Bôas SG, Mas S, Åkesson M, Smedsgaard J, Nielsen J. Mass spectrometry in metabolome analysis. *Mass spectrometry reviews*. 2005;24(5):613-46.
8. Holmes E, Wilson ID, Nicholson JK. Metabolic Phenotyping in Health and Disease. *Cell*. 2008;134(5):714-7.
9. Brennan L. Metabolomics in nutrition research—a powerful window into nutritional metabolism. *Essays in biochemistry*. 2016;60(5):451-8.
10. O'Sullivan A, Gibney MJ, Brennan L. Dietary intake patterns are reflected in metabolomic profiles: potential role in dietary assessment studies. *The American journal of clinical nutrition*. 2011;93(2):314-21.
11. Heinzmann SS, Brown IJ, Chan Q, Bictash M, Dumas ME, Kochhar S, et al. Metabolic profiling strategy for discovery of nutritional biomarkers: proline betaine as a marker of citrus consumption. *The American journal of clinical nutrition*. 2010;92(2):436-43.
12. Heinzmann SS, Holmes E, Kochhar S, Nicholson JK, Schmitt-Kopplin P. 2-Furoylglycine as a Candidate Biomarker of Coffee Consumption. *J Agric Food Chem*. 2015;63(38):8615-21.
13. Bazanella M, Maier TV, Clavel T, Lagkouvardos I, Lucio M, Maldonado-Gomez MX, et al. Randomized controlled trial on the impact of early-life intervention with bifidobacteria on the healthy infant fecal microbiota and metabolome. *The American journal of clinical nutrition*. 2017;106(5):1274-86.

14. Walker A, Pfitzner B, Harir M, Schaubeck M, Calasan J, Heinzmann SS, et al. Sulfonolipids as novel metabolite markers of *Alistipes* and *Odoribacter* affected by high-fat diets. *Scientific Reports*. 2017;7(1):11047.
15. Walker A, Pfitzner B, Neschen S, Kahle M, Harir M, Lucio M, et al. Distinct signatures of host–microbial meta-metabolome and gut microbiome in two C57BL/6 strains under high-fat diet. *The Isme Journal*. 2014;8:2380.
16. Smirnov KS, Maier TV, Walker A, Heinzmann SS, Forcisi S, Martinez I, et al. Challenges of metabolomics in human gut microbiota research. *International Journal of Medical Microbiology*. 2016;306(5):266-79.
17. Kübeck R, Bonet-Ripoll C, Hoffmann C, Walker A, Müller VM, Schüppel VL, et al. Dietary fat and gut microbiota interactions determine diet-induced obesity in mice. *Molecular Metabolism*. 2016;5(12):1162-74.
18. Lee T, Clavel T, Smirnov K, Schmidt A, Lagkouravdos I, Walker A, et al. Oral versus intravenous iron replacement therapy distinctly alters the gut microbiota and metabolome in patients with IBD. *Gut*. 2017;66(5):863-71.
19. Trezzi J-P, Vlassis N, Hiller K. The Role of Metabolomics in the Study of Cancer Biomarkers and in the Development of Diagnostic Tools. In: Scatena R, editor. *Advances in Cancer Biomarkers: From biochemistry to clinic for a critical revision*. Dordrecht: Springer Netherlands; 2015. p. 41-57.
20. Sillner N, Walker A, Koch W, Witting M, Schmitt-Kopplin P. Metformin impacts cecal bile acid profiles in mice. *Journal of chromatography B, Analytical technologies in the biomedical and life sciences*. 2018;1083:35-43.
21. Walker A, Lucio M, Pfitzner B, Scheerer MF, Neschen S, de Angelis MH, et al. Importance of Sulfur-Containing Metabolites in Discriminating Fecal Extracts between Normal and Type-2 Diabetic Mice. *Journal of Proteome Research*. 2014;13(10):4220-31.
22. Vincent IM, Barrett MP. Metabolomic-Based Strategies for Anti-Parasite Drug Discovery. *Journal of Biomolecular Screening*. 2015;20(1):44-55.
23. Schauer N, Semel Y, Roessner U, Gur A, Balbo I, Carrari F, et al. Comprehensive metabolic profiling and phenotyping of interspecific introgression lines for tomato improvement. *Nature Biotechnology*. 2006;24(4):447-54.
24. Klupczynska A, Derezinski P, Kokot ZJ. METABOLOMICS IN MEDICAL SCIENCES--TRENDS, CHALLENGES AND PERSPECTIVES. *Acta poloniae pharmaceutica*. 2015;72(4):629-41.
25. Zhang A, Sun H, Wang P, Han Y, Wang X. Modern analytical techniques in metabolomics analysis. *Analyst*. 2012;137(2):293-300.
26. Rochfort S. Metabolomics reviewed: a new "omics" platform technology for systems biology and implications for natural products research. *Journal of natural products*. 2005;68(12):1813-20.
27. Johnson CH, Ivanisevic J, Siuzdak G. Metabolomics: beyond biomarkers and towards mechanisms. *Nature Reviews Molecular Cell Biology*. 2016;17:451.

28. Sender R, Fuchs S, Milo R. Revised Estimates for the Number of Human and Bacteria Cells in the Body. *PLoS Biol.* 2016;14(8):e1002533-e.
29. Almeida A, Mitchell AL, Boland M, Forster SC, Gloor GB, Tarkowska A, et al. A new genomic blueprint of the human gut microbiota. *Nature.* 2019;568(7753):499-504.
30. Eckburg PB, Bik EM, Bernstein CN, Purdom E, Dethlefsen L, Sargent M, et al. Diversity of the human intestinal microbial flora. *Science.* 2005;308(5728):1635-8.
31. Leser TD, Molbak L. Better living through microbial action: the benefits of the mammalian gastrointestinal microbiota on the host. *Environmental microbiology.* 2009;11(9):2194-206.
32. Lederberg J. Of Men and Microbes. *New Perspectives Quarterly.* 2003;20(3):52-5.
33. Turnbaugh PJ, Gordon JI. An invitation to the marriage of metagenomics and metabolomics. *Cell.* 2008;134(5):708-13.
34. Forster SC, Kumar N, Anonye BO, Almeida A, Viciani E, Stares MD, et al. A human gut bacterial genome and culture collection for improved metagenomic analyses. *Nature Biotechnology.* 2019;37(2):186-92.
35. Bergman EN. Energy contributions of volatile fatty acids from the gastrointestinal tract in various species. *Physiological reviews.* 1990;70(2):567-90.
36. Kau AL, Ahern PP, Griffin NW, Goodman AL, Gordon JI. Human nutrition, the gut microbiome and the immune system. *Nature.* 2011;474(7351):327-36.
37. Backhed F, Ding H, Wang T, Hooper LV, Koh GY, Nagy A, et al. The gut microbiota as an environmental factor that regulates fat storage. *Proceedings of the National Academy of Sciences of the United States of America.* 2004;101(44):15718-23.
38. Lloyd-Price J, Arze C, Ananthakrishnan AN, Schirmer M, Avila-Pacheco J, Poon TW, et al. Multi-omics of the gut microbial ecosystem in inflammatory bowel diseases. *Nature.* 2019;569(7758):655-62.
39. Heinken A, Thiele I. Systems biology of host-microbe metabolomics. *Wiley interdisciplinary reviews Systems biology and medicine.* 2015;7(4):195-219.
40. Dorrestein PC, Mazmanian SK, Knight R. Finding the missing links among metabolites, microbes, and the host. *Immunity.* 2014;40(6):824-32.
41. Vernocchi P, Del Chierico F, Putignani L. Gut Microbiota Profiling: Metabolomics Based Approach to Unravel Compounds Affecting Human Health. *Frontiers in microbiology.* 2016;7:1144.
42. Sonnenburg JL, Backhed F. Diet-microbiota interactions as moderators of human metabolism. *Nature.* 2016;535(7610):56-64.

43. Nicholson JK, Holmes E, Kinross J, Burcelin R, Gibson G, Jia W, et al. Host-gut microbiota metabolic interactions. *Science*. 2012;336(6086):1262-7.
44. Bourriaud C, Robins RJ, Martin L, Kozlowski F, Tenailleau E, Cherbut C, et al. Lactate is mainly fermented to butyrate by human intestinal microfloras but inter-individual variation is evident. *Journal of applied microbiology*. 2005;99(1):201-12.
45. Russell WR, Duncan SH, Flint HJ. The gut microbial metabolome: modulation of cancer risk in obese individuals. *The Proceedings of the Nutrition Society*. 2013;72(1):178-88.
46. Gao Z, Yin J, Zhang J, Ward RE, Martin RJ, Lefevre M, et al. Butyrate improves insulin sensitivity and increases energy expenditure in mice. *Diabetes*. 2009;58(7):1509-17.
47. Kespolh M, Vachharajani N, Luu M, Harb H, Pautz S, Wolff S, et al. The Microbial Metabolite Butyrate Induces Expression of Th1-Associated Factors in CD4+ T Cells. *Frontiers in Immunology*. 2017;8(1036).
48. Fassler C, Arrigoni E, Venema K, Brouns F, Amado R. In vitro fermentability of differently digested resistant starch preparations. *Molecular nutrition & food research*. 2006;50(12):1220-8.
49. Samuelsson LM, Young W, Fraser K, Tannock GW, Lee J, Roy NC. Digestive-resistant carbohydrates affect lipid metabolism in rats. *Metabolomics*. 2016;12(5):79.
50. Karu N, Deng L, Siae M, Guo AC, Sajed T, Huynh H, et al. A review on human fecal metabolomics: Methods, applications and the human fecal metabolome database. *Analytica Chimica Acta*. 2018;1030:1-24.
51. Zheng X, Qiu Y, Zhong W, Baxter S, Su M, Li Q, et al. A targeted metabolomic protocol for short-chain fatty acids and branched-chain amino acids. *Metabolomics*. 2013;9(4):818-27.
52. Pandak WM, Bohdan P, Franklund C, Mallonee DH, Eggertsen G, Björkhem I, et al. Expression of sterol 12 α -hydroxylase alters bile acid pool composition in primary rat hepatocytes and in vivo. *Gastroenterology*. 2001;120(7):1801-9.
53. Benson RSP, Sidhu SS, Jones MN, Case RM, Thompson DG. Fatty acid signalling in a mouse enteroendocrine cell line involves fatty acid aggregates rather than free fatty acids. *The Journal of Physiology*. 2002;538(1):121-31.
54. Chiang JY. Bile acid metabolism and signaling. *Comprehensive Physiology*. 2013;3(3):1191-212.
55. Hammons JL, Jordan WE, Stewart RL, Taulbee JD, Berg RW. Age and Diet Effects on Fecal Bile Acids in Infants. *Journal of pediatric gastroenterology and nutrition*. 1988;7(1):30-8.
56. Gérard P. Metabolism of cholesterol and bile acids by the gut microbiota. *Pathogens*. 2013;3(1):14-24.

-
57. Xie G, Zhang S, Zheng X, Jia W. Metabolomics approaches for characterizing metabolic interactions between host and its commensal microbes. *Electrophoresis*. 2013;34(19):2787-98.
58. Aw W, Fukuda S. Toward the comprehensive understanding of the gut ecosystem via metabolomics-based integrated omics approach. *Seminars in immunopathology*. 2015;37(1):5-16.
59. Islam KB, Fukiya S, Hagio M, Fujii N, Ishizuka S, Ooka T, et al. Bile acid is a host factor that regulates the composition of the cecal microbiota in rats. *Gastroenterology*. 2011;141(5):1773-81.
60. Fiorucci S, Distrutti E. Bile Acid-Activated Receptors, Intestinal Microbiota, and the Treatment of Metabolic Disorders. *Trends in Molecular Medicine*. 2015;21(11):702-14.
61. Goodwin BL, Ruthven CR, Sandler M. Gut flora and the origin of some urinary aromatic phenolic compounds. *Biochemical pharmacology*. 1994;47(12):2294-7.
62. Dodd D, Spitzer MH, Van Treuren W, Merrill BD, Hryckowian AJ, Higginbottom SK, et al. A gut bacterial pathway metabolizes aromatic amino acids into nine circulating metabolites. *Nature*. 2017;551(7682):648-52.
63. Beloborodova N, Bairamov I, Olenin A, Shubina V, Teplova V, Fedotcheva N. Effect of phenolic acids of microbial origin on production of reactive oxygen species in mitochondria and neutrophils. *Journal of Biomedical Science*. 2012;19(1):89.
64. Beloborodova NV, Khodakova AS, Bairamov IT, Olenin AY. Microbial origin of phenylcarboxylic acids in the human body. *Biochemistry (Moscow)*. 2009;74(12):1350-5.
65. Aragozzini F, Ferrari A, Pacini N, Gualandris R. Indole-3-lactic acid as a tryptophan metabolite produced by *Bifidobacterium* spp. *Applied and Environmental Microbiology*. 1979;38(3):544-6.
66. Li P, Hotamisligil GS. Host and microbes in a pickle. *Nature*. 2010;464:1287.
67. Heinzmann SS, Schmitt-Kopplin P. Deep Metabotyping of the Murine Gastrointestinal Tract for the Visualization of Digestion and Microbial Metabolism. *Journal of Proteome Research*. 2015;14(5):2267-77.
68. Maier TV, Lucio M, Lee LH, VerBerkmoes NC, Brislawn CJ, Bernhardt J, et al. Impact of Dietary Resistant Starch on the Human Gut Microbiome, Metaproteome, and Metabolome. *mBio*. 2017;8(5).
69. Melnik AV, da Silva RR, Hyde ER, Aksenov AA, Vargas F, Bouslimani A, et al. Coupling Targeted and Untargeted Mass Spectrometry for Metabolome-Microbiome-Wide Association Studies of Human Fecal Samples. *Analytical chemistry*. 2017;89(14):7549-59.

-
70. Probert CSJ, Jones PRH, Ratcliffe NM. A novel method for rapidly diagnosing the causes of diarrhoea. *Gut*. 2004;53(1):58-61.
71. Marchesi JR, Holmes E, Khan F, Kochhar S, Scanlan P, Shanahan F, et al. Rapid and Noninvasive Metabonomic Characterization of Inflammatory Bowel Disease. *Journal of Proteome Research*. 2007;6(2):546-51.
72. Dragsted LO, Gao Q, Scalbert A, Vergères G, Kolehmainen M, Manach C, et al. Validation of biomarkers of food intake—critical assessment of candidate biomarkers. *Genes & Nutrition*. 2018;13(1):14.
73. Llorach R, Garcia-Aloy M, Tulipani S, Vazquez-Fresno R, Andres-Lacueva C. Nutrimetabolomic Strategies To Develop New Biomarkers of Intake and Health Effects. *Journal of Agricultural and Food Chemistry*. 2012;60(36):8797-808.
74. Jones DP, Park Y, Ziegler TR. Nutritional metabolomics: progress in addressing complexity in diet and health. *Annual review of nutrition*. 2012;32:183-202.
75. Wild CP. Complementing the genome with an "exposome": the outstanding challenge of environmental exposure measurement in molecular epidemiology. *Cancer epidemiology, biomarkers & prevention : a publication of the American Association for Cancer Research, cosponsored by the American Society of Preventive Oncology*. 2005;14(8):1847-50.
76. McNiven EMS, German JB, Slupsky CM. Analytical metabolomics: nutritional opportunities for personalized health. *The Journal of Nutritional Biochemistry*. 2011;22(11):995-1002.
77. Astarita G, Langridge J. An Emerging Role for Metabolomics in Nutrition Science. *Lifestyle Genomics*. 2013;6(4-5):181-200.
78. Rangel-Huerta OD, Gil A. Nutrimetabolomics: An Update on Analytical Approaches to Investigate the Role of Plant-Based Foods and Their Bioactive Compounds in Non-Communicable Chronic Diseases. *International journal of molecular sciences*. 2016;17(12):2072.
79. Celis-Morales C, Livingstone KM, Marsaux CF, Macready AL, Fallaize R, O'Donovan CB, et al. Effect of personalized nutrition on health-related behaviour change: evidence from the Food4Me European randomized controlled trial. *International journal of epidemiology*. 2017;46(2):578-88.
80. Elnenaei MO, Chandra R, Mangion T, Moniz C. Genomic and metabolomic patterns segregate with responses to calcium and vitamin D supplementation. *The British journal of nutrition*. 2011;105(1):71-9.
81. Yen S, McDonald JA, Schroeter K, Oliphant K, Sokolenko S, Blondeel EJ, et al. Metabolomic analysis of human fecal microbiota: a comparison of feces-derived communities and defined mixed communities. *J Proteome Res*. 2015;14(3):1472-82.
82. Arrieta MC, Stiemsma LT, Dimitriu PA, Thorson L, Russell S, Yurist-Doutsch S, et al. Early infancy microbial and metabolic alterations affect risk of childhood asthma. *Science translational medicine*. 2015;7(307):307ra152.

-
83. Despres JP, Lemieux I. Abdominal obesity and metabolic syndrome. *Nature*. 2006;444(7121):881-7.
84. Chow J, Panasevich MR, Alexander D, Vester Boler BM, Rossoni Serao MC, Faber TA, et al. Fecal Metabolomics of Healthy Breast-Fed versus Formula-Fed Infants before and during In Vitro Batch Culture Fermentation. *Journal of Proteome Research*. 2014;13(5):2534-42.
85. Mai V, Torrazza RM, Ukhanova M, Wang X, Sun Y, Li N, et al. Distortions in development of intestinal microbiota associated with late onset sepsis in preterm infants. *PLoS One*. 2013;8(1):e52876.
86. Mai V, Young CM, Ukhanova M, Wang X, Sun Y, Casella G, et al. Fecal microbiota in premature infants prior to necrotizing enterocolitis. *PLoS One*. 2011;6(6):e20647.
87. de Weerth C, Fuentes S, de Vos WM. Crying in infants: on the possible role of intestinal microbiota in the development of colic. *Gut microbes*. 2013;4(5):416-21.
88. Huffnagle GB. The microbiota and allergies/asthma. *PLoS pathogens*. 2010;6(5):e1000549.
89. Kalliomaki M, Collado MC, Salminen S, Isolauri E. Early differences in fecal microbiota composition in children may predict overweight. *The American journal of clinical nutrition*. 2008;87(3):534-8.
90. Harmsen HJ, Wildeboer-Veloo AC, Raangs GC, Wagendorp AA, Klijn N, Bindels JG, et al. Analysis of intestinal flora development in breast-fed and formula-fed infants by using molecular identification and detection methods. *Journal of pediatric gastroenterology and nutrition*. 2000;30(1):61-7.
91. Penders J, Thijs C, Vink C, Stelma FF, Snijders B, Kummeling I, et al. Factors influencing the composition of the intestinal microbiota in early infancy. *Pediatrics*. 2006;118(2):511-21.
92. Arrieta MC, Stiemsma LT, Amenyogbe N, Brown EM, Finlay B. The intestinal microbiome in early life: health and disease. *Front Immunol*. 2014;5:427.
93. Walker WA, Iyengar RS. Breast milk, microbiota, and intestinal immune homeostasis. *Pediatric Research*. 2014;77:220.
94. Dessi A, Briana D, Corbu S, Gavrieli S, Cesare Marincola F, Georgantzi S, et al. Metabolomics of Breast Milk: The Importance of Phenotypes. *Metabolites*. 2018;8(4).
95. Hellwig M, Henle T. Baking, Ageing, Diabetes: A Short History of the Maillard Reaction. *Angewandte Chemie International Edition*. 2014;53(39):10316-29.
96. Pischetsrieder M, Henle T. Glycation products in infant formulas: chemical, analytical and physiological aspects. *Amino acids*. 2012;42(4):1111-8.

-
97. Alexy U, Kersting M, Sichert-Hellert W, Manz F, Schoch G. Macronutrient intake of 3- to 36-month-old German infants and children: results of the DONALD Study. Dortmund Nutritional and Anthropometric Longitudinally Designed Study. *Annals of nutrition & metabolism*. 1999;43(1):14-22.
98. Riva E, Verduci E, Agostoni C, Giovannini M. Comparison of the nutritional values of follow-on formulae available in Italy. *The Journal of international medical research*. 2007;35(1):20-37.
99. Wiame E, Delpierre G, Collard F, Van Schaftingen E. Identification of a pathway for the utilization of the Amadori product fructoselysine in *Escherichia coli*. *The Journal of biological chemistry*. 2002;277(45):42523-9.
100. Katz C, Cohen-Or I, Gophna U, Ron EZ. The ubiquitous conserved glycopeptidase Gcp prevents accumulation of toxic glycated proteins. *mBio*. 2010;1(3).
101. Bui TP, Ritari J, Boeren S, de Waard P, Plugge CM, de Vos WM. Production of butyrate from lysine and the Amadori product fructoselysine by a human gut commensal. *Nat Commun*. 2015;6:10062.
102. Fuhrer T, Zamboni N. High-throughput discovery metabolomics. *Current opinion in biotechnology*. 2015;31:73-8.
103. Griffin JL, Atherton H, Shockcor J, Atzori L. Metabolomics as a tool for cardiac research. *Nature reviews Cardiology*. 2011;8(11):630-43.
104. Schmitt-Kopplin P, Gelencser A, Dabek-Zlotorzynska E, Kiss G, Hertkorn N, Harir M, et al. Analysis of the unresolved organic fraction in atmospheric aerosols with ultrahigh-resolution mass spectrometry and nuclear magnetic resonance spectroscopy: organosulfates as photochemical smog constituents. *Analytical chemistry*. 2010;82(19):8017-26.
105. Novakova L, Solichova D, Solich P. Advantages of ultra performance liquid chromatography over high-performance liquid chromatography: comparison of different analytical approaches during analysis of diclofenac gel. *Journal of separation science*. 2006;29(16):2433-43.
106. Lenz EM, Wilson ID. Analytical strategies in metabolomics. *J Proteome Res*. 2007;6(2):443-58.
107. Buszewski B, Noga S. Hydrophilic interaction liquid chromatography (HILIC)--a powerful separation technique. *Analytical and bioanalytical chemistry*. 2012;402(1):231-47.
108. Alpert AJ. Hydrophilic-interaction chromatography for the separation of peptides, nucleic acids and other polar compounds. *Journal of chromatography*. 1990;499:177-96.
109. Guo Y, Gaiki S. Retention and selectivity of stationary phases for hydrophilic interaction chromatography. *Journal of chromatography A*. 2011;1218(35):5920-38.

-
110. Guo Y, Gaiki S. Retention behavior of small polar compounds on polar stationary phases in hydrophilic interaction chromatography. *Journal of chromatography A*. 2005;1074(1-2):71-80.
111. Brenton AG, Godfrey AR. Accurate mass measurement: terminology and treatment of data. *J Am Soc Mass Spectrom*. 2010;21(11):1821-35.
112. Meher AK, Chen Y-C. Electrospray Modifications for Advancing Mass Spectrometric Analysis. *Mass Spectrom (Tokyo)*. 2017;6(Spec Iss):S0057-S.
113. Forcisi S, Moritz F, Kanawati B, Tziotis D, Lehmann R, Schmitt-Kopplin P. Liquid chromatography-mass spectrometry in metabolomics research: mass analyzers in ultra high pressure liquid chromatography coupling. *Journal of chromatography A*. 2013;1292:51-65.
114. Nolting D, Malek R, Makarov A. Ion traps in modern mass spectrometry. *Mass spectrometry reviews*. 2019;38(2):150-68.
115. Gross JH. *Mass Spectrometry: A Textbook*. Berlin, Heidelberg: Springer Berlin Heidelberg; 2011.
116. Šebeková K, Klenovics KS, Šebeková KB. Advanced glycation end products in infant formulas. *Handbook of dietary and nutritional aspects of bottle feeding*, 2015. p. 421-40.
117. Finot PA, Magnenat E. Metabolic transit of early and advanced Maillard products. *Progress in food & nutrition science*. 1981;5(1-6):193-207.
118. Erbersdobler HF, Lohmann M, Buhl K. Utilization of Early Maillard Reaction Products by Humans. In: Friedman M, editor. *Nutritional and Toxicological Consequences of Food Processing*. Boston, MA: Springer US; 1991. p. 363-70.
119. Henle T, Schwenger V, Ritz E. Preliminary studies on the renal handling of lactuloselysine from milk products. *Czech Journal of Food Sciences*. 2000;18(Special Issue):101-2.
120. Erbersdobler HF, Faist V. Metabolic transit of Amadori products. *Die Nahrung*. 2001;45(3):177-81.
121. Scano P, Murgia A, Demuru M, Consonni R, Caboni P. Metabolite profiles of formula milk compared to breast milk. *Food Research International*. 2016;87:76-82.
122. Bowen BP, Northen TR. Dealing with the Unknown: Metabolomics and Metabolite Atlases. *Journal of the American Society for Mass Spectrometry*. 2010;21(9):1471-6.
123. Boiteau RM, Hoyt DW, Nicora CD, Kinmonth-Schultz HA, Ward JK, Bingol K. Structure Elucidation of Unknown Metabolites in Metabolomics by Combined NMR and MS/MS Prediction. *Metabolites*. 2018;8(1):8.
124. Bonner R, Hopfgartner G. SWATH data independent acquisition mass spectrometry for metabolomics. *TrAC Trends in Analytical Chemistry*. 2018.

125. Hemmler D, Heinzmann SS, Wöhr K, Schmitt-Kopplin P, Witting M. Tandem HILIC-RP liquid chromatography for increased polarity coverage in food analysis. *Electrophoresis*. 2018;39(13):1645-53.

List of Figures

Figure 1-1. Factors shaping the metabolome of an organism or biological sample.	2
Figure 1-2. Distribution of metabolomics publications in different research areas in 2018. Number of publications were obtained by searching the corresponding keywords (e.g. metabolom* & nutrition) in the PubMed Central (PMC) database for the year 2018. The fractions were calculated by dividing the number obtained from each area by the total number of publications found with the keyword metabolom* (5,430).....	3
Figure 1-3. Schematic overview and principles of non-targeted and targeted metabolomics.	17
Figure 1-4. Schematic structures of HILIC stationary phases. (A) Unbonded silica, (B) BEH (Ethylene Bridged Hybrid) amide (Waters, ACQUITY UPLC™, Eschborn, Germany), (C) zwitterionic phase (iHILIC®-Fusion, HILICON AB, Umea, Sweden).	19
Figure 1-5. Scheme of an iontrap MS (adapted from amaZon ETD user manual, Bruker Daltonics GmbH).....	21
Figure 1-6. Scheme of an orthogonal hybrid QTOF-MS (adapted from maXis™ user manual version 1.1, Bruker Daltonics GmbH).....	22
Figure 1-7. Outline of the chapters included in the thesis.....	24
Figure 5-1. Heat map of highly discriminative metabolites mass signals between infants exclusively breastfed (B, blue), exclusively formula-fed without probiotics (F-, orange) and with probiotics (F+, green) over time (month 1 – 24) analyzed by HILIC UHPLC-QTOF-MS (negative ionization mode). Peak areas were unit variance scaled for visualization.....	32

-
- Figure C.S1.** Chemical composition of feces from 1-month-old infants, who were exclusively fed with breast milk (average of signal intensity of $n = 16$ fecal samples), acquired by FT-ICR-MS in negative ionization mode. Calculated molecular formulas were categorized into 4 compositional groups: CHO (blue), CHON (orange), CHOS (green) and CHONS (red). The van Krevelen diagram plots the H/C vs. O/C atomic ratios of the computed molecular formulas. 86
- Figure C.S2.** Identification of Lys Amadori products performed with HILIC LC-MS/MS (positive ionization mode). (A) Extracted ion chromatogram of FruLys ($[M+H]^+ = 309.1656 \pm 0.005$ Da) in feces (orange), purchased compound (blue) and spiking of the purchased Amadori product into the pooled fecal extract (green). (B) Collision induced dissociation MS/MS experiments (20 eV) of the FruLys standard and (C) of pooled fecal samples (MS/MS match: fit score 99.5%). (D) Chemical structure of FruLys. (E) Extracted ion chromatogram of LacLys ($[M+H]^+ = 471.2185 \pm 0.005$ Da) in feces (orange), prepared reference compound (blue) and spiking of the prepared Amadori product into the pooled fecal extract (green). (F) MS/MS (20 eV) of prepared LacLys standard and (G) of pooled fecal samples (MS/MS match: fit score 99.9%). (H) Chemical structure of LacLys. 87
- Figure C.S3.** 2D ^1H - ^1H TOCSY NMR spectrum of the reference standard leucylisoleucine (800 MHz, in 15% D_2O aqueous NMR buffer containing TSP). 88
- Figure C.S4.** 2D ^1H - ^1H TOCSY NMR spectrum of the prepared and purified FruLeulle standard (800 MHz, in 15% D_2O aqueous NMR buffer containing TSP). 88
- Figure C.S5.** 2D ^1H - ^1H TOCSY NMR spectrum of extracted FruLeulle from fecal samples (800 MHz, in 15% D_2O aqueous NMR buffer containing TSP). 89
- Figure C.S6.** 2D ^1H - ^1H TOCSY NMR spectrum of extracted LacLeulle from fecal samples (800 MHz, in 15% D_2O aqueous NMR buffer containing TSP). 89

Figure C.S7. Acid hydrolysis of infant formula. Fragmentation patterns of the putative N-(2-furoylmethyl) amino acids (A) furosine, (B) N-(2-furoylmethyl)-leucine and (C) N-(2-furoylmethyl)-leucylisoleucine measured with C8 RP-UHPLC-MS/MS in positive ionization mode with a collision energy of 20 eV. MS/MS of (D) lysine and (E) leucine are shown for comparison.....	90
Figure C.S8. Excretion of (A) FruLeulle and (B) FruLys in $\mu\text{mol/g}$ feces during the first year of life. Samples from 6 exemplary formula-fed infants were chosen for quantification.	91
Figure C.S9. ^1H NMR spectra used for quantification of (A) FruLeulle (7.3 mmol/L) and (B) FruLys (12.4 mmol/L) reference stock solutions using 1 mg/mL TSP as internal standard.	92

Curriculum Vitae

Name Nina Sillner
Birthday 15.12.1989
Birthplace Nürnberg, Germany
Nationality German

Education and scientific work experience

- 12/2015 – 06/2019** **Ph.D., Research Associate**
Technical University of Munich, ZIEL Institute for Food & Health and Helmholtz Zentrum München, Analytical BioGeoChemistry, Germany
- Screening of small biomolecules (metabolomics) using mass spectrometry coupled to liquid chromatography (HPLC-MS)
 - Coordination and analysis of more than thousand biological samples from an infant cohort study to investigate the influence of nutrition and gut microbiome composition on the early-life metabolome
 - Multivariate data analysis and statistics using software like Genedata Expressionist®, SIMCA, SigmaPlot and R
 - Development and validation of HPLC-MS methods for quantification of bile acids in intestinal samples from mice and non-targeted screening of metabolites in human stool samples
 - Writing of method development protocols used by colleagues
 - Supervision of technical assistants and bachelor students
 - Presentation of research results at several international conferences and publications in peer-review journals
- 04/2015 – 06/2015** **Scientific assistant,**
Fraunhofer Institute for Process Engineering and Packaging IVV, Department Sensory Analytics, Freising, Germany
- Method development and optimization for analysis of volatile metabolites in human samples (urine, breath and milk) using proton-transfer-reaction mass spectrometry

- 04/2015 – 09/2015** **Master Thesis**
*Fraunhofer Institute for Process Engineering and Packaging IVV,
 Department Sensory Analytics, Freising, Germany*
- Title: Monitoring of garlic substances in breath, urine and breast milk via proton-transfer-reaction mass spectrometry (grade: 1.0)
 - Design of a nutrition study and recruitment of volunteers
- 10/2013 – 09/2015** **Master of Science “Molecular Science“**
Friedrich-Alexander-University Erlangen-Nürnberg, Germany
- Specialization: Molecular Life Science
 - Final grade: 1.1
- 09/2014 – 02/2015** **Exchange semester, Chemistry**
ETH (Swiss Federal Institute of Technology) Zurich, Switzerland
- 10/2010 – 09/2013** **Bachelor of Science “Molecular Science“**
Friedrich-Alexander-University Erlangen-Nürnberg, Germany
- Thesis title: Untersuchungen zum Einfluss von Silizium Nanopartikeln auf *C. glutamicum* und *C. elegans*
 - Final grade: 1.8
- 06/2010** **Higher education entrance qualification**
 German “Abitur” grade 1.4
Johannes-Scharrer-Gymnasium Nürnberg, Germany

Honors and Awards

- 2018** Scientific poster prize at Seeon Conference, Germany
- 2018** Travel grant from GDCh, Division Analytical Chemistry
- Since 08/2010** Online scholarship from e-fellows.net
- 09/2014 –
02/2015** Swiss European Mobility Program scholarship for exchange semester at the ETH Zurich, Switzerland
- 2010** Future prize in biology (“Biozukunftspreis”) from the “Natur Mensch Kultur” foundation for excellent achievements in the subject biology

Eidesstattliche Erklärung

Ich erkläre an Eides statt, dass ich die bei der promotionsführenden Einrichtung Wissenschaftszentrum Weihenstephan für Ernährung, Landnutzung und Umwelt der Technischen Universität München zur Promotionsprüfung vorgelegte Arbeit mit dem Titel:

Optimization of liquid chromatography-mass spectrometry-based methods for the discovery of microbial and nutritional metabolites

In Chemie am ZIEL – Institute for Food & Health unter der Anleitung und Betreuung durch apl.-Prof. Dr. Philippe Schmitt-Kopplin ohne sonstige Hilfe erstellt und bei der Abfassung nur die gemäß § 6 Abs. 6 und 7 Satz 2 angegebenen Hilfsmittel benutzt habe.

(x) Ich habe keine Organisation eingeschaltet, die gegen Entgelt Betreuerinnen und Betreuer für die Anfertigung von Dissertationen sucht, oder die mir obliegenden Pflichten hinsichtlich der Prüfungsleistungen für mich ganz oder teilweise erledigt.

(x) Ich habe die Dissertation in dieser oder ähnlicher Form in keinem anderen Prüfungsverfahren als Prüfungsleistung vorgelegt.

(x) Ich habe den angestrebten Doktorgrad noch nicht erworben und bin nicht in einem früheren Promotionsverfahren für den angestrebten Doktorgrad endgültig gescheitert.

Die öffentlich zugängliche Promotionsordnung der TUM ist mir bekannt, insbesondere habe ich die Bedeutung von § 28 (Nichtigkeit der Promotion) und § 29 (Entzug des Doktorgrades) zur Kenntnis genommen. Ich bin mir der Konsequenzen einer falschen Eidesstattlichen Erklärung bewusst.

Mit der Aufnahme meiner personenbezogenen Daten in die Alumni-Datei bei der TUM bin ich einverstanden.

München, den

.....

